THE ROLE OF MOISTURE PROFILING TOWARDS UNDERSTANDING PHARMACEUTICAL SOLID STATE FUNCTIONALITY

Validation and the application of a moisture profiling analytical tool for investigation into the characterisation of and prediction of the effects of compaction and storage on different lactose physical forms

Louise SEYMOUR

Submitted for the degree of Doctor of Philosophy

School of Pharmacy

Faculty of Life Sciences

University of Bradford

2015

Abstract

THE ROLE OF MOISTURE PROFILING TOWARDS UNDERSTANDING PHARMACEUTICAL SOLID STATE FUNCTIONALITY

KEYWORDS: Moisture profiling, equilibrium relative humidity, compaction, storage stability, lactose physical forms, solid state properties, thermal properties.

The majority of therapeutic pharmaceutical formulations are presented in the solid form. Moisture is able to play an important role in the functional performance of pharmaceutical solids. Moisture profiling is able to provide novel information with regards to the behaviour of moisture within materials using equilibrium relative humidity as a measurement.

The hypothesis investigated explores the changes in equilibrium relative humidity of pharmaceutical material induced by physical, chemical or storage conditions, these are able to be monitored using the innovative moisture profiler system.

The aims within this were to primarily validate the moisture profiler and secondly evaluate the effects of moisture on physical forms and with respect to effects of compaction, finally this was compared to conventional characterisation methods.

Preliminary explorations were conducted in order to assess the validity of the moisture profiler, from this lactose was selected as a suitable pharmaceutical material for further work.

Processing effects were then examined, firstly storage at elevated relative humidity of different forms of lactose were explored, and this was carried out with supplementary analysis. Secondly the effects of tabletting were explored, different compaction forces were investigated to observe if this had any notable effects on equilibrium relative humidity of the different lactose forms. Finally subsequent storage of the compacts were examined in order to explore if there were any changes in the equilibrium relative humidity.

Acknowledgements

It would not have been possible to write this doctoral thesis without the help and support of the kind people around me, to only some of whom it is possible to give particular mention here.

I would like to thank my academic supervisors, firstly Professor Robert Forbes for his guidance and support throughout this research project, his patience and academic experience have been invaluable and help make this thesis possible. Secondly, Dr. Wendy Hulse for her constant words of encouragement, help and friendship, I am truly indebted to her.
I would also like to thank the EPSRC and Reckitt Benckiser who provided financial support for this work.

I would also like to thank Dr Peter Moir, from Relequa for the loan of the moisture profiler.

Finally, special thanks to my family, especially parents for their continual and never ending support over the last eight years, without this support, none of this would have been possible, thank you does not seem to express the extent of gratitude I have for them

Contents

List of symbols and abbreviations

α	Alpha
β	Beta
γ	Gamma
λ	Wavelength
θ	Theta
2θ	Two theta
Å	Angstrom
ϕ	Relative humidity
δ^-	Delta negative
δ^+	Delta positive
Δ T	Change in temperature
API	Active pharmaceutical ingredient
a_w	Water activity
DSC	Differential scanning calorimetry
DVS	Dynamic vapour sorption
ERH	Equilibrium relative humidity
FDA	Food and drug adminstration
IUPAC	International union of pure and applied chemistry
HDPE	High density polyethylene
PXRD	Powder x-ray diffraction
p	Vapour pressure of substances
p^o	Vapour pressure of pure water
P	Pressure
RH	Relative humidity
RH_o	Critical relative humidity
SEM	Scanning electron micrography
TGA	Thermogravimetric analysis
V	Volume

List of figures

List of tables

List of appendices

1. INTRODUCTION

1.1 General introduction

The majority of therapeutic drugs that are dispensed are present in the solid form. Active pharmaceutical ingredients (API's) and excipients are therefore routinely present in the solid state and are delivered to patients in an approved dosage from such as tablets or capsules. Solids are able to provide a convenient, stable format for delivery and storage. Therefore, understanding and controlling the chemistry of API's and excipients is a crucial part of the drug development process (Morissette et al., 2004).

Both APIs and excipients are able to exist in numerous solid state forms including, co-crystals, hydrates, polymorphs, solvates and amorphous solids. Consequently, each form exhibits different physicochemical properties that can directly influence the bioavailability, manufacturing, stability and many other performance characteristics of the final dosage form (Byrn et al., 1999). Consequently the physical and chemical properties of the solid state must be fully understood. Complete comprehension of this area can lead to better design and control of drug performance (Byrn et al., 1994).

The physical and chemical properties of pharmaceutical solids are crucially dependent upon the presence of water; it is able to influence areas such as compaction, dissolution, flow, stability and storage (Brittain, 1995). Materials used in the pharmaceutical arena may come into contact with water during various ways such as; during manufacturing, storage at high relative humidity (RH), residual water or transfer between components (Khankari and Grant, 1995).

1.2 Solid state chemistry

When formulating a new pharmaceutical product, both the solid state chemical and physical properties must be fully understood. Therefore, it is important to examine the fundamental principles from the beginning. There are three general states of matter; gas, liquid and solid. The differences between these can be seen in Figure 1.1.

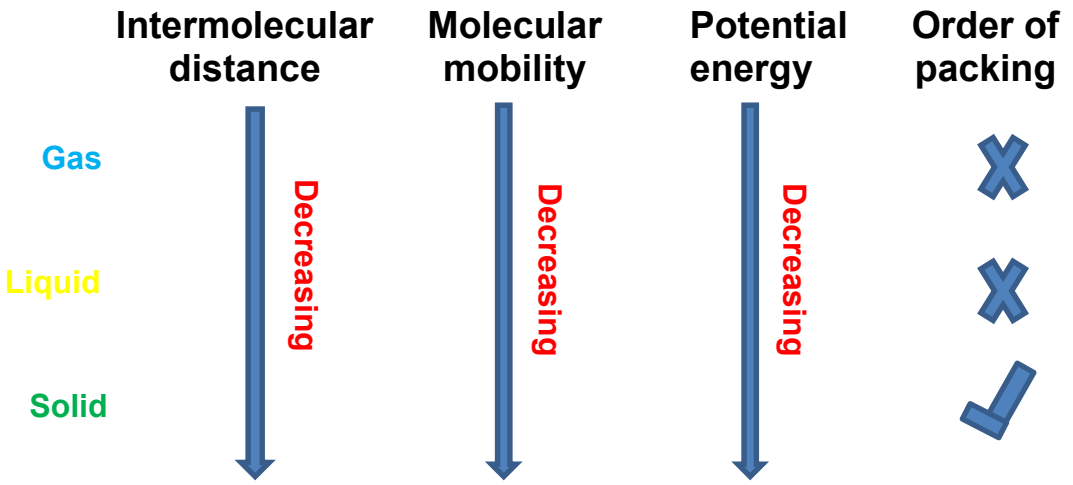

Figure 1.1. Differences exhibited by the three states

It can be seen that solids are different when compared to other states, hence the research into the study of solid state properties is essential. (Aulton, 2009, Zografi et al., 1988).

Materials that exist in the solid state can be further categorised into either amorphous or crystalline, or they may be a mixture of both. The basic taxonomy of the solid state can be seen in Figure 1.2.

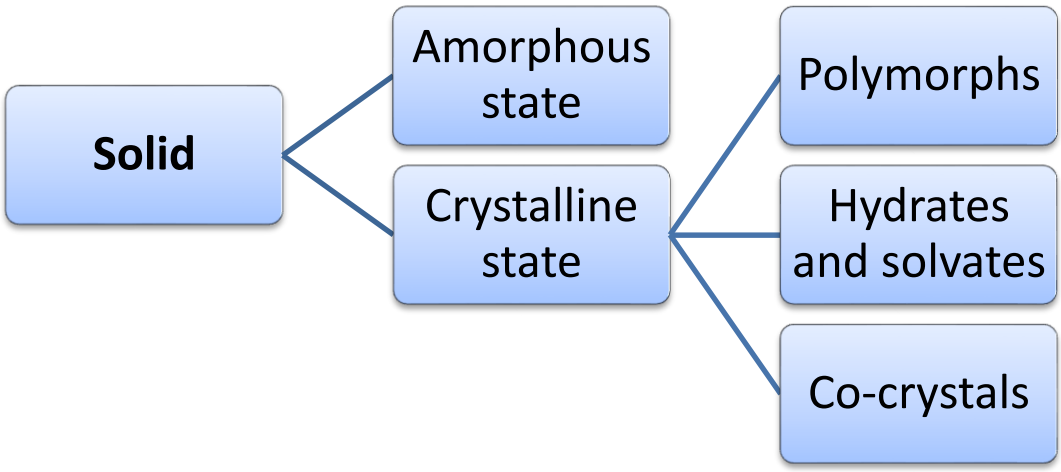

Figure 1.2. Taxonomy of the solid state

1.2.1 Amorphous state

Amorphous solids essentially have a complete absence of internal order with a random composition of molecules. An amorphous solid can be defined as possessing short range order, but does not possess long range order of molecular packing or have a defined molecular conformation (Yu, 2001). This results in amorphous forms being more unstable than their crystalline counterparts (Bhugra and Pikal, 2008). This instability has both good and bad consequences, it allows amorphous material to be of great pharmaceutical use, the dissolution rate is generally increased which gives rise to the possibility of enhanced drug bioavailability (Pikal et al., 1978). Amorphous solids are also found to enhance pharmaceutical formulations by other manners, such as enhancing solubility and compressibility (Craig et al., 1999, Cal et al., 1996).

Amorphous material may be produced by many routes; the four main methods are shown in Figure 1.3. The most common of these being super cooling of a melt, this

produces amorphous material because the cooling process occurs rapidly which therefore prevents crystallisation taking place.

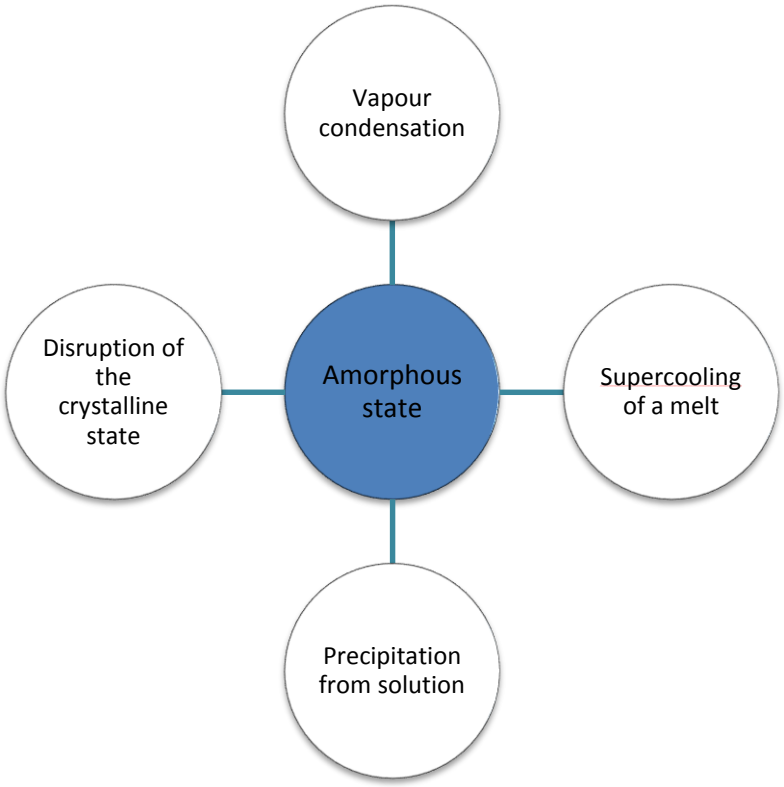

Figure 1.3. Main methods employed to produce amorphous pharmaceutical materials

Adapted from (Hancock and Zograf, 1997).

Figure 1.3. Main methods employed to produce amorphous pharmaceutical materialsFigure 1.3 illustrates the production of an amorphous solid using the super cooling process, relative to its crystalline counterpart.

In the formation of amorphous material, the liquid also known as the melt is cooled rapidly. It is apparent that there is no discontinuity in enthalpy or volume seen at the melting temperature (T_m). The material then reaches the super cooled region, which is sometimes referred to as the rubbery state. The material undergoes further cooling and at a characteristic temperature specific to the material, a

change in slope is observed. The intersection of the change in slope is termed the glass transition (T_g). The T_g is the distinguishing feature of the amorphous form and is representative of the temperature when the material is kinetically unable to attain equilibrium (Shah et al., 2006). Hence, a non-equilibrium state is produced, giving rise to higher internal energy, greater than that of the super cooled liquid. This results in enhanced thermodynamic properties, compared to that of the crystalline state. At this point the bonding between molecules does not alter significantly to that exhibited by a liquid.

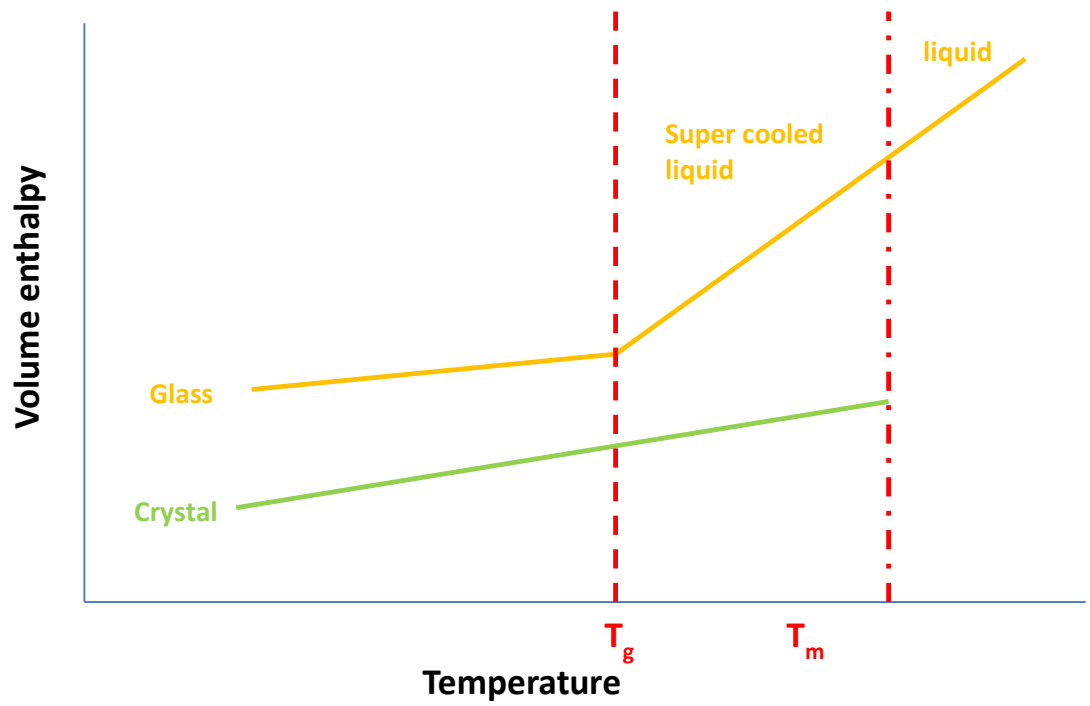

Figure 1.4. Variation of enthalpy (or volume) with temperature

Graphic representation of amorphous material being produced via supercooling

1.2.2 Crystalline state

The majority of dosage forms are presented in the crystalline state (Craig et al., 1999). The process of crystallisation is routinely employed for separation, purification and production of pure material (F. Doherty et al., 2007). As can be seen in Figure 1.2, a crystalline material can be further classified into a polymorph, hydrate or solvate or a co-crystal. Each of the above forms are all discussed individually within this chapter.

The definition of the crystalline state is best described in comparison to that of the amorphous state. Crystalline solids exhibit both long and short range order. Long range order refers to the uniformity and periodicity of the surrounding molecules and the short range order gives indication of the neighbouring molecular co-ordination (Cui, 2007). The term crystalline is therefore used to describe the arrangement of atoms within a solid. The structural units, called unit cells are repeated systematically and indefinitely through three dimensions in space. Therefore, each unit cell is the exact same size, have the same number of molecules (or ions) that are arranged identically (Florence and Attwood, 2006).

The unit cell of a crystal is specified by the lengths of the edges and the angles between these (Kennon, 1978). Consequently a unit cell has very distinct parameters; these can be seen in Figure 1.5. The symmetry of a unit cell gives rise to seven crystal systems, which in turn can be classified into one of fourteen bravais lattices and then further into 230 different space groups (Vippagunta et al., 2001, Lewis and Edwards, 2001).

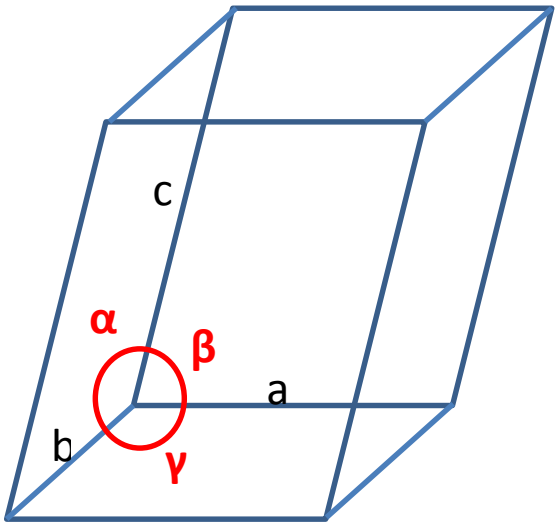

a, b, and c correspond to lengths of the sides. α, β and γ correspond to the angles between the sides.
α = angle between b and c
β = angle between a and c
γ = angle between a and b

Figure 1.5. Unit cell parameters of a crystal system (Adapted from (Levinson, 2001))

1.2.3 Polymorphism

The term polymorph is used to describe the existence of a substance in more than one crystal form (Sanders et al., 2000). A simple example of polymorphism is observed in carbon; which is able to exist in two forms as the cubic diamond or hexagonal graphite. A compound has more than one molecular composition when it is in the solid state and it has been suggested that the majority of all organic compounds can form polymorphs (Haleblian and McCrone, 1969). Subsequently polymorphic compounds exhibit different crystal structures and physicochemical properties.

Polymorphs can therefore have a huge impact in the pharmaceutical industry. True polymorphs are chemically identical but differ in their physical properties. Therefore polymorphic compounds could display different crystal shape, density, melting point, solubility and vapour pressure (Rodríguez-Spong et al., 2004, Llinàs and Goodman, 2008, Aulton, 2009). The above properties are important to take into account when conducting pre-formulation studies. As polymorphism can

subsequently affect other areas such as chemical stability, physical stability and bioavailability (Singhal and Curatolo, 2004), which may have beneficial or detrimental effects.

A variety of techniques may be employed to differentiate between polymorphic forms; routine methods include x-ray single crystal analysis, x-ray powder diffractometry (PXRD), infrared spectroscopy, raman spectroscopy, differential scanning calorimetry (DSC), optical or scanning electron microscopy (SEM) and solid state nuclear magnetic resonance spectroscopy.

1.2.4 Hydrates, solvates and co-crystals

Hydrates, solvates and co-crystals are all similar solid state forms in the fact that they all contain more than one molecular entity. Within the pharmaceutical context, for a potential drug, one of these molecules would be the active pharmaceutical ingredient and the other molecule is either water, organic solvent or another crystalline solid respectively forming the corresponding hydrate, solvate or co-crystal (Vishweshwar et al., 2006). Both components concerned contribute to both the long and short range order that the crystalline structure exhibits (Cui, 2007).

1.3 Moisture

1.3.1 General introduction

The term moisture is used in reference to the existence of a liquid, this is typically water. The liquid is usually present in small trace amounts and can be found as a vapour or condensed upon a surface, it can be found in the air as humidity, within foods and other various commercial products.

Moisture sorption properties of pharmaceutical materials are recognised as a critical factor in determining storage, stability, processing and application performance. (York, 1983)

Moisture does not only impact on the pharmaceutical industry, it has many implications on a variety of trades, ranging from the food, construction and soil industries to name a few.

1.3.2 Equilibrium relative humidity

Equilibrium relative humidity (ERH) can also be termed water activity (a_w) and is fundamentally, a measure of the free water present within a substance or pharmaceutical dosage form for example (Bell L and Labuza, 2000). It can be defined as the ratio of the water vapour pressure of the substance to the vapour pressure of pure water, when both are at the same temperature:

Equation 1

$$a_w = \frac{p}{p_o}$$

Where: p = vapour pressure of a substance; p_o = vapour pressure of pure water.

ERH is simply a derivative of a_w, in which it has been developed and expressed as a percentage:

Equation 2

$$ERH = a_w \times 100$$

ERH is obviously related to relative humidity (RH); RH is based upon the principle that air is able to hold water vapour. The ability of air to hold the water vapour can be directly measured and is expressed as a percentage (% RH); this measurement is

directly dependent upon the temperature. Water vapour is constantly being sorbed or desorbed from material surfaces. Within a closed environment, the movement of the water vapour will eventually after the relevant amount of time, reach equilibrium. This can be seen in Figure 1.6.

At equilibrium the water activity of a sample is equal to the relative humidity of the environment in which it is contained. An understanding of whether water will be sorbed or desorbed from a material is crucial in preventing degradation. It is important to distinguish the difference and importance of measuring ERH and measuring water content. For example, considering two separate materials that will initially have different water contents and water activities. If these are stored at 35 % RH, they will eventually reach a water activity of 0.35, and hence have an ERH value of 35 %. However, both materials have the ability to exhibit different water contents. Similarly, consider two materials with different water activities but the same water content. If these are mixed together, then the water will adjust between the two materials, until eventually an equilibrium water activity is achieved. Therefore, water activity and consequently ERH is able to potentially provide valuable information for pharmaceutical areas such as formulation design, manufacturing environment and packaging stipulations.

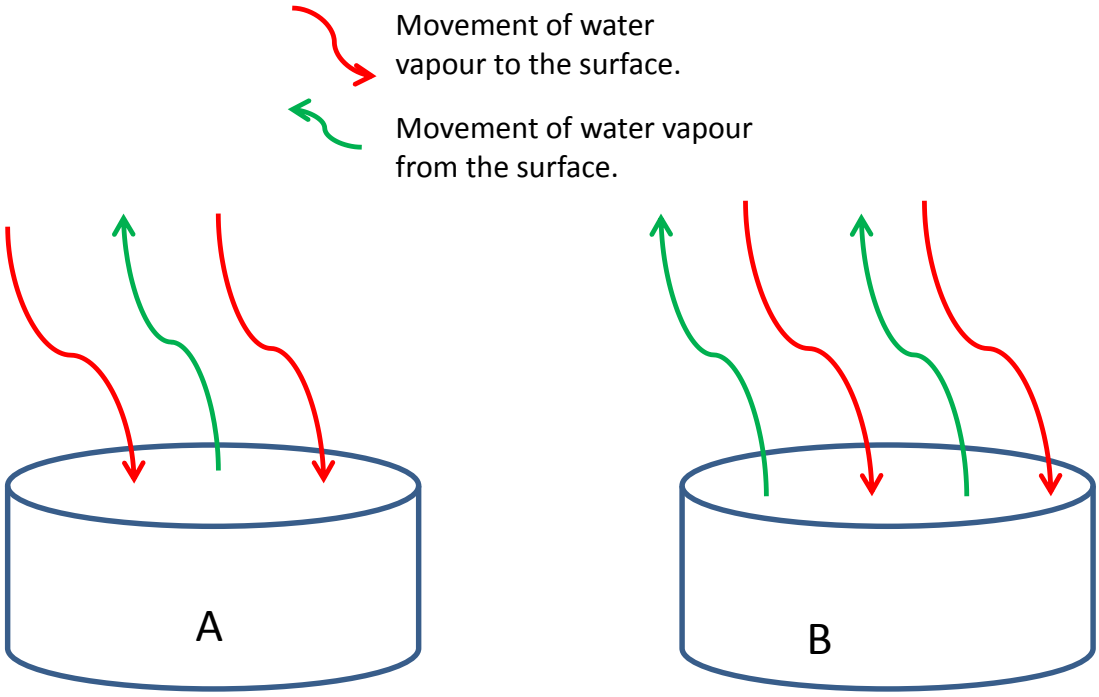

Figure 1.6. Movement of water vapour in a closed environment on a solid surface

A) Illustrates water vapour movement not at equilibrium B) Illustrates water vapour movement when it reaches equilibrium, this is the point when ERH is attained.

1.3.3 Pharmaceutical importance of ERH

Moisture uptake is a significant concern for many powdered industrial materials (Bergren, 1994). Pharmaceutically ERH is significant for one main reason; the stability of the product. Water vapour is able to cause an effect in three main ways:

1) Microbial growth

2) Physical stability

3) Chemical stability.

Therefore moisture can have a considerable effect on the final pharmaceutical product. If a final dosage form is able to pick up moisture this can lead degradation of chemical and physical properties. This is appreciably more important than the

problem of microbial growth, even though microbial growth can cause implications too.

1.3.4 Sources of moisture

The interaction of water vapour with pharmaceutical solids can occur at any point, from synthesis of the raw materials to storage of the actual finished dosage form (Zografi et al., 1988). There are three main sources of the water vapour which interact with the solid (Zografi and Hancock, 1994):

I. Residual water present from processing.

II. Present in the surrounding environment.

III. Chemical reactions taking place within the solid state, producing water.

1.4 Water – solid interactions

1.4.1 Introduction

Water is able to interact via two possible routes;

1) Interaction only at the surface of the solid, known as adsorption

2) Interaction causing penetration within the bulk solid arrangement (United States Pharmacopeial Convention., 1995).

This gives rise to three possible ways in which the water is located within a solid. It is able to firstly from a monolayer of adsorbed water on the surface. Then it can become adsorbed within the solid and thirdly it is able to form multilayers of water. However the latter is not adsorbed water it is condensed water. The above is described schematically and can be seen in Figure 1.7.

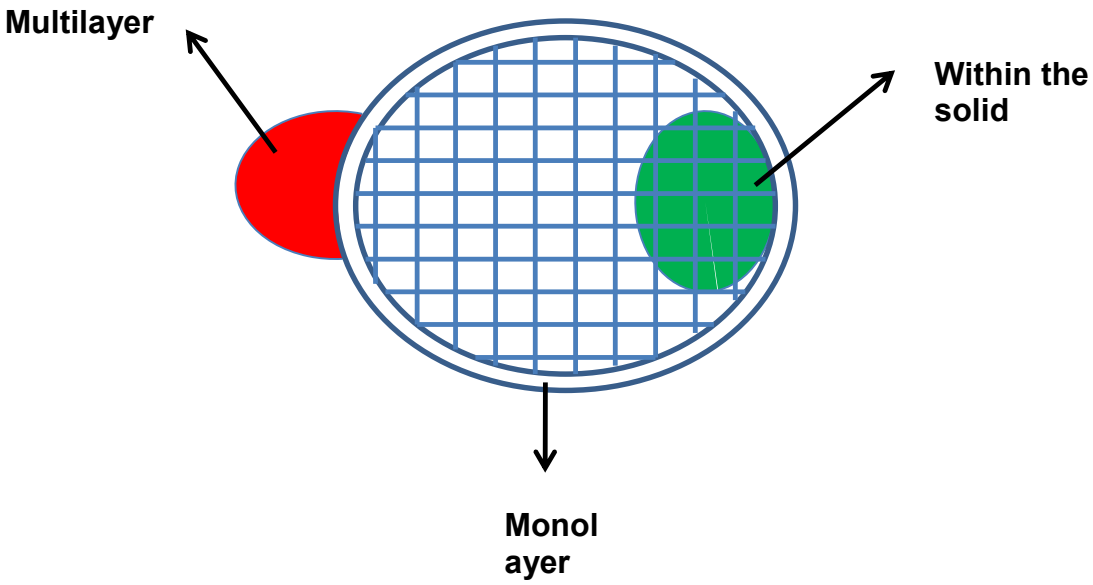

Figure 1.7. The possible ways water can be located within a solid. Adapted from (York, 1981)

Uptake of water molecules by water soluble solids usually occurs when water is in the vapour form; the process by which this can occur is seen in Figure 1.8 .

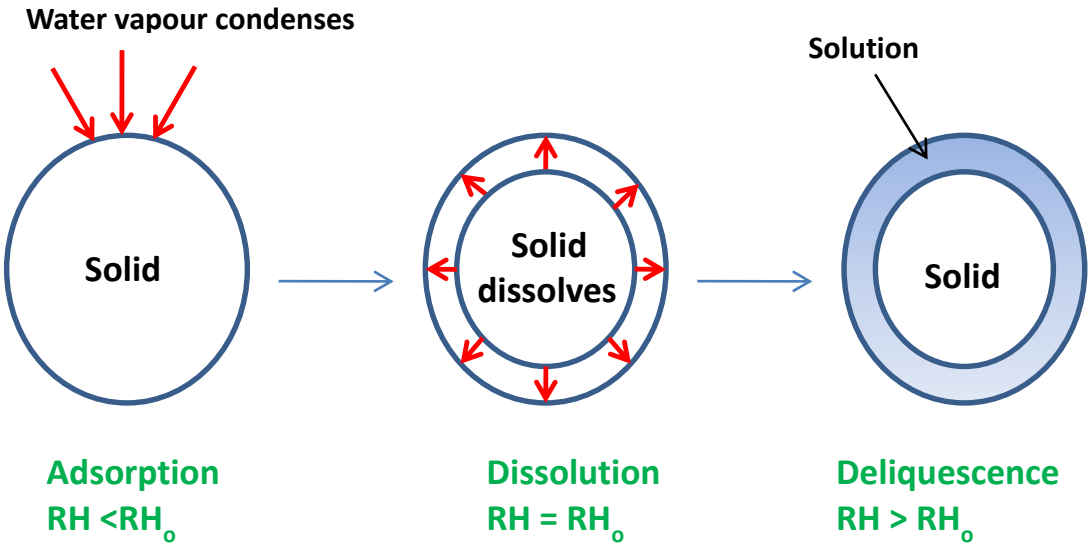

Figure 1.8. Water vapour adsorption processes Adapted from (van Campen et al., 1983)

As a rule adsorbed water is not dramatically able to impact and affect the solid properties. Water vapour is required to condense at the solid surface before any change can occur. Condensation occurs when $RH<RH_O$ (where RH_O is the critical relative humidity). However, at high RH's the adsorbed water vapour becomes capable of starting to dissolve the solid surfaces, dissolution occurs when $RH=RH_O$, and does not occur below the RH_O of the solid. If a high RH is sustained, then the adsorbed water will continue to dissolve the solid. This eventually causes deliquescence of the solid which leads to the formation a saturated solution (van Campen et al., 1983, Brittain, 1995). Deliquescence occurs when the $RH>RH_O$.

1.4.2 Hydrate formation

Many solids are able to form and exist as hydrates, materials that have the ability to form crystal hydrates, do so in a stepwise process. They firstly adsorb water molecules on to the external surface (Brittain, 1995). If more water molecules are available, these will be adsorbed into the anhydrous crystal, converting it into the hydrated form and the water molecules are bound within the crystal lattice. The strength of the resultant water-solid interactions is dependent upon the hydrogen bonds that are formed within the crystal lattice (Zografi, 1988). Hydrogen bonding is discussed in greater detail in section 1.4.3.

The hydration of a crystalline material is a function of the water activity of the solid. The crystalline hydrate is essentially a two component system that is specified by pressure, temperature and water activity.

1.4.3 Intermolecular forces

Water molecules are constructed of two hydrogen atoms that are found to be covalently bonded to an oxygen atom that is centrally located. Water is a "polar" molecule, meaning that there is an uneven distribution of electron density.

Two types of intermolecular forces that exist are hydrogen bonds and van der Waals forces, both are types of electrostatic interactions. Hydrogen bonding is an intermolecular force of attraction that exists when hydrogen molecules are attached to electronegative atom (X). X is able to produce an uneven electron cloud charge distribution. This forms a highly polarised hydrogen bond between the electronegative atom and hydrogen molecule (H-X). Formation of this bond causes X to develop a slight negative charge and H to develop a slight positive charge, causing a dipole to be formed (Figure 1.9). A hydrogen bond is brought about when the hydrogen atom that is covalently bonded to X is able to strongly interact with another electronegative atom (Y). Hydrogen bonding is therefore directly responsible for many physio-chemical properties that a material possess (Zografi et al., 1988).

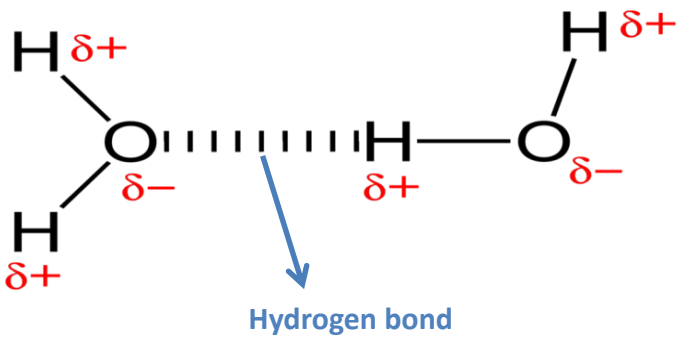

Figure 1.9. Diagram representing hydrogen bonding

In this case the hydrogen bond is between two water molecules. The hydrogen atoms are covalently bonded to the oxygen atom, with the hydrogen bond being formed between the two molecules. The oxygen atom is electronegative compared to the hydrogen atoms; they are δ^- δ^+ respectively, resulting in the formation of a hydrogen bond.

"Van der Waals" forces is a general expression used to describe intermolecular forces to include dipole-dipole and London forces (Ebbing and Gammon, 2009). Both are similar in that they are electrostatic interactions between molecules that possess no, or only a partial formal charge. The permanent dipole of a molecule has the ability to alter the electron distribution of an adjacent molecule, inducing a dipole moment (Figure 1.10). Hence, van der Waals forces are weak, attractive forces that are only able to exist over short distances. The forces are important in many different areas, but are important within the solid-state area because they can directly influence physical properties (such as melting point, hardness and conductivity) that a solid material may possess. This is due to the fact that along with chemical bonds, intermolecular forces help form the structural unit and hold the molecules together. It is the solids structure that is responsible for the physical properties exhibited (Ebbing and Gammon, 2009).

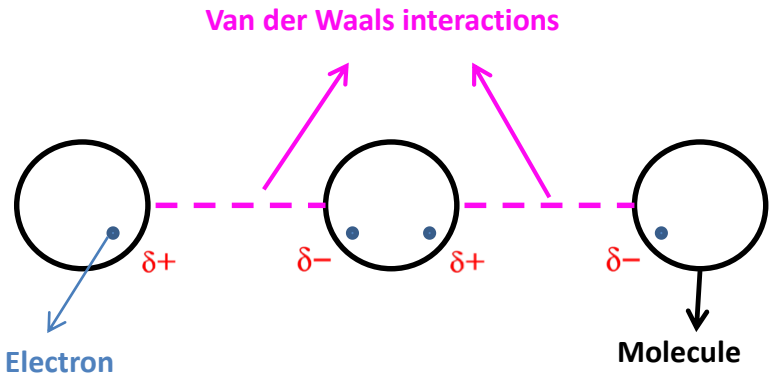

Figure 1.10. Diagram representing van der Waals interactions between molecules

1.4.4 Amorphous solids and water

As discussed previously, a solid can be considered as being on a spectrum between being essentially amorphous or crystalline. Amorphous solids are comprised of a disordered arrangement of molecules and consequently do not possess a distinguishable crystal lattice. This therefore means that amorphous material is able to absorb significantly greater amounts than its crystalline counterpart.

Amorphous material is able to exist in two distinctive states, the glassy state and the rubbery state (Strickley and Anderson, 1997).

1.4.5 Crystalline solids and water

Crystalline solids interact differently with water than amorphous solids, due to amorphous solids absorbing a large amount of water within the bulk structure. Water can interact with solids that are crystalline in four ways:

1. Adsorption on the solid surface.
2. Inclusion into micro-porous regions through a mechanism called capillary condensation.
3. Formation of a crystal hydrate.
4. Deliquescence (Ahlneck and Zografi, 1990).

For all four types of interaction, the water molecules become adsorbed to the surface of the solid, forming monolayer's, which at very high humidity's may increase to a maximum of two – three layers. (Ahlneck and Zografi, 1990).

The mechanism by which water sorption takes place is dependent upon various factors the solid exhibits, such as; crystal structure, water solubility, porous structure and the ability to readily form hydrates. (Dawoodbhai and Rhodes, 1989). This is because of the close packing and high degree of order exhibited by the crystal lattice, hence most crystalline solids will adsorb water molecules onto the surface and not within the structure (United States Pharmacopeial Convention., 1995). The adsorption of water molecules is dependent upon the polarity of the crystalline solid surface, which is relative to the surface area (Newman and Brittain, 1995).

1.5 Aims

From the introduction, it is evident that moisture plays an important role in the functional performance of pharmaceutical powders and materials. The main research question that this thesis therefore addresses is whether it is possible to obtain information on the physical form of a material and consequently behaviour or performance by assessing equilibrium relative humidity with time. Or put another way, is it possible to assess the state or performance of a material by simply measuring the materials interaction with moisture. In the current era of process analytical technology, it is very desirable if we could use a moisture

profiling tool as a predicator of process endpoint or process performance. The sub-aims of this thesis were to:

- Establish and assess the validity of a novel instrument that monitors equilibrium relative humidity with time (moisture profiler). Consequently, this can only be done after selecting and fully characterising a suitable pharmaceutical excipient to be used for the duration of the study.
- Detect any solid state changes induced by storage at elevated storage RH, including the effects upon the resultant moisture profiles.
- Investigate the effects of compaction and then subsequent storage on the solid state of lactose forms, lactose being the selected material. Then evaluate the relationship between any changes in the samples with regards to solid state analysis in correlation with the evolved relative humidity-time moisture profiles. The ambition here is to explore and establish if moisture profiling is able to detect any changes in materials solid-state properties after processing.

1.6 Material selection

It was appropriate in this instance to choose a model material that would produce alternative crystalline forms upon exposure to moisture. It was also necessary that the different systems exhibited by the material show significantly different physical and chemical behaviour. After careful consideration lactose was selected from the excipients as the behaviour and forms are well characterised. Several other excipients were also evaluated in early studies.

1.6.1 Lactose

Lactose is a disaccaharide that occurs in the milk of mammals, it is comprised of galactose and glucose. Lactose exists in two isomeric forms, α and β, these are optically active (Angberg, 1995). Both α and β structures can be seen in Figure 1.11 . This shows that the anomeric forms exist due to the conformation of the hydroxyl group attached to the C1 carbon. Equatorial orientation of the hydroxyl groups gives rise to the β anomer, whereas axial orientation gives rise to the α anomer. Only the α anomer is able to incorporate water of crystallisation into the actual crystal lattice with a 1:1 stoichiometry. Therefore, throughout this thesis when lactose monohydrate is mentioned this refers to the α anomer.

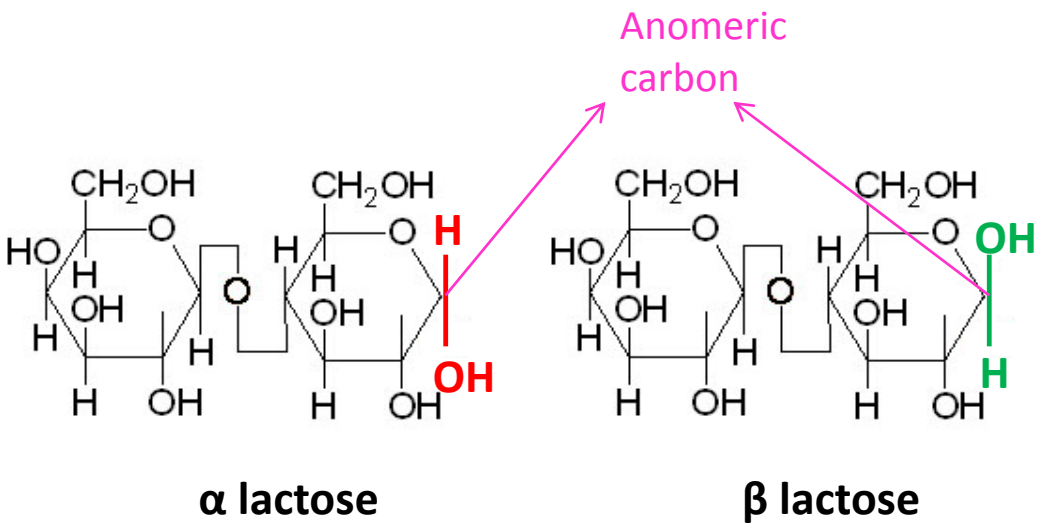

Figure 1.11. Molecular structures of α and β lactose

Lactose is found to exist in four forms (Ziffels and Steckel, 2010) these can be seen in Figure 1.12. It is evident that the α anomer is able to exist in both the monohydrate and anhydrate forms, however, the β anomer is only able to exist in the anhydrous form.

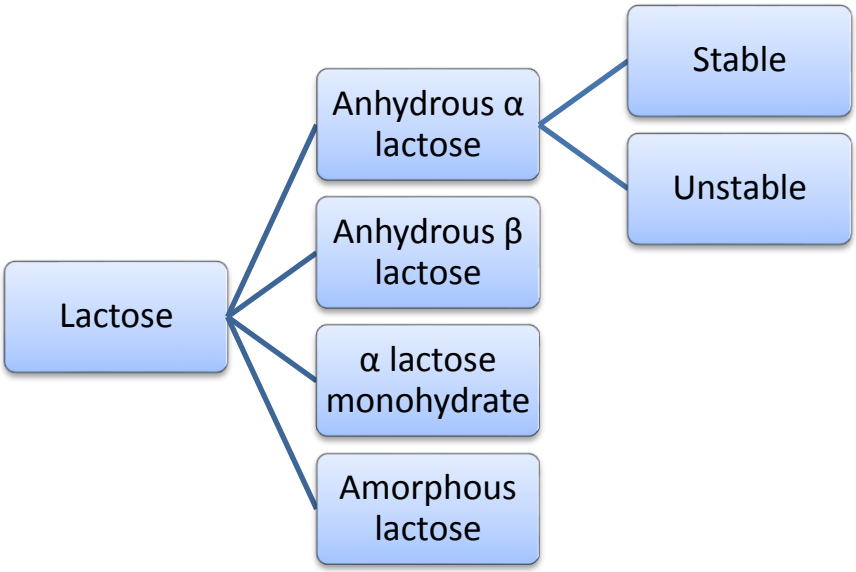

Figure 1.12. Different forms of lactose

It is necessary to clarify the different forms of lactose that exist in relation to polymorphism. The generic definition of polymorphism being a material that exhibits different crystal structures within the solid state, but when in solution demonstrates identical characteristics. From Figure 1.11 it is obvious that the two forms shown are anomers related by muturotation, therefore technically α and β are not strictly polymorphs. However, a spontaneous equilibrium exists in the ratio 40:60 between anhydrous α and β lactose respectively. This therefore agrees with the earlier definition, as polymorphs are said to exist if rapid conversion between forms occurs in solution (Kirk et al.' 2007). The classification of lactose as a polymorph is debatable; however the different forms of lactose have been commonly described as polymorphs. Therefore throughout the context of this work and thesis, all forms will be referred to as polymorphs, thereby maintaining the terminology.

1.6.2 The interaction of moisture with lactose

Figure 1.12 shows that lactose occurs in different forms and section 1.4 highlights that different solid state are able to interact differently with moisture. Therefore, the different lactose forms will interact differently. Under atmospheric conditions lactose monohydrate adsorbs minimal water at RH less than 70%. However, in contrast the anhydrous form will convert to the monohydrate at 70% RH, as a direct result of water being incorporated into the crystal lattice. If humidity reaches above 95% then this is able to promote deliquescence which is followed by recrystallisation.

1.6.3 Applications

Lactose has a huge variety of uses and its applications are not solely limited to the pharmaceutical industry. For example, lactose is used in the food industry as a free flowing or agglomerating agent and to enhance flavours of food. Lactose is used as a precursor for several more valuable food grade derivatives, due to reactive functional groups contained within the molecule.

Within the pharmaceutical arena lactose is one of the most significant excipient in the production of the solid oral dosage form (Ziffels and Steckel, 2010). This is due to the biological inactivity lactose exhibits, its main use is as an inert filler within tablets and capsules. Lactose is also employed to aid dispersion in dry powder inhalers. It is able to act as a carrier for the desired drug, due to its much larger size.

2. MATERIALS AND METHODS

2.1 Introduction

This chapter focuses on the specific materials used and methods employed for sample preparation. It also highlights the specific analytical techniques utilised throughout for physicochemical characterisation.

2.2 Materials

Material	Manufacturer	Batch/Lot number
α Lactose monohydrate	Reckitt Benckiser	00026660
Anhydrous lactose	Fluka	17814
Acesulfame potassium	Reckitt Benckiser	359988
Buprenorphine hydrochloride	Reckitt Benckiser	G08062
Citric acid	Reckitt Benckiser	411361
Magnesium stearate	Reckitt Benckiser	00026660
Maize/starch	Reckitt Benckiser	375540
Naloxone hydrochloride dihydrate	Reckitt Benckiser	P02065
Povidone	Reckitt Benckiser	00023288
Sodium citrate	Reckitt Benckiser	316453

All materials were used as received unless stated otherwise.

2.3 Preparation of amorphous lactose material

2.3.1 Freeze drying

Freeze drying is also known as lyophilisation and is commonly used within the biotechnology and pharmaceutical industries to enhance stability of formulations (Tsinontides et al., 2004). Freeze drying is the process by which a solvent is removed from a frozen product by sublimation, hence the solvent goes straight to the gaseous phase by-passing the liquid phase (Velardi and Barresi, 2008). This leaves the solute or substrate almost entirely or in some cases completely in their anhydrous state (Franks, 1998).

Freeze drying is a three step process that comprises of;

1) Freezing, this is essentially solidification.

2) Primary drying, this is fundamentally sublimation.

3) Secondary drying, this involves the desorption of unfrozen water (Abdelwahed et al., 2006, Franks, 1998).

Freeze dried lactose was conducted using a Heto FD 8.0 CD 8030 Freeze dryer (Heto Lab equipment Ltd, UK). In order to obtain freeze dried lactose, aqueous solutions were prepared from α lactose monohydrate, the solution was heated until a clear solution (20% w/w solids in the molar ratio of 9:1 of α lactose monohydrate), was obtained as reported (Haque and Roos., 2004). The samples were then pipetted in 2.5ml aliquots in 10 ml crimp neck vials. The procedure involved three stages: 24 hour freezing at -50°C, followed by primary drying at -20°C, secondary drying for up to twenty four hour at 0°C, then up to 20°C. Samples were then stored in a desiccator over silica until required for analysis.

2.3.2 Spray drying

Spray drying is the process by which the feed is transformed from a fluid state into a dried particulate form via a one step process (Goula and Adamopoulos, 2005)

Spray drying has a huge range of applications spanning across numerous industries. Such as the; chemical, food, biochemical and pharmaceutical industries (Broadhead et al., 1992). In this case, the pharmaceutical applications are of most importance. Material produced through the spray-drying process has been employed during manufacture of solid dosage forms since the 1940s (Broadhead et al., 1992, Corrigan, 1995).

Spray drying is increasingly being used as an alternative to milling in the production of particles of suitable size for inhalation (Tajber et al., 2009, Sham et al., 2004).

In some cases the spray drying technique is employed in order to produce amorphous material. In the solution the solute is present in a disordered state, which is then dried rapidly. This means it does not have time to crystallise and results in an amorphous product being formed (Gabbott, 2008).

Spray drying was carried out using a Buchi 190 mini spray dryer, a schematic diagram of this apparatus can be seen in Figure 2.1. In order to obtain spray dried lactose, aqueous solutions were prepared from α lactose monohydrate, the solution was heated until a clear solution (20% w/w solids in the molar ratio of 9:1 of α lactose monohydrate), was obtained. The samples were atomised using a two fluid nozzle (0.5mm), with the atomising air and solution passing individually. The nozzle operates using compressed air (6 bar pressure) that is sourced from an in-house supply; this is then cooled by a constant flow of cold water. The spray drier was allowed to thermally equilibrate before drying of samples was initiated. Solutions to be spray dried were supplied to the nozzle using 1mm silicone tubing. The drying air flow rate used was 500 L/hour and the liquid feed rate employed was around 13 ml/min. The conditions above resulted in inlet and outlet temperatures of 120-150°C and 60-70°C respectively. Samples were then stored in a desiccator over silica until required for analysis.

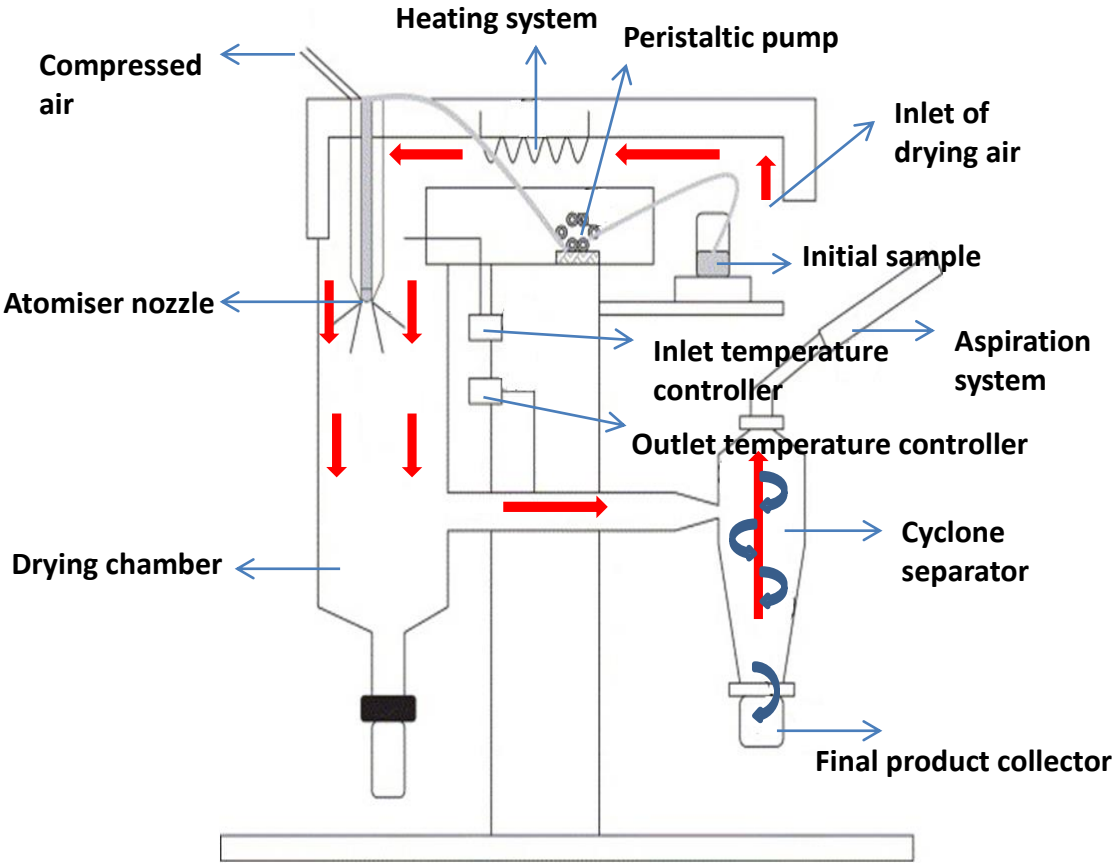

Figure 2.1. Schematic representation of the Buchi 190 mini spray dryer

2.4 Analytical techniques

2.4.1 Thermogravimetric analysis

Thermogravimetric analysis (TGA) is the measurement of the mass of a sample as a function of temperature. TGA measures mass changes associated with a sample that are induced by thermal variation.

The data obtained from the TGA can be used to determine many properties a material may exhibit, such as solvate or hydrate stoichiometry. TGA is a very useful tool and compliments DSC analysis through verification of thermal events such as decomposition and degradation. TGA can also be used to investigate the thermal

stability of materials and examine the kinetics related to the thermal events. However, it is important to highlight that although TGA analysis can be used to determine solvate or hydrate properties, it cannot distinguish between the two. Other techniques would need to be employed to establish this.

TGA instruments all consist of a similar design with an electronic microbalance (onto which the sample is placed), furnace, temperature controller and an instrument that is able to record the output of all these components.

TGA data was acquired using the thermogravimeteric analysis module of TA Instruments Q500 series thermal analysis system (TA Instruments, West Sussex, UK). Material of sample size 1-5 mg was analysed in an open aluminium pan attached to a microbalance heating in a predetermined temperature range dependant on the material, using a scanning rate of 10°C/min. Measurements were carried out in triplicate and the sample weight was monitored by the microbalance throughout the experimental period, to an accuracy of ± 1µg. The TGA was calibrated using nickel standard. The percentage weight lost from the sample prior to decomposition was attributed to be due to loss of water.

The data obtained from TGA analysis is represented and referred to as a thermogram (traces, curves or plots). Figure 2.2 shows a typical TGA trace that would be obtained for a sample of lactose monohydrate. A step change is evident within the trace at approximately a temperature of 100°C, due to the sample losing weight. The mass change can be calculated and then the stoichiometry of water within the sample can be calculated. So in this example, a mass loss of 0.2202 mg is observed, which corresponds to a percentage difference of 5.151 %, which is

corresponds to the water (or volatiles) within the sample which is lost during heating.

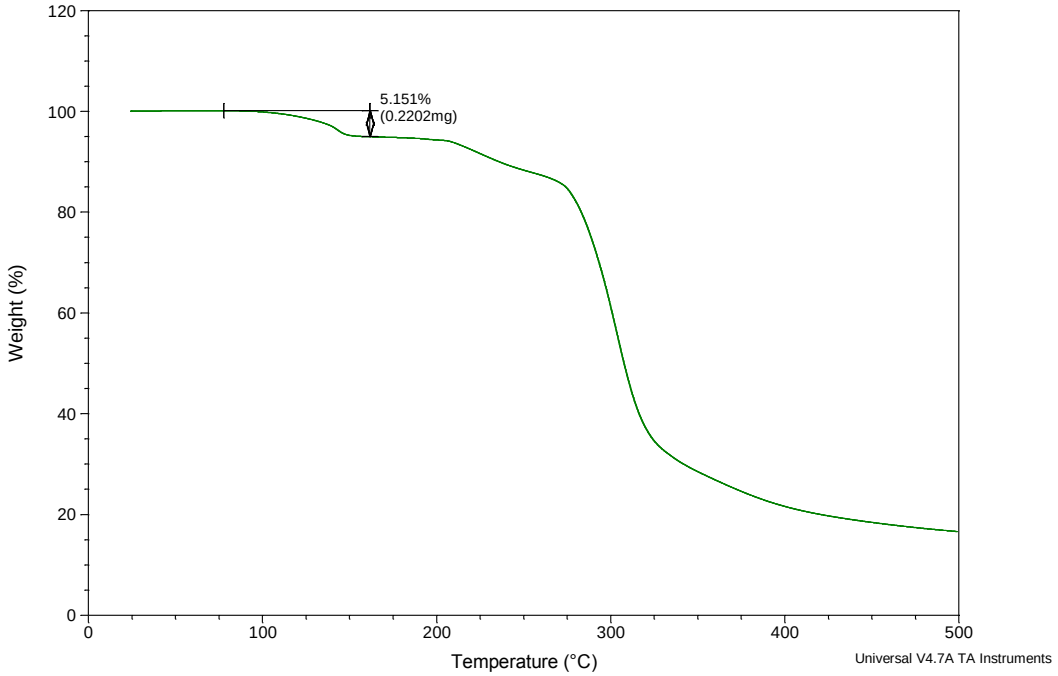

Figure 2.2. Typical TGA trace obtained for lactose monohydrate

2.4.2 Differential scanning calorimetry

DSC is a frequently used thermal method within the pharmaceutical industry for physicochemical characterisation of powders (Bond et al., 2002). DSC is a technique in which the energy input into a sample and into a reference is measured, as a function of time or temperature, whilst both the sample and reference are subjected to a controlled temperature program. The two predominant DSC methods are 'power compensation DSC' and 'heat-flux DSC (Swarbrick and Boylan, 2002). Power compensation DSC involves a system by which the sample and reference are housed in two different furnaces and hence are heated using separate furnaces.

Heat flux DSC is comprised of a system in which the sample and the reference are heated individually but are in the same furnace, as seen in Figure 2.3. The sample is contained within shallow sample pans in order to ensure maximum thermal contact between the sample, sample pan and the heat flux plate such that symmetrical heating of the sample and reference pans is employed. The difference in power required to keep the pans at identical temperatures is measured, which is expressed graphically as a function of temperature. DSC also has the ability to establish gas flow through the cell, which is able to assist in: heat transfer, removal of volatiles and provide the atmosphere required.

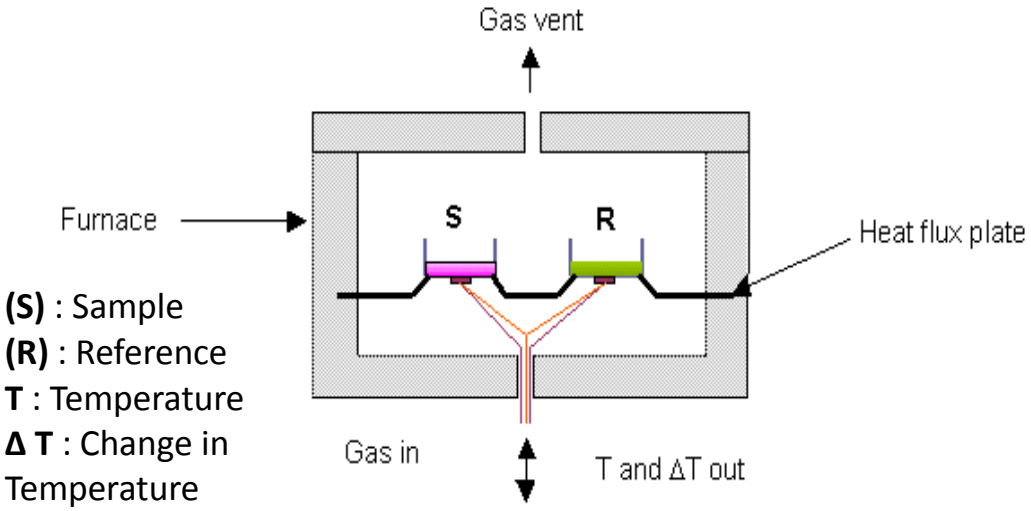

Figure 2.3. Schematic representation of heat flux DSC

DSC measurements were acquired using the Q2000, TA Instruments Limited, Crawley UK, which is an example of a heat flux system. The DSC is calibrated using pure Indium (M.P. 156 °C) and Zinc (M.P. 419 °C) standards at a heating rate of 10 °C/min. The sample (between 1-10 mg) was placed into an aluminium pan, to which an aluminium lid was then crimped and an empty aluminium pan was used as a reference. The sample is then heated at the same rate as the calibration

standards (10 °C/min) across various preselected temperature ranges dependent upon the sample.

DSC thermograms are plots of the difference between heat flows to a sample and reference against temperature and/or time. Figure 2.4 shows typical transition peaks that may occur within a thermogram and can be identified, depending upon the material. The glass transition (T_g) is observed when an amorphous solid or glass, goes through a phase change to form a less viscous, rubbery solid or paste. Also seen in Figure 2.4 is crystallisation and melting peaks, which are exothermic and endothermic processes respectively. If a sample absorbs energy, as in this case, the enthalpy change is endothermic and the peak is sometimes described as an endotherm. If the sample releases energy the enthalpy change is exothermic, hence the term exotherm. In some circumstances the baseline from the start of an experiment slopes upwards or downwards and in a lot of instances, changes level after a transition event, this is due to the difference in specific heat capacity between the sample and the reference. Potential enthalpic peaks and corresponding processes that can assist in data interpretation can be seen in Table 2.1.

Table 2.1. Possible enthalpic peaks and relevant processes

Process	Endotherm	Exotherm
Solid-solid transition	•	•
Crystallisation		•
Melting	•	
Vapourisation	•	
Sublimation	•	
Polymerisation	•	
Decomposition	•	•

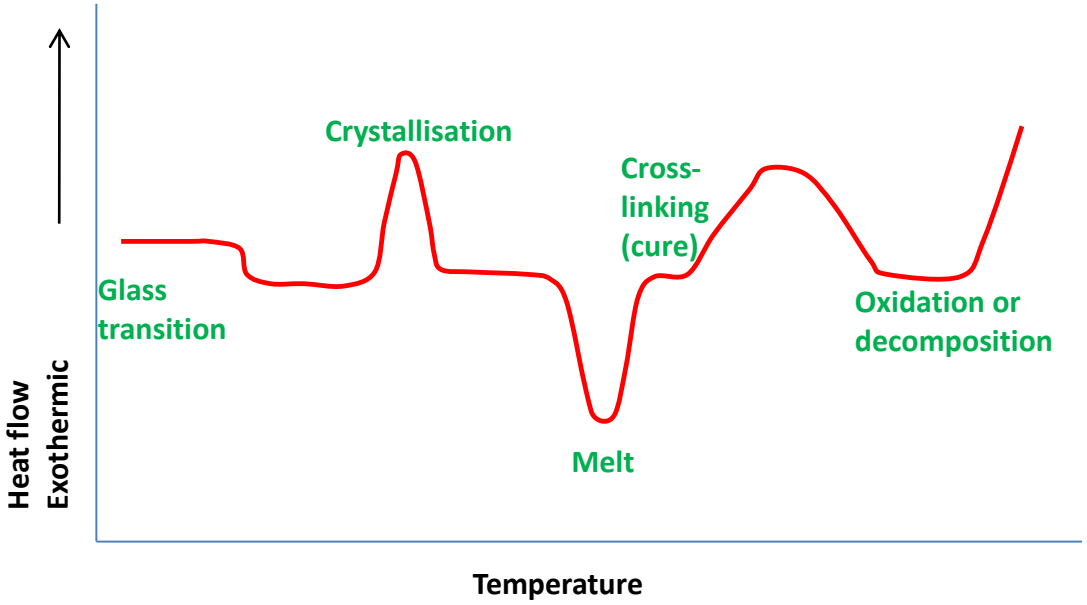

Figure 2.4. DSC thermogram showing typical peaks that may be observed

2.4.3 Dynamic vapour sorption

Dynamic vapour sorption (DVS) is a gravimetric technique that is essentially a measurement of change in mass of a sample, as a function of relative humidity (Willson and Beezer, 2003). It has a wide range of applications over various industries. In this work DVS is being used qualitatively, in order to assess amorphous content of material, because amorphous areas are thermodynamically unstable (Columbano et al., 2002). Other techniques also have the ability to quantify amorphous content such as PXRD and DSC; however these only have detection limits of around 10 % (Hogan and Buckton, 2001), whereas DVS is able to detect amorphous content to as low as 0.5 % (Mackin et al., 2002). Until the development and introduction of automated machines, moisture sorption measurements were carried out statically. The process involves placing a pre-weighed sample into an environment maintained at a constant RH, such as a

desiccator containing a saturated salt solution. At regular intervals the sample would be removed and weighed until equilibrium had been reached. The procedure has many drawbacks:

- Time consuming – can take weeks or months to produce an isotherm.
- Reduced accuracy – sample has to be removed from environment in order to be weighed.
- Does not provide kinetic data.

However, the above method has now been superseded by automated, dynamic methods. **Error! Reference source not found.** shows the schematic representation of an automated system.

Moisture sorption experiments were carried out using an IGAsorp moisture sorption analyser (Hiden Isochemica, UK). The balance was calibrated using 20 mg (GO4O163), 50 mg (GO48706) and 100 mg (GO4O16O) standards (KERN and Sohn GmbH, Germany). Humidity conformance was established using Lithium bromide and Lithium chloride humidity standards (Rotronic ag, Switzerland). Calibration was performed using 10%, 50% and 80% salt solutions. The solutions were placed into pyrex bulbs and dried to 0% RH for 120 minutes. The humidity was then raised to 2% below the humidity standard value and increased in steps of 1% until an upper limit of 2% above the humidity standard value.

Samples (50-60mg) were placed in stainless steel sample baskets. The sequence of isothermal steps incorporated drying the samples to 0% RH until constant weight was achieved. The RH was then increased in increments of 10% to a maximum of 95%

RH. The samples were then dried by decreasing the RH in increments of 10% to a final value of 0% RH before being returned to 40% RH in 10% humidity steps.

Information on the sorption mechanism of water on the surface of powders can be gained from the shape of the resultant isotherm; this is because it is dependent upon the interaction of the vapour molecules and the solid material (Roos, 1995). The physisorption isotherms can categorised into six major types based upon the IUPAC classification (Sing et al., 1985), these can be seen in Figure 2.5. A type one is a Langmuir isotherm and is typical of anti-caking agents. These tend to absorb water on to polar sites and the non-swelling capillaries. This can lead to a high amount of moisture being retained at low water activities (Bell and Labuza, 2000). Type two isotherms are termed a sigmoid isotherm, and as can be seen they are typically S-shaped and characteristic of isotherms given by biological material. They exhibit sudden changes amount of moisture adsorbed at low and high water content. Type three isotherms are typically exhibited by crystalline material. As can be seen by the isotherm, very little moisture gain is seen initially because interaction only takes place on the surface. As the water activity increases the water dissolves the material and the sample deliquesces, which is represented by the large increase in amount adsorbed. Type four and five isotherms both contain hysteresis loops; these are related to capillary condensation taking place within the mesopore structures. Hysteresis loops exist in various shapes (Sing et al., 1985). Type four isotherms are typically exhibited by mesoporous industrial adsorbents. Type five isotherms are rare and are representative of weak adsorbent-adsorbate

interactions. Type six isotherms are associated with stepwise adsorption on a uniform non-porous material (Rouquerol et al., 1999).

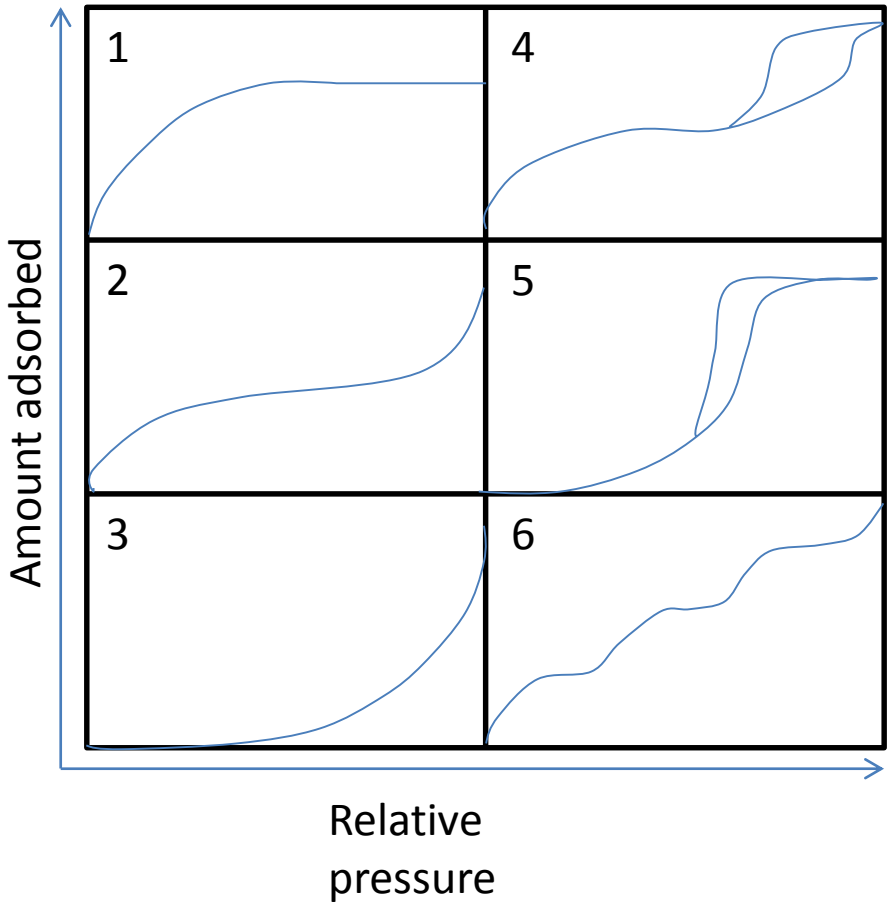

Figure 2.5. Classification of moisture isotherms based upon resultant shapes Adapted from (Sing et al., 1985).

2.4.4 Powder x-ray diffraction

PXRD is a common analytical technique, which is of particular importance when polymorphism exists in crystalline solids (Qiu, 2009). X-rays are a form of electromagnetic radiation that in relation to the electromagnetic spectrum occur directly before the ultra-violet region.

PXRD operates on the basis that when a crystalline sample is bombarded by X-rays, the sample will diffract these, resulting in scattering. The resultant scatter is almost

exclusively due to the electrons present within the atoms (Hammond, 2009), and is unique to the sample. This phenomenon that is observed is described by Braggs Law.

Braggs Law describes the diffraction of the emitted X-rays by the atoms from within the crystal lattice in terms of reflection; where angle of incidence is equal to the angle of reflection. The diffraction of the X-rays from a crystalline sample is illustrated in Figure 2.6. Braggs Law is given as:

Equation 3

$$n\lambda = 2d_{hkl} \sin \theta$$

Where: n = order of reflection; λ = wavelength of radiation, d_{hkl} = lattice plane spacing and θ = angle of incidence/reflection.

PXRD's usually consist of the following main components, an X-ray source, sample holder, detector and a device capable of acquiring the geometry of the incidence/diffraction angles.

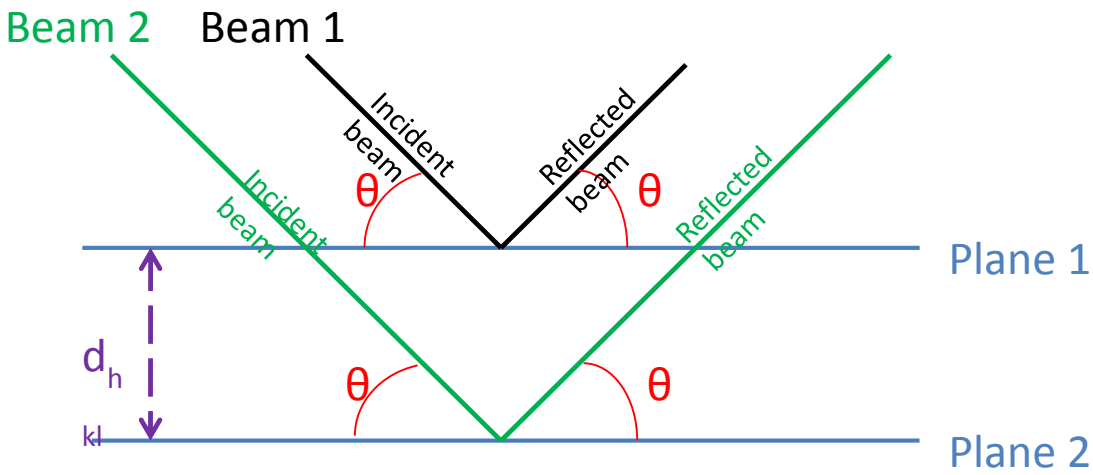

Figure 2.6. Diagram of x-ray diffraction and reflection from two crystal planes

The x-ray tube is located is located in a vacuum sealed tube, to which a current is applied, causing the filament to be heated and electrons to be emitted (increasing the current causes an increased number of electrons to be generated). A separate high voltage charge is the applied within the tube, this enables the electrons to be accelerated towards a metal target, (such as copper, chromium and cobalt) to which they collide. This results in X-rays being produced, which are directed towards the sample. The detector then records the diffracted X-ray signals. These can then be processed and transformed into a count rate.

The angle between the X-ray source, sample, and detector are able to be altered at controlled rates between predetermined limits, allowing the for the powder pattern to be generated. Figure 2.7 shows a typical PXRD instrument, in which the goniometer is set up for a theta-theta configuration. The sample is held in a fixed position and the X-ray tube and detector rotated around the sample; to form a two-theta angle between the tube and the detector.

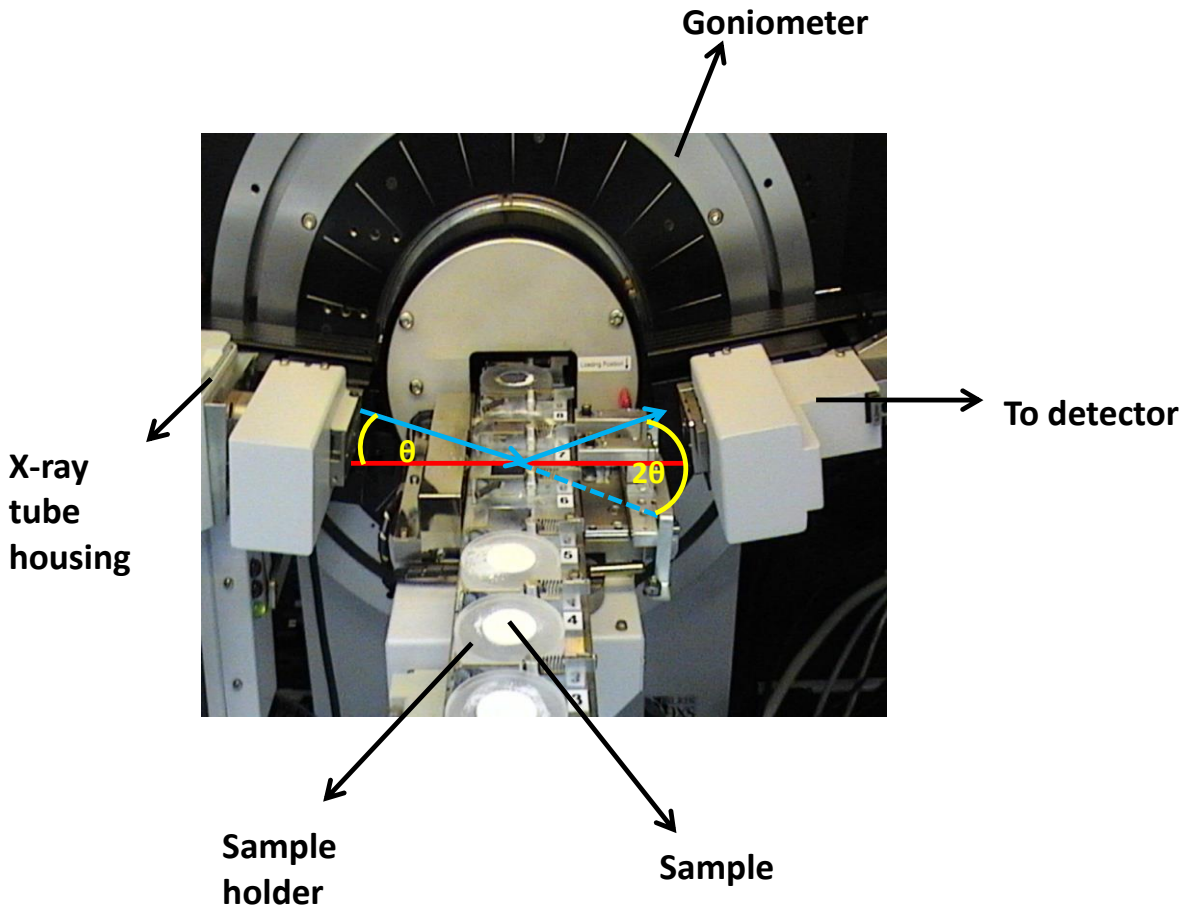

Figure 2.7. Typical PXRD instrumentation

The picture depicts the upper design of a Bruker D8 advance powder x-ray diffractometer. Illustrated is the significant geometric measurements mentioned previously. The red line indicates the sample level, x-ray beams are shown in blue and the resultant incident (θ) and diffraction (2θ) angles are shown in yellow.

It is important to emphasise that situations can occur when a truly representative powder pattern may not be obtained from the sample. This is caused by the particles within the sample not being arranged randomly within the sample holder. The effect is demonstrated in Figure 2.8. In the case of preferred orientation, only selected planes of the sample material become exposed. The possible outcomes from this are:

A) Larger peak intensities are seen due to preferentially exposed faces.

B) Some peaks may not be observed at all due to the faces not being exposed.

In order to try and overcome the predicament of preferred orientation, two precautions can be employed:

A) The sample holders used have grooved or ridged bases.

B) The sample holders are rotated during data accumulation.

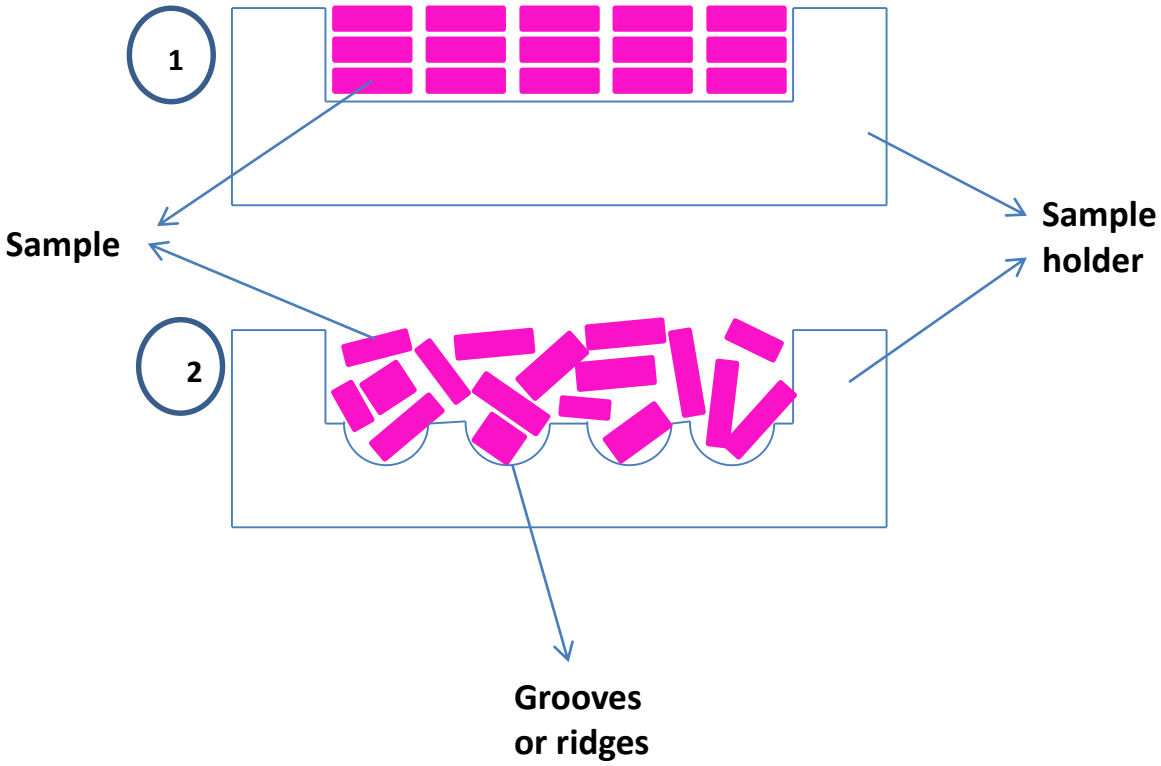

Figure 2.8. Sample arrangements using different sample holders

1) An example of a flat based sample holder, the molecules within the sample are observed to be ordered, which leads to preferred orientation. 2) An example of a sample holder with grooves within the base, this causes the sample molecules to be randomly packed.

X-ray powder patterns were obtained using a Bruker D-8 advance powder x-ray diffractometer. Samples were placed into the sample holder, where the material was subjected to manual compaction in order to produce a flat plane for analysis.

The scanning range used was 10-40° 2θ, with a step size scanning mode of 0.01, at a rate of 1 second.

The instrument is calibrated using powdered silicon crystals. However it is possible to use any polycrystalline powder as long as it exhibits high stability and sharp diffraction lines.

PXRD data obtained is displayed in a PXRD pattern. A typical PXRD pattern can be seen in Figure 2.9 . Braggs Law (Equation 3) can be used to calculate the d-spacing that relates to the diffraction angle, the d-spacing is the distance between the hkl planes shown in Figure 2.6.

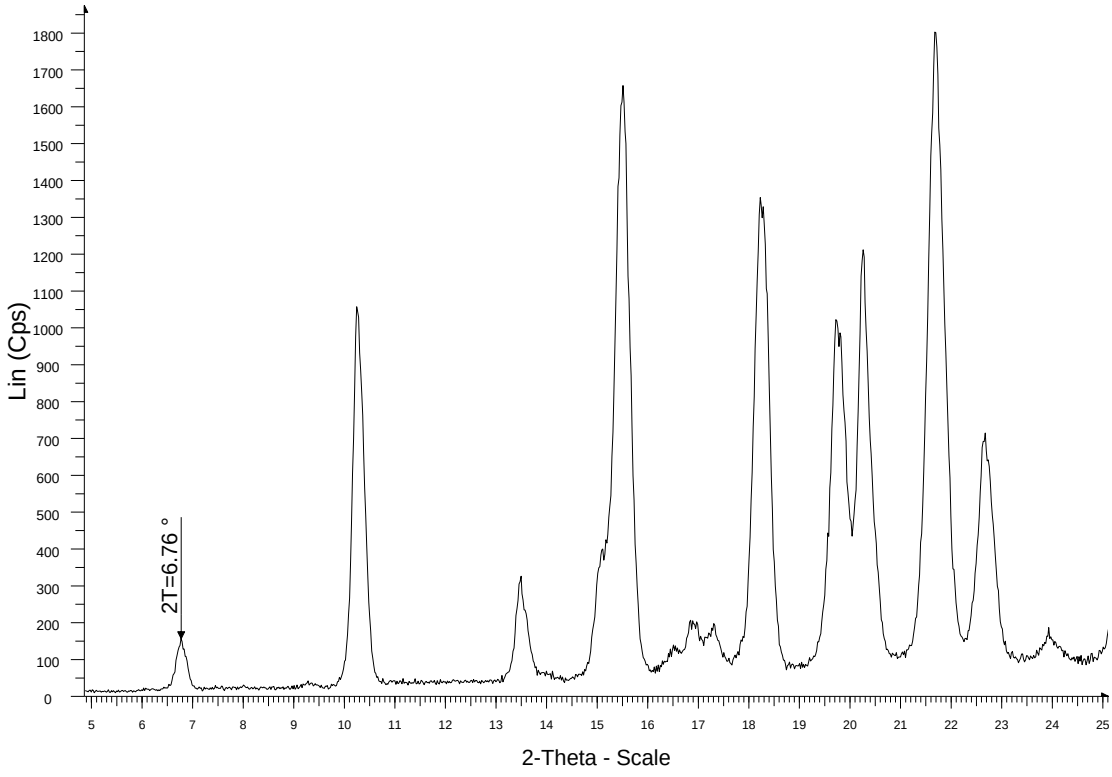

Figure 2.9. Typical PXRD pattern Peak labelled at 2θ = 6.76°, resultant d-spacing is 13.1 Å.

PXRD data can also be obtained for amorphous material, the typical patterns show a raised “halo” background. This raised background is due to an increased amount

of x-ray scattering being produced, as the molecules and hence associated atoms and electrons are not present in a regular repeating arrangement.

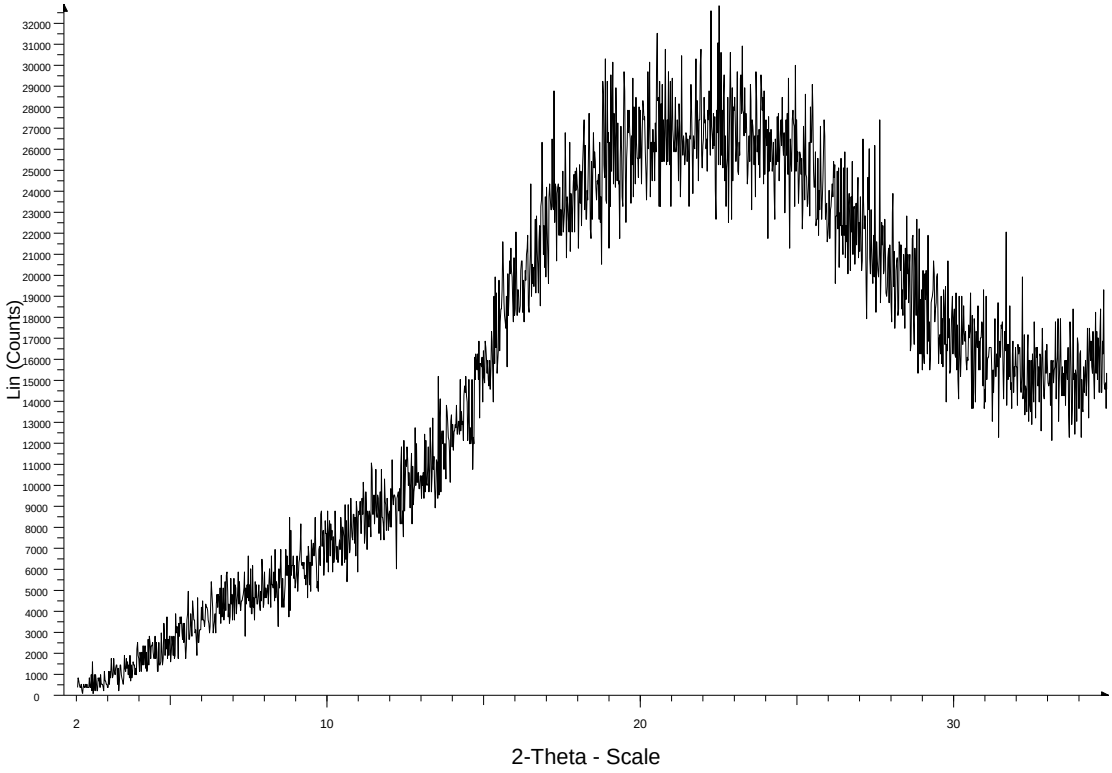

Figure 2.10. Typical PXRD pattern for amorphous material

2.4.5 Scanning electron microscopy

SEM is used within the pharmaceutical industry to attain three dimensional images of a material. SEM analysis primarily allows for examination of surface topography, but it is also able to give information on interactions between excipients and API's and it is also able to show solid-state changes that may be evident due to changes in habit.

SEM works on the basis that images are created by focusing high energy electrons onto the sample. Interaction of the electrons results in the formation of secondary and back scattered electrons which are responsible for the imaging capability of the SEM (Newman and Brittain, 1995).

Most SEM's consist of several main components; electron gun, column, lenses, sample chamber and a detector (Newman and Brittain, 1995). The electron gun is responsible for generating electrons which are generated by an electric current being passed through a tungsten filament. The resultant emitted electrons are drawn down towards the microscope column, due to a voltage difference present in the housing of the electron gun. The electrons are then focused and directed towards the sample by electromagnetic lenses. The electrons interact with the sample, producing secondary and backscattered electrons.

Secondary electrons occur when a weakly bound inner electron from within the nucleus becomes expelled. The electrons that originate from the surface of the sample reveal the topographical information. All possible interactions of the electron beam with the sample surface can be seen in Figure 2.12.

Secondary electrons are detected via a scintillator-photomultiplier device. Visible light is emitted from the reaction between the secondary electrons with the scintillator material (phosphorous or aluminium based coatings), which is then detected via the photomultiplier tube. The resultant signal is transmitted to the grid of a cathode ray tube, which is in sync with the scanning of the electron beam. An image is the produced as the beam travels over the sample. Differences in brightness at any point on the grid of the cathode ray tube are connected to the signal strength from that specific point on the sample. The resultant image is then observed digitally on screen.

In contrast, backscattered electrons are more energetic and bound more tightly. These electrons occur when incident electrons become scattered due to

interactions taking place with an atomic nucleus/nuclei where there is negligible loss of energy. The likelihood that backscattered electrons are produced increases with atomic number; the higher the atomic number, the larger the positive charge associated with the nucleus. This approach can therefore yield some chemical information of the sample. However, it is important to observe that most pharmaceutical compounds are comprised of elements with low atomic numbers (such as carbon and hydrogen), and hence would not be imaged by backscattered electrons. A schematic illustration of a scanning electron microscope can be seen in Figure 2.11.

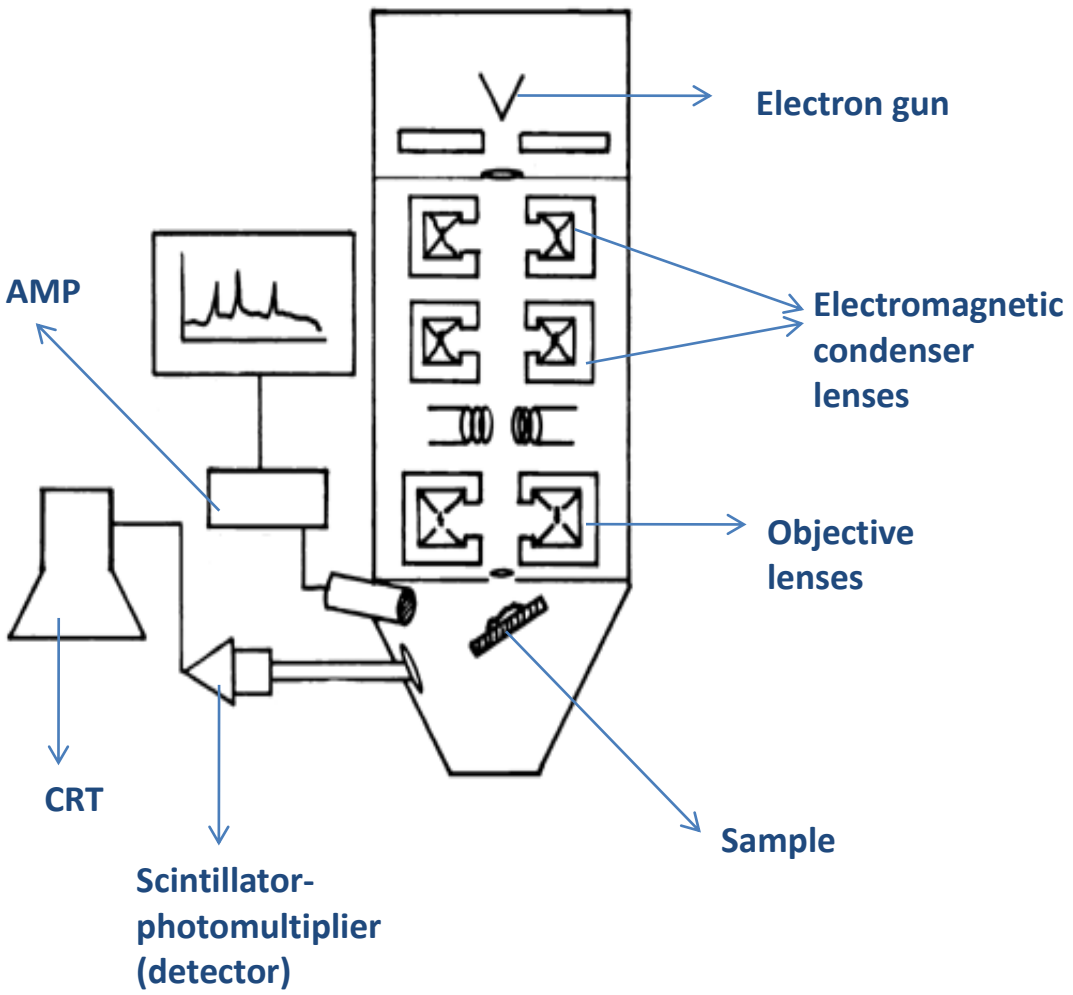

Figure 2.11. Schematic representation of a scanning electron microscope

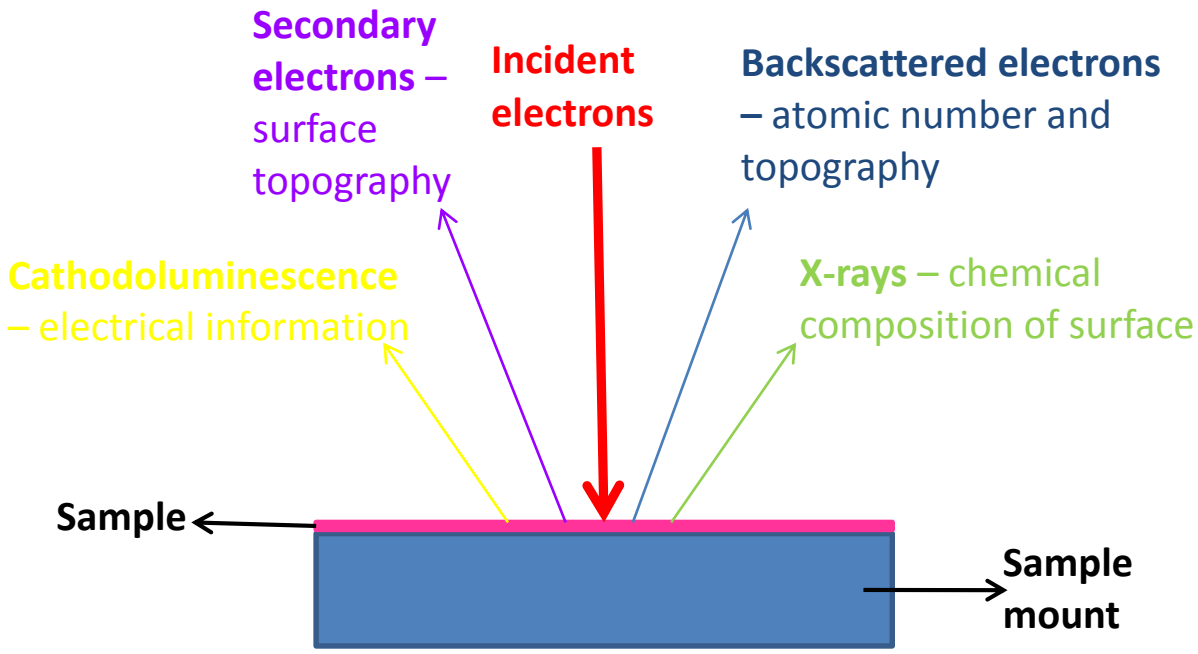

Figure 2.12. Diagram illustrating interactions that are possible between the electron beam and sample surface

SEM of all materials was carried out using a FEI Quanta 400 (Oxford, UK). Material for analysis was mounted onto an aluminium stub using an adhesive carbon tab and placed into the sample chamber of the instrument. Some organic compounds may require coating with a thin layer of metal (for example gold) sputter. This enables charge build up to be reduced which would cause intense brightness; hence the resultant image is visibly clear.

2.4.6 Moisture profiling

Moisture profiling is a unique and innovative analytical technique that is used for generating moisture profiles which record relative humidity in a closed chamber with time. This thesis explores the utility of the method to give novel information regarding the behaviour of moisture within a sample. This is of particular

importance to the pharmaceutical industry; the instrument can be seen in Figure 2.13.

Figure 2.13. Moisture profiler test system

The moisture profiler essentially gives information regarding the moisture within a material. Unlike other analytical techniques that quantify moisture, the profiler gives a measurement of the unbound or free water located in the material.

Water is associated with a material it can be classified into varying states, bound or unbound (Barbosa-CÃ¡novas, 2007). Bound water exhibits different characteristics to unbound water. Bound water has more structural bonding present, hence it is not able to act as a solvent; the vapour pressure it exerts is insignificant, meaning that the water molecules are unable to escape as water vapour and finally the bound water is more closely compacted therefore exhibits a greater density (Vaclavik, 2007). Unbound water is also termed free water, and possesses different

properties than bound water, and is free to move and interact and is more easily removed.

The moisture profiler has many underlying fundamental principles. The first basic assumption is that water vapour behaves and acts like a gas. Gases can be classified into either a real gas or an ideal gas. Both behave slightly different to each other and their corresponding properties are summarised in Table 2.2.

Table 2.2. Differences between real and ideal gases

Real gas	Ideal gas
Do not obey gas laws at standard temperature and pressure	Do obey gas laws at standard temperature and pressure
Obeys the Van der waals equation: $\left[\frac{P + an^2}{V^2}\right]$ (V-nb) = nRT	Obeys the ideal gas equation: PV=nRT
Has volume, mass and velocity	Has no volume, but has mass and velocity
Can have electronic interactions	Does not have the potential for electronic interactions
Are able to liquefy when cooled to their boiling point	Can be compressed or cooled infinitely, but does not liquefy.

Water vapour behaves as an ideal gas; this is of course within certain specification limits (standard temperature and pressure). As seen in Table 2.2 ideal gases abide and obey the gas laws. There are three significant gas laws that are relevant, these being:

I. Boyles Law

II. Charles Law

III. Daltons Law of partial pressures

The three laws can be combined in order to derive a measurement for the moisture profile of samples and the resultant ERH established. The relationship between the three gas laws and ERH is as follows:

Boyles Law (Equation 4) describes the relationship of the behaviour of an ideal gas under constant temperature. It states that the volume of a gas is inversely proportional to pressure at a constant temperature. For example, if the volume of gas doubled, then the pressure exerted with the system would decrease by half, this is represented graphically in Figure 2.14.

Equation 4

$$P \times V = \text{Constant}$$

Where V= volume, P = pressure

Charles's Law (Equation 5) describes the behaviour and relationship of an ideal gas at a constant pressure. It states that for a fixed amount of gas at a constant pressure, the volume of gas will increase as the temperature increases. For example, if the temperature of gas was to double, then the volume occupied by the gas would also double, this is represented graphically in Figure 2.14.

Equation 5

$$V/T = \text{Constant}$$

Where: V = volume, T = temperature

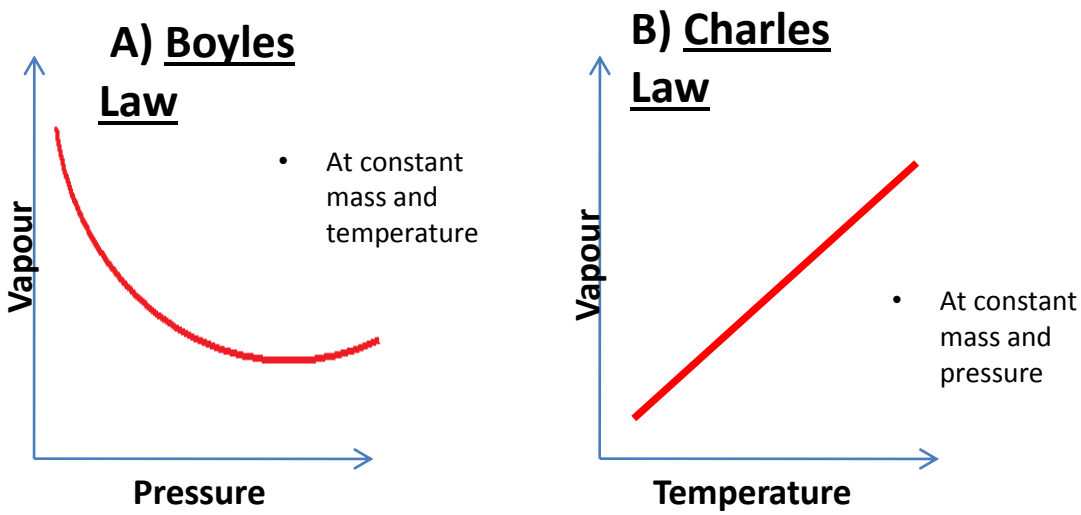

Figure 2.14 Diagram graphically representing Boyles and Charles Law exhibited by ideal gases.

A) Represents Boyles Law, showing the relationship between pressure and volume when mass and temperature are constant. B) Represents Charles Law, showing the relationship between temperature and volume when mass and pressure remain constant.

The final law obeyed by an ideal gas is Daltons Law of partial pressures (Equation 6). This states that the total pressure exerted within a mixed gaseous system is equal to the sum of all the partial pressures of each individual component.

Equation 6

$$P_{total} = P_1 + P_2 + P_3 + P_n$$

Where P = pressure, n = integer

In order to acquire a theoretical basis for measurement of ERH, RH obviously has to be taking into consideration; RH being the amount of water vapour present within a gaseous mixture of air and water vapour. RH is normally expressed as a percentage and is calculated by Equation 7.

Equation 7

$$\phi = \frac{P}{P_s} \times 100$$

Where ϕ = relative humidity, P = vapour pressure, P_s = vapour pressure at saturation

This shows that RH of an air/water mixture is defined as the ratio of partial pressures exerted by water vapour (present within the mixture) to the saturated vapour pressure at the specific temperature.

Then by taking into consideration Charles's Law (Equation 5), a substitution can be made to Equation 7, due to the fact that the moisture profiling system provides a fixed volume during data accumulation. Therefore Equation 8 can be derived in which RH is dependent upon temperature; this is the basis of the measurements recorded by the profiler.

Equation 8

$$\phi = \text{Constant} \times T$$

Where ϕ = % RH and T is temperature

The moisture profiling system essentially consists of 5 major components;

1) High density polyethylene (HDPE) container

2) Combination temperature-RH probe

3) Data logger

4) Sample holder (depending upon material being analysed)

5) Computer or other device for viewing the data.

The schematic representation can be seen in Figure 2.15.

In order for a moisture profile to be generated, the material to be analysed is introduced into the instrument, this can be done in two ways and is entirely dependent upon the sample:

I. The sample is a powder formulation for example. These require placing within a sample holder. The sample holder containing the powder is then fitted into the HDPE container lid and then lid is then screwed on to the HDPE container.

II. Where the sample does not require a sample holder, such as a tablet. The sample is placed directly into the HDPE container and the lid screwed on.

Enclosed within the HDPE container is a combined temperature and relative humidity probe, which when switched on is able to monitor and record both temperature and relative humidity within the closed environment of the HDPE container. These are both logged until the time when the user determines that an ERH point has been reached. This is when there is no further change in the RH of the sample and it remains constant. The moisture profiler data logger is powered independently via a 9 volt battery; this is able to directly store the humidity and temperature data. The acquired data can then be transferred to a computer. The software allows for graphic representation or can viewed in an excel format to allow data to be combined.

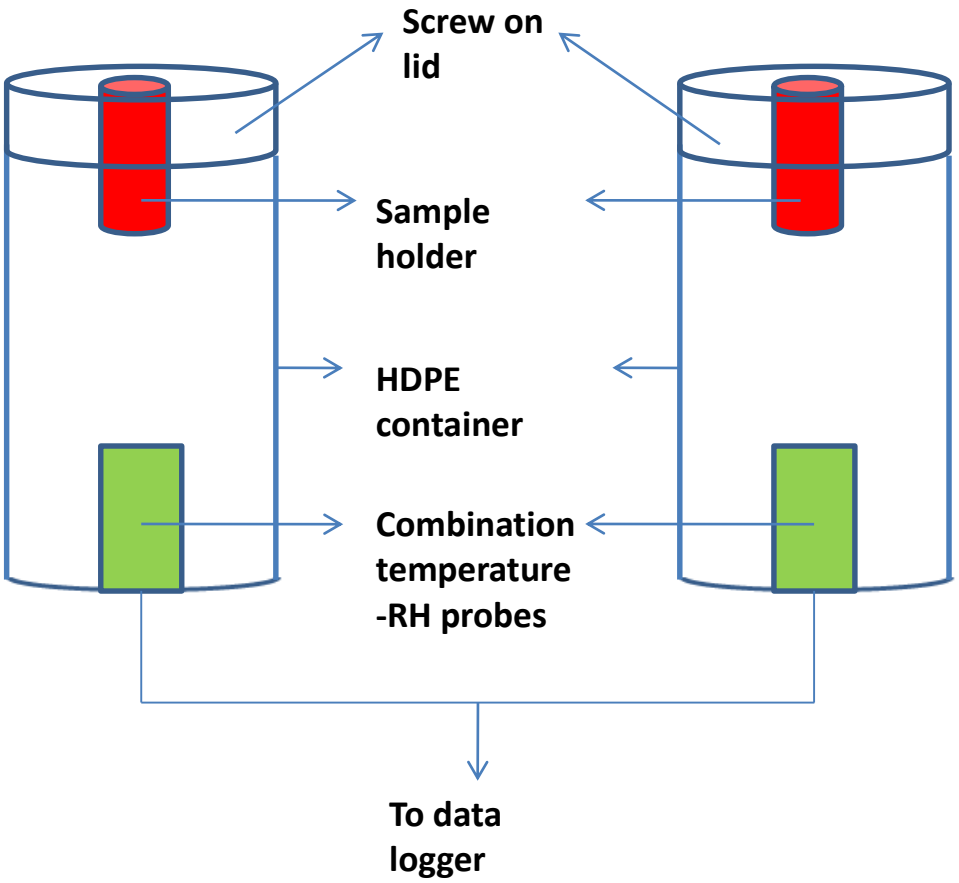

Figure 2.15. Schematic representation of the moisture profiler instrumentation (adapted from (Moir, 2007)

The ERH point of a sample was tested using the portable moisture profiler test system. Material to be tested was placed within the unit, typically; 250 mg of powdered sample was placed within a sample holder which then fitted within the lid. If the material was a tablet or capsule, one was placed whole within the HDPE container to be were situated in close proximity to the combination temperature-RH probes. The test was then initiated and the moisture profile generated according to the material behaviour. The temperature was also recorded. ERH of the material was taken as the point when there was no further change in %RH. The run was terminated and considered to be complete when the change in %RH was less than 0.1% for 10 consecutive readings, a reading is taken every 5 minutes.

Some studies were conducted where the whole profiler of the profiler system was placed in a stability oven throughout the analysis. This was done in order to maintain temperature and prevent fluctuations of RH due to temperature variation. The moisture profiler records both temperature and %RH data simultaneously and these are presented in a moisture profile. A typical moisture profile for a sample can be seen in Figure 2.16, which also serves to demonstrate the inverse temperature relationship whereby; warm air is able to hold more water than cold air, so at higher temperatures the same material will exhibit a lower ERH. Thereby reinforcing that, the RH measured by the profiler is strictly temperature dependant.

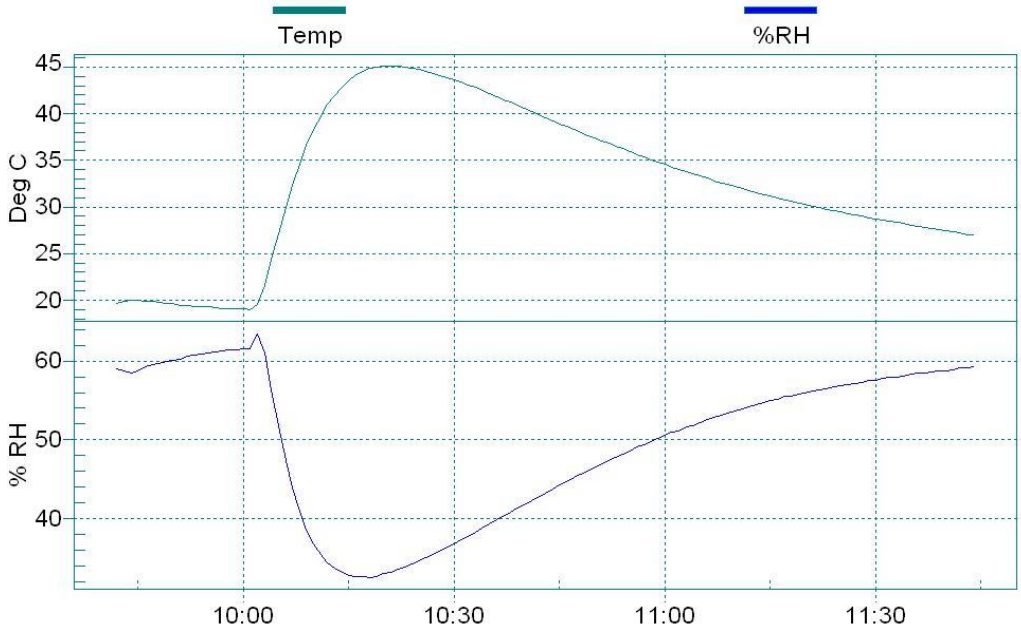

Figure 2.16. Typical moisture profile generated by the moisture profile system

The material is able to behave in two ways:

1) Take moisture up from the closed environment, observed by a decrease in the internal % RH of the container.

2) Give moisture out into the environment, seen by an increase in the internal %RH of the container. These typical behaviour profiles can be seen in Figure 2.17.

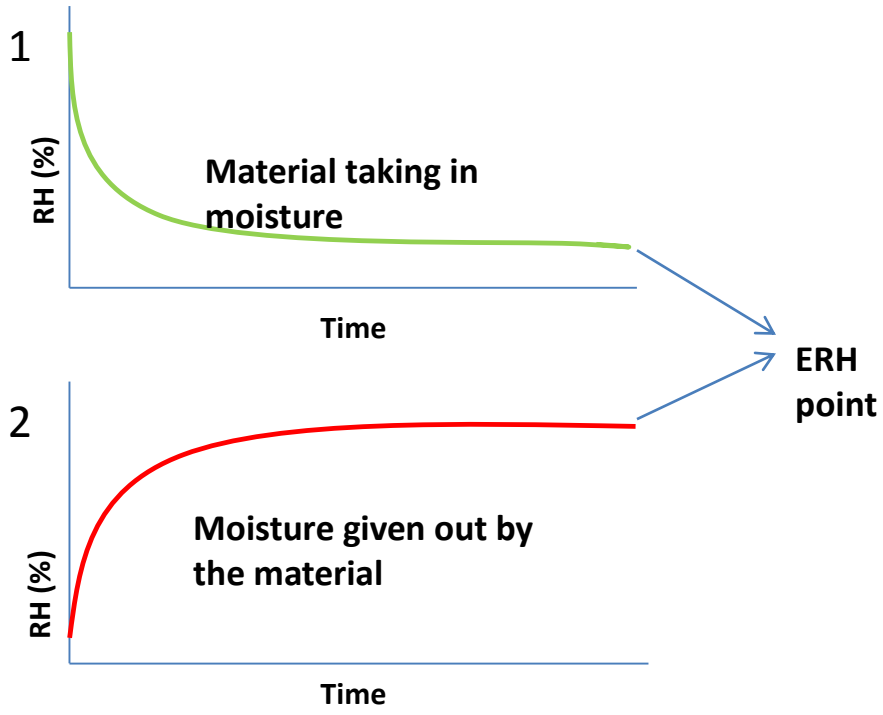

Figure 2.17 Typical types of moisture profile behaviour

2.5 Compaction studies

2.5.1 Tablet compaction

Tablet compaction was carried out using a compaction studies press (Caleva Process Solutions Ltd, UK). A predetermined weight (450 mg) was hand filled into a circular die and compressed at a speed 10mm/s with a 10 mm flat faced punch to produce tablets of approximately 2.7 mm in thickness. Compaction to force

experiments were carried out using the same sample size and die at compaction forces of 25, 30, 35 and 40 kN, with the compaction speed being kept constant.

The thickness and diameter of the tablets were measured using an ID-C Digimatic indicator (Mitututoyo Corporation), this was measured immediately after ejection and/or storage. Tablet weight was also recorded at the same time.

The crushing strength has been described by Brook and Marshall as "the compressional force that when applied diametrically to a tablet, just fractures it" (Brook and Marshall, 1968). Crushing strength of tablets was obtained using a Schleuniger Hardness tester (Copley Instruments, UK). The tablets requiring testing were placed flat down on the bed of the hardness tester and the crushing strength measured of the circular tablets.

Tablet strength was determined by crushing strength and tensile strength measurements. The tensile strength was calculated using Equation 9

Equation 9

$$\text{Tensile strength} = 2F/\pi DT$$

Where F is the crushing strength (N), D and T are the diameter and thickness (mm) of the tablet respectively.

3. VALIDATION OF A METHOD TO CONTINUOUSLY MONITOR WATER ACTIVITY – MOISTURE PROFILING

3.1 Introduction

Qualification of an analytical method is of huge importance with respect to ensuring quality, safety and efficacy of pharmaceuticals; consequently before an analytical method can be employed routinely it must first be validated to ensure that it is appropriate for its intended purpose (Rozet et al., 2007). The importance of method validation emerged and was emphasised in the late 1940's when the issue of how mathematics and statistics are a crucial prerequisite to development of new analytical methods was raised by the American Chemical Society and Merck & Co (Araujo, 2009, Clarke, 1947).

Since then, method validation has developed and evolved rapidly, into a commonly recognised procedure. With the ultimate purpose of the validation of an analytical method being to ensure that future measurements in routine analysis will be close enough to the unknown true value for the content of the analyte within the sample (González and Herrador, 2007). Presently there are several regulatory bodies that offer guidelines with respect to method validation, such as International Organisation of Standardisation (ISO), International of Union of Pure and Applied Chemistry (IUPAC), Food and Drug Administration (FDA) and the International Conference on Harmonisation (ICH). The requirements and procedures of validation of analytical methods were eventually brought together and combined. These can be seen in guidelines such as the Q2A and Q2B produced by the ICH (Gad, 2007).

According to the validation guidelines specified in ICH Q2B there are several validation characteristics that must be adhered to, these are;

- Specificity
- Linearity
- Quantitation limit
- Detection limit
- Range
- Accuracy
- Precision
- Robustness

3.2 Methods

3.2.1 Specificity

Specificity refers to the ability of a method to differentiate between the analytes of interest (Ahuja and Dong, 2005). Therefore, with respect to moisture profiling, the issue of specificity relates to whether it can successfully detect different levels of free moisture contained within samples.

Specificity can be assessed using a straight calibration curve. This therefore means carrying out a conformance check with standards of known RH and consequently the ERH. Standard salt solutions were used to generate ERH's of 10, 50 and 75%. Water was used to generate an ERH of 100 % and a desiccant (silica) was used to generate 0% ERH at ambient conditions. The results were then plotted and expressed graphically.

3.2.2 Linearity

Linearity refers to the ability of the analytical method to provide a linear response across the intended method range (American Chemical and American Chemical Society. Committee on Analytical, 2006). Linearity should be determined over a range, with a minimum of five concentrations being used. Therefore, for moisture profiling linearity can be assessed and established using samples of known RH. Desiccant was used to generate a RH value of 0%, salt solutions were used to generate RH's of 10, 50 and 75% RH and pure water used to generate 100 %RH.

3.2.3 Quantification and detection limit

The limit of quantification (LOQ) and limit of detection (LOD) are related in that LOQ=LOD because the moisture profiling system is not an assay method LOQ=LOD. The ICH describes the quantification limit as the lowest amount of analyte within a sample that is able to be quantitatively determined with appropriate precision and accuracy and the detection limit as the lowest amount of analyte that is able to be detected. With respect to moisture profiling, specific reference standards of sufficiently low RH were not available and so the tests were unable to be performed.

3.2.4 Range

The range of an analytical method is the detection of the upper and lower levels of an analyte that has been demonstrated to be determined with a suitable level of precision, accuracy and linearity. The range is therefore determined by analysing samples of known ERH and assessing how high and how low the instrument is able

to detect and measure ERH. However, as with LOD and LOQ specific reference standards of appropriate RH's were unavailable, so this was unable to be performed.

3.2.5 Accuracy

Accuracy of an analytical measurement is the closeness of a result to that of a given standard or accepted reference value (Huynh-Ba, 2008). In this work the accuracy of the moisture profiling system was determined using comparison of calibration standards of known %RH.

3.2.6 Precision

ICH describes precision of an analytical measurement as the nearness in agreement of a series of measurements obtained by multiple analyses of sub-samples the same homogenous sample under the same conditions. In this work the precision of the moisture profiler was determined by analysing subsamples of the same sample a number of times using the same conditions.

Precision measurements are split into three sub-measurements;

1. Repeatability; precision measurements taken over a short interval of time. The repeatability of the moisture profiler was analysed by performing the same test on the same day, the number of tests that can be performed using this technique are limited however due to the length of time required for each test. Repeatability was assessed using lactose monohydrate; five runs were performed on the same day.
2. Intermediate precision; precision measurements taking into account inter-laboratory variations, i.e. different days, different analyst, different

equipment. The intermediate precision of the moisture profiler was analysed by performing the same test once a day over a number of days. As there was only one operator and one set of equipment intermediate precision was limited to day to day variability. Intermediate precision was assessed using lactose monohydrate; five runs were performed each day for five consecutive days.

3. Reproducibility; Reproducibility expresses the precision between laboratories. This testing was not possible in this work due to space restrictions and will therefore not be reported.

3.2.7 Robustness

The robustness of an analytical procedure is a measure of its capacity to remain unaffected by small, but deliberate, variations in method parameters and provides an indication of its reliability during normal usage. The robustness of the moisture profiler was established using the following tests;

1. Change in sample size – Change in sample size was assessed of powders being placed into the sample holder and its influence was examined using lactose monohydrate.
2. Operating temperature – Different temperature directly effects the ERH value obtained, but the same material was ran at 25°C and then at 40°C to ensure temperature variability did not affect the repeatability of results obtained
3. Variability of starting RH – The instrument has no inbuilt device to ensure the starting RH of the sample chamber is constant; therefore it's able to

fluctuate. Precondition parameters were employed to alter the starting RH; desiccant was used to produce a low starting RH, an elevated initial RH was produced raising the surrounding sample chamber environment RH. The same material was then placed into the different sample chamber environments and allowed to reach equilibrium, to see if the same ERH value was reached.

3.3 Results;

3.3.1 Specificity

Specificity can be evaluated graphically by plotting the value of the RH of standards of known % RH value against the ERH value obtained for that standard. Such a plot is presented in Figure 3.1, and it demonstrates that the moisture profiler is able to differentiate between different levels of moisture and so consequently is specific.

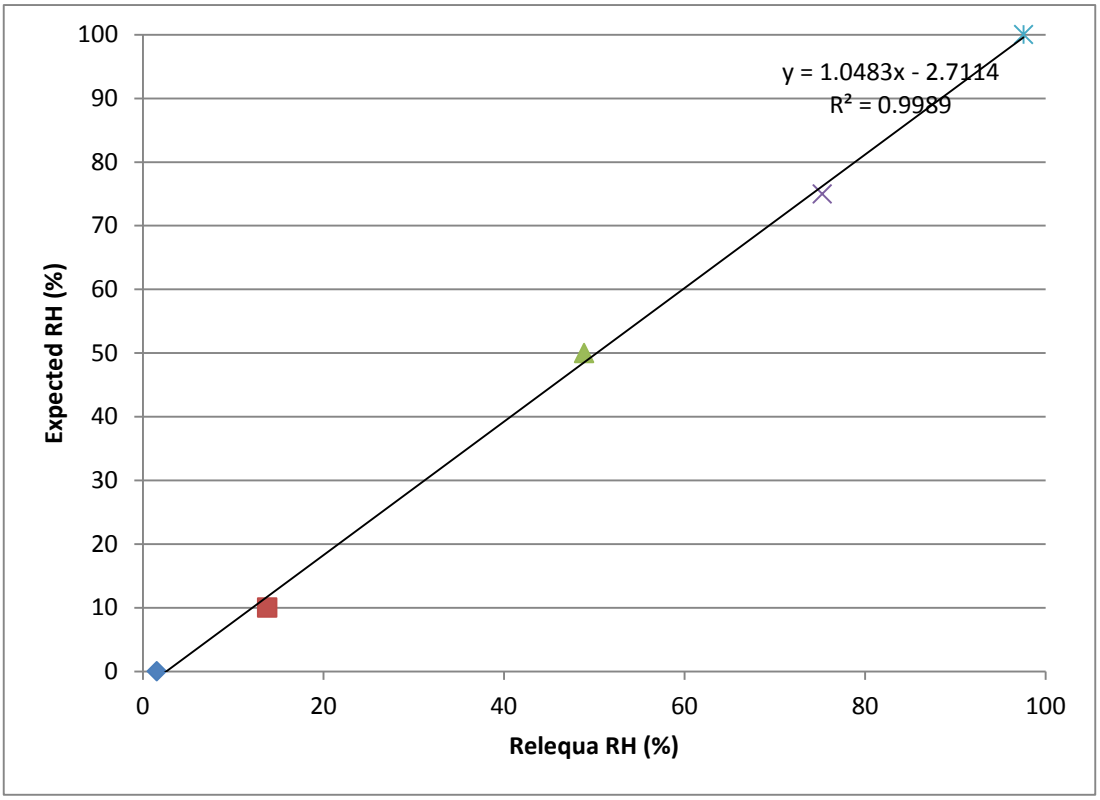

Figure 3.1. Specificity expressed graphically of the moisture profiler

3.3.2 Linearity

Linearity is frequently evaluated graphically in the form of a calibration curve (it can also be expressed mathematically), linearity with respect to the moisture profiler is shown in Figure 3.2 and is portrayed graphically. The figure demonstrates the range of the analytical procedure and a minimum of five concentrations have been employed. During method validation the linearity of the calibration curve should be assessed and the working range of the calibration curve determined. This is usually determined by examining the correlation coefficient, and resultant calibration curves where the correlation co-efficient it greater than 0.995 is usually considered to be linear, which is the case here.

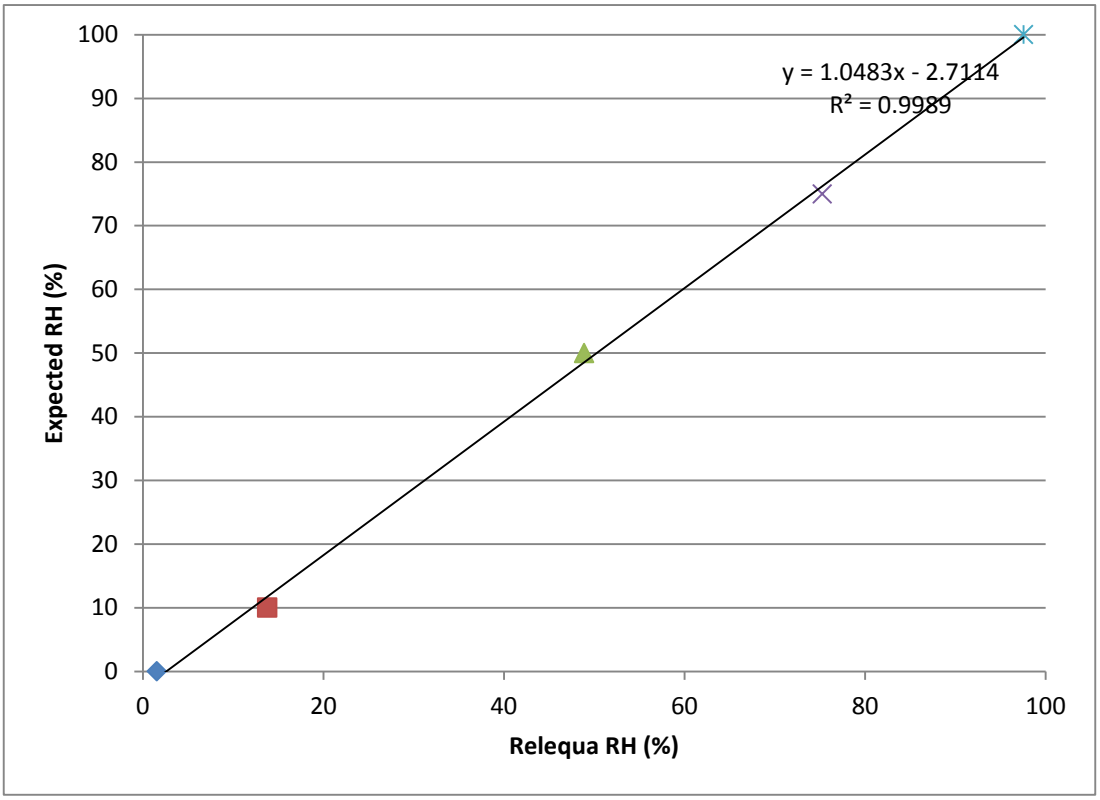

Figure 3.2. Graph establishing linearity using calibration standards

3.3.3 Quantification and detection limit

The LOQ and LOD were unable to be evaluated in this instance.

3.3.4 Range

The range has to be determined with a suitable level of precision, accuracy and linearity, and is expressed usually in the same units as the test results, so with respect to moisture profiling this would be expressed in terms of percentage. The range is determined upon the standards and is shown in Table 3.1 and demonstrates the range of the moisture profiler is 1% to 100%.

Table 3.1. Range exhibited by the moisture profiler

Standard	Moisture profiler result
Desiccant (Silica)	1.567
10 %	13.230
50 %	49.481
75 %	75.672
100%	97.656

3.3.5 Accuracy

Accuracy is the closeness of the analytical measurement obtained compared to that of a known standard. Table 3.2 shows the closeness of the values obtained compared to that of the standards used. From this it is evident that at intermediate values, these being 50 % RH and 75 % RH, at which the instrument appears to be more accurate than the values at the extremes of the limits, these being 1-10% RH and 100% RH.

Table 3.2. Comparison of moisture profile results for RH to known RH standards

Standard	Moisture profiler result	Closeness
Desiccant (0 %)	1.6	+ 1.6
10 %	13.2	+ 3.2
50 %	49.5	- 0.5
75 %	75.7	+ 0.7
100%	97.7	- 2.4

3.3.6 Precision

Precision is the degree of agreement among individual test results. Precision with respect to moisture profiling is evaluated by focusing upon repeatability and assessment of the intermediate precision. Intermediate precision, formerly ruggedness, is able to be evaluated because measurements were taken on different days, therefore intra-laboratory variations could be assessed. Precision can be expressed as the standard deviation or relative standard deviation, the standard deviation assessing repeatability is show in Table 3.3. Taking into account all measurements, the standard deviation is ± 0.9 % with regards to the intermediate precision measurements.

Table 3.3. Repeatability and intermediate precision measurements and associated standard deviation of lactose monohydrate samples run at 25°C

	Day 1	Day 2	Day 3	Day 4	Day 5
Run 1 (% RH)	28.5	28.4	29.2	28.7	27.6
Run 2 (% RH)	29.3	28.9	30.7	28.7	26.6
Run 3 (% RH)	29.0	29.4	29.1	29.1	26.6
Run 4 (% RH)	29.1	28.9	29.4	29.0	26.6
Run 5 (% RH)	28.9	29.6	29.2	28.7	28.1
Standard deviation (% RH)	29.0 ± 0.2	29.0 ± 0.4	29.5 ± 0.7	28.4 ± 0.2	27.1 ± 0.7

3.3.7 Robustness

Robustness is basically a measure of the reliability of a method. In order to evaluate the robustness of the moisture profiler, various method parameters were altered in order to determine the effect, if any, upon the results obtained. Various changes were employed, the first being change in sample size, this was assessed using lactose monohydrate and results are shown in Table 3.4.

Table 3.4.Effect of sample size of lactose monohydrate on the final ERH values

Sample size (mg)	Final ERH value (% RH)
50	46.1
100	46.1
150	47.7
200	47.9

The data in Table 3.4 demonstrate that sample size had minimal effects upon the final ERH value attained. It was therefore decided that a constant sample size of 200 mg would be used throughout for powdered materials that would require use of the sample holder.

The second change employed was to see if operating temperature had an effect upon the ERH. Table 3.5 shows that ERH obtained for lactose monohydrate when run at 40°C. It is clear that temperature has an effect upon the ERH value, as warm air is able to hold more water than colder air, so the increased operating temperature will result in lowers ERH value. However, this does show that the results are reproducible and repeatable regardless of operating temperature.

Table 3.5. Effect of operating temperature upon the reproducibility of final ERH values of lactose monohydrate samples

	Final ERH value at 40°C (% RH)
Run 1	10.6
Run 2	10.1
Run 3	10.2
Run 4	10.9
Run 5	10.9
Standard deviation (% RH)	0.4

The effect of the initial RH of the sample chamber on the resultant final RH was investigated. It was of interest to determine whether employing a RH above or below the resultant ERH affected the final ERH.

Figure 3.3 -Figure 3.6 show the effects of different starting RH for materials; acesulfame potassium, maize starch, povidone and sodium citrate. For the above materials the profiles suggest that the starting RH has no notable effect upon the final ERH value attained, but is able to influence the behaviour (shape of the moisture profile) so this therefore must be considered if there is any change in the behaviour the sample exhibits. The data presented in Figure 3.7 and Figure 3.8 for magnesium stearate and sodium citrate respectively shows that if a high RH or a low RH is used as the initial RH then the final ERH is different, the final ERH obtained between the two starting points is circa 10% or more for each sample. Why do these two samples behave in a different manner from the previous four? Therefore, is it more appropriate to approach ERH from a higher or lower RH than

the resultant ERH? On balance, it would seem that approaching ERH from a higher initial RH is more appropriate and has more merit. It follows that for a sample to truly equilibrate there should be an excess of water vapour available. It is possible for some samples as demonstrated above, that by approaching from below ERH, insufficient water vapour is available to the sample in order to provide a true ERH and what is actually measured is an apparent ERH.

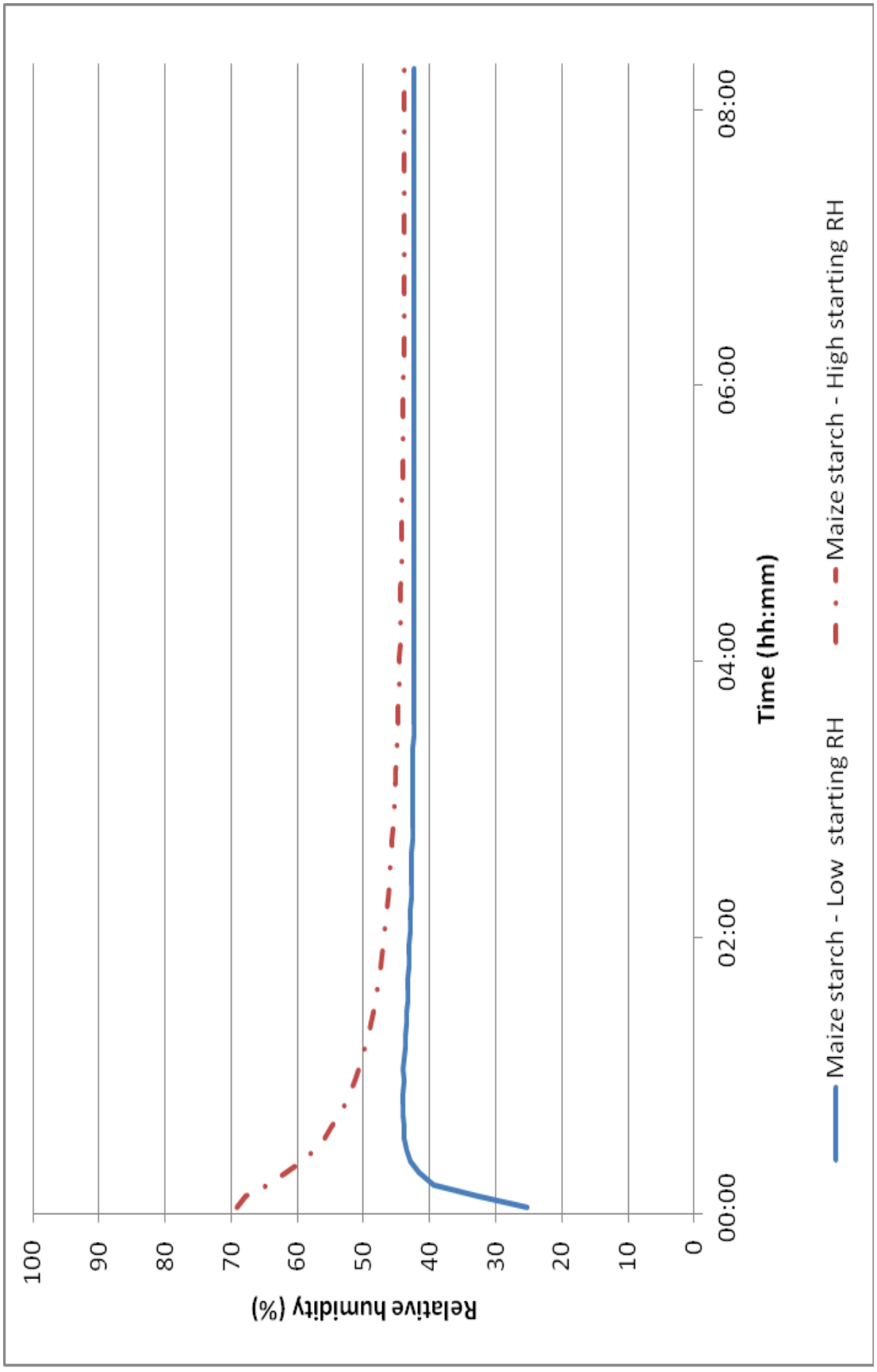

Figure 3.3. Moisture profile for maize starch with low and high starting RH

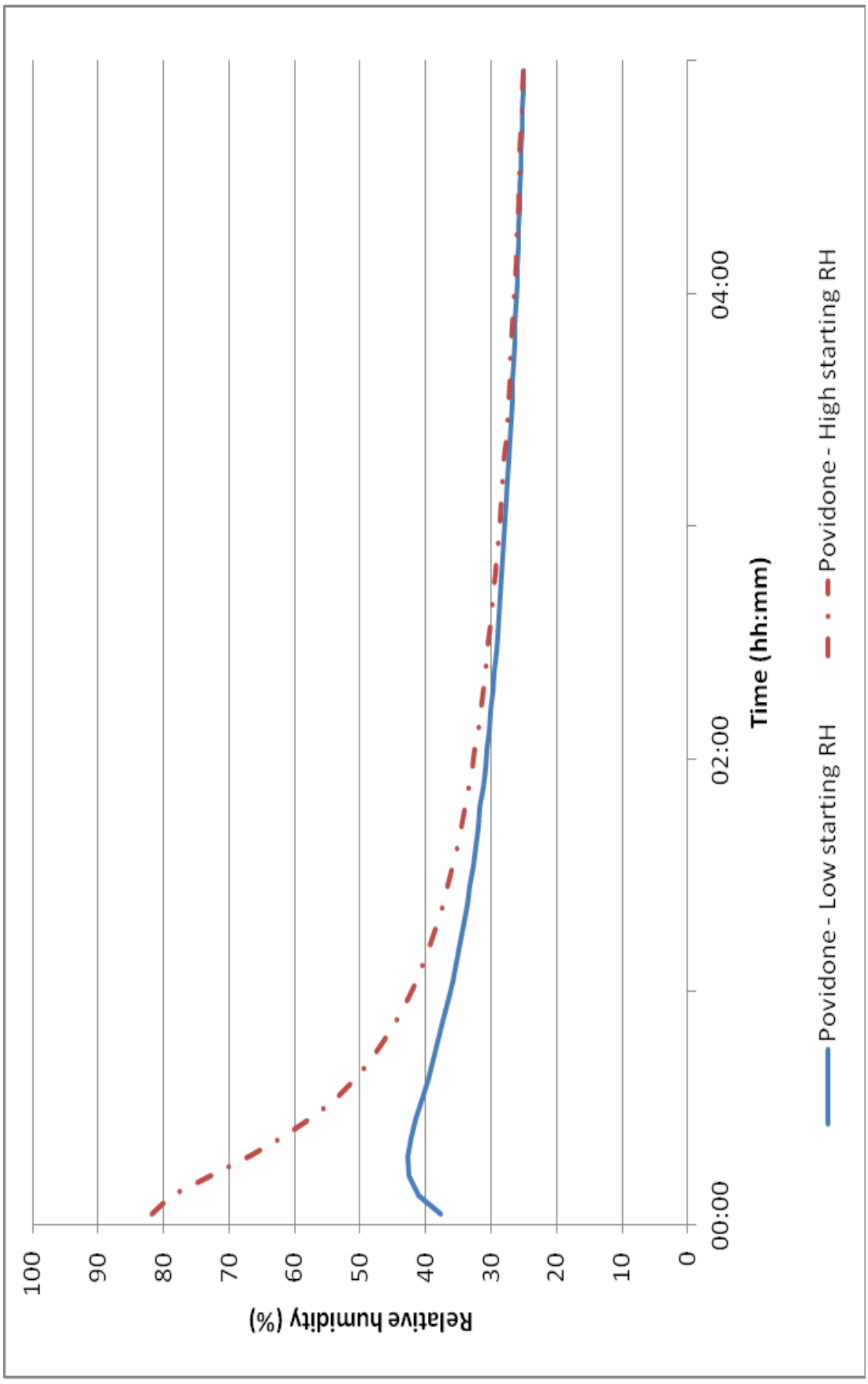

Figure 3.4. Moisture profile for Povidone with low and high starting RH

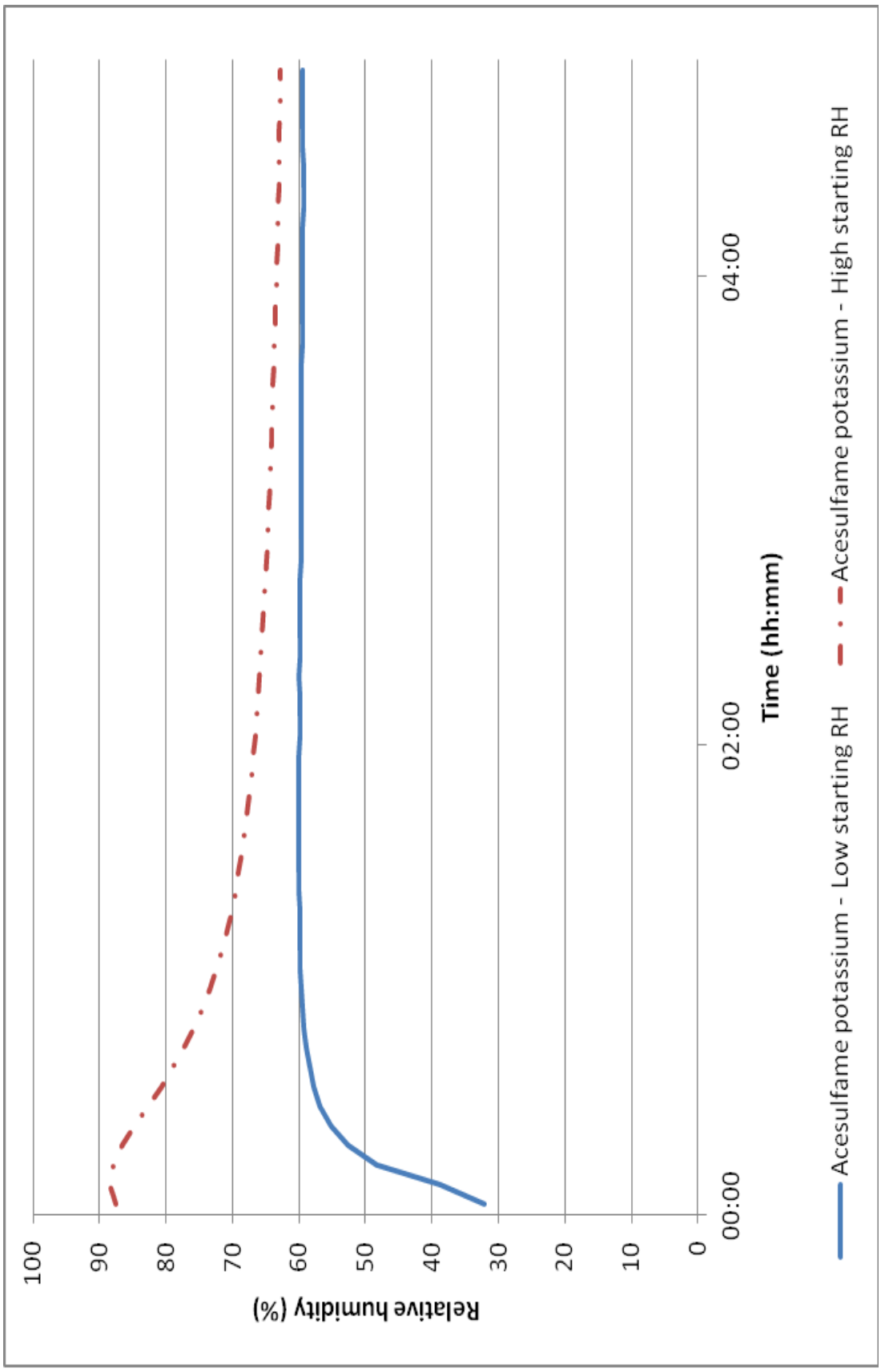

Figure 3.5. Moisture profile for acesulfame potassium with low and high starting RH

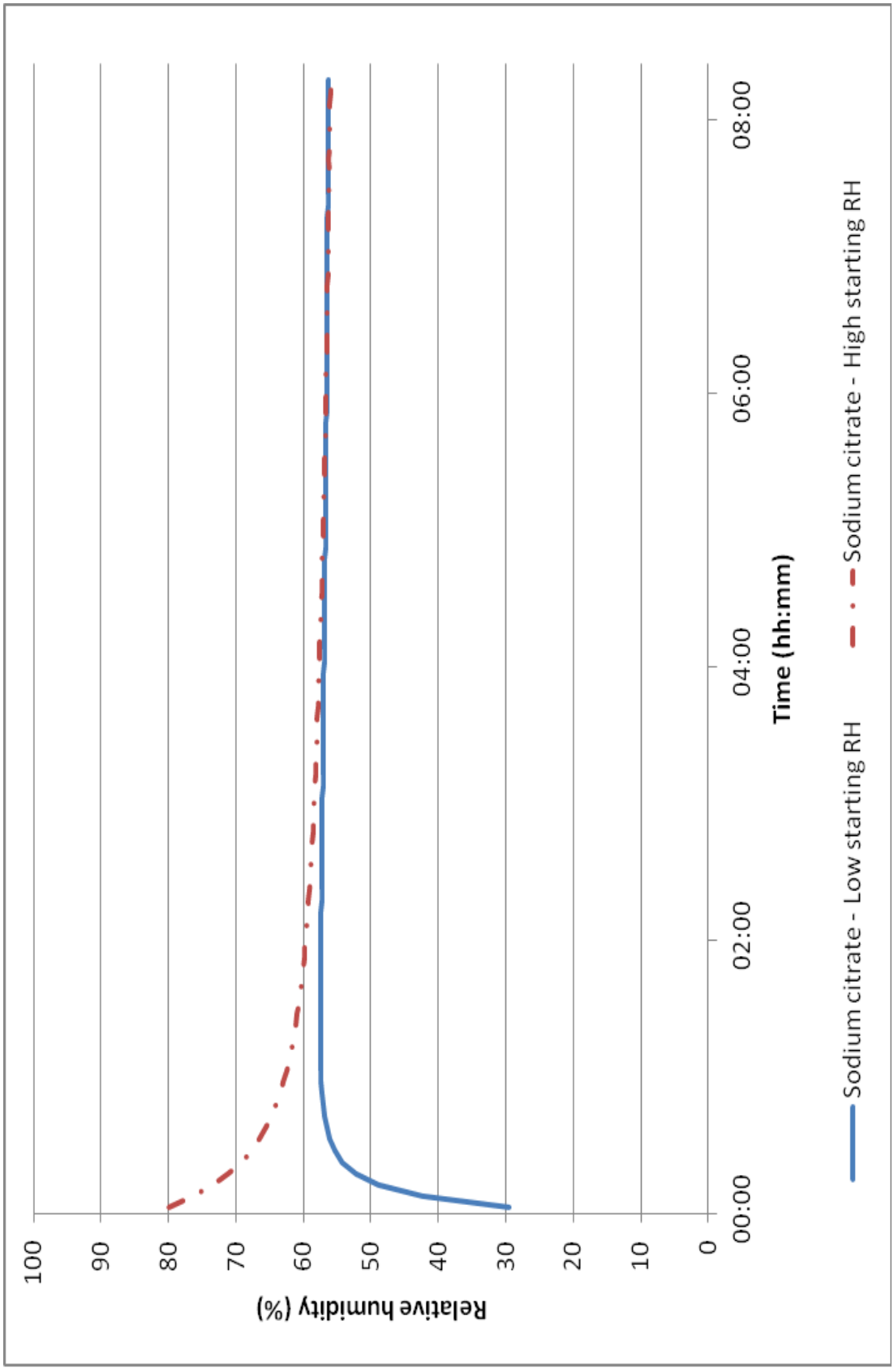

Figure 3.6. Moisture profile for sodium citrate with low and high starting RH

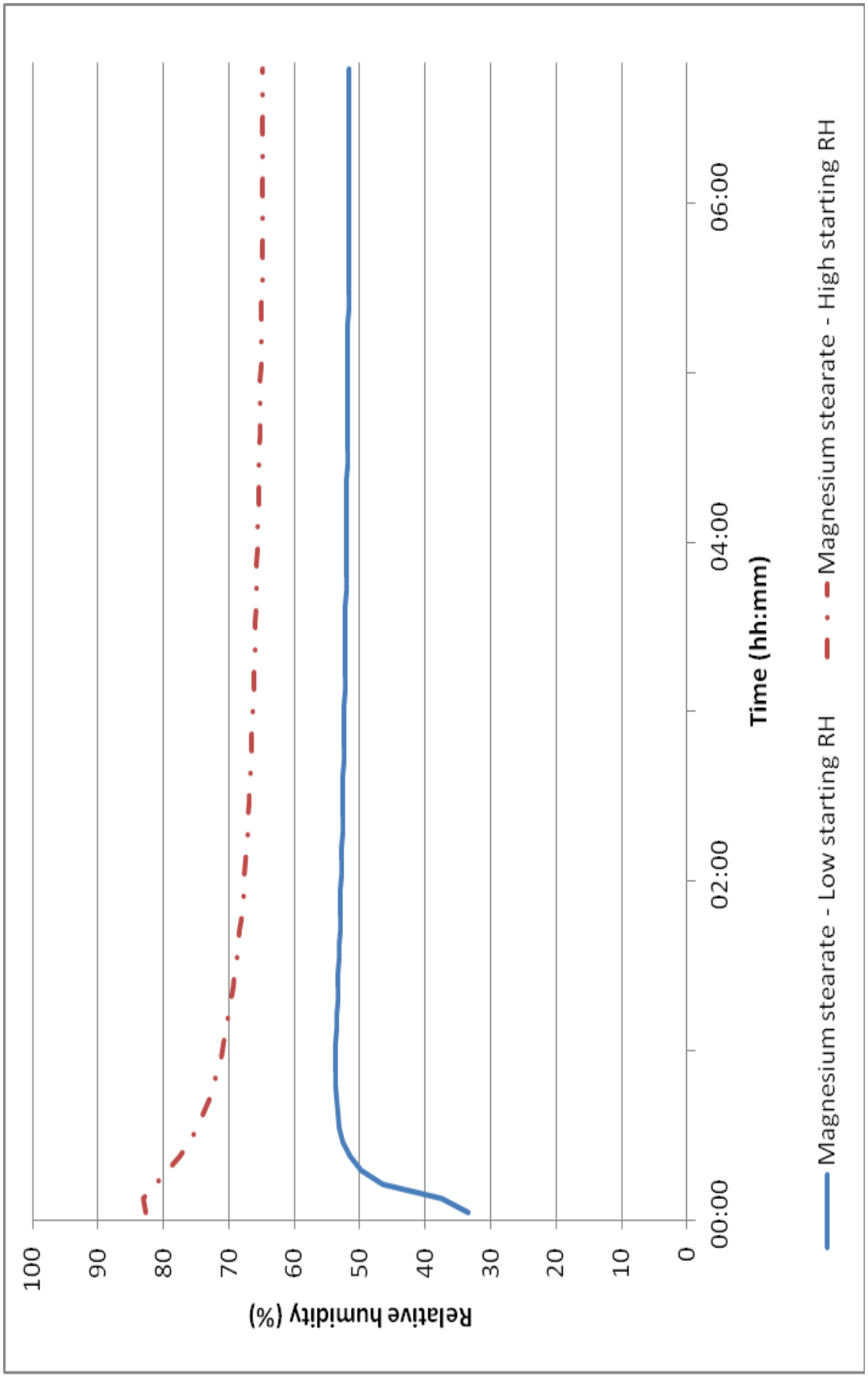

Figure 3.7. Moisture profile for magnesium stearate with low and high starting RH

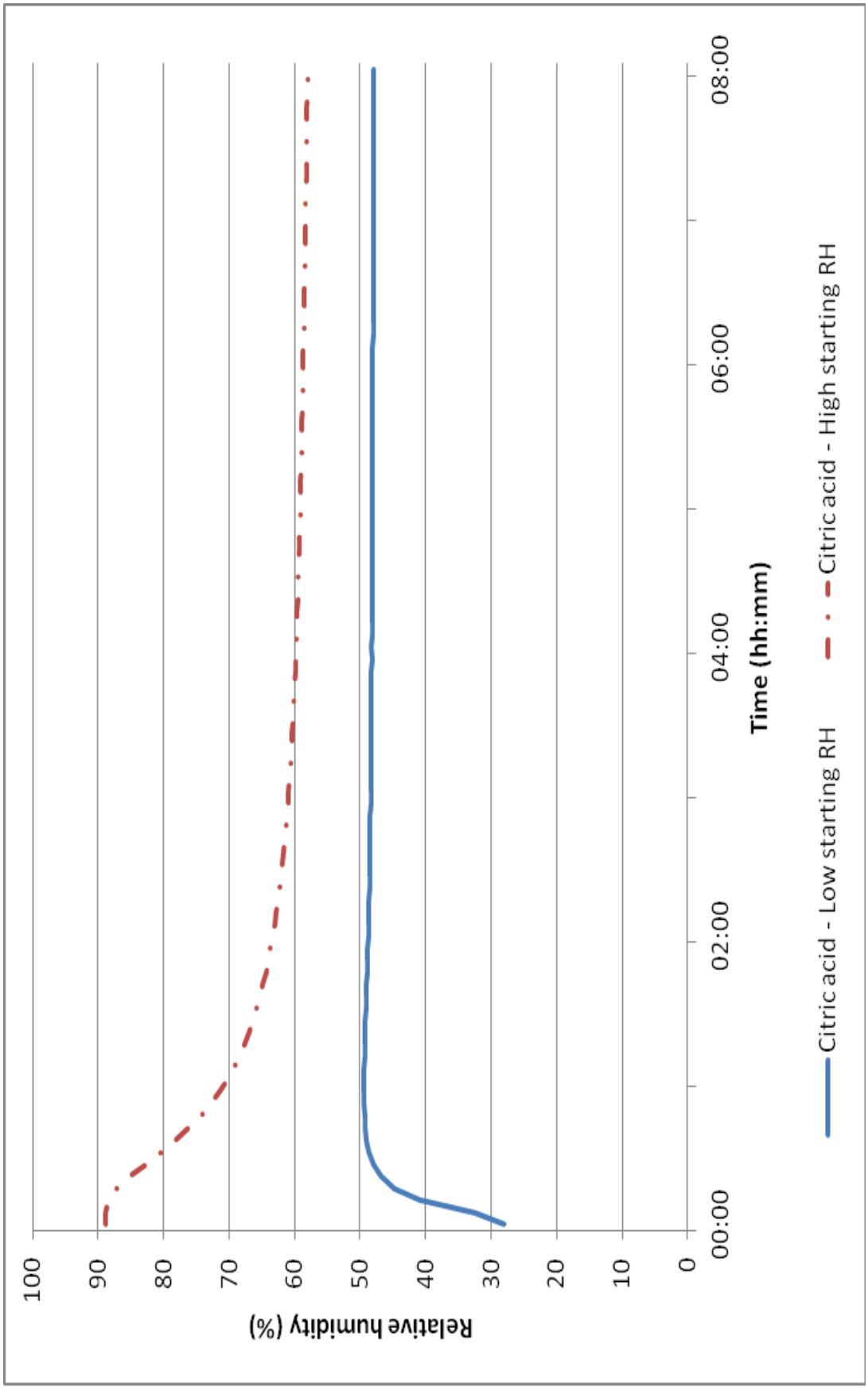

Figure 3.8. Moisture profile for citric acid with low and high starting RH

3.4 Discussion

Validation of the moisture profiler was carried out using several different methods. Measurement of ERH was carried out on a series of calibrated standards and lactose, which was to be used in future experimental work. The moisture profiler method proved to be linear within the range of 0% RH and 100% RH, and the highest accuracy was obtained at the median %RH. The LOD was not evaluated due to the lack of suitable standards, however, for the context of this work, the instrument did not need to be evaluated for LOD as it was to be used to establish ERH% of materials only. The intermediate precision of the instrument was carried out by analysing five samples each day for five days. This method is commonly used in industry during validation of instrumentation and that is why it was employed here. The moisture profiler gave good reproducibility both inter and intra-day indicating that the techniques is both sensitive and repeatable. The final set of tests carried out were robustness which involved evaluation the effects of temperature and starting %RH. The moisture profiler results obtained indicated that sample size effects were minimal; however, a sample size of 200mg was determined to be optimal for ERH measurements. The starting ERH had no effect on the final ERH for four samples, indicating that such samples could be loaded into the instrument without the need for a controlled %RH environment. However it was noted that the resultant ERH for two samples was dependent upon the initial ERH. It was consequently determined that approaching ERH from a high starting RH was the most appropriate way of obtaining an ERH.

The work in this chapter has validated the moisture profiler as a suitable method to determine the ERH of pharmaceutically materials. The ERH behaviour of these materials (after various processes) will now be evaluated in depth in future chapters and compared to conventional physicochemical methods to determine whether any novel information can be gained by using the moisture profiler analytical method.

4. PRELIMINARY EXPLORATIONS OF THE PHARMACEUTICAL APPLICATIONS OF MOISTURE PROFILING

4.1 Objective

The potential areas for exploration of this novel method are wide-ranging. Therefore this chapter is primarily focused upon the initial areas of investigation. Thereby the principal objective was to initially scope out and identify possible areas to focus further research upon. This was done by assessing the potential of the instrument by extending the basic areas touched upon during the previous validation process.

Firstly a range of excipients will be tested within the moisture profiler in order to determine whether different materials will give rise to different moisture profiles and ERH values and to see if any materials would be of specific interest during further research opportunities. The materials used were: acesulfame potassium, buprenorphine hydrochloride, citric acid, lactose monohydrate, maize/starch, magnesium stearate, naloxone hydrochloride, povidone and sodium citrate.

Secondly the effect of sample size on the moisture profile obtained will be further probed, extending the work previously undertaken in Chapter 3 to include another material, povidone. This material was chosen based upon the difference in ERH values that it had displayed after the excipients were screened above. The material yielded an ERH noticeably lower than the other excipients. The effect of Lactose monohydrate sample weight variation will also be examined again but at a later stage of this chapter in conjunction with temperature variation.

Another subject of preliminary investigation was the determination of ERH of blends of material. The research question asked here is whether the moisture

profiler is able to detect and indicate differences in mixtures of excipients based upon the resultant moisture profiles and ERH values. Firstly povidone and sodium citrate mixtures were analysed. Secondly, exploration was undertaken of the use of the moisture profiler to distinguish differences between blends of different physical forms of the same material namely crystalline and amorphous lactose.

Finally the temperature effects with respect to the moisture profiler will be examined. This was explored by placing lactose monohydrate in the instrument for an extended period of time, whilst not controlling the surrounding temperature environment, thereby monitoring the variances of ERH with temperature fluctuations that occur naturally. Finally, as mentioned earlier, the effect of sample weight differences for lactose monohydrate undertaken elevated temperature was also investigated.

4.2 Exploration of moisture profiles of excipients

Each material was individually subjected to moisture profiling analysis, when ERH was attained analysis was halted; therefore analysis time is dependent upon each individual material. Figure 4.1-Figure 4.9 demonstrates typical moisture profiles obtained for each material; Table 4.1 shows the final ERH values attained for each material.

All materials except buprenorphine hydrochloride and naloxone hydrochloride demonstrate an initial decrease in %RH before equilibrium is attained, thereby indicating that the materials take in moisture from the sample chamber environment. This therefore suggests that enough moisture was present in the

surrounding sample environment for the materials to give a representative ERH value.

Materials, buprenorphine hydrochloride and naloxone hydrochloride conversely demonstrate opposite behaviour in that an initial increase in %RH is observed, indicating that these materials give out moisture to the environment before reaching equilibrium. As previously mentioned to obtain a true moisture profile and ERH value there needs to be sufficient moisture available in the first instance for the material to be able to absorb moisture from the surrounding, even if this is later desorbed back into the surrounding sample chamber environment for equilibrium to be attained. Therefore if these materials are selected for further research this has highlighted that these materials would need an increased starting RH while conducting moisture profiling analysis.

Table 4.1 demonstrates the different ERH values that were observed by the range of excipients used in this case in order to identify possible materials for future research. Interestingly many ERH values were around 40%. The exceptions to this were Naloxone Hydrochloride and Povidone, which gave the highest and lowest ERH's respectively.

All materials underwent complete physical characterisation in order to confirm complete identity. These can be seen in Appendix 4.1 – Appendix 4.23 and have been included for completeness. These were consistent with literature. Complete characterisation of lactose monohydrate can be found in the following chapter 5.

Table 4.1. Final % RH readings from moisture profiling experiments for a range of pharmaceutical materials

Material	Final % RH	
	Run 1	Run 2
Acesulfame potassium	38.4	40.6
Buprenorphine hydrochloride	51.0	52.6
Citric acid	39.5	40.8
Lactose monohydrate	38.8	41.6
Maize/starch	39.9	41.4
Magnesium stearate	38.7	36.9
Naloxone hydrochloride	51.7	50.3
Povidone	28.2	29.0
Sodium citrate	37.6	38.9

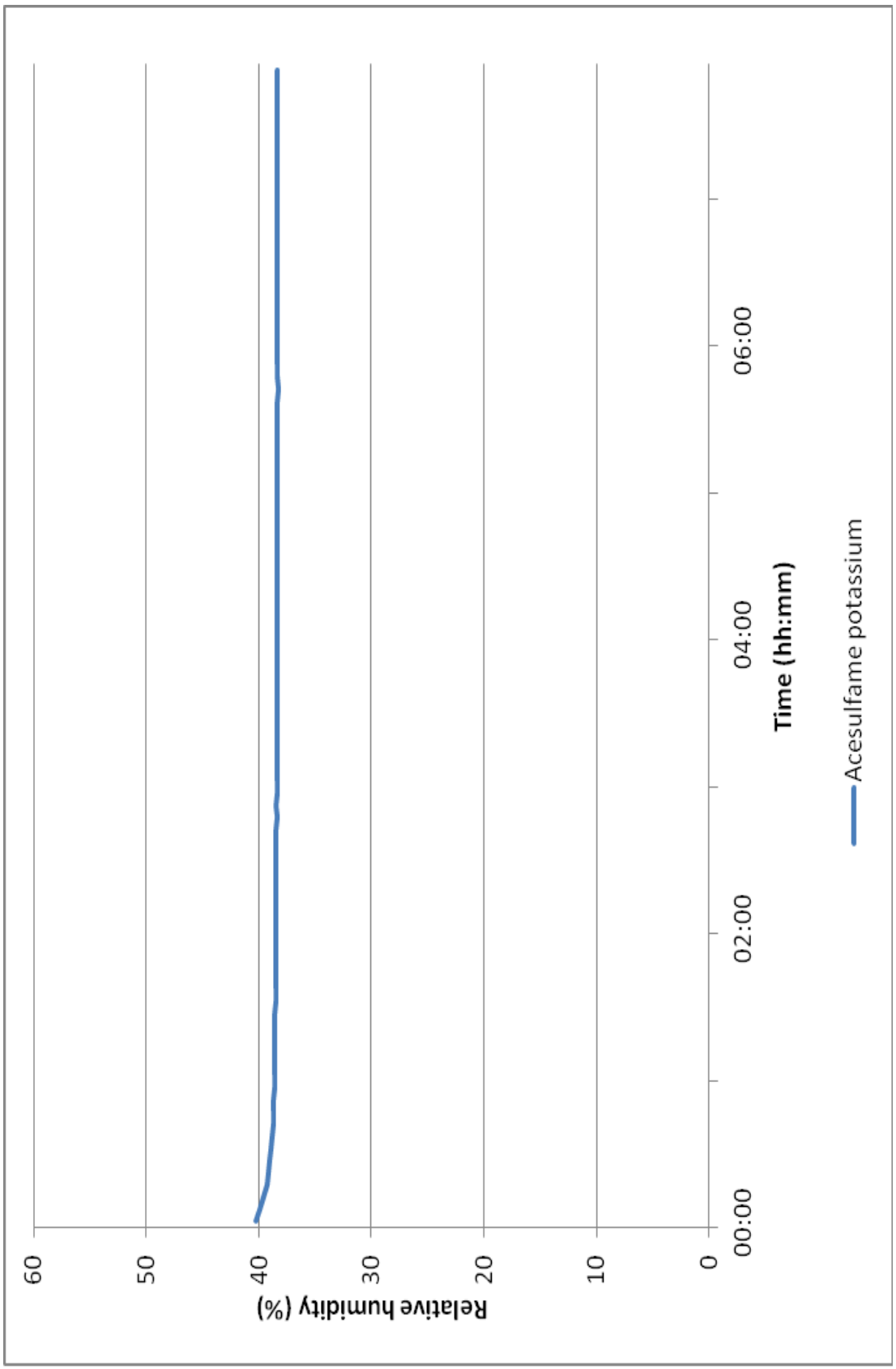

Figure 4.1. Representative moisture profile for acesulfame potassium

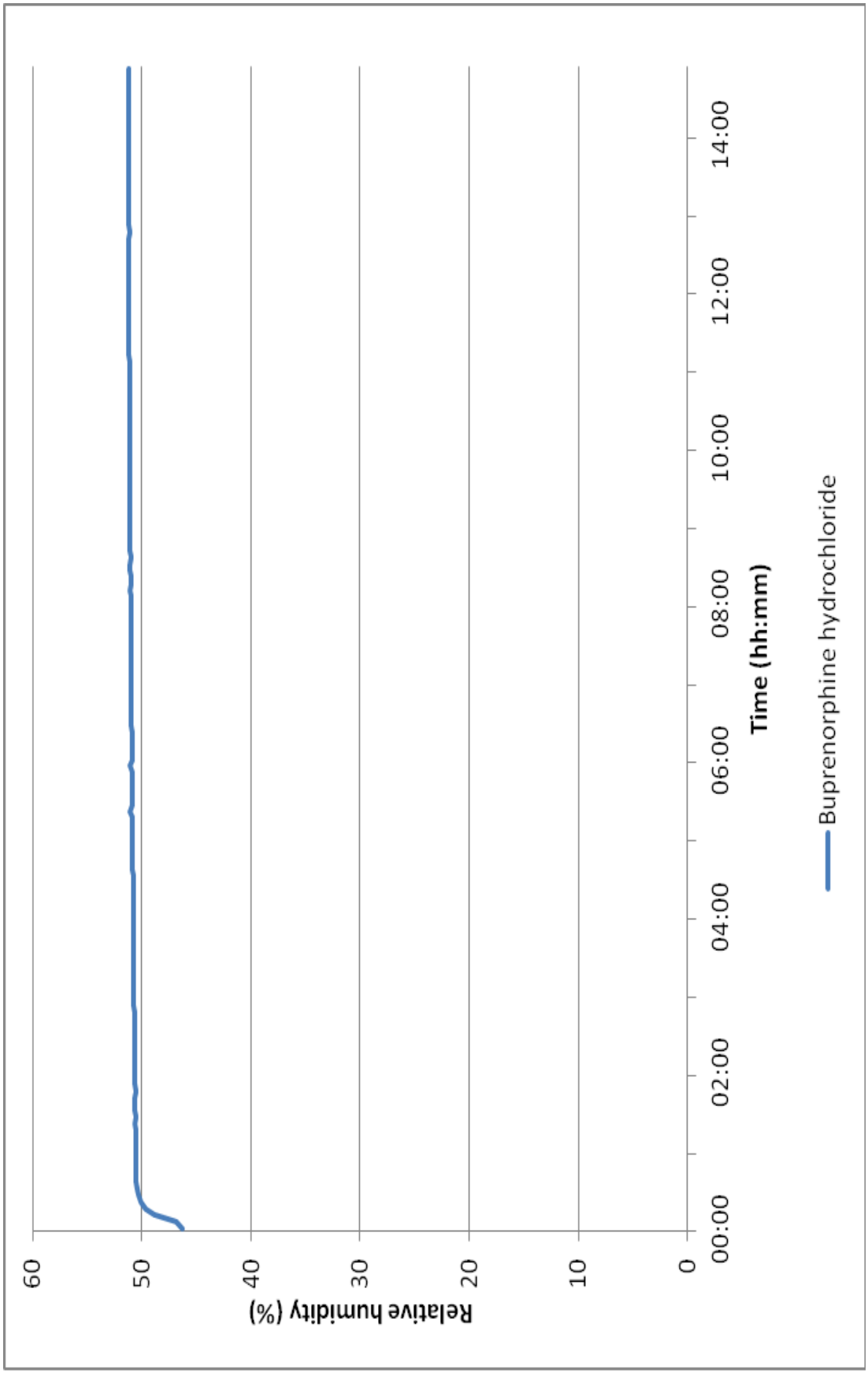

Figure 4.2. Representative moisture profile for buprenorphine hydrochloride

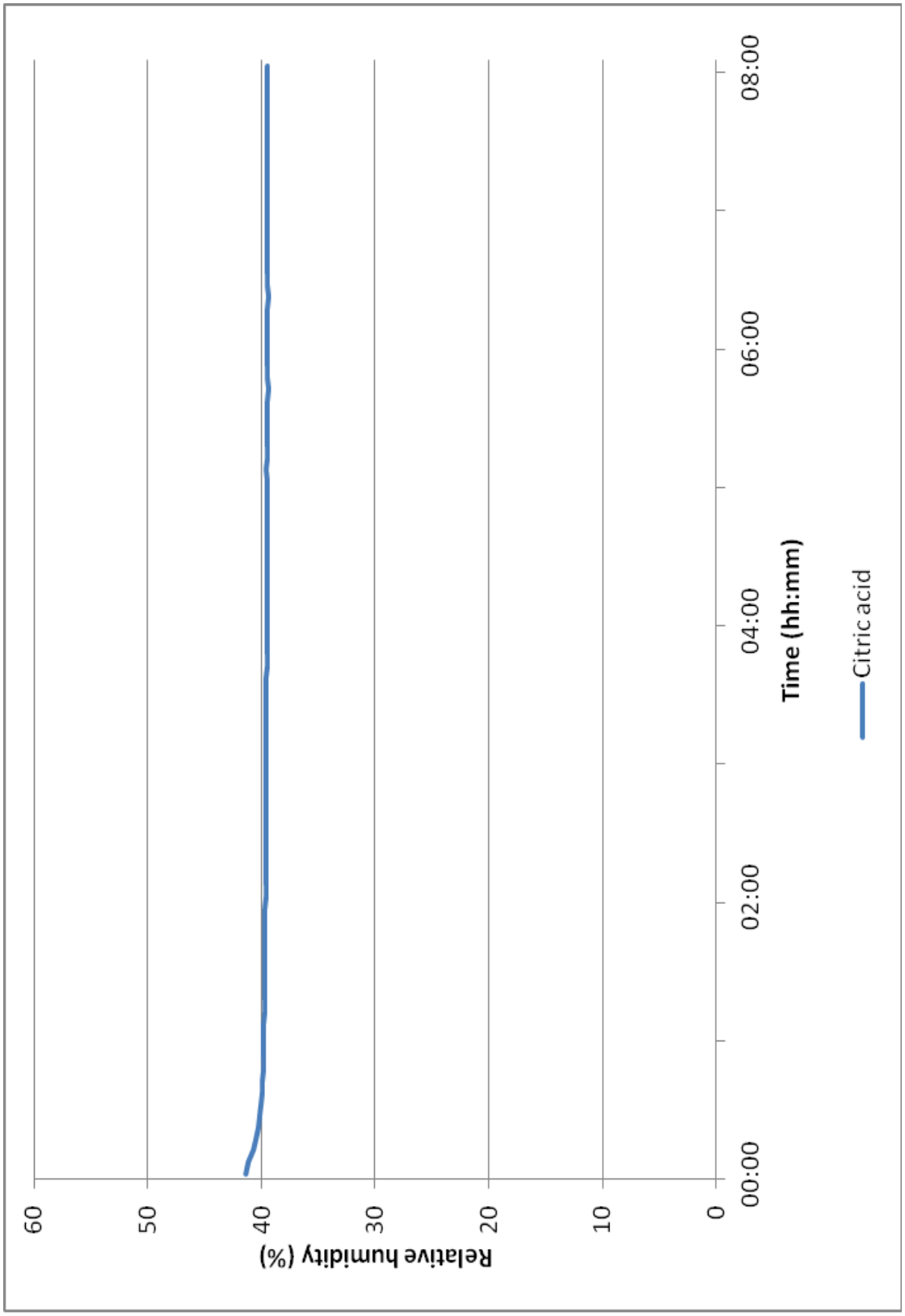

Figure 4.3. Representative moisture profile for citric acid

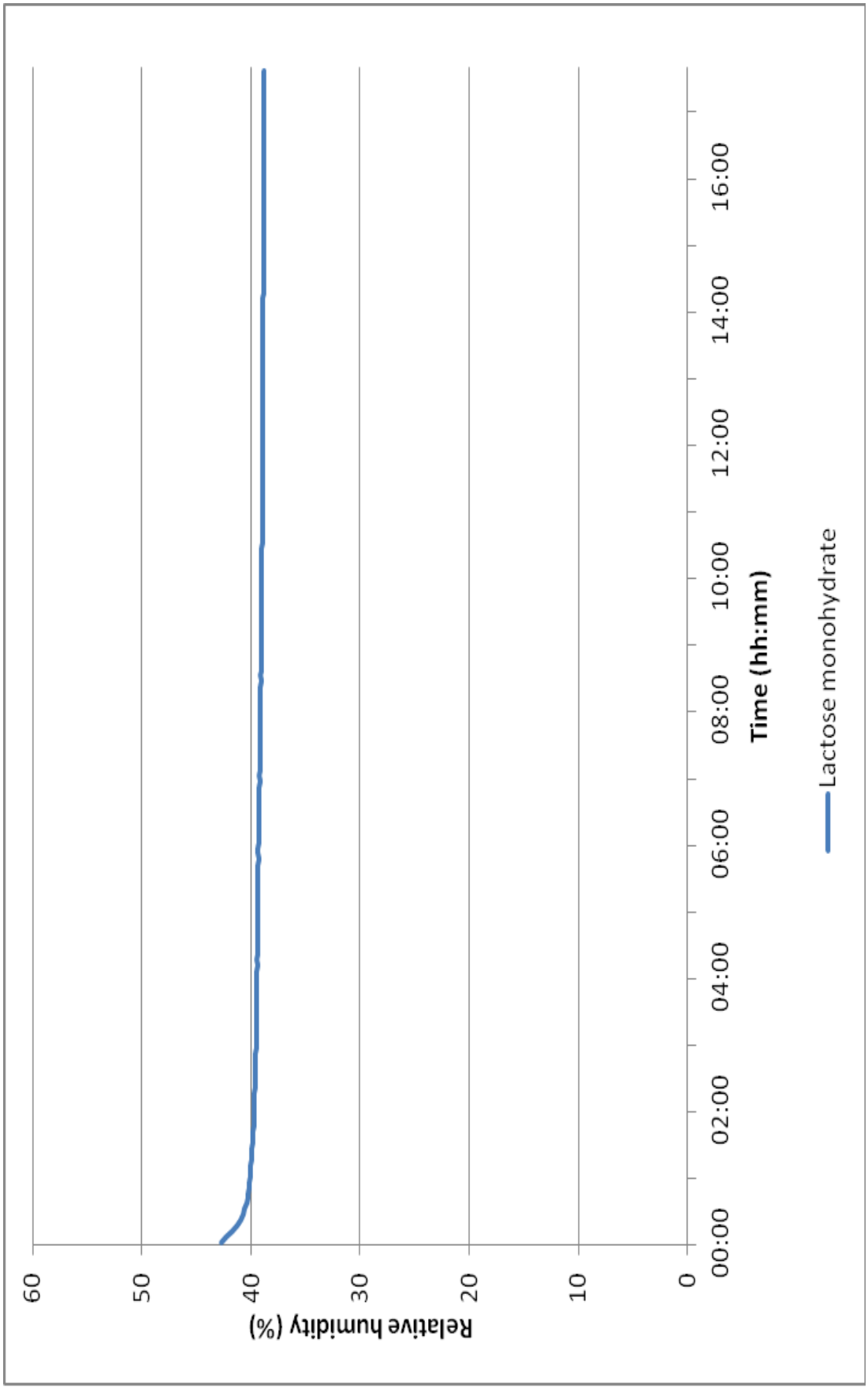

Figure 4.4. Representative moisture profile for lactose monohydrate

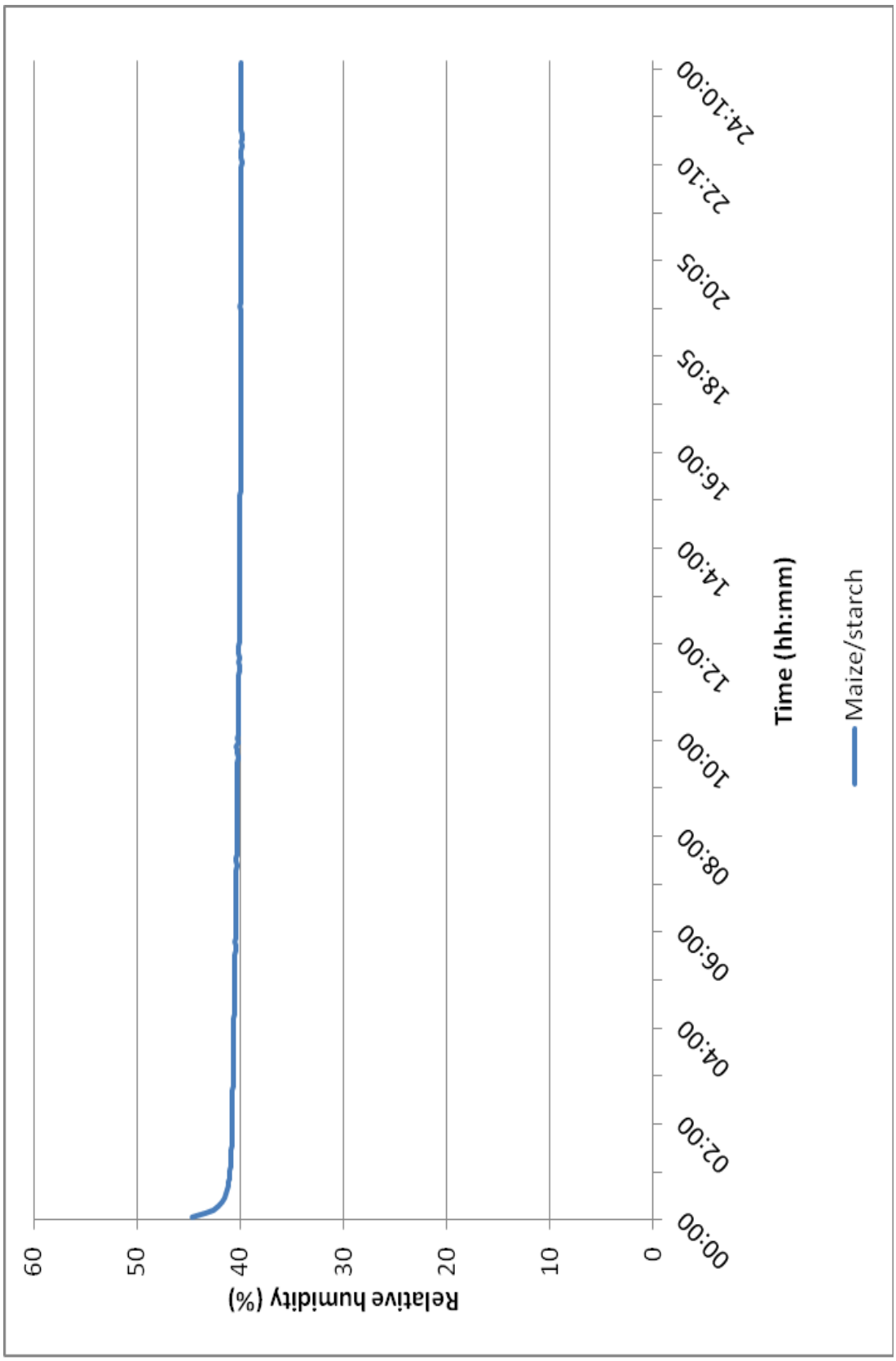

Figure 4.5. Representative moisture profile for maize/starch

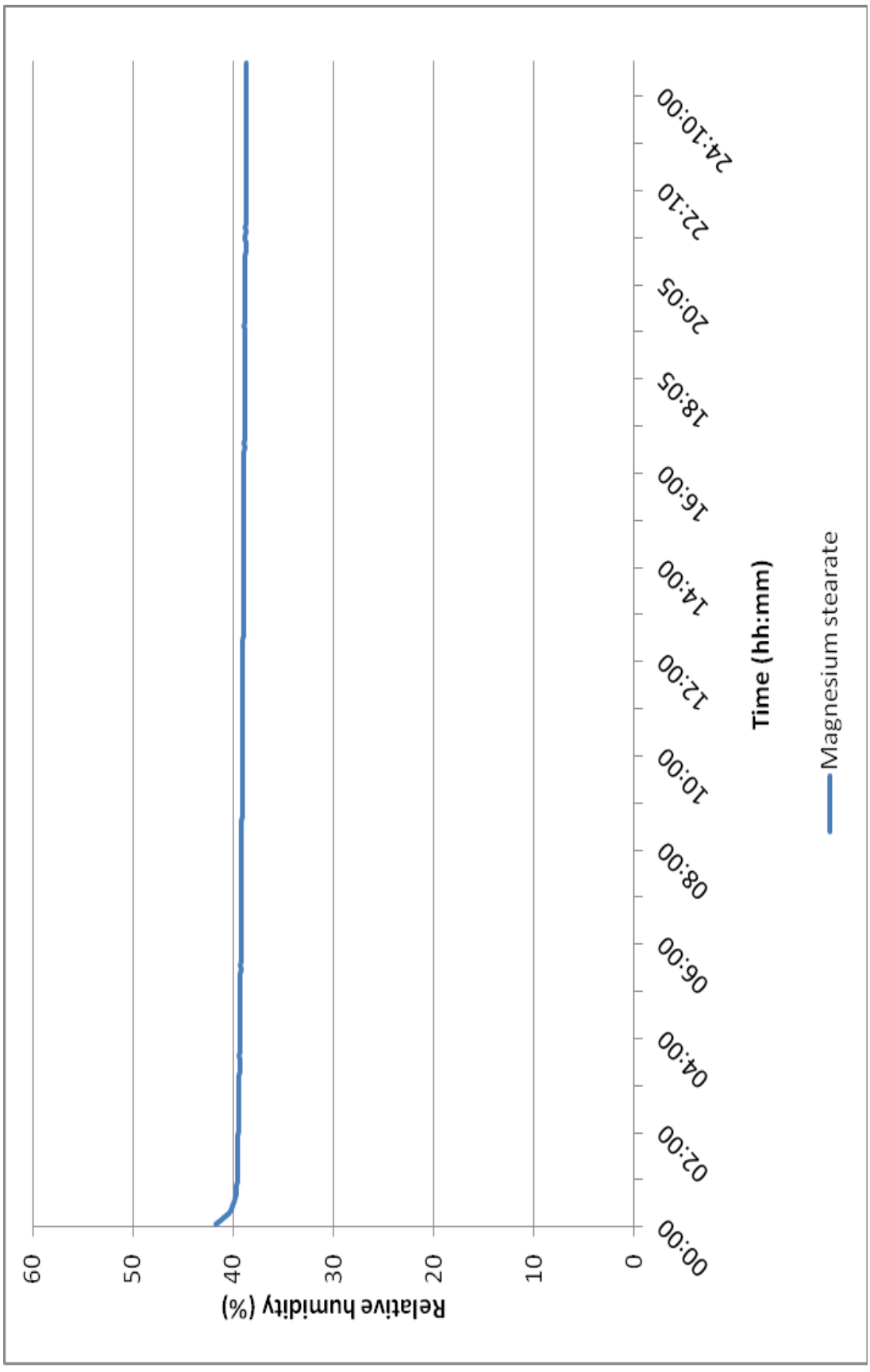

Figure 4.6. Representative moisture profile for magnesium stearate

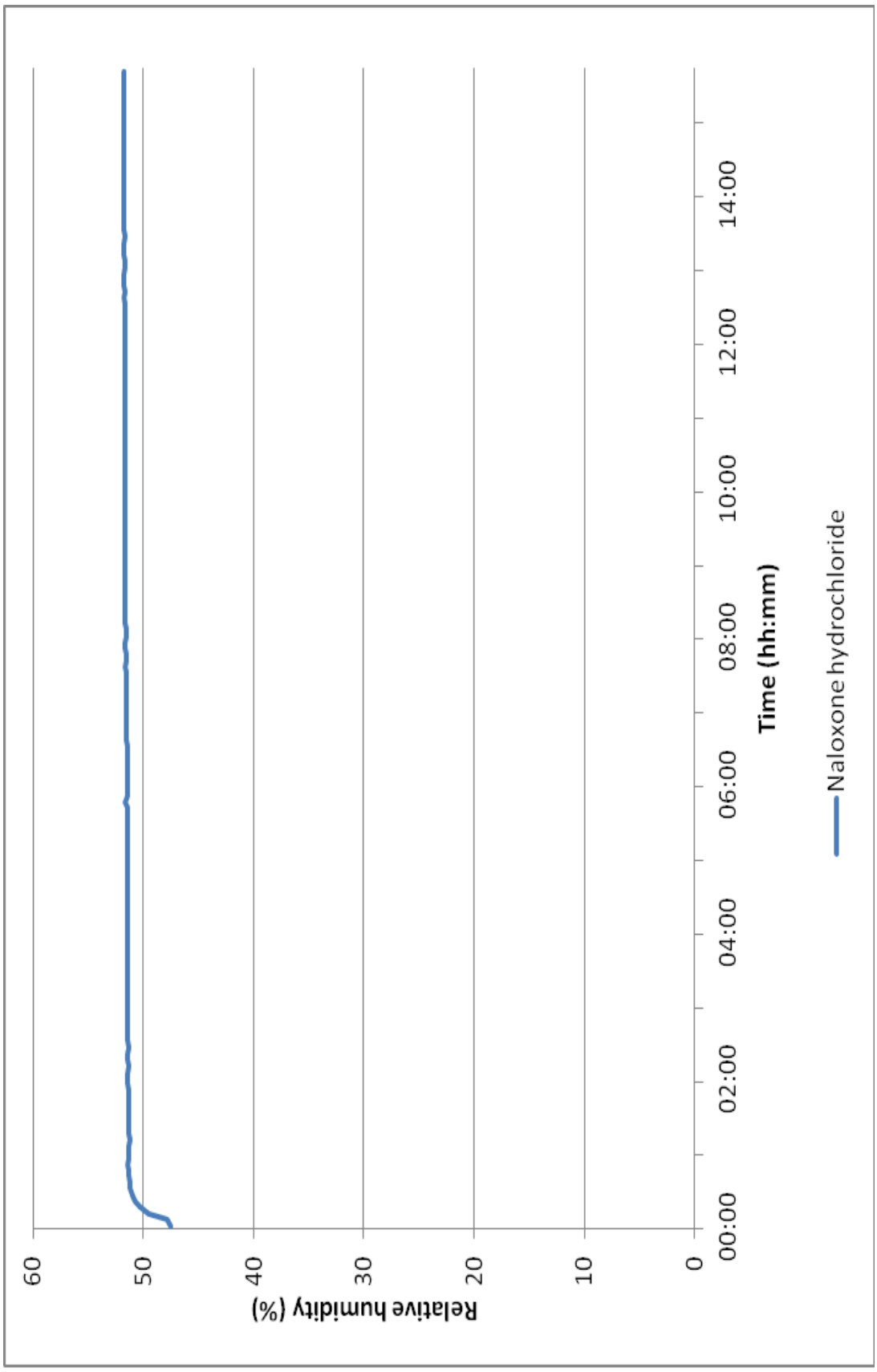

Figure 4.7. Representative moisture profile for naloxone hydrochloride

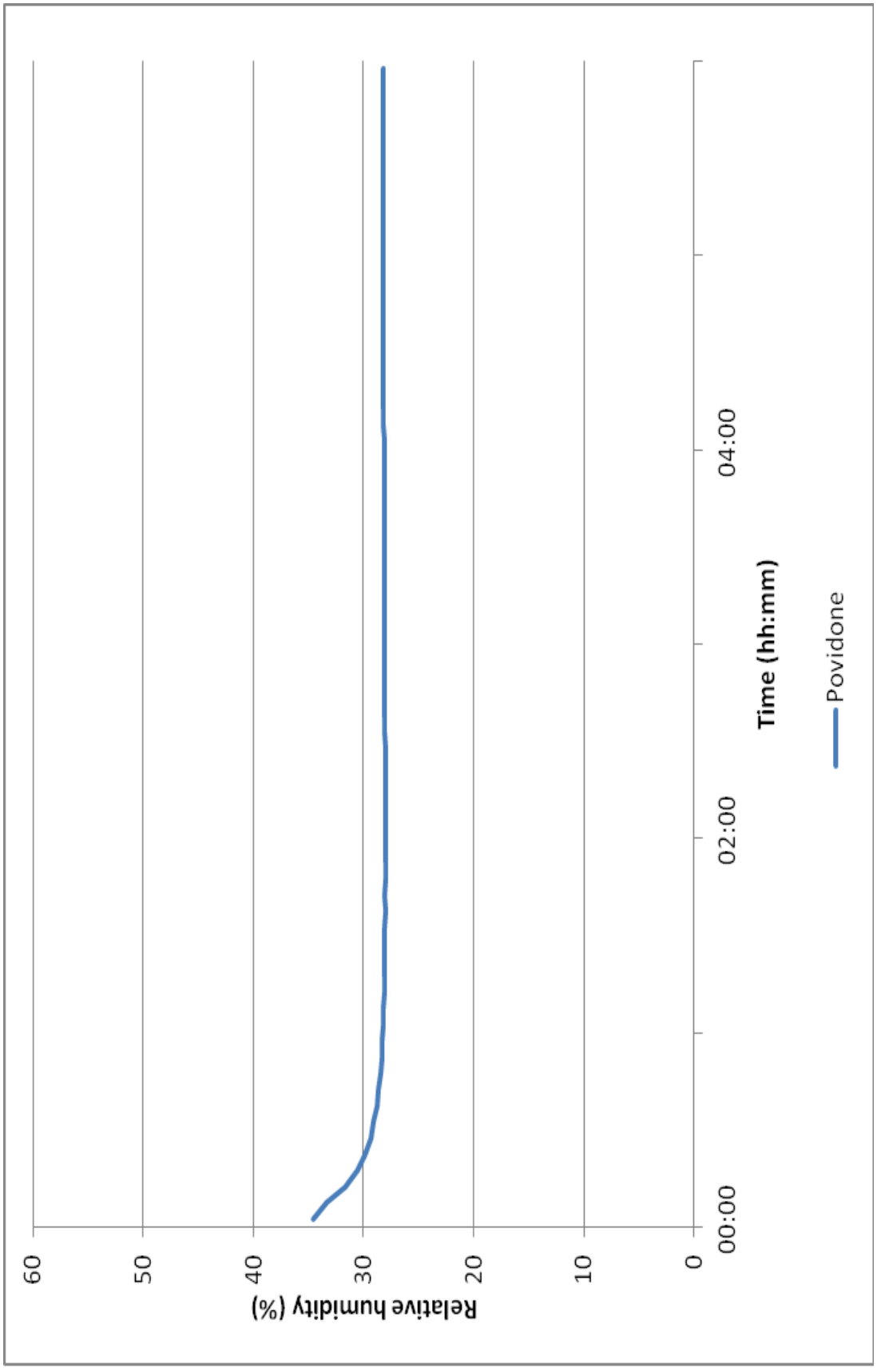

Figure 4.8. Representative moisture profile for povidone

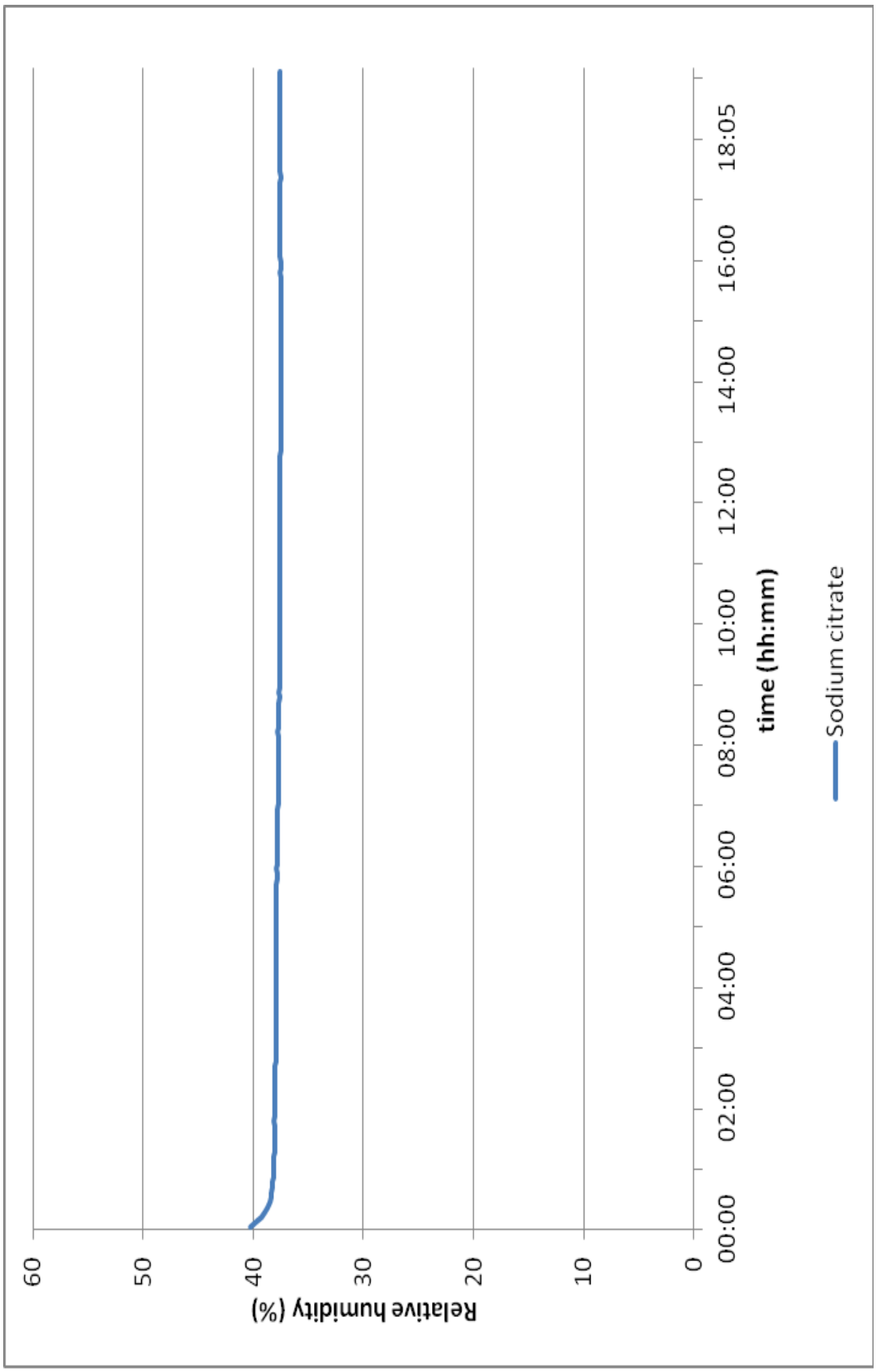

Figure 4.9. Representative moisture profile for sodium citrate

4.3 Effect of sample size upon resultant moisture profiles

The effect of the sample weight of lactose monohydrate on resultant moisture profile has been discussed previously. In summary for this sample, sample weight did not significantly affect the ERH. Here, we present the results of the same analysis for the material Povidone. Moisture sorption profiles for Povidone were determined using the same sample weights as previously used for lactose monohydrate, namely 50, 100, 150 and 200 mg. The analyses were carried out at 25°C and two repetitions at each sample weight were undertaken. Figure 4.10 shows the resultant representative moisture profiles for povidone using the different sample weights. Table 4.2 details the final ERH values from both repetitions carried out.

Examination of the data shows that the moisture profiles demonstrate a trend that different sample weights give rise to different final ERH values. Another trend is observed that the final ERH is lower with increasing sample weight and that the final ERH is converging with higher sample weight. Each profile for the individual sample weights shows an initial decrease which indicates that enough moisture was present in the surrounding sample environment for the material to uptake as much moisture as required. Interestingly for this sample final ERH is sample weight dependent. Thus it is sensible to compare materials of similar weight. Table 4.2 shows the differences observed for the sample weights used and the differences between the repetitions carried out. The standard deviation between all data (all sample weights and repetitions) being ±3.1. This reiterates that it would be beneficial for future research concerning powders that a sample weight is decided

upon, so that any changes seen during moisture profile analysis is not due to sample size variability.

Table 4.2. Final ERH values for povidone using sample sizes 50, 100, 150 and 200 mg

Sample size (mg)	Final % RH	
	Run 1	Run 2
50	32.6	32.3
100	27.8	30.2
150	25.7	26.2
200	25.1	25.9

Figure 4.10. Representative moisture profiles for povidone at sample weights 50, 100, 150 and 200 mg

4.4. Exploration into the ability of the moisture profiler to indicate differences in the composition of mixtures of materials by ERH

The ability of the moisture profiler to be able to discriminate ERH differences between mixtures of materials, and to further develop this concept to see if it is able to give an indication into the predominant physical form within a mixture was of interest. Two systems were evaluated using the moisture profiler. A mixture of sodium citrate and povidone provided the first test system. A mixture of lactose monohydrate and freeze-dried (amorphous) lactose provided the second system.

4.4.1 Results from mixtures of sodium citrate and povidone

The moisture profiler was used to evaluate mixtures of sodium citrate and povidone made up in the following ratio's respectively; 10:90, 50:50, and 90:10 % w/w and then placed in the moisture profiler.

Figure 4.11 shows the representative moisture profiles obtained for the mixtures of sodium citrate and povidone. The profiles for the three mixtures are not greatly different despite a 10% difference in ERH of the pure starting materials. Interestingly from the moisture profiles, it is evident that in this case sodium citrate is the more dominant material, in this case, with respect to ERH and moisture. The moisture profile for mixture 90% sodium citrate: 10% povidone gives the highest ERH, and even with only 10% sodium citrate present in the mixture this still gives a similar ERH value. This brief investigation shows that mixtures of materials are able to affect the resultant ERH values but not necessarily in a linear fashion even though it has been shown that the extent to which the values are affected is dependent upon the mixture ratios. This provides useful information and gives rise

to the possibilities of exploring more formulation and processing effects as further research areas.

Figure 4.11. Representative moisture profiles for mixtures of sodium citrate and povidone

4.4.2 Moisture profiling of mixtures of lactose monohydrate and freeze dried lactose

We wished to use the moisture profiler to explore whether mixtures of an amorphous and a crystalline material gave intermediate values between a 100% crystalline and a 100% amorphous sample. Lactose monohydrate and freeze dried lactose were chosen as representative of a crystalline and amorphous material (for confirmatory XRD data can be seen in section 0).

Mixtures of crystalline lactose monohydrate and amorphous freeze dried lactose were prepared in the following ratio's respectively; 10:90, 50:50, 90:10 w/w and then placed in the moisture profiler. Figure 4.12 shows the representative moisture profiles for the mixtures of lactose monohydrate and freeze dried lactose. From the shape of the profiles, it is evident that mixtures of the same material with differing physical forms give rise to different ERH values. For the profile of the 10% lactose monohydrate: 90% freeze dried lactose mixture, a higher ERH value than other mixtures was obtained. This finding is consistent with the amorphous nature of the freeze dried material, which is metastable and will tend to crystallise, expelling water as it does so (Chidavaenzi et al., 1997).

This brief exploration into the effects of the physical mixtures shows again that the ERH and ERH stability of mixtures is influenced by the nature of the blend and are not trivial to predict. What is clear is that it is important, that in order to fully understand the nature of the ERH profiles, that well characterised materials are used initially and that that the solid state properties of the material at the end of ERH testing are further evaluated. The blend studies performed here therefore

indicate further possible areas for future research, to include examination of the effects of different physical forms of the same material with respect to their moisture behaviour and any changes in that behaviour during processing towards the manufacture of solid dosage forms.

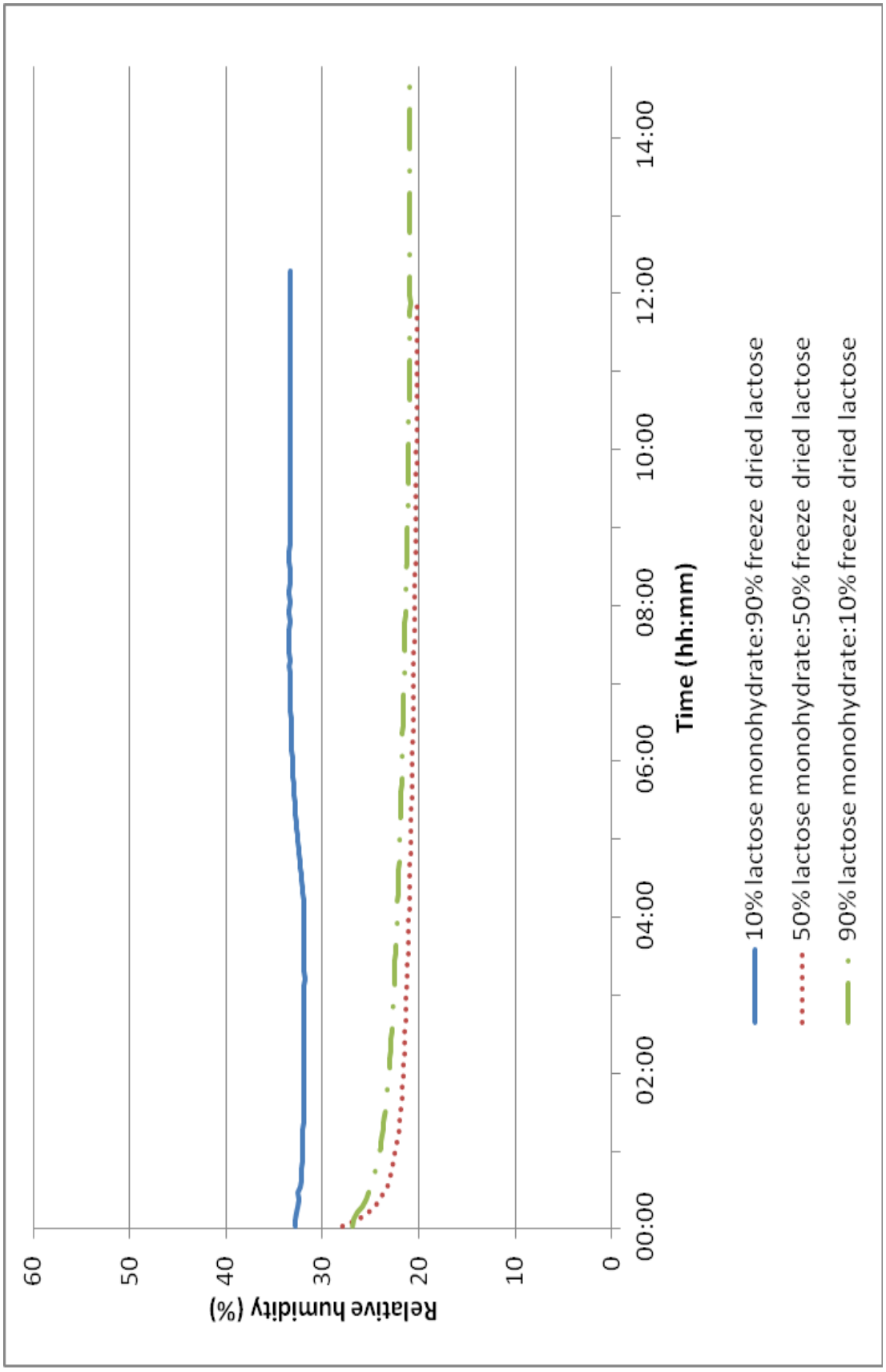

Figure 4.12. Representative moisture profiles for mixtures of lactose monohydrate and freeze dried lactose

4.5 Investigation into the effects of temperature fluctuations on moisture profiles

The final area of preliminary exploration was to evaluate how ERH varied in an uncontrolled temperature environment and whether it was important to control temperature. The effects of temperature were explored because of the inverse relationship that exists between ERH and temperature. The test was done by removing the moisture profiler from the temperature controlled oven and leaving the sample chamber exposed for a prolonged period of time. The test was performed without a sample and then with a sample in order to assess the impact that temperature has on the relative humidity (consequently ERH value) of the surrounding air within the closed environment and what effects this can have upon a sample. The test material chosen was lactose monohydrate. For an additional evaluation, different sample sizes of lactose monohydrate were tested in the moisture profiler at an increased temperature in order to observe if previous differences in ERH values were still apparent at an increased operating temperature.

4.5.1 Moisture profiles with no temperature control

Firstly, the moisture profiler was removed from the temperature controlled oven and the lid from the sample tube removed. Data was logged over a prolonged period of time (in excess of 24 hours). Figure 4.13 shows the resultant moisture profile and also shows the temperature log for the exact same time period. The profile shows that initially a decrease in temperature occurred, due to the temperature in the room being lower than in the temperature controlled oven. The decrease in temperature was accompanied by an increase in RH; consistent with

cold air being able to hold less moisture. This brief and very basic investigation into the temperature effects but demonstrates that without a sample present RH is affected by temperature fluctuations.

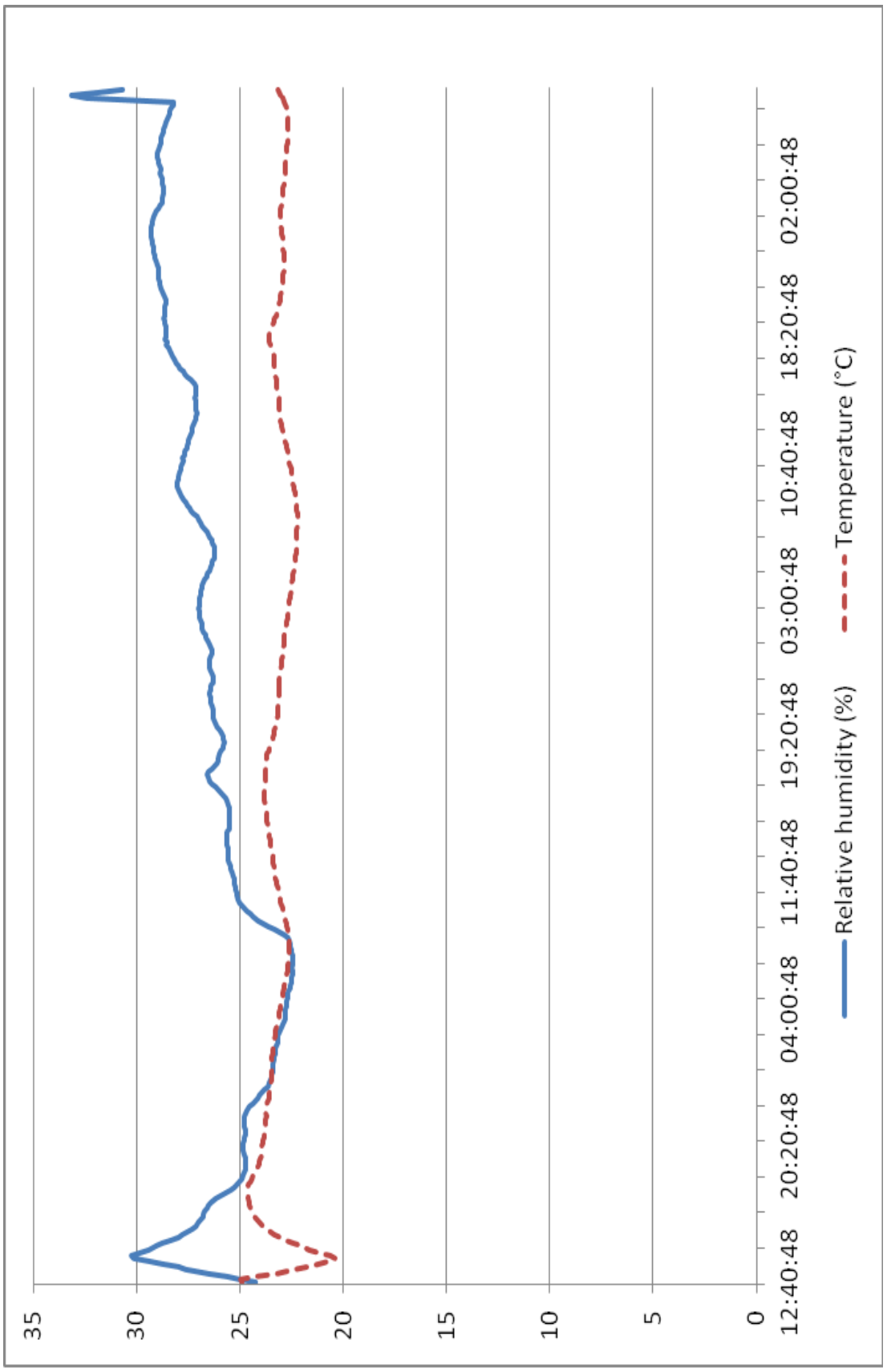

Figure 4.13. Representative moisture profile demonstrating fluctuations of RH a room based upon the inverse relationship with temperature

4.5.2 Moisture profile study of Lactose monohydrate with no temperature control

Lactose monohydrate was also analysed as described previously (removal of moisture profiler from temperature controlled oven and left for prolonged period of time to assess fluctuations that occurred). However, for this study, the sample holder closure was used in order to retain the closed environment system and observe the effects that surrounding temperature fluctuations have whilst a material is being analysed. Figure 4.14 shows the resultant moisture profile with the temperature data that was recorded at the exact same time the RH measurement was taken. Scrutiny of the data shows that, contrary to what is theoretically predicted there is not a strong inverse relationship, in that a decrease in temperature is not always accompanied by a corresponding increase in resultant RH for the material. However we can observe that fluctuations in temperature influence ERH. The preliminary study therefore highlights that temperature is able to affect the RH even while a material is under analysis. This is evidently only an extremely basic investigation but demonstrates the necessity to control the temperature, in order to limit the number of variables.

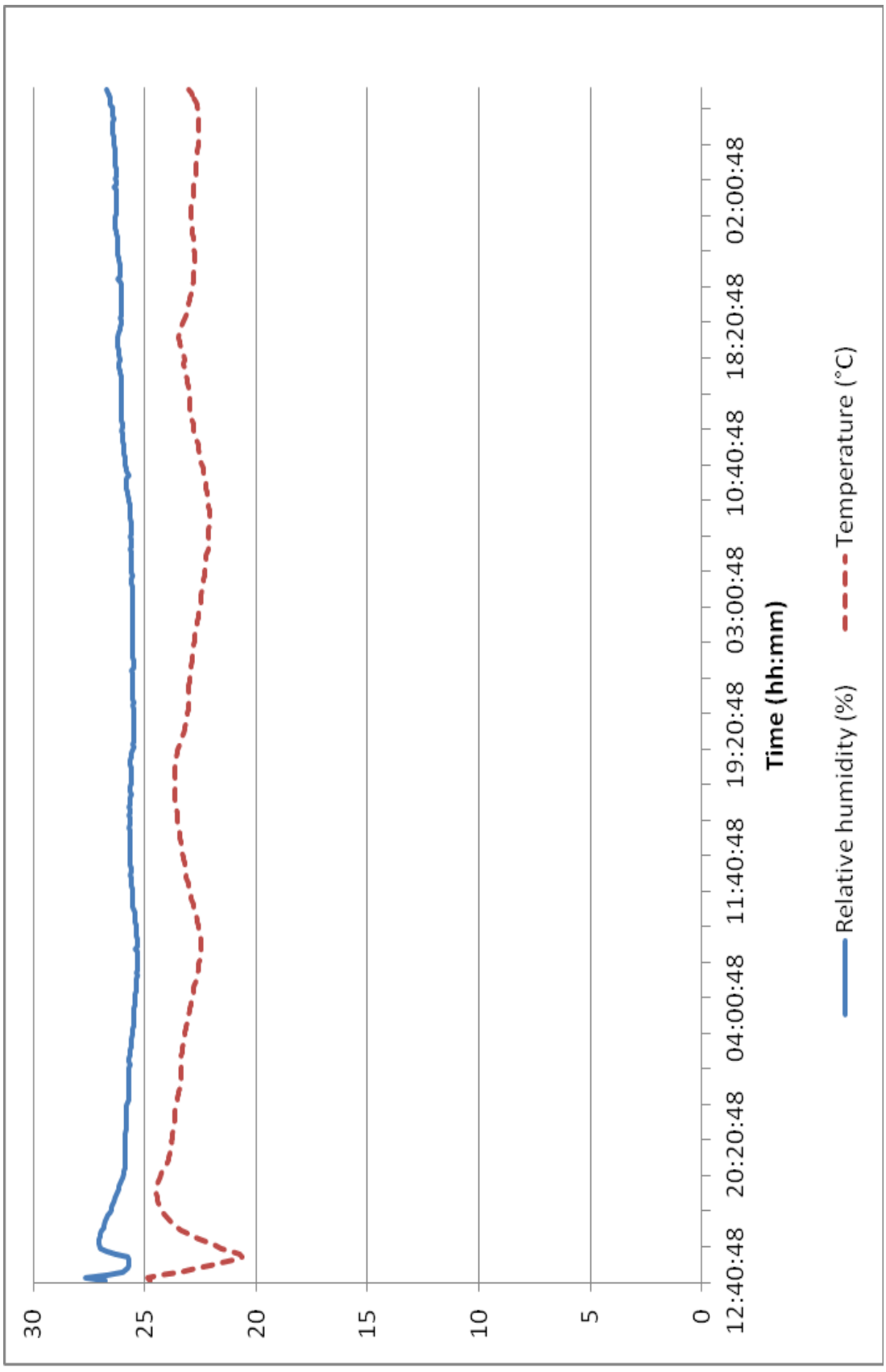

Figure 4.14. Moisture profile demonstrating the influence of temperature during analysis of lactose monohydrate

4.5.3 Moisture profile study of Lactose monohydrate at elevated temperature and with different sample size

It has previously been shown that sample size is able to have a slight impact upon final ERH values obtained for the materials studied, lactose monohydrate and povidone. This issue was re-investigated in order to see if previous differences in final ERH values due to sample size are still evident if the operating temperature was increased to 40°C. Sample weights 200 and 750mg were used so that a clear difference in any changes could be observed.

Figure 4.15 shows representative moisture profiles for the two sample sizes and shows that only a slight difference in final ERH is noted even at elevated operating temperature. The result is confirmatory that ideally a standard sample size be employed throughout future work. It is important to note that although the samples do not attain ERH from an elevated starting RH, which we have discussed as a better methodological approach, the behaviour within the moisture profiles for both sample weights is qualitatively the same.

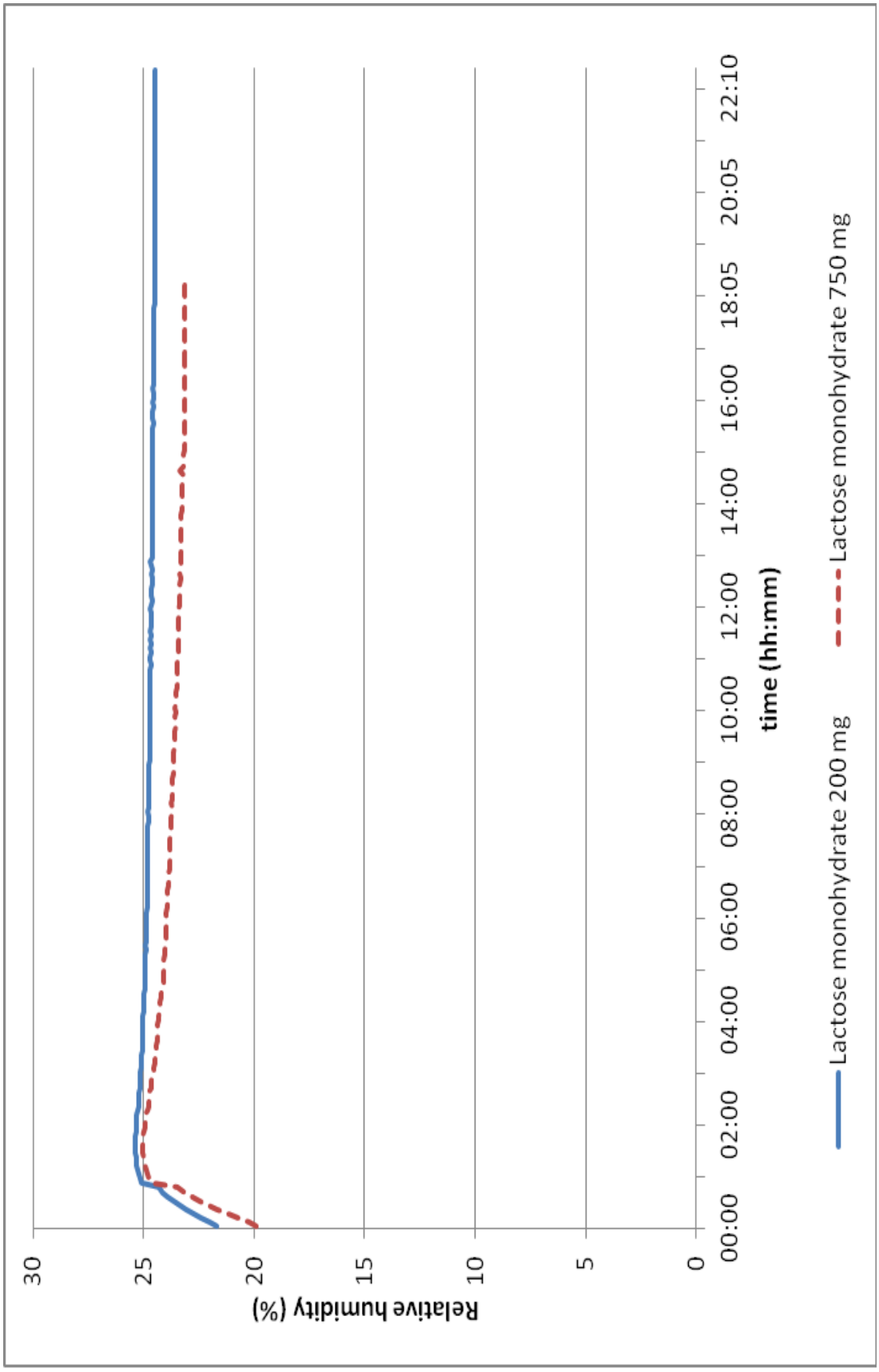

Figure 4.15. Representative moisture profiles for lactose monohydrate at 200 and 750mg sample weights at 40°C

4.6 Discussion

The operational capabilities and scoping of applications for the novel moisture profiler instrument have been evaluated in this chapter. Initial exploration of the applications of moisture profiling and potential areas of research was probed. Firstly explored was how the ERH profiles for a range of pharmaceutical materials differed within the moisture profiler. The results showed and reinforced previously drawn conclusions that some materials adsorb moisture from the closed sample environment, and that some do the opposite and desorb moisture. However, ideally there must be sufficient moisture present within the sample chamber so that it is available for the material to uptake if it wants to dependent upon the nature of the material. The results demonstrated that there was sufficient moisture available for all materials, with the exception of buprenorphine hydrochloride and naloxone hydrochloride. Both these materials demonstrated that during moisture profiling analysis the starting RH meant an initial increase was observed within the moisture profile. This could therefore mean that the insufficient moisture was available for uptake and that a true ERH value may not have been attained, as the materials may have wanted to absorb more moisture. Further work to clarify this behaviour would need to be explored should these materials be used in further research beyond the exploratory study here. Characteristic ERH's for the various materials were identified. The highest and lowest ERH values obtained for the range of different materials varied by over 20%.

The influence of sample size on the moisture profile obtained was explored for a second material, povidone. Examination of the data showed that the moisture

profiles demonstrated a trend that different sample weights give rise to different final ERH values. Another trend was observed that the final ERH was lower with increasing sample weight and that the final ERH was converging with higher sample weight. Interestingly for this sample final ERH is sample weight dependent. Thus it is sensible in further studies to compare materials of similar weight. This therefore reinforces the conclusion previously drawn to use 200mg sample size for powdered materials requiring use of the sample holder.

The behaviour in the moisture profiler of mixtures of excipients and mixtures of different physical forms of the same material were determined for sodium citrate:povidone and lactose monohydrate:freeze dried lactose systems respectively in varying ratios. The results from this brief investigation showed that mixtures of materials were able to affect the resultant ERH values but not necessarily in a linear fashion even though it has been shown that the extent to which the values are affected is dependent upon the mixture ratios. More detailed research in this area is required as the samples may have been changing physically during the analysis

An examination of the effect of temperature fluctuations revealed that temperature is able to have an effect upon ERH. The results reinforced a prior conclusion drawn, that a defined and controlled operating temperature is beneficial for future work as it reduces a variability.

5 SOLID STATE CHARACTERISATION

5.1 Introduction

In order to provide material that is of a consistent quality for formulation, it is essential to study the solid state properties (Anderson, 2000). Complete characterisation is therefore necessary in order to fully understand the chemical and physical properties of both API's and excipients present in the final dosage form (Bugay, 2001).

As previously discussed, lactose is a raw material that is used in large quantities in both pharmaceutical and food industries. Lactose is reported to exist in various different solid state forms, these being: lactose monohydrate, anhydrous lactose and amorphous lactose (Kirk et al.2007). These forms consequently exhibit different physical properties and therefore it is important that they are fully characterised.

The implications of polymorphism within the pharmaceutical industry are significant. Different polymorphs differ physically and behave as if they were completely different chemical entities, yet they are not. Each polymorph may exhibit different solubility, density, crystal shape and vapour pressure. Therefore it is essential to characterise the solid state properties of commercial products prior to usage to assess the suitability of a product for use.

All forms of lactose to be used in the experimental work need to be fully characterised structurally, thermally and physically to clarify behaviour. Moisture profiling will also be employed to distinguish differences between different lactose forms with respect to moisture behaviour.

5.2 Objectives

Full characterisation, both structurally and thermally of the different physical forms of lactose that will be used for further work is required. The different physical forms will be completely characterised initially using thermal techniques TGA and DSC, in conjunction with structural technique PXRD. SEM, DVS and moisture profiling will also be carried out. Methods of the above techniques have been detailed in chapter 2.

5.3 Results of Thermogravimetric analysis

5.3.1 Thermogravimetric analysis results for lactose monohydrate

The lactose monohydrate TGA thermal profile (Figure 5.1) demonstrates weight loss of approximately 5%, which corresponds to the theoretical molar content of water of hydration. The weight loss occurs after 100°C indicating that the weight loss is probably due to crystalline lattice water.

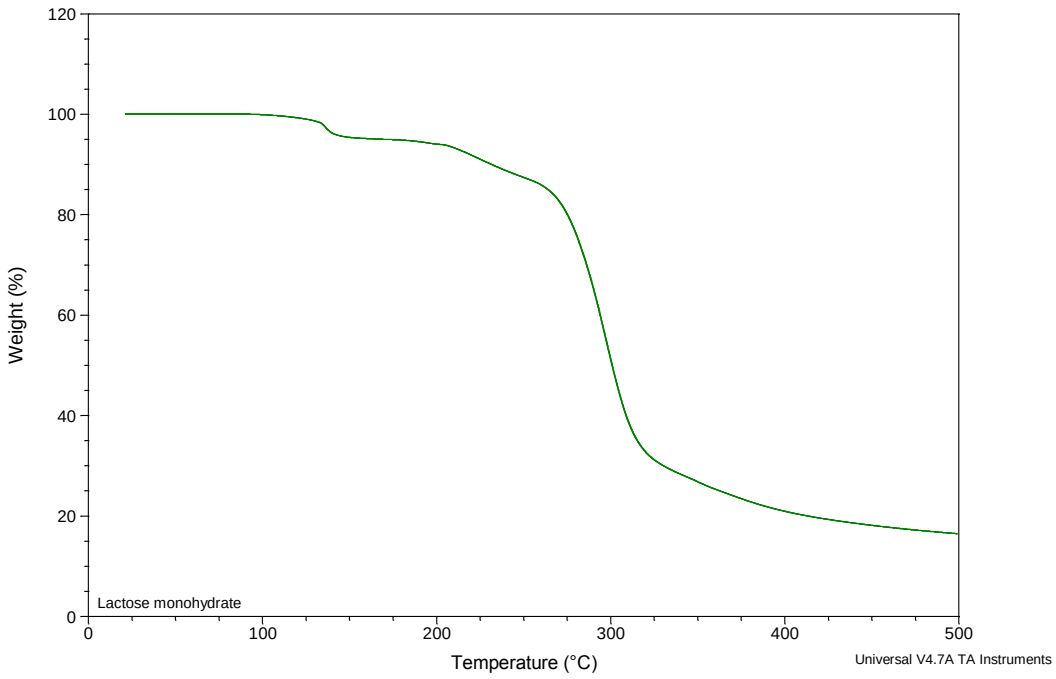

Figure 5.1. Representative TGA thermal profile for lactose monohydrate

5.3.2 Thermogravimetric analysis results for anhydrous lactose

Anhydrous lactose TGA thermal profiles (Figure 5.2) show confirms the material is predominately anhydrous in nature as no evidence of water loss associated with the hydrate.

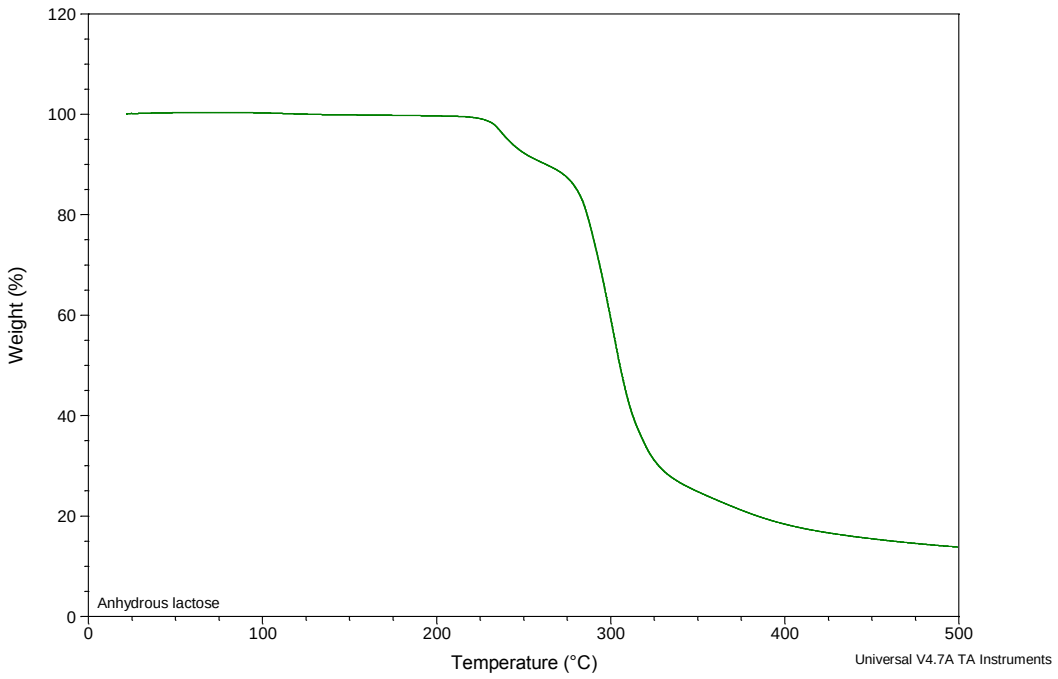

Figure 5.2. Representative TGA thermal profile for anhydrous lactose

5.3.3 Thermogravimetric analysis results for freeze dried lactose

Freeze dried lactose was manufactured according to the method given in 2.3.1. The thermal profile obtained for the sample (Figure 5.3), shows a weight loss in the temperature region 30-130°C; which is likely due to residual water (Darcy and Buckton, 1997). Between 130 and 200°C only minor weight fluctuations are evident.

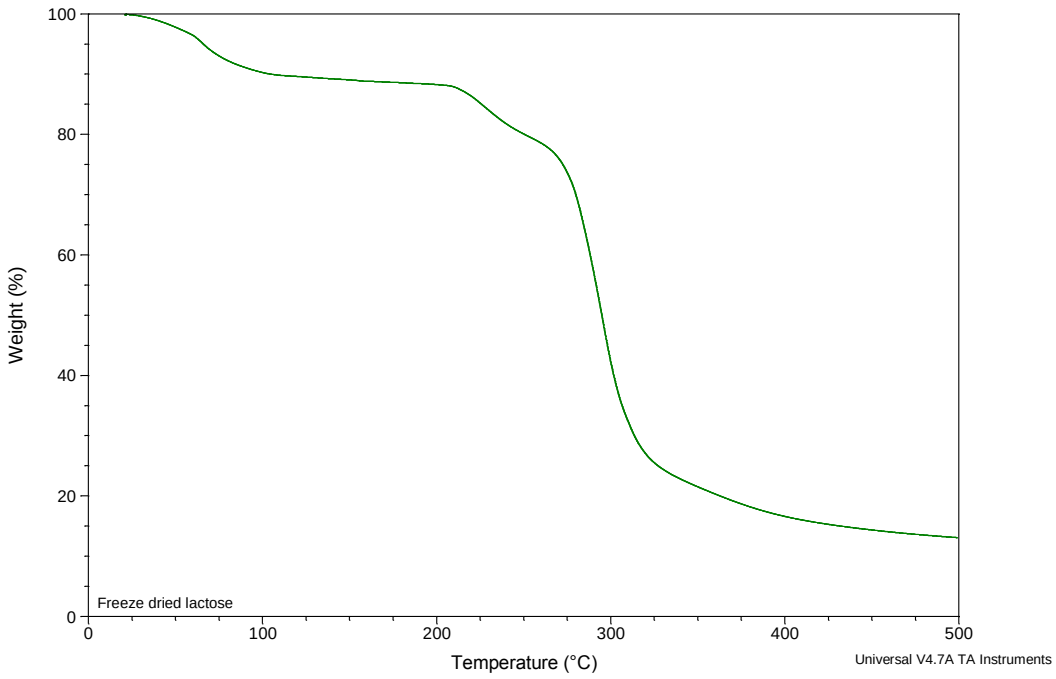

Figure 5.3. Representative TGA thermal profile for freeze dried lactose

5.3.4 Thermogravimetric analysis results for spray dried lactose

Spray dried lactose was prepared according to the method given in 2.3.2. The thermal profile (Figure 5.4) shows an initial weight loss which is likely to be due to residual water that remains after the spray drying process.

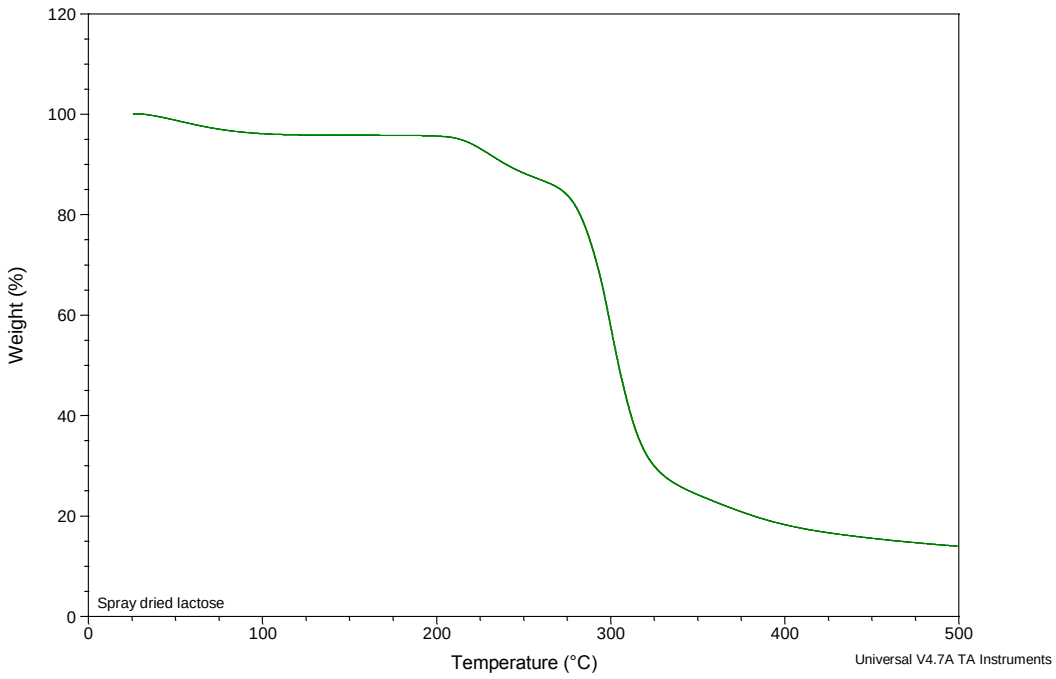

Figure 5.4. Representative TGA thermal profile for spray dried lactose

5.4 Results from Differential Scanning Calorimetry

5.4.1 Results of DSC analysis for lactose monohydrate

The DSC thermal profile (Figure 5.5) shows two distinctive endotherms. The first is at 147.30°C (± 0.29°C, n=3), which is due to dehydration of the crystalline lattice water. The second endothermic peak at 212.44°C (± 0.21°C, n=3) is due to melting of the crystalline solid (Berlin et al., 1971, Listiohadi et al., 2009). The material then undergoes decomposition. The position of the melting endotherm and absence of an endothermic peak at approximately 230°C, suggests that the lactose is primarily the α polymorph (Chidavaenzi et al., 1997).

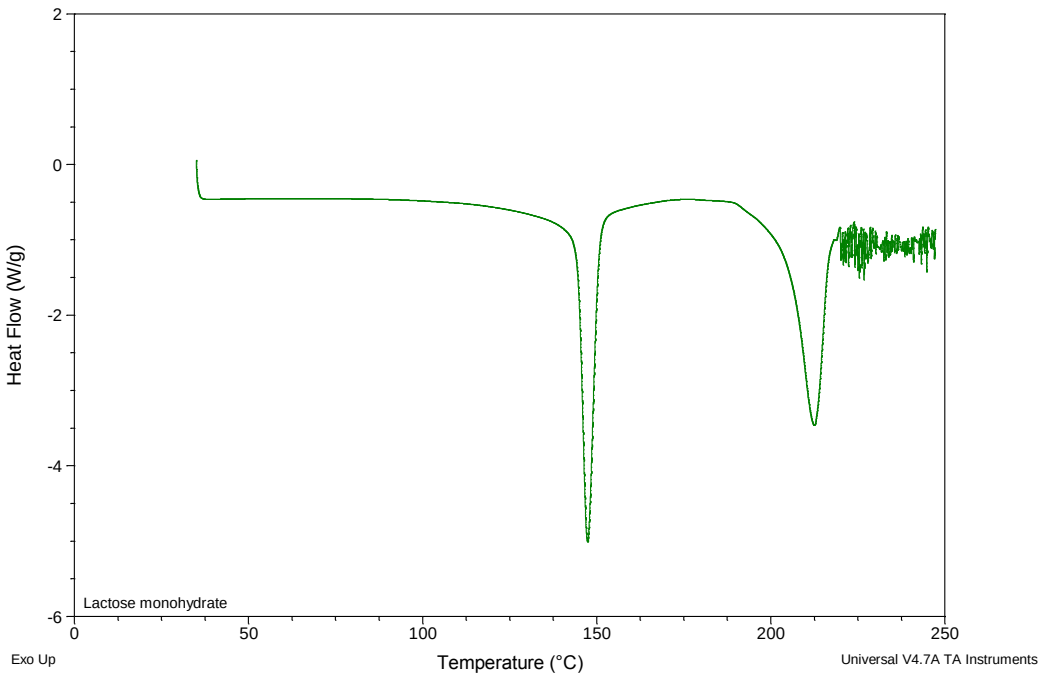

Figure 5.5. Representative DSC thermal profile for lactose monohydrate

5.4.2 Results of DSC analysis for anhydrous lactose

The DSC thermal profile (Figure 5.6) shows a single exotherm at 232.93°C (± 0.34°C, n=3), which is characteristic of the melting associated with the β polymorph of the anhydrous material (Listiohad et al., 2008). Commercial anhydrous lactose has been found to contain up to 50% α lactose monohydrate. The ability of anhydrous lactose to take up moisture from the surrounding environment due to its hygroscopic nature (Brackel, 2007). Thereby, converting the β anhydrous lactose to α lactose monohydrate is the mechanism whereby this occurs. It has been extensively cited in literature, that exposure to humidity incorporates water into the crystal lattice facilitating conversion into the crystalline α lactose monohydrate (Shah et al., 2008, Ford and Timmins, 1989).

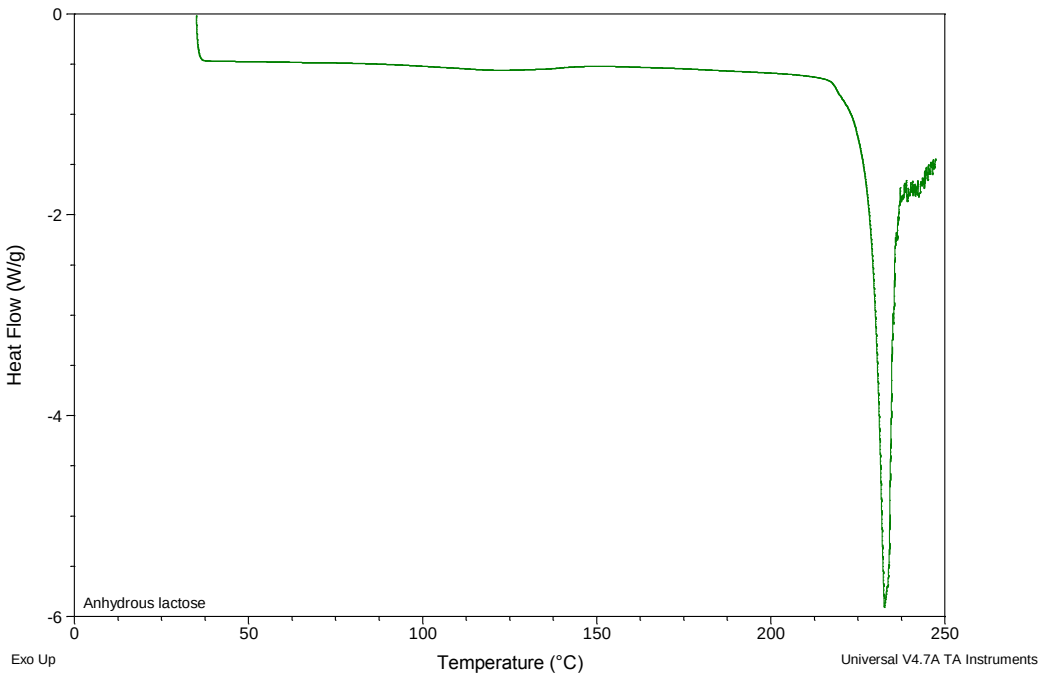

Figure 5.6. Representative DSC thermal profile for anhydrous lactose

5.4.3 Results of DSC analysis for freeze dried lactose

The DSC thermal profile (Figure 5.7) shows peaks typical of amorphous lactose. Firstly, the broad endothermic peak over an approximate temperature range 35-120°C, is due loss of surface water. A slight exotherm is visible at 119.75°C (±0.43 °C, n=3), which is attributed to T_g of amorphous material, this is usually found in the range 100-120°C. An endotherm at 189.65°C (±0.86°C, n=3) is due to crystallisation of the amorphous material, which is facilitated by the thermal technique promoting mobility. Crystallisation is confirmed by the subsequent onset of melting of the material. Two melting endotherms are visible at 216.33 °C (±0.38°C, n=3) and 225.89°C (±0.67°C, n=3), which are attributed to the melting of the α and β forms respectively. The material then undergoes decomposition.

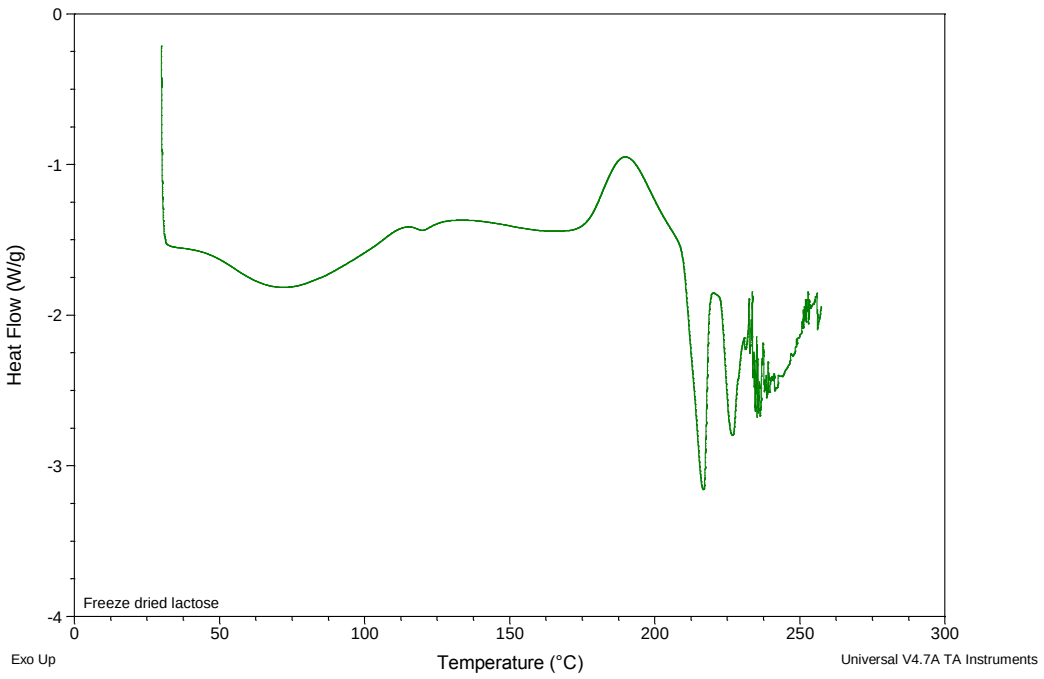

Figure 5.7. Representative DSC thermal profile for freeze dried lactose

5.4.4 Results of DSC analysis for spray dried lactose

The representative DSC thermal profile for spray dried lactose (Figure 5.8) shows several thermal events. A broad endotherm at 81.84°C (±0.73 °C, n=3) is due to residual moisture remaining from the spray drying process. An indication that the material is initially amorphous in structure is shown in that a glass transition (T_g) is also observed in the thermal profile. In this instance it is observed as a disruption of the baseline at 118.89 °C (±0.97 °C, n=3) (Chidavaenzi et al., 1997). An exothermic peak is visible at 163.30°C (±0.44°C, n=3), which is perceived to be crystallisation of the amorphous material (Sebhatu et al., 1997). It is important to emphasise that the sample material was amorphous prior to DSC analysis (X-ray data to be presented later). The rising temperature during analysis facilitated crystallisation which is evidenced by the subsequent melting endotherm. A melting endotherm is

present at 213.93°C (±0.33°C, n=3). The endotherm is attributed to the melting of the crystalline lactose, present in the α polymorphic form. Absence of an endothermic peak at 235°C (due to melting of β lactose) suggests that during crystallisation only the α polymorph was formed and is being detected within the detection limits of the instrument. However, because the DSC has relatively low sensitivity, the peaks may not be visible (Angberg, 1995), or possibly be hidden within the decomposition peaks.

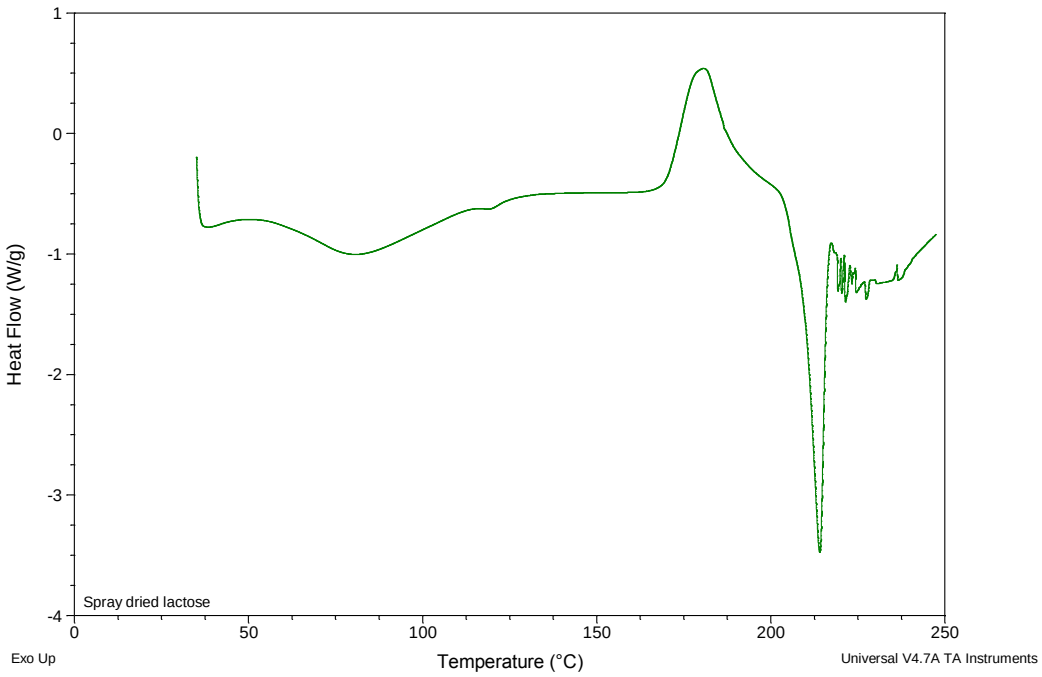

Figure 5.8. Representative DSC thermal profile for spray dried lactose

5.5 Dynamic vapour sorption

Moisture uptake is able to play a major role in both chemical and physical stability of the solid dosage form. It is therefore necessary given the nature of this work that material be evaluated with respect to moisture uptake upon exposure to humidity using DVS. The method was as described in section 2.4.3.

5.5.1 Results of DVS analysis for lactose monohydrate

The moisture sorption isotherm from DVS analysis for lactose monohydrate is shown in Figure 5.9 . Analysis shows that the adsorption step the sample gradually increases in weight until 60% RH, when a weight loss is observed, which is followed by a weight gain which is gradual up until 90 % RH is reached when a sharper increase is observed. This behaviour is characteristic of polymorphic conversion induced by exposure to the elevated RH'S. The desorption step shows a steep decrease in weight until 80% RH is reached, where the weight change then becomes gradual.

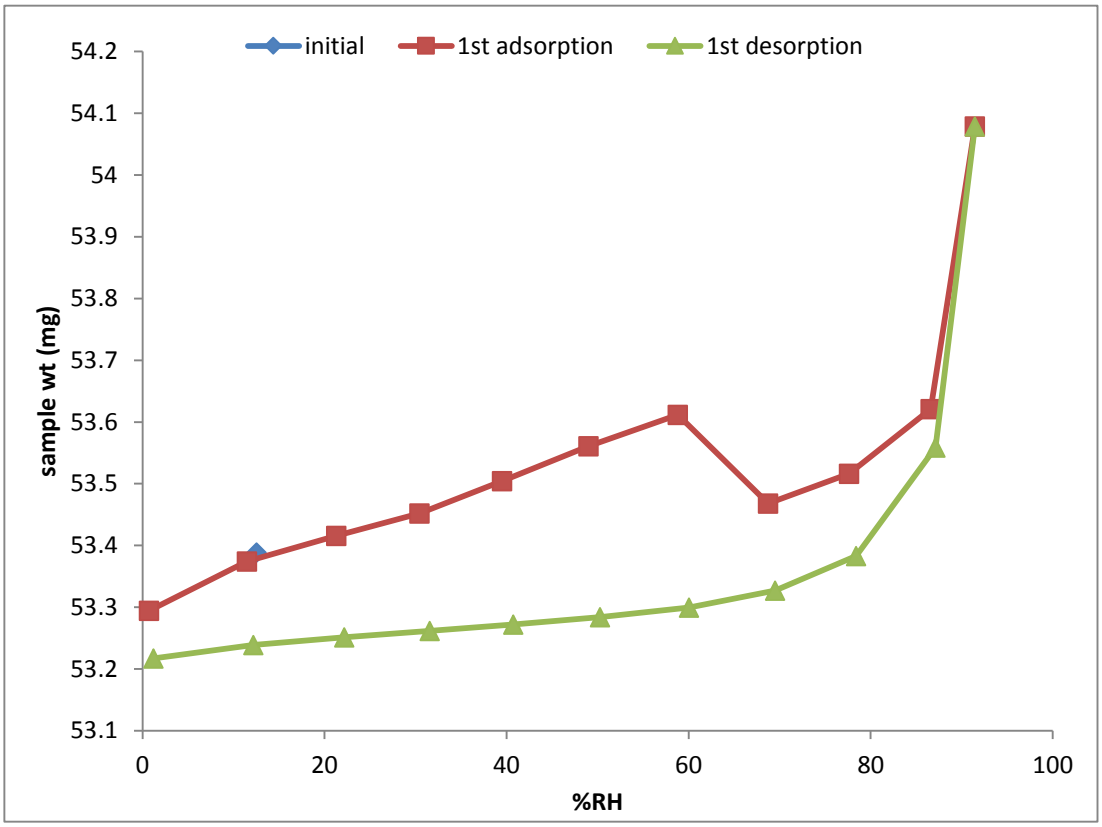

Figure 5.9. DVS isotherm for lactose monohydrate

5.6 Powder X-Ray Diffraction

PXRD patterns were obtained for each material using the method described in 2.4.4.

5.6.1 Results of XRPD analysis for lactose monohydrate

The PXRD diffractogram of lactose monohydrate is shown in Figure 5.10. The pattern is consistent with those reported in the literature (Lerk et al.; 1984A). The diffractogram indicates a high degree of crystallinity which is expected for this material.

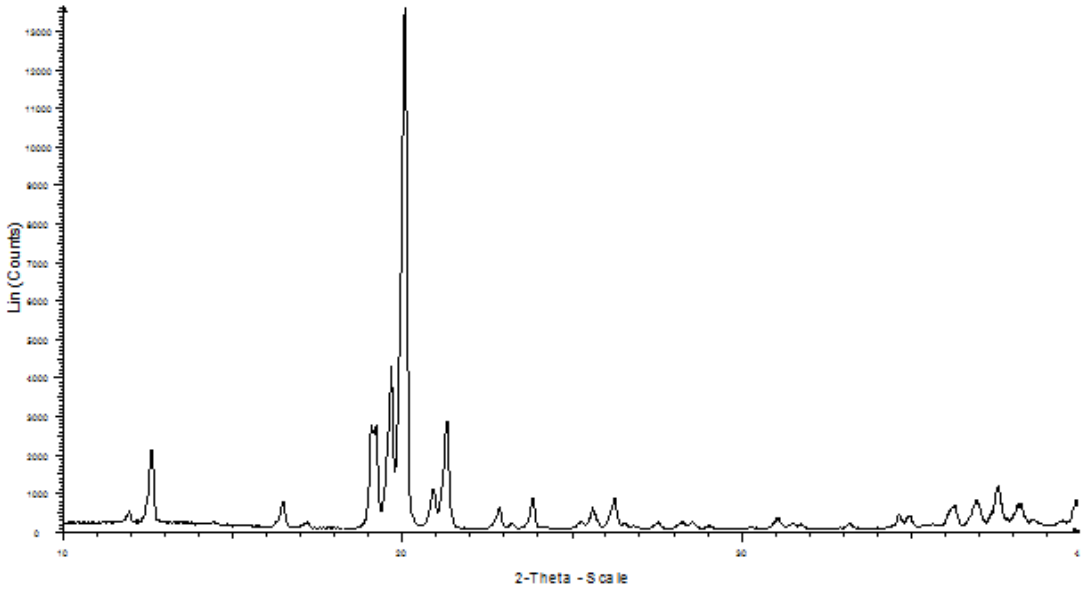

Figure 5.10. Representative PXRD pattern for lactose monohydrate

5.6.2 Results of XRPD analysis for anhydrous lactose

The PXRD diffractogram of anhydrous lactose is shown in Figure 5.11. The presence of a characteristic peak at 10.5°2θ helps distinguish this β polymorph from the anomeric equivalent.

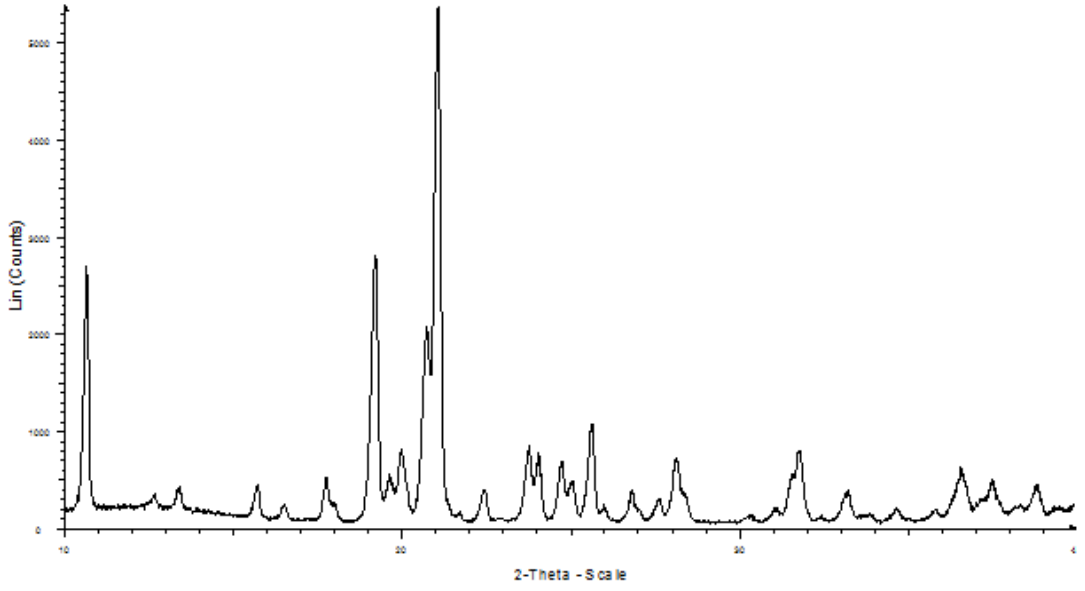

Figure 5.11. Representative PXRD pattern for anhydrous lactose

5.6.3 Results of XRPD analysis for freeze dried lactose

The PXRD diffractogram of freeze dried lactose is shown in Figure 5.12. The analysis confirms that the material has amorphous character, which is indicated by the characteristic broad halo.

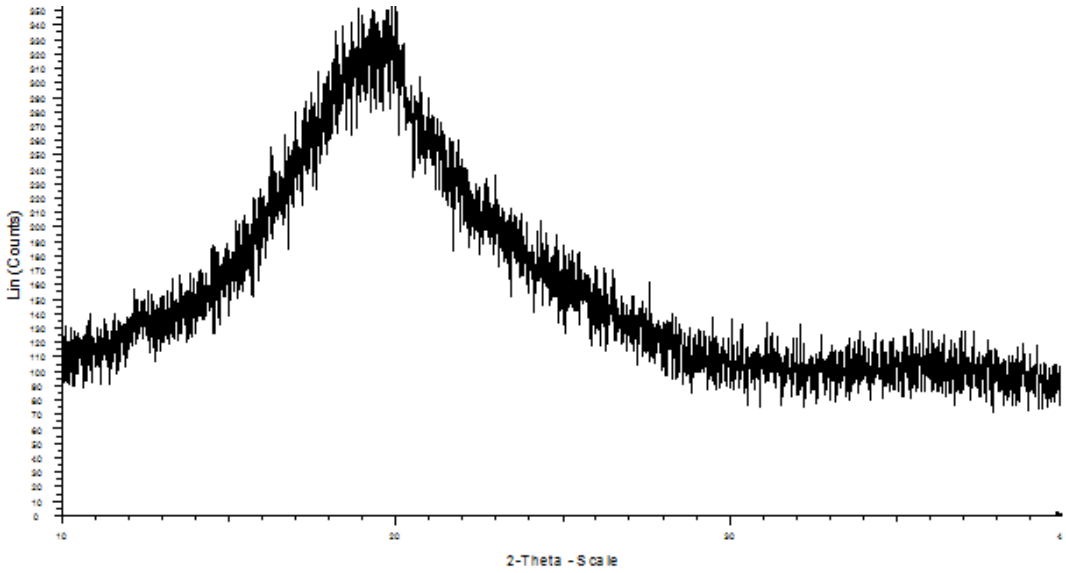

Figure 5.12. Representative PXRD pattern for freeze dried lactose

5.6.4 Results of XRPD analysis for spray dried lactose

The PXRD diffractogram of spray dried lactose is shown in Figure 5.13; analysis confirms that the material has amorphous character which is signified by the characteristic broad halo. However, it is evident that some low levels of crystallinity are present. This may be a direct result of the PXRD analysis; the material is hygroscopic in nature, so is able to pick up moisture which can facilitate conversion. Or it may be due to the spray drying process not completely producing amorphous material.

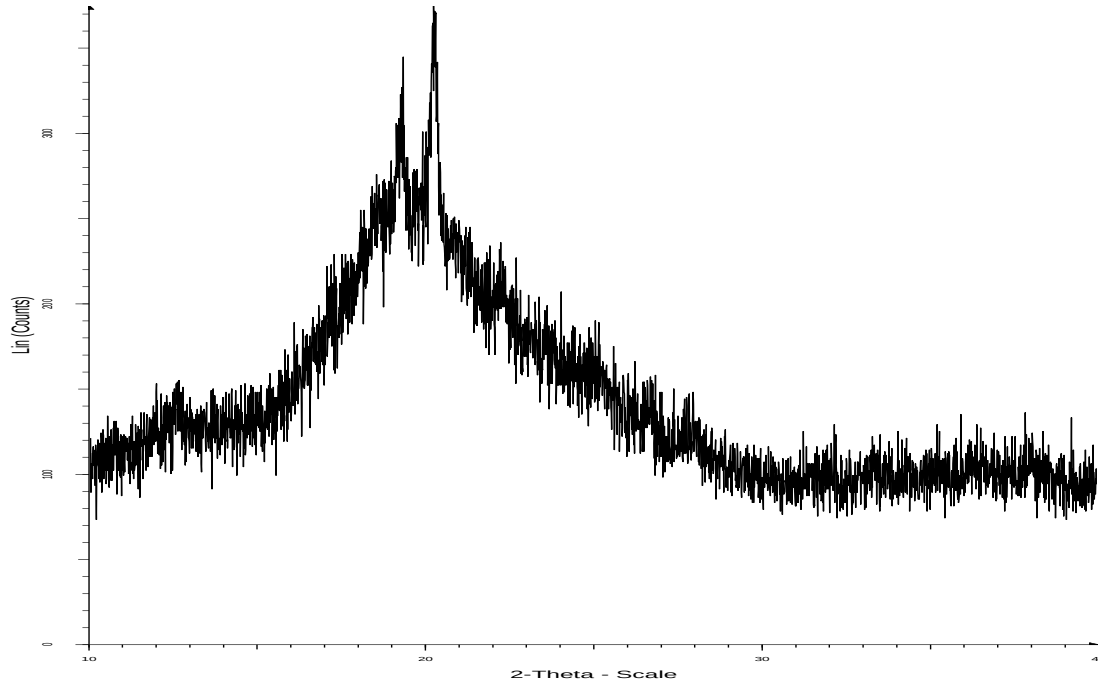

Figure 5.13. Representative PXRD pattern for spray dried lactose

5.7 Scanning electron microscopy

SEM pictures were obtained for each material and were used to visualise the shape, size and surface morphology initially of materials used within this work.

5.7.1 SEM results for lactose monohydrate

A representative SEM micrograph is shown in Figure 5.14 which displays the typical tomahawk shape. Some irregular surfaces are visible, which probably occur as a direct result of the manufacturing process.

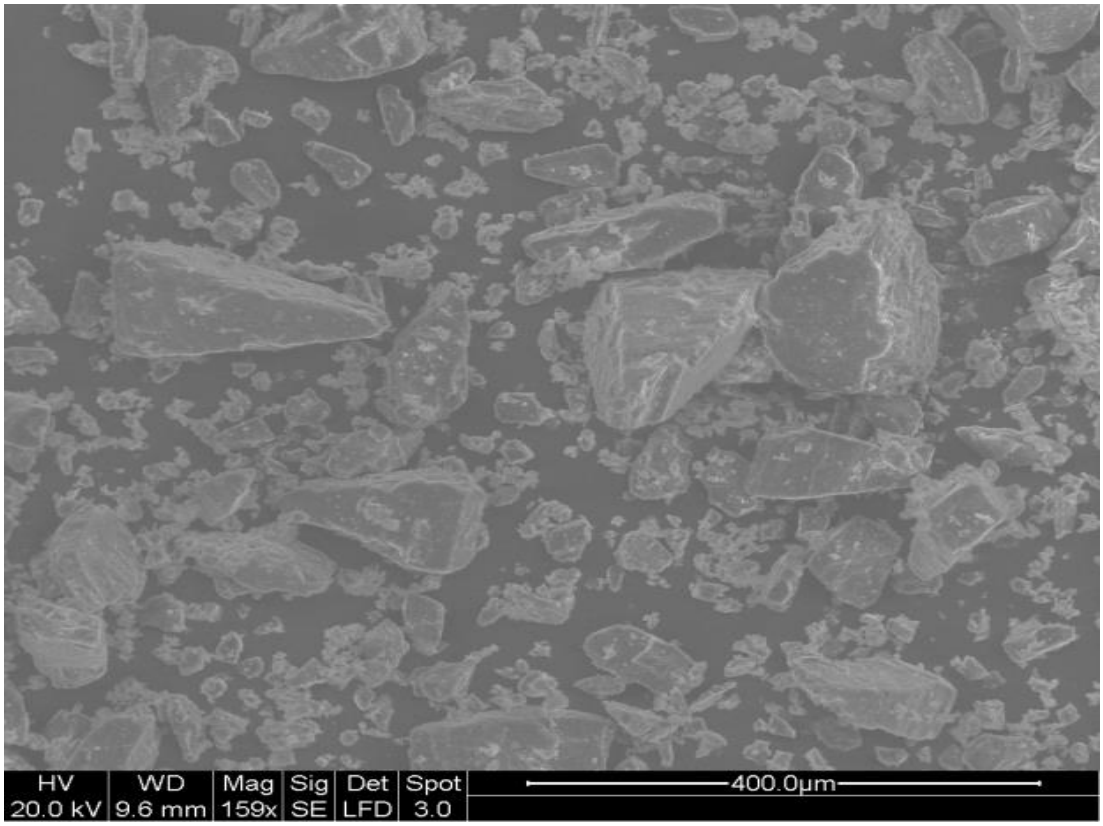

Figure 5.14. Representative SEM micrograph for lactose monohydrate

5.7.2 SEM results for anhydrous lactose

A representative SEM micrograph is shown in Figure 5.15. Anhydrous lactose exhibits rougher and more irregular surfaces than those seen for lactose monohydrate. A possible reason for this is due to the dehydration process.

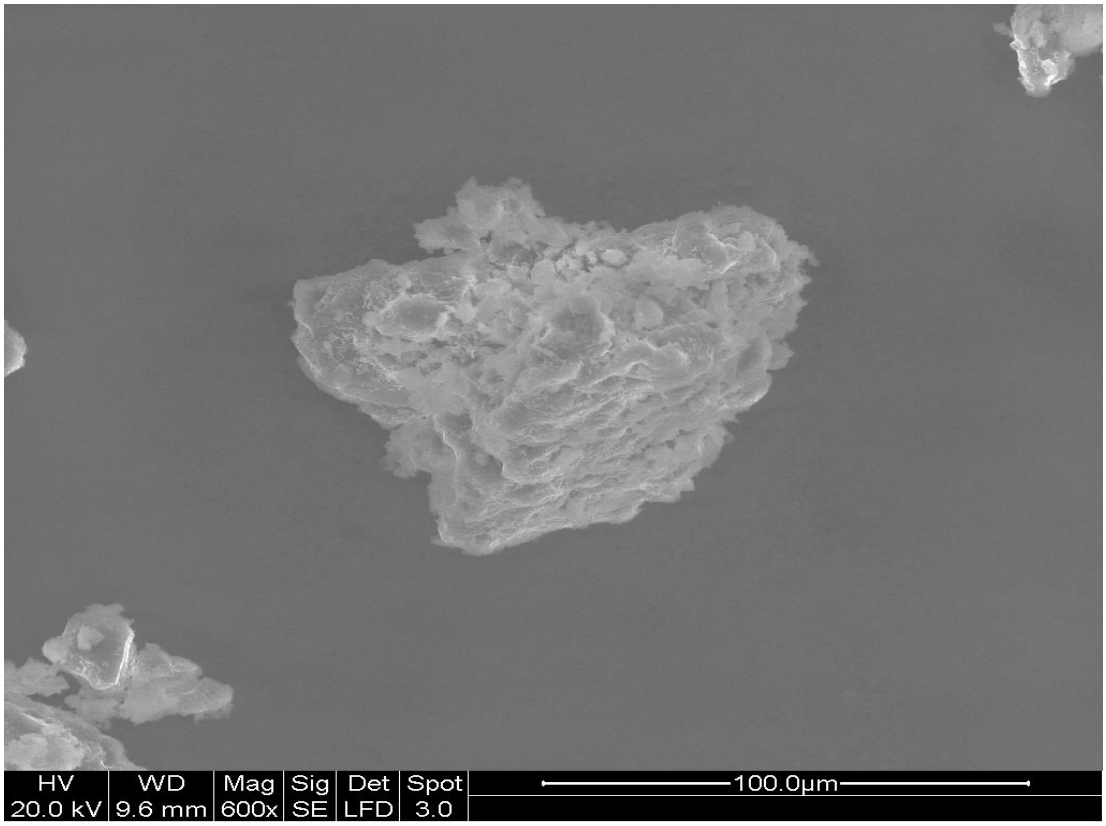

Figure 5.15. Representative SEM micrograph for anhydrous lactose

5.7.3 SEM results for freeze dried lactose

The representative SEM micrograph Figure 5.16 shows that freeze dried lactose bears a resemblance to a fractured plane of window glass.

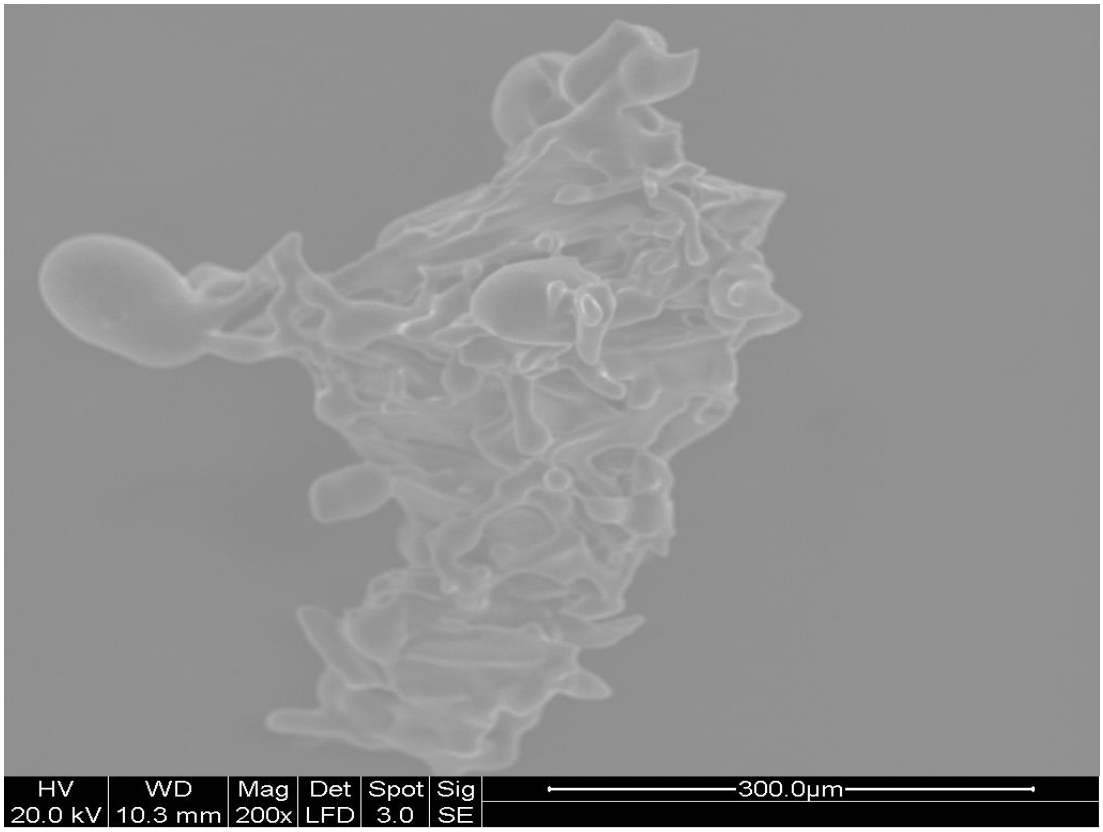

Figure 5.16. Representative SEM micrograph of freeze dried lactose

5.7.4 SEM results for spray dried lactose

A representative SEM micrograph is shown in Figure 5.17. Spray dried lactose exhibits spherical particles which are characteristic of the general morphology of a spray dried amorphous material. The image further reveals that all surfaces are smooth without any cracks. Such features are in complete contrast to the amorphous material produced by the freeze drying process.

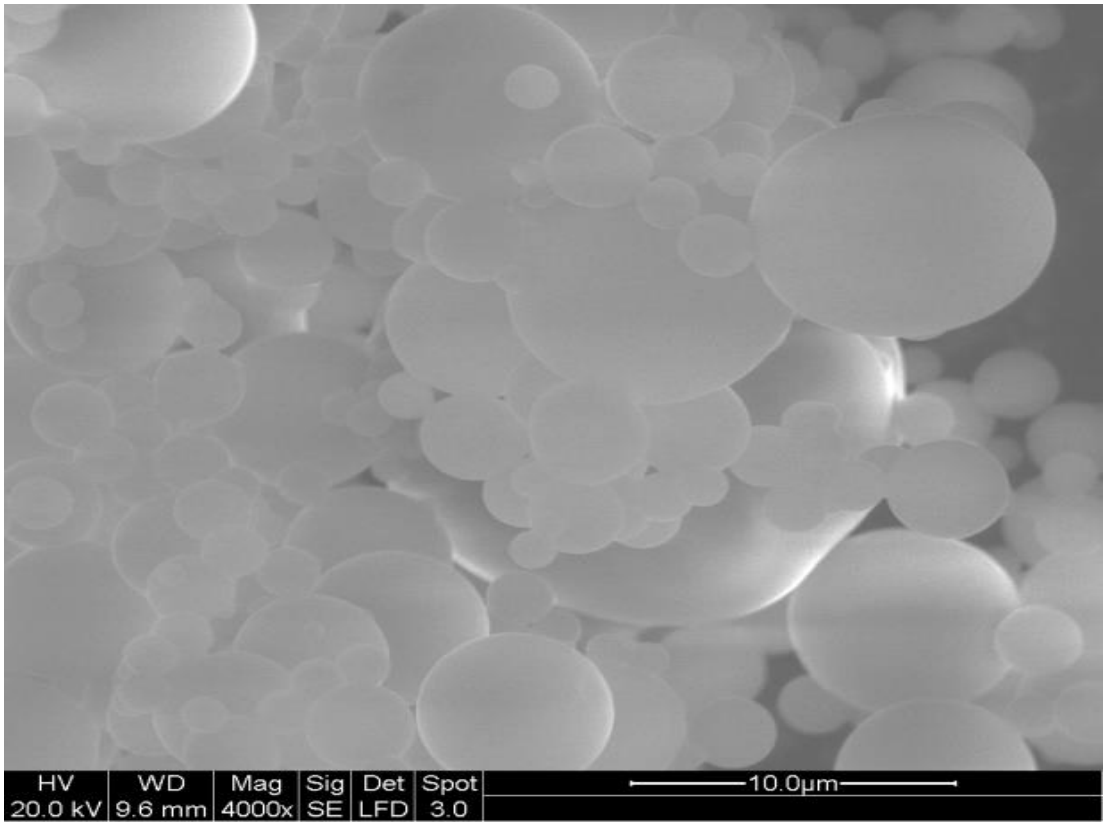

Figure 5.17. Representative SEM micrograph of spray dried lactose

5.8 Moisture profiling

Moisture profiling analysis is able to provide a novel way of evaluating the behaviour of moisture within materials, by considering the ERH that is generated by the material. The different forms of lactose were each subjected to moisture profiling analysis as described in section 2.4.6, in order to determine if the samples exhibited different ERH's and see how the moisture associated with the materials behaved in a closed environment.

5.8.1 Moisture profiling analysis results for lactose monohydrate

The moisture profile for lactose monohydrate is shown in Figure 5.18 and shows that lactose monohydrate exhibits an ERH in this instance of 40.9 %RH (±0.9 %RH, n=3).

The behaviour exhibited by the material within the sample chamber is also of importance. The material shows an initial increase in %RH before reaching equilibrium. This behaviour is indicative of the material exchanging moisture with the sample environment. In this case moisture is given out from the material to the sample chamber environment.

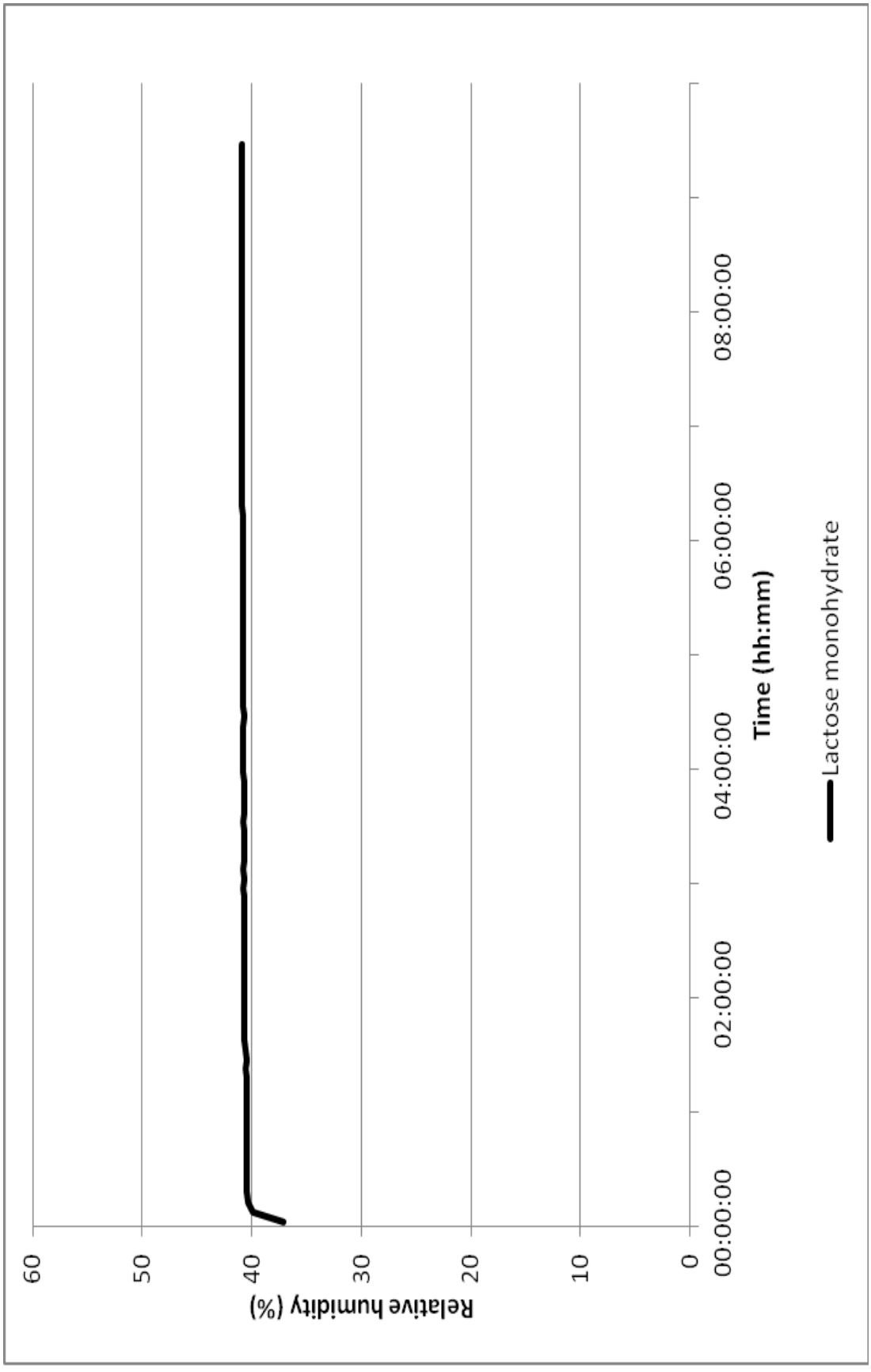

Figure 5.18. Representative moisture profile for lactose monohydrate

5.8.2 Moisture profiling analysis results for anhydrous lactose

The moisture profile for anhydrous lactose is shown in Figure 5.19 and shows that anhydrous lactose exhibits a ERH of 35.3 % (± 0.9 %RH, n=3), which is approximately 5% lower than that of the hydrated form.

The behaviour of the material within the sample chamber is also important. The material shows a very slight initial increase in RH before equilibrium is reached. This is indicative of the material giving out moisture to the surrounding sample environment, demonstrating that in this instance anhydrous lactose possesses low hygroscopicity, this property makes it an ideal excipient for moisture sensitive API's.

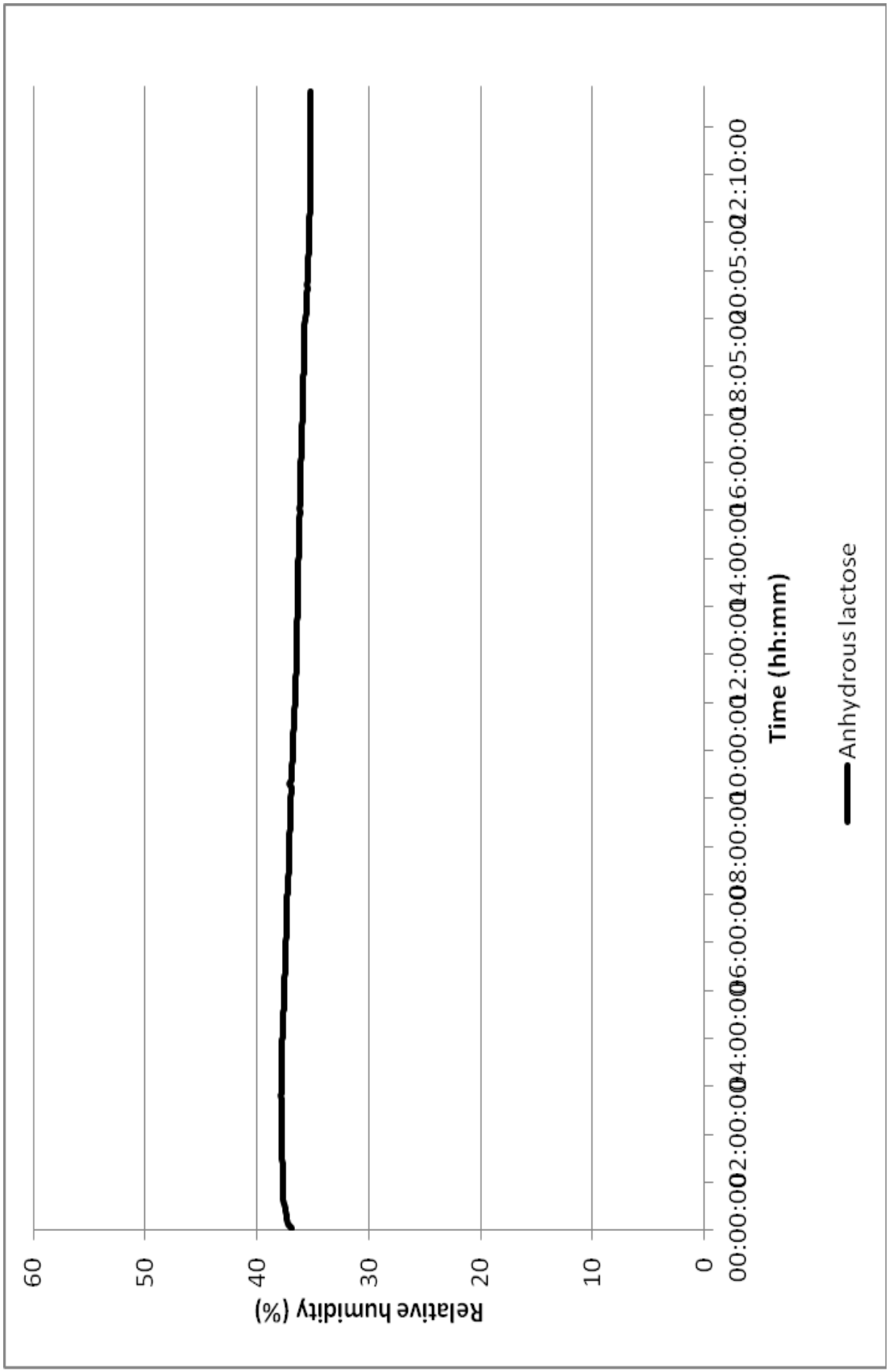

Figure 5.19. Representative moisture profile for anhydrous lactose

5.8.3 Moisture profiling analysis results for freeze dried lactose

A representative moisture profile for freeze dried lactose is shown in Figure 5.20, which exhibits an ERH of 30.4 % RH (±2.6 %RH, n=3).

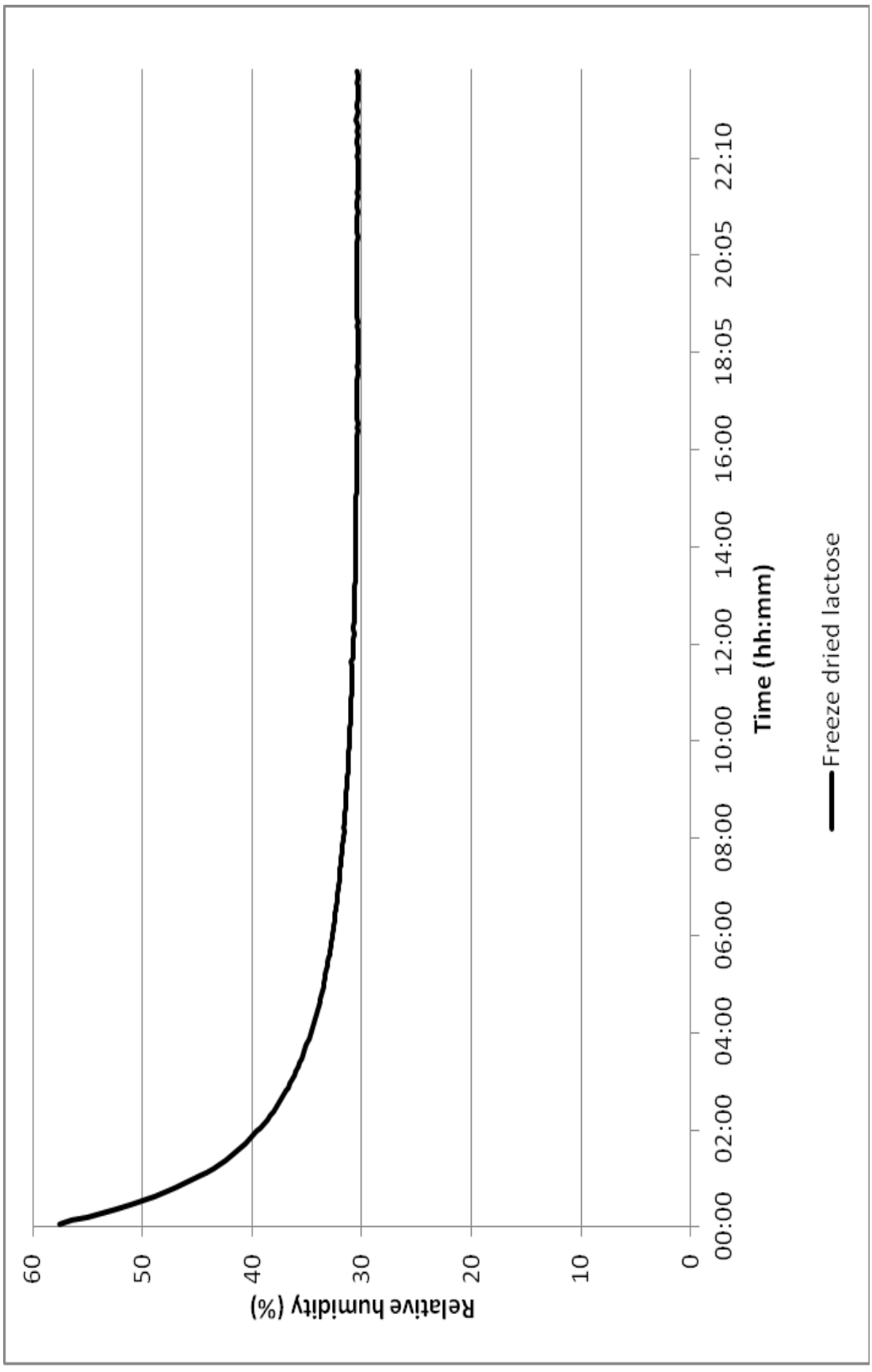

Figure 5.20. Representative moisture profile for freeze dried lactose

5.8.4 Moisture profiling analysis results for spray dried lactose

The moisture profile for spray dried lactose is shown in Figure 5.21 and shows that spray dried lactose exhibits an ERH of 28.8 % RH (± 1.0 %RH, n=3). This is the lowest value obtained for all the forms.

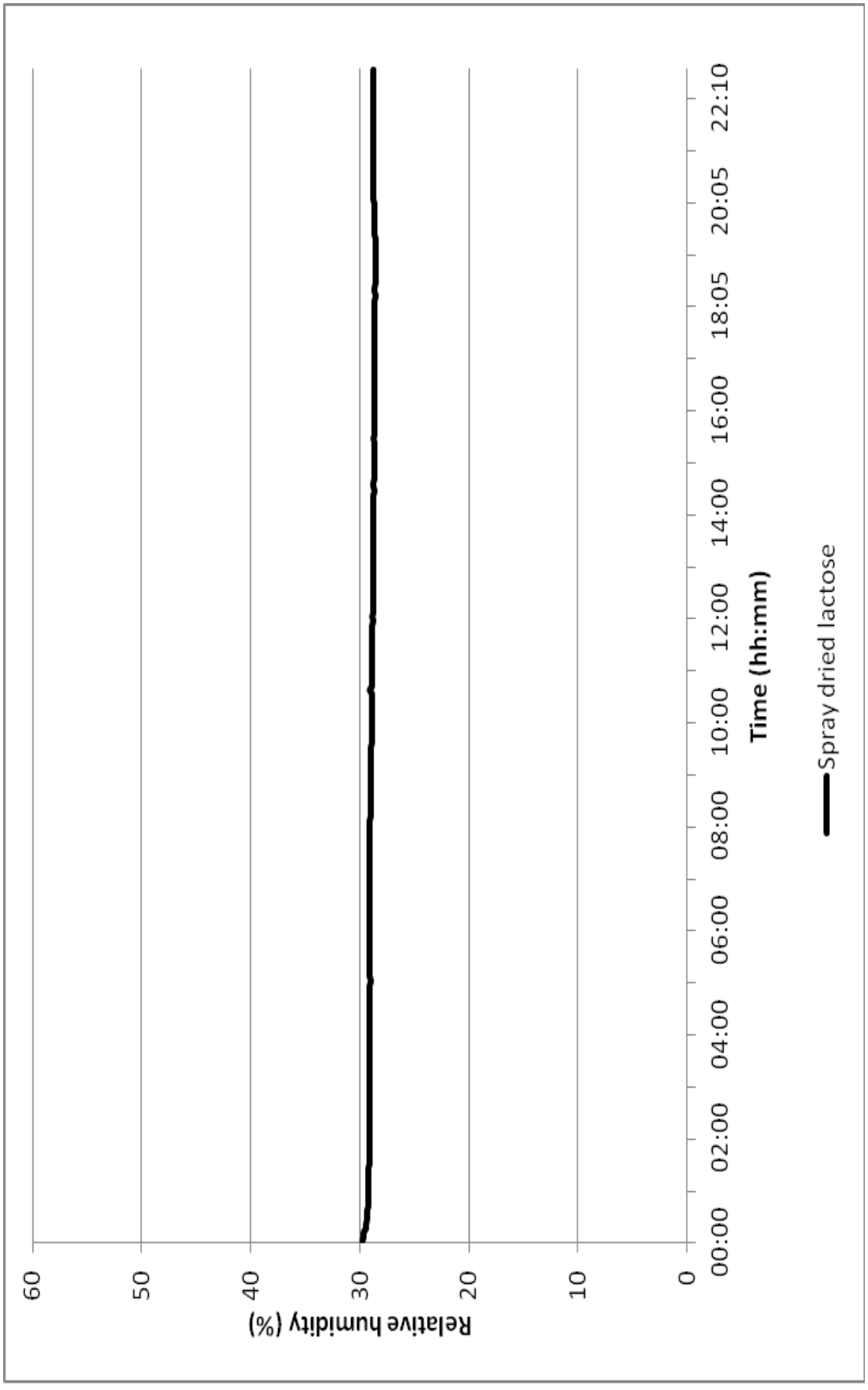

Figure 5.21. Representative moisture profile for spray dried lactose

5.9 Conclusion

Complete thermal and structural characterisation of the four different forms of lactose to be used in the experimental work was completed using a variety of analytical techniques.

The various techniques employed have shown that they can be used to complement each other and give in-depth information on the polymorphic forms and hydration/dehydration behaviour of lactose. Thermal analysis showed that recrystallization of amorphous lactose occurs when freeze/spray dried lactose is heated and is a well reported method of detecting/characterising amorphous material. This difference in physicochemical character could also be detected by the moisture profiler which showed distinct differences between the spray/freeze dried material and the starting materials. These benchmark measurements will be used to see if moisture profiling can detect solid-state changes on processing.

To evaluate the sensitivity of the moisture profiler to more subtle physical changes a series of samples will be stored and tabletted under various conditions. The results are presented in the following chapters.

6 INVESTIGATION IN TO THE USE OF MOISTURE PROFILING TO EXPLORE PHYSICAL FORM CHANGES DUE TO HUMIDITY

6.1 Introduction

Process induced changes and storage stability of both raw API and final dosage form are of major concern within the pharmaceutical industry (Dalton and Hancock, 1997). Any changes in either physical or chemical properties can result in a loss of highly valuable materials and manufacturing time or in extreme cases can lead to product recalls. Process and storage induced changes include the physicochemical changes of recrystallization and polymorphic conversion. The characterisation of these physical changes is extremely important when developing dosage forms and a great deal of analytical effort and instrument advances are constantly being developed to aid in this analytical challenge. Conventional methods are sometimes time consuming and lack sensitivity so new technology that can save both time and money whilst increasing sensitivity of detection and an understanding into material characteristics is extremely attractive to the pharmaceutical industry. Polymorphic conversions and recrystallisation of partial or wholly amorphous systems can be induced by moisture both during processing and storage (Strydom et al., 2009). It is therefore essential to establish the relationship between moisture and dosage forms and APIs as part of the development process. The concept of monitoring ERH with time has been has been developed (by Relequa), as a unique tool for moisture profiling and can give information on the behaviour of moisture within pharmaceuticals.

We have used the moisture profiler to analyse a series of well characterised model compounds of different physical forms, both amorphous and crystalline, to

establish if moisture profiling can predict/measure the polymorphic and amorphous to crystalline conversion within samples.

6.2 Objective

The primary objective is to examine and assess if moisture profiling is able to detect and therefore distinguish between any changes that may occur in the different physical forms upon storage.

The material used to determine the suitability and sensitivity of the moisture profiler in order to detect changes in physical form was lactose as it is widely used in industry and its physical behaviour is well reported in the literature (Garnier et al., 2008, Listiohadi et al., 2009). The two different physical forms of lactose that were selected are lactose monohydrate and freeze dried lactose. They have differing physical properties; lactose monohydrate has two polymorphic forms which may interconvert (Kirk et al., 2007). Freeze dried lactose is amorphous and can convert to a crystalline anhydrous form, or if enough moisture is present it can convert to the polymorphic monohydrate form. This complex behaviour will evaluate the robustness and sensitivity of the instrument and also the methods used.

6.3 Method

Samples of lactose monohydrate and freeze dried lactose were initially analysed (t=0), through a variety of analytical techniques; moisture profiling, thermogravimetric analysis, differential scanning calorimetry and powder x-ray diffraction to fully characterise their physical forms prior to experimental work. The initial characterisation would allow for any time dependant physical changes to be detected.

Samples of both materials were then placed into a glass dessicator containing a saturated salt solution, in order to produce a controlled humidity chamber. The saturated salt solution was prepared from analytical grade sodium chloride salt and purified water, giving a RH of approximately 75 % at room temperature (Winston and Bates, 1960). The room temperature was monitored twice daily to ensure that no gross fluctuations in temperature occurred.

The relevant material was placed into a dessicator, then after twenty four (t=24) and seventy two hours (t=72) of storage they were analysed using the techniques that were used before storage.

6.4 Results of assessment of physical form change of lactose monohydrate

6.4.1 Physical form analysis

TGA data (Figure 6.1) shows that the initial dehydration onset is consistent throughout all of the samples, demonstrating similar weight losses of approximately 5% in the region of 105-150°C, which is in agreement with the theoretical molar content of water of hydration associated with lactose monohydrate (Berlin et al., 1971, Abdelwahed et al., 2006, Otsuka et al., 1991, Shukla and Price, 1991). The TGA thermograms display no weight loss below 100°C, suggesting that any free water that was potentially sorbed during storage is not present in large enough quantities to play a significant role or is below the limit of detection for the method used on the TGA. It was anticipated that moisture profiling would be more sensitive to determine if any free water is present by comparing the ERH readings of t=0 to t=24 and t=72.

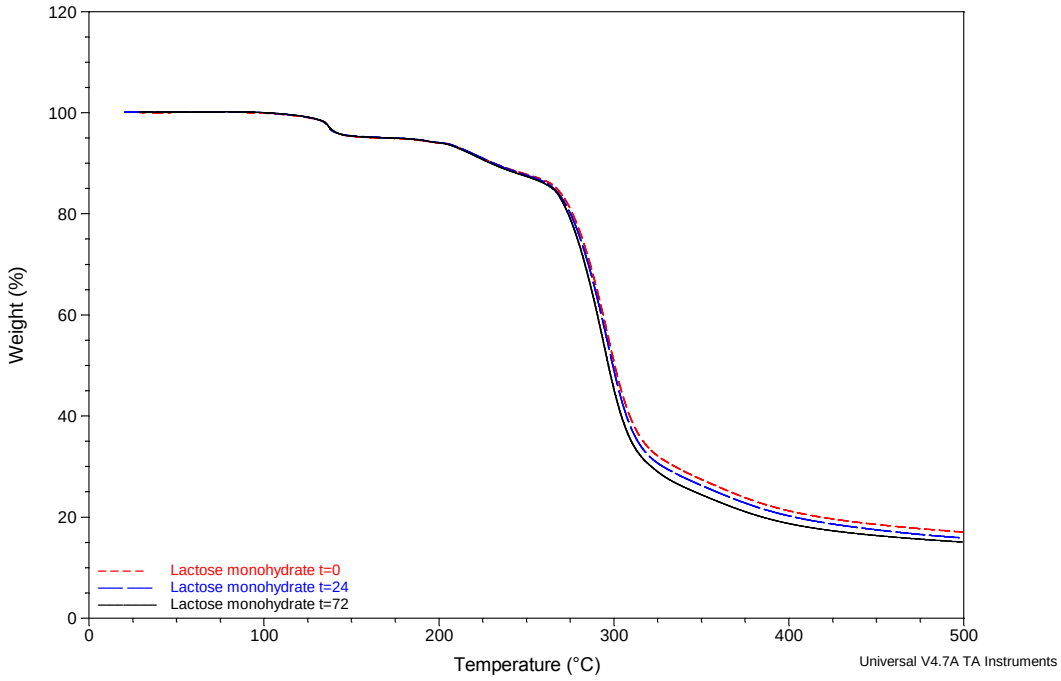

Figure 6.1. Representative TGA thermal profiles for lactose monohydrate after storage at 75% RH at t=0, t=24 and t=72

Figure 6.2 shows the DSC thermal profiles of lactose monohydrate after storage at 75% RH at t=0, t=24 and t=72, the DSC results are summarised in Table 6.1.

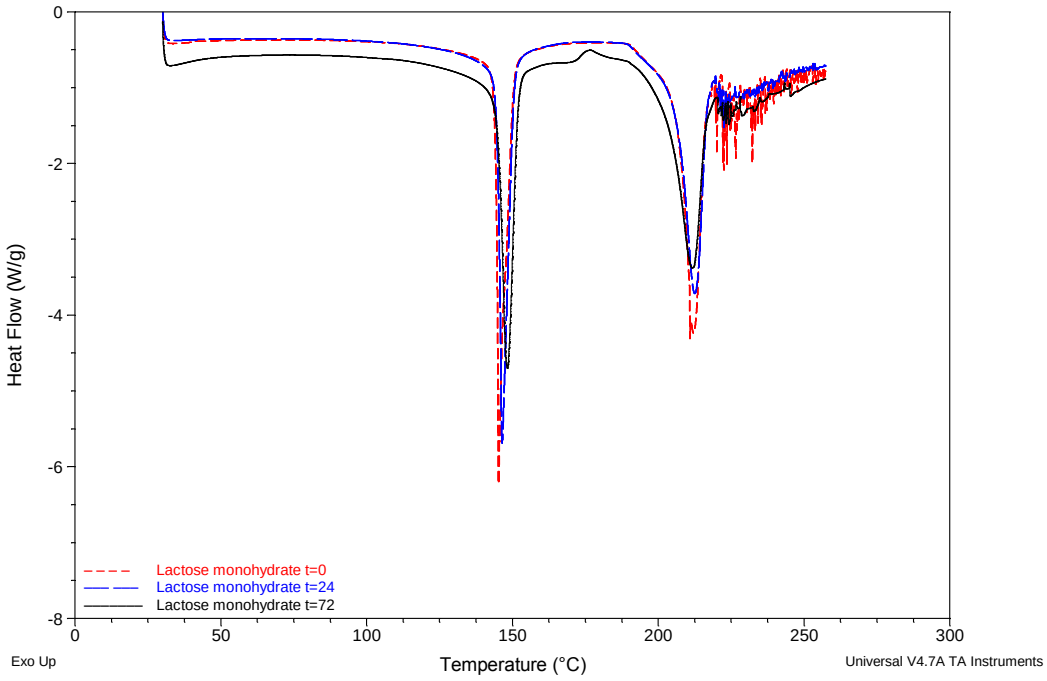

Figure 6.2. Representative DSC thermal profiles for lactose monohydrate after storage at 75% RH at t=0, t=24 and t=72

The DSC profiles for lactose monohydrate at t=0 and t=24 both show two similar endothermic peaks. The first endotherm at approximately 145°C is due to dehydration of the crystalline lattice water (Berlin et al., 1971). Dehydration occurs in several steps; firstly cleavage of interactions between lactose and water, followed by vaporisation of water and then the conversion of the crystal lattice (Khankari et al., 1992). The second endotherm observed at approximately 211°C is the melting of the crystalline solid, once melted the material then undergoes decomposition (Berlin et al., 1971, Listiohadi et al., 2009).

The representative DSC profiles for lactose monohydrate at t=72 hours is different from the t=0 and t=24 profiles. The same endothermic events at approximately

145°C and 211°C are present, which have previously been attributed to dehydration and melting respectively. However, an exothermic peak in the region of 176°C is observed, analysis of the TGA thermal profiles shows that there is no substantial weight loss associated with this exotherm. This therefore suggests that the peak is due to mutorotation of α-lactose to the β lactose which is reported in the literature (Listiohadi et al., 2009). This is feasible because all of the tightly bound crystal lattice water may not have been removed during the first endothermic event. Thereby the residual water that remains is sufficient enough to facilitate mutorotation above temperatures of 150°C (Listiohadi et al., 2009, Shariare et al., 2011.). It is likely that storage at elevated RH acted as an extra source of moisture and thereby aided the mutorotation process.

Table 6.1. Summary of DSC thermal profiles for lactose monohydrate obtained at times t=0, t=24 and t=72 hours

Sample	Water of crystallisation		Mutorotation of lactose		Melting	
	Peak Max (°C)	Enthalpy (J/gmol^{-1})	Peak Max (°C)	Enthalpy (J/gmol^{-1})	Peak Max (°C)	Enthalpy (J/gmol^{-1})
t=0	**145.15** (±0.96)	**161.33** (± 6.88)	-	-	**211.59** (± 0.75)	**165.20** (±3.34)
t=24	**146.56** (±0.38)	**164.50** (± 3.58)	-	-	**212.19** (± 0.24)	**159.1** (± 6.10)
t=72	**147.99** (±0.20)	**167.53** (± 2.72)	**176.31** (± 0.28)	**5.99** (± 0.52)	**211.01** (± 0.58)	**155.07** (± 1.60)

To establish if polymorphic conversion of lactose could be induced by increased humidity a sample was subjected to DVS analysis. The DVS isotherm for lactose are shown in Figure 6.3. In the first adsorption step the sample gradually increases in weight, and then at 60% RH a weight loss can be seen followed again by gradual

weight increase up to approximately 90% RH where a sharper increase in weight is observed. This behaviour is characteristic of a polymorphic conversion; exposure to the high humidity causes the initial polymorphic form to change into the second polymorph. Upon polymorphic conversion there is a small amount of water lost due to changes in the lattice structure, as the lattice changes water is free to move and is expelled. Having changed to the second polymorph the behaviour of the sample in the second adsorption is noticeably very different to the first confirming that a change of physical form has occurred. There is no gross hysteresis visible indicating that higher order hydrates (i.e. di- or tri-) are formed after the first desorption. There is a small difference in the initial weight on the first and second isotherms; this may be due to the slight differences in water content of the two polymorphs.

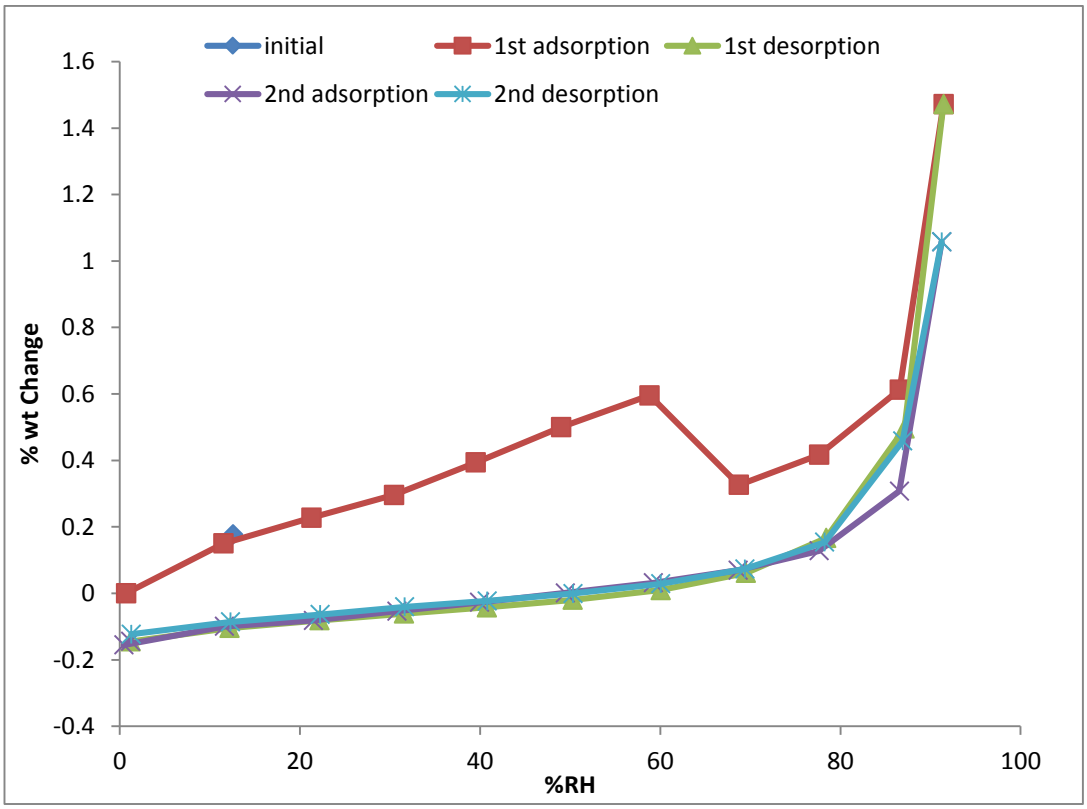

Figure 6.3. DVS isotherm for lactose monohydrate

PXRD of lactose monohydrate at t=0, t=24 and t=72 are shown in Figure 6.4. The individual PXRD patterns obtained are consistent with the α-lactose monohydrate polymorph and correspond well with those reported in the literature (Lerk et al., 1984a). DSC analysis revealed mutorotation of the different lactose forms. Absence of any peaks associated with the presence of β-lactose, is due to the fact that the mutorotation is facilitated by both the increased storage RH and the increased temperature during the analytical process. This temperature is absent in PXRD analysis so no presence of the β-anhydrous lactose is observed.

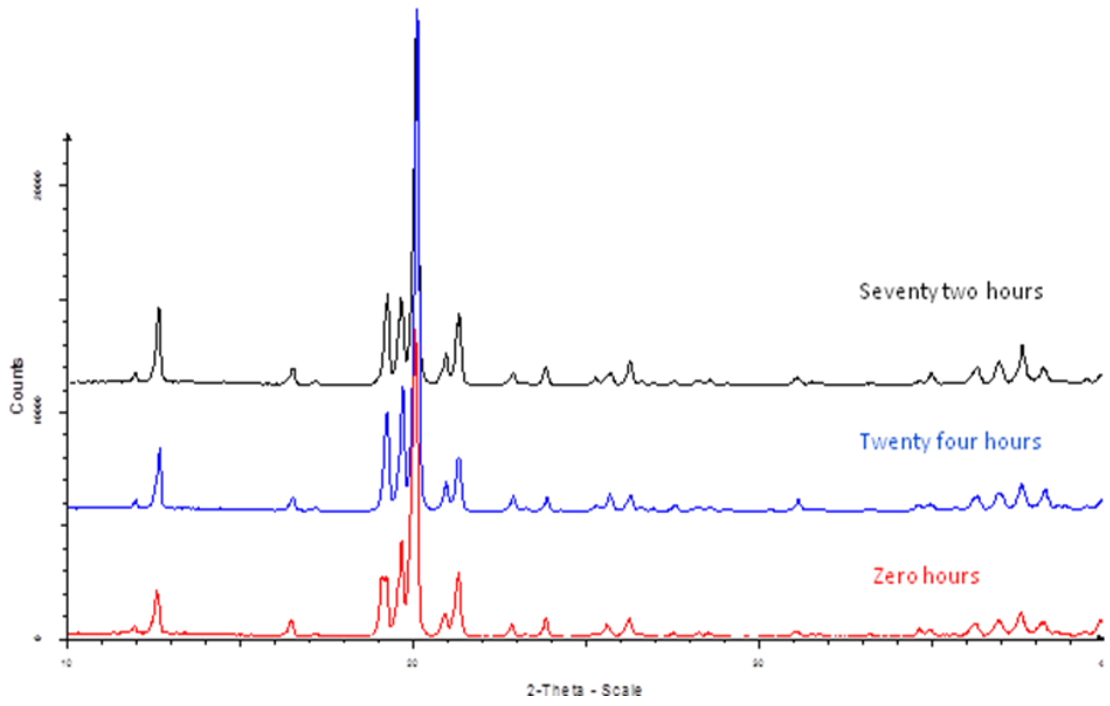

Figure 6.4. PXRD of lactose monohydrate after storage at 75% RH at t=0, t=24 and t=72 hours

6.4.2 Moisture profiling results for lactose monohydrate

Moisture profiling of lactose monohydrate at t=0, t=24 and t=72 showed an increase in the ERH with increasing storage time, with an overall ERH increase of 2.771% (between t=0 and t=72). Representative moisture profiles for lactose

monohydrate at t=0, t=24 and t=72 can be seen in Figure 6.5 and the final %RH which is consequently the point taken to be the ERH of the material, is summarised in Table 6.2.

The behaviour exhibited by the samples within the moisture profiler is also important and can be readily visualised in real time during analysis. In this case, all samples give rise to similar ERH values; however the behaviour during the analysis is visibly different. Both t=0 and t=24 samples show an initial increase in %RH, before then reaching equilibrium with the surrounding test environment. This behaviour indicates that the material is giving out some of the moisture (either crystal lattice or surface) to the atmosphere within the sample chamber. Sample t=72, demonstrates that the sample initially takes in moisture from within the sample chamber, causing the overall internal RH to be lowered, before the ERH of the sample is achieved over time. In this case, the initial behaviour of the material is influenced by the starting %RH of the container, as the final ERH are very similar to each other, and the complementary analysis supports that no physical changes had occurred.

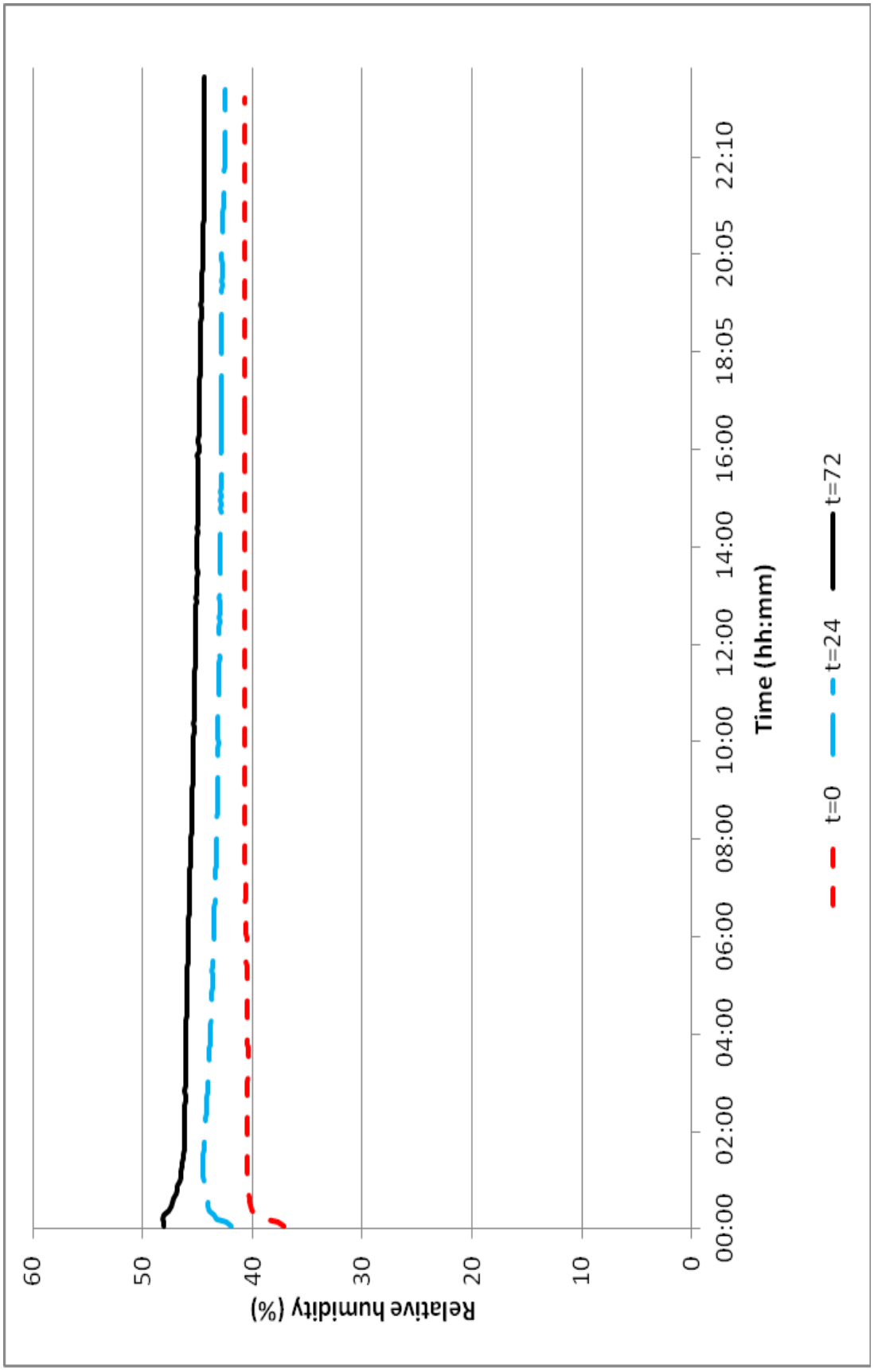

Figure 6.5. Moisture profiles for lactose monohydrate obtained after storage at 75% at times t=0, t=24 and t=72 hours

Table 6.2. Final ERH readings for lactose monohydrate obtained at times t=0, t=24 and t=72 hours

Storage time (hours)	Final % RH	
	Rep 1	Rep 2
t = 0	40.7	45.0
t = 24	42.5	44.9
t = 72	44.4	45.0

The ERH data for lactose monohydrate shown in Table 6.2 illustrates that the only notable differences in the ERH values is for the difference in the ERH readings for the samples t=0 and t=72 (Figure 6.6). This can be attributed to the increased storage RH, allowing water to be adsorbed onto the surface, but not incorporating it into the crystal lattice, resulting in only a slight increase in ERH. Lactose monohydrate adsorbs minimal atmospheric water at RH less than 70% at room temperature, so storage above this (75% RH) gives suitable conditions for atmospheric water to be adsorbed.

The physical analysis carried out in conjunction with moisture profiling reveals that the adsorbed moisture upon the materials surface is negligible as no detectable change in mass is observed in the TGA below 100°C. DSC analysis showed that elevated storage RH and temperature helped to promote muturotation of the different lactose forms, as seen with PXRD analysis, this temperature is absent. As moisture profiling is carried out at a controlled temperature of 25°C no change in form will be induced, so any change in ERH is not due to the conversion of different lactose forms.

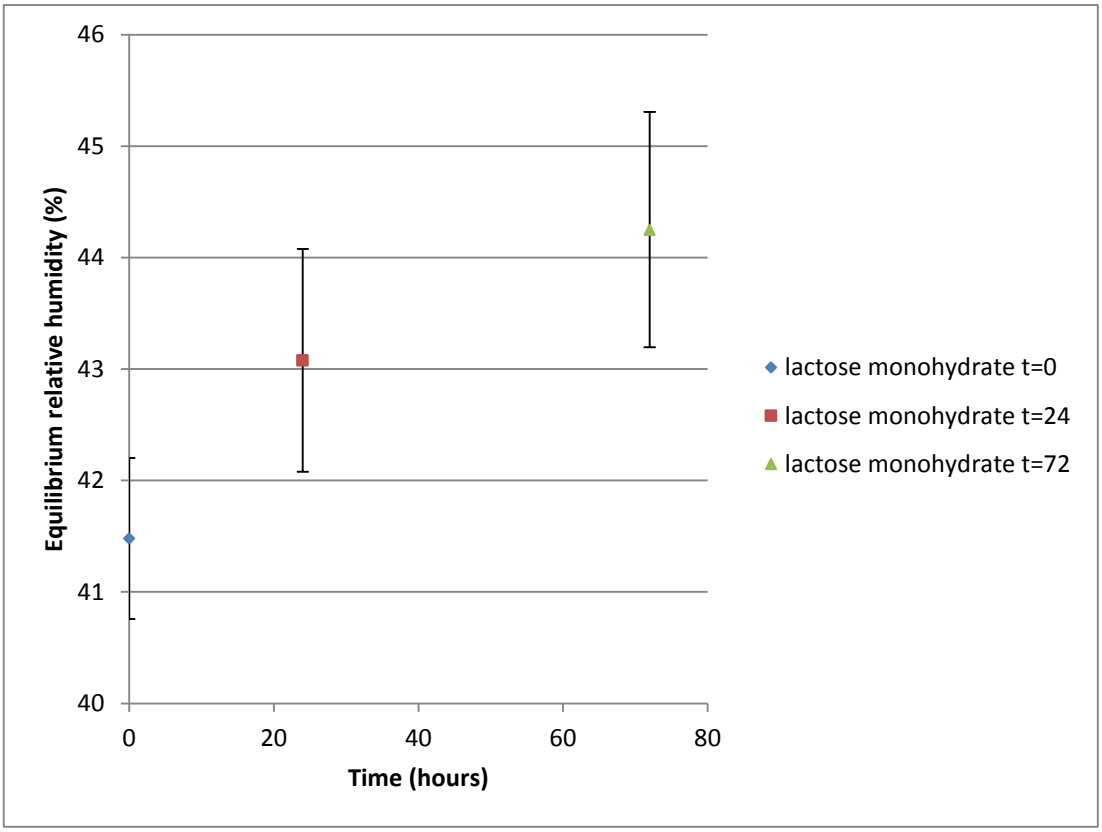

Figure 6.6. Comparison of ERH results obtained for lactose monohydrate at times t=0, t=24 and t=72 hours

6.5 Results of assessment of physical form change of freeze dried lactose

6.5.1 Physical form analysis results for freeze dried lactose

The results from TGA analysis (Figure 6.7) shows that after exposure of freeze dried lactose to 75% RH there is an apparent difference in the thermal profiles of the t=0 and t=24 hour samples, with t=24 and t=72 hour samples exhibiting similar behaviour.

The TGA thermal profile of the initial starting material, t=0, shows three distinctive weight losses. The first weight loss being in the temperature range 30 - 130°C, this is attributed to loss of surface water (Darcy and Buckton, 1997). Between 130-200°C; typical crystallisation of the amorphous lactose is observed, this is evident

due to little fluctuation in weight change over this temperature range. As reported in the literature (Figura, 1993, GombÃs et al., 2002) the crystallisation of the material was confirmed by the presence of an accompanying exothermic peak in further thermal analysis (DSC) , obtained at approximately 190°C (Figure 6.8). The material then melts and simultaneously undergoes decomposition which is indicated by a small weight loss followed immediately by a much larger weight loss on the TGA thermogram.

TGA thermal profiles of the material at t=24 and t=72 hours storage at 75% RH demonstrate similar behaviour to each other but different to that of the material at t=0, suggesting a physical change was induced during the storage at elevated RH. The TGA analysis of material at t=24 and t=72 hours both show TGA behaviour which is characteristic of crystalline α-lactose monohydrate.

The thermal profiles demonstrate three distinct weight losses. The first weight loss observed is due to loss of water due to crystallisation. Literature states the theoretical molar content of water associated with the lactose monohydrate is equivalent to 5% (Berlin et al., 1971, Shukla and Price, 1991, Otsuka et al., 1991). However, the weight loss percentages displayed by t=24 and t=72 are slightly below this expected value, (3.679% and 3.865 % respectively) reiterating the possibility that some amorphicity remains within the sample.

Further heating resulted in a small weight loss followed immediately by a larger weight loss which corresponds to the decomposition on melting of the samples. This is consistent with literature of a TGA thermal profile for α-lactose monohydrate (Figura, 1993, Listiohadi et al., 2009).

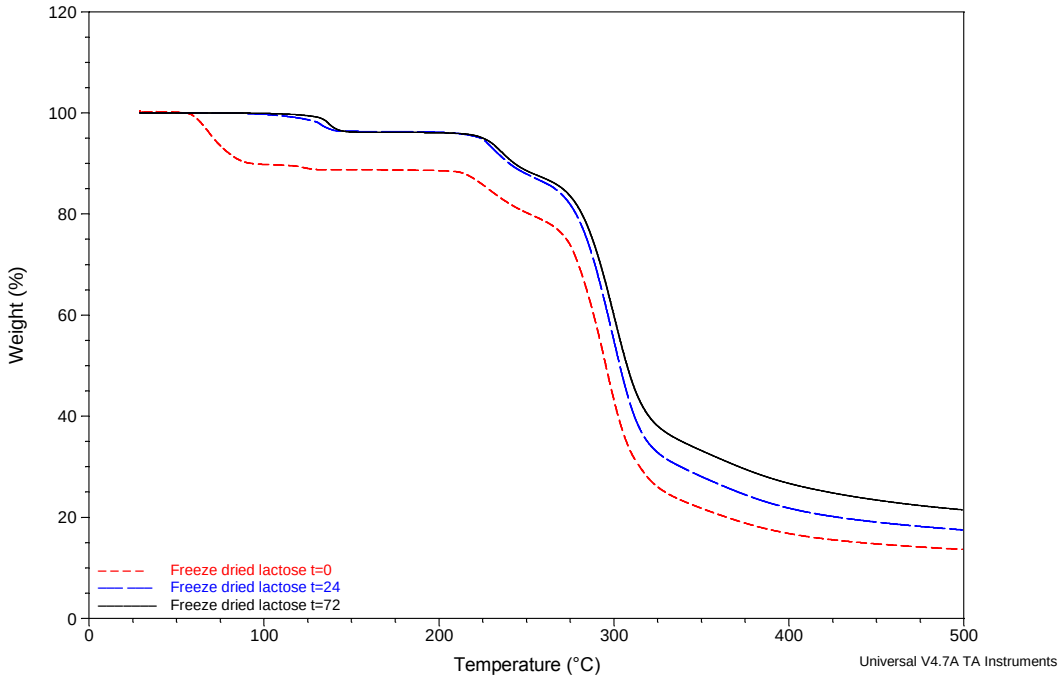

Figure 6.7. Representative TGA thermal profiles obtained for freeze dried lactose after storage at 75% RH at times t=0, t=24 and t=72 hours

Representative DSC thermal profiles for freeze dried lactose after storage at t=0, t=24 and t=72 hours can be seen in Figure 6.8 and a summary of the DSC thermal events in Table 6.3.

The DSC profile for freeze dried lactose t=0 shows a combination of peaks typical of amorphous lactose. The initial broad peak signifies loss of surface water; this is followed by a small exothermic event at approximately 120°C, which is attributed to loss of water of crystallisation, which suggests the material was not completely amorphous, and some crystalline areas remained. An endotherm at approximately 190°C is attributed to crystallisation of the amorphous material, which This is reiterated by the onset of melting of the sample shortly after (Figura, 1993,

GombÃs et al., 2002). Two melting peaks are present at approximately 216°C and 226°C which are attributed to α-lactose melt and β-lactose melt respectively. The thermal profile did not clearly show a curve indicating the glass transition, which would appear before crystallisation onset at 190°C. The glass transition is not always visible in the DSC; especially as the heating rate 10°C/min was employed. The glass transition of dry amorphous lactose is reported to be 101°C (Lloyd et al., 1996).

Both representative DSC thermal profiles for t=24 and t=72 samples evidently exhibit similar behaviour. An endothermic peak is visible at approximately 145°C is attributed to the desolvation of water associated with the crystal lattice, corresponding to literature values (Berlin et al., 1971). It is apparent that the t=72 endotherm peak corresponding to desolvation is sharper, signifying that storage for longer periods of time at elevated RH increases the crystallinity. It is known that exposure to 50% RH or more at 25°C causes amorphous lactose to collapse, trapping water within its mass which then undergoes crystallisation (Buckton et al., 1998). The two melting peaks are also visible in the t=24 and t=72 samples, however, the α-lactose melt is significantly smaller than the β-lactose melt, suggesting that storage at elevated RH not only facilitated crystallisation but also mutorotation of molecules by incorporation of water via a partial alpha structure, causing the β-lactose to be more predominant.

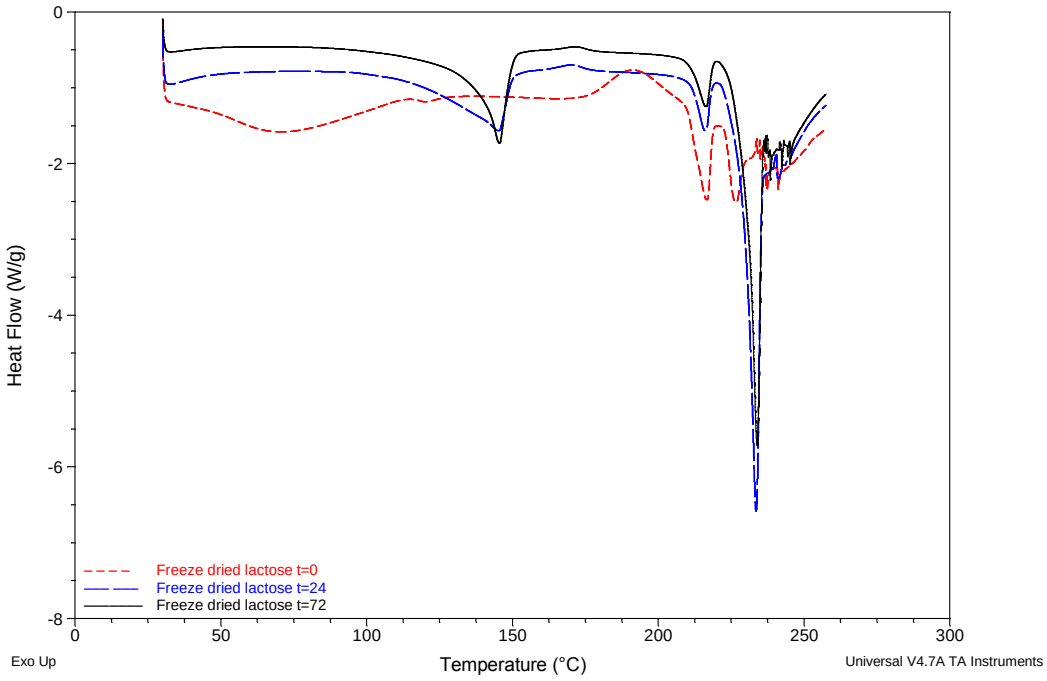

Figure 6.8. Representative DSC thermal profiles obtained for freeze dried lactose at times t=0, t=24 and t=72 hours

Table 6.3. Summary of DSC thermal profiles obtained for freeze dried lactose at times t=0, t=24 and t=72 hours (n=3)

	Water of crystallisation		Crystallisation of amorphous lactose		α-melt		β-melt	
	Peak Max (°C)	Enthalpy (J/gmol^{-1})	Peak Max (°C)	Enthalpy (J/gmol^{-1})	Peak Max (°C)	Enthalpy (J/gmol^{-1})	Peak Max (°C)	Enthalpy (J/gmol^{-1})
t=0	**120.60** (± 0.14)	**2.186** (±0.136)	**191.4** (±0.27)	**42.88** (±3.30)	**216.13** (±0.38)	**44.40** (± 3.37)	**225.56** (±0.40)	**16.33** (± 0.89)
t=24	**145.17** (± 0.08)	**100.31** (± 1.80)	-	-	**215.60** (± 0.21)	**20.08** (± 2.26)	**233.58** (±0.37)	**138.80** (± 1.90)
t=72	**145.30** (±0.15)	**111.00** (± 3.71)	-	-	**216.02** (±0.33)	**26.65** (± 4.25)	**233.22** (±0.54)	**117.53** (± 1.72)

PXRD analysis of freeze dried lactose at times t=0, t=24 and t=72 hours are shown in Figure 6.9. PXRD analysis confirmed that the initial t=0 material was predominantly

amorphous indicated by the characteristic broad halo in the PXRD pattern. Upon storage at 75% RH, PXRD data shows that this amorphous material was converted by a number of processes, into the crystalline state. Compared to the PXRD results for lactose monohydrate starting material, the t=24 and t=72 hour PXRD patterns seem more disordered as demonstrated by broader peaks. The results suggest that the samples are not completely crystalline. The PXRD profiles for these latter samples are consistent with the alpha form of lactose.

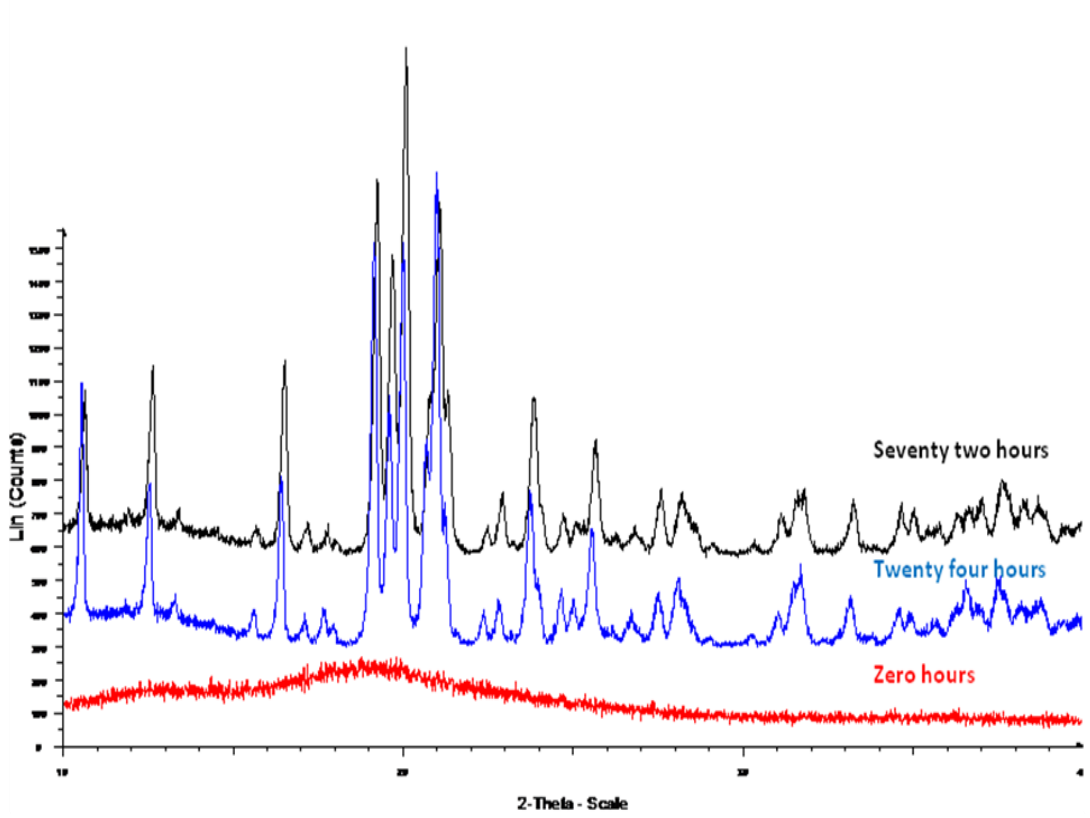

Figure 6.9. PXRD analysis for freeze dried lactose after storage at 75% RH at t=0, t=24 and t=72 hours

6.5.2 Moisture profiling results for freeze dried lactose

Moisture profiles for freeze dried lactose after storage at 75% RH at times t=0, t=24 and t=72 (Figure 6.10) demonstrate that with prolonged exposure to elevated humidity, ERH was also increased, with the overall approximate difference between

t=0 and t=72 being 19%. Representative moisture profiles can be seen in Figure 6.10 and the final ERH readings are summarised in Table 6.4.

The behaviour exhibited by the samples prior to the ERH being attained is also of interest. All samples have similar onset RH's, suggesting that the cause of the behaviour is due to the material. Sample t=0 displays behaviour typical of freeze dried material in that it takes in moisture from within the closed environment, thereby lowering the RH within, and allowing the lower ERH to be achieved. The behaviour demonstrated suggests that the sample is hygroscopic in nature, which is consistent with the physical form analysis carried out confirming that the t=0 sample was amorphous and by nature amorphous lactose is thermodynamically unstable and hygroscopic (Ibach and Kind, 2007).

Conversely the moisture profile data for the samples obtained after storage at t=24 and t=72 hours displays behaviour in the opposite manner. The profiles show that these samples give out moisture to the surrounding environment, before ERH is achieved. The fact that no stable ERH is immediately achieved is suggestive that storage of the samples caused a change within the material, which is consistent with the physical form analysis. Thereby moisture profiling is able to demonstrate that the storage at elevated RH causes the amorphous lactose to absorb moisture as it is metastable (Elmonsef Omar and Roos, 2007, Nickerson, 1962). Subsequent plasticisation increases the molecular mobility and consequently lowers the glass transition temperature (Ibach and Kind, 2007, Zografi and Hancock, 1994). The above is able to promote rearrangement of the lactose molecules into the crystalline state (Roos and Karel, 1990, Troy and Sharp, 1930, Slade et al., 1991).

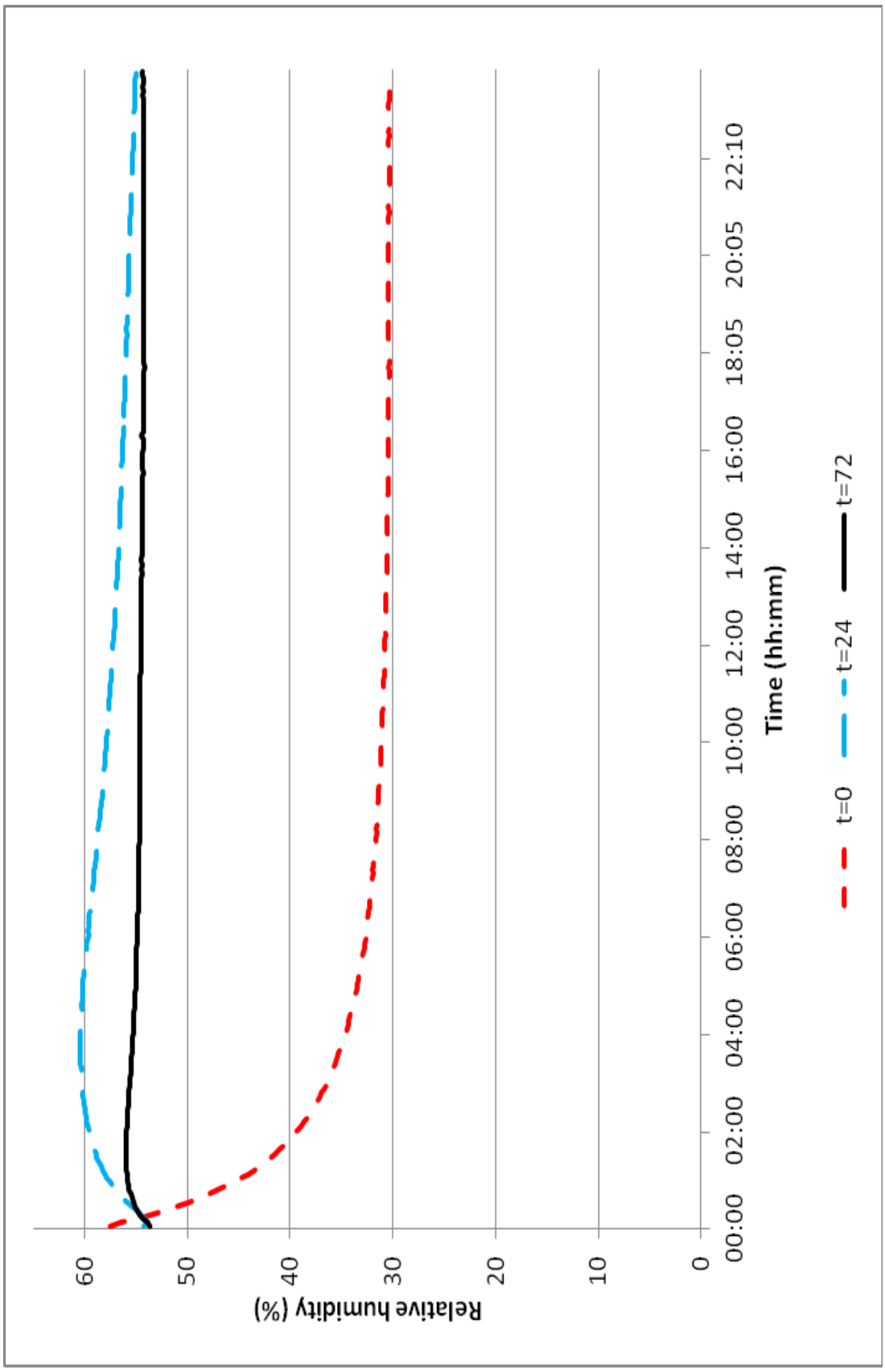

Figure 6.10. Representative moisture profiles obtained for freeze dried lactose after storage at 75% RH at time t=0, t=24 and t=72 hours

Table 6.4 Final ERH readings obtained for freeze dried lactose at time t=0, t=24 and t=72 hours

Storage time (hours)	Final % RH	
	Rep 1	Re 2
t = 0	30.4	32.7
t = 24	55.0	56.5
t = 72	54.3	54.3

In terms of the final ERH obtained, data shown in Table 6.4 indicates that the only notable difference in the data is between t=0 and t=24 hours. The difference is substantial and evidently corresponds with storage of the samples and the physical form changes associated with this. Therefore, this notable difference is expected to occur due to a change in free water within the sample.

No notable difference in the final ERH value is observed between the t=24 and t=72 hour samples. This finding is consistent with the prior conversion from amorphous lactose to crystalline lactose. Although it is necessary to highlight that there is a difference in the shape of the moisture profiles of the t=24 and t=72 hour samples. As previously discussed and can be seen in the moisture profiles, the behaviour of both samples with regards to the general shape is the same; moisture is given out to the surroundings. However, for the t=72 moisture profile the expression of moisture into the sample chamber to raise ERH is not as large. The suggested explanation for this is that higher levels of free water are initially available in the t=24 hour sample and it is not fully converted to the crystalline form (consistent with disorder shown in PXRD data) and that after t=72 hours the sample exhibits behaviour more consistent with that of crystalline lactose monohydrate due to the

prolonged exposure to the elevated storage RH, suggesting its more stable due to increased crystallinity.

A slight decrease in the final ERH is observed between t=24 and t=72 hours, which is attributed to a decrease in free water. Storage at elevated RH brought about adsorption and absorption of moisture to the material surface. The increased storage time has allowed the adsorbed moisture to cause a physical form change within the material. This is supported by an increase in crystallinty in the physical form analysis.

If left for a longer storage period of time it is expected that the ERH would continue to decrease until a ERH value similar to that of the lactose monohydrate at t=0 is attained, where the water is predominantly incorporated within the lattice rather than remaining adsorbed on the surface.

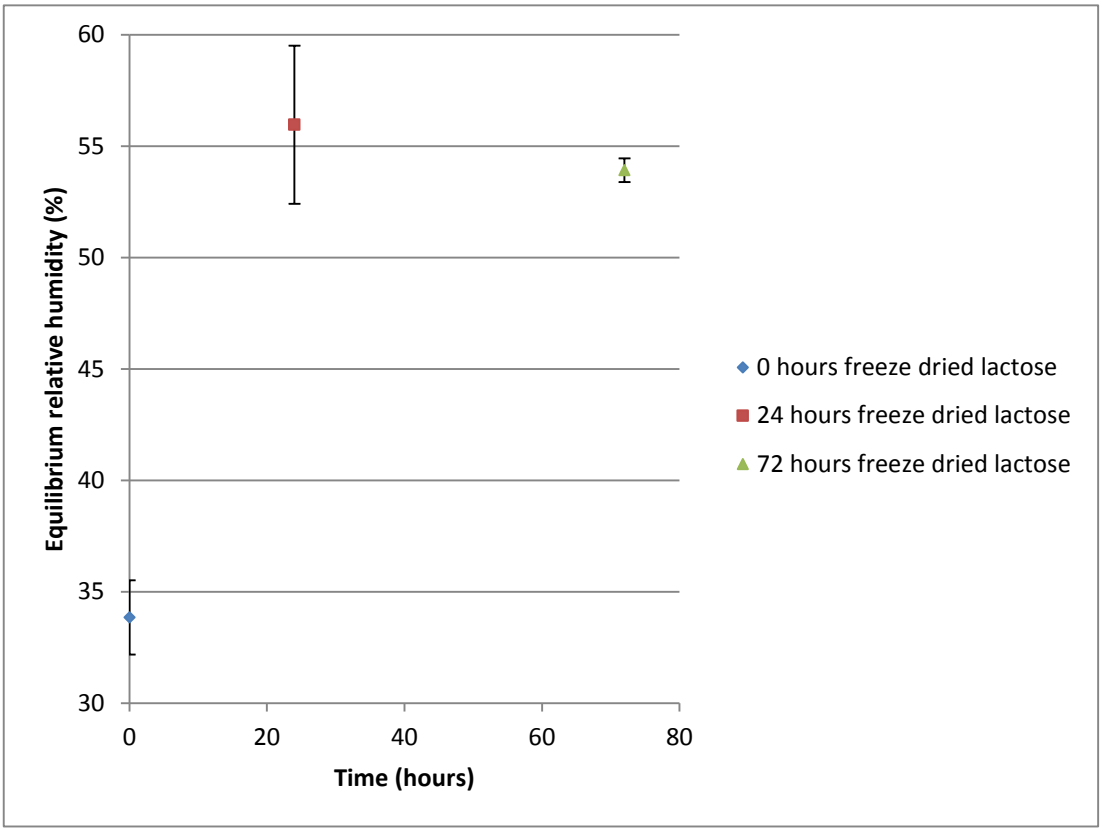

Figure 6.11. ERH results for freeze dried lactose after storage at 75% RH at t=0, t=24 and t=72 hours

6.6 Conclusion

The ability of moisture the profiling instrument to reflect physical changes within lactose samples was probed. Moisture profiling was able to clearly distinguish between the crystalline and amorphous forms of lactose, with amorphous freeze dried lactose generating a lower ERH value than crystalline lactose monohydrate.

Moisture profiling was also able to detect that upon storage at elevated RH, no physical change occurred with the lactose monohydrate sample, which was confirmed by supplementary analysis. Moisture profiles for the storage of freeze dried lactose reflected that a physical change had occurred upon storage at elevated RH. The physical changes were confirmed by supplementary analysis. Therefore, moisture profiling was successful in detecting the change from

amorphous to crystalline lactose upon storage at high relative humidity. In the next chapter the use of moisture profiling to detect changes in a sample on processing will be explored.

7 THE USE OF MOISTURE PROFILING TO ASSESS THE EFFECT OF COMPACTION FORCE ON DIRECTLY COMPRESSED LACTOSE TABLET EQUILIBRIUM RELATIVE HUMIDITY

7.1 Introduction

Direct compression is viewed as the method of choice for manufacturing tablets containing moisture sensitive API's and excipients (Jivraj et al., 2000). Compaction of pharmaceutical powders is employed in order to increase powder density, attain minimal porosity and create maximum inter-particulate contact, so that robust tablets can be produced.

Compaction behaviour is different for the various forms of lactose (Shah et al., 2008), all which have been extensively studied and documented in literature (Busignies et al., 2004, Ziffels and Steckel). It has even been demonstrated that for the same crystal form, different grades from different suppliers are able to exhibit different powder properties due to manufacturing (Whiteman and Yarwood, 1988). Compaction can cause physical form conversion of materials, which may hinder any favourable compaction properties that the material possesses. It also may consequently cause the bioavailablity of an API present within the final formulation to be altered (Blanco et al., 2010).

It is therefore essential to establish the effect of processing, in this instance the effect of direct compression upon the behaviour of moisture within material. In this chapter we test the hypothesis that moisture profiling can be used in order to monitor free moisture changes within materials that are due to direct compression.

7.2 Objectives

The overall aim was to evaluate the effect upon ERH and consequently the behaviour of lactose on applying a range of compaction forces during the direct compression process of tablet manufacture. This was completed by:

- Examining the solid state properties of material before compaction.
- Examining the solid state properties and the resultant crushing and tensile strengths and how these are affected by increasing compaction force.
- Examining the ERH value and moisture profiles before and after storage and compaction.

Lactose was chosen as the material of investigation because it is widely used within the industry and therefore its physical behaviour is well documented throughout the literature (Garnier et al., 2008, Listiohadi et al., 2009). Three different physical forms of lactose were selected to be studied; lactose monohydrate, anhydrous lactose and spray dried lactose. As they all exhibit differing physical properties and they are therefore able to behave differently under compaction it was consequently anticipated that they would behave differently in the moisture profiler.

7.3 Methods

Samples of lactose monohydrate, anhydrous lactose and spray dried lactose were obtained (Section 2.3) and tabletted using direct compression. Direct compression of the tablets was performed using a single punch die. The material was weighed on an analytical balance and manually poured into the 10 mm circular die. The weight of material used was kept constant at 450 mg (± 1.99 mg) throughout, producing

tablets of approximately 4.7 mm in thickness. Various compaction forces were employed; these were 25, 30, 35 and 40 kN. In order to fully characterise the physical form and detect any physical changes upon compaction, the resultant tablets and initial powder were analysed through a variety of analytical techniques; TGA, DSC, PXRD crushing and tensile strength was also measured. The extensive characterisation would help in any interpretation of ERH data.

7.4 Lactose monohydrate; Results and discussion

7.4.1 Thermo gravimetric analysis results for lactose monohydrate compacts

The results of TGA analysis (Figure 7.1) show that all samples display similar behaviour whether compacted or not. All samples have the same initial dehydration onset and demonstrate an approximate 5% weight loss in the region of 105-150°C, which is consistent with the theoretical water content of α-lactose monohydrate (Berlin et al., 1971, Otsuka et al., 1991). The data therefore suggests that compaction of the lactose monohydrate causes no notable change in the amount of moisture contained within the material. Subsequent moisture profiling analysis may be able to show if the location of the moisture has been affected by compaction.

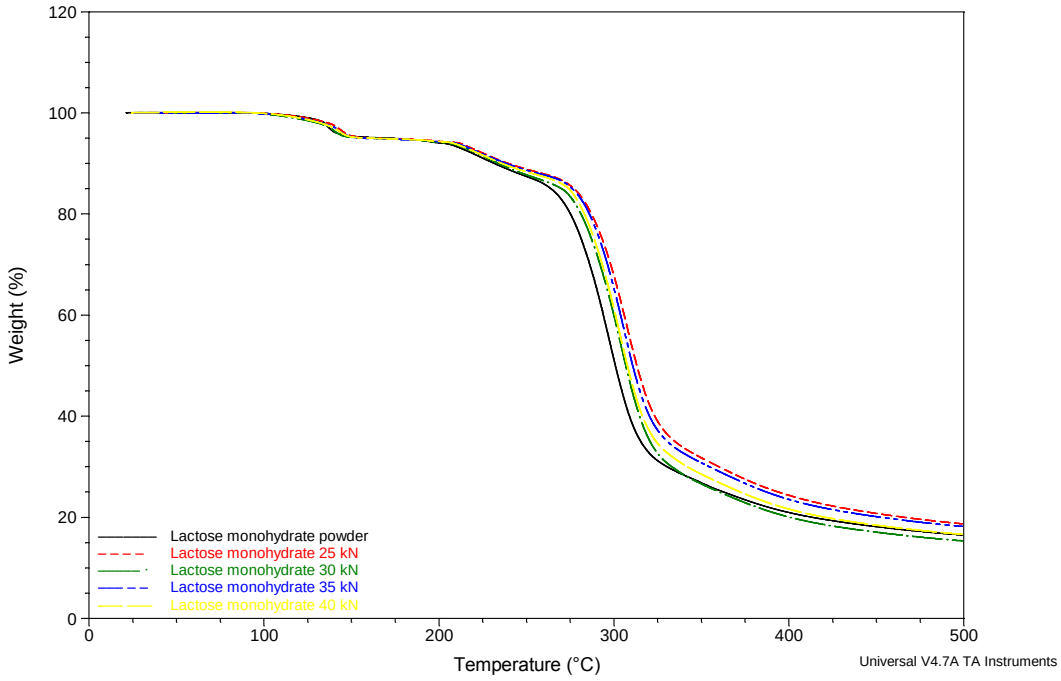

Figure 7.1. Representative TGA thermal profile for lactose monohydrate tablets under direct compression at 25, 30, 35 and 40 kN pressures

7.4.2 DSC results for lactose monohydrate compacts

DSC analysis of the effects of compaction upon lactose monohydrate showed that all the thermal profiles demonstrated the characteristic peaks associated with the material (Figure 7.2 and Figure 7.3). The first endotherm at approximately 145°C is due to dehydration of the crystal lattice (Lerk et al., 1984a). High temperature is required to remove the crystalline water from within the lattice as the water is secured by an extensive hydrogen bonding network. While the second endotherm at approximately 212°C is due to melting of the crystalline solid, the material then undergoes decomposition (Lerk et al., 1984a, Lerk et al., 1984b).

Figure 7.2 shows the effects of compaction of lactose monohydrate at 25 kN, as already mentioned no polymorphic changes have been induced and the material

still exhibits the characteristic peaks. However, it is noticeable that there is a decrease in the position of the dehydration endotherm upon compaction. This is likely to be due to the compaction process disrupting the crystal lattice. Therefore it is easier for the water to be removed, so a subsequent decrease in the temperature required to cause dehydration is observed. Figure 7.3 shows DSC analysis for further directly compressed lactose monohydrate tablets at increasing compaction pressures, with the general trend being that decrease in the temperature of the dehydration endotherm (Table 7.1) relative to the starting material are observed. This behaviour is accompanied by a general decrease in enthalpy associated with the endotherm.

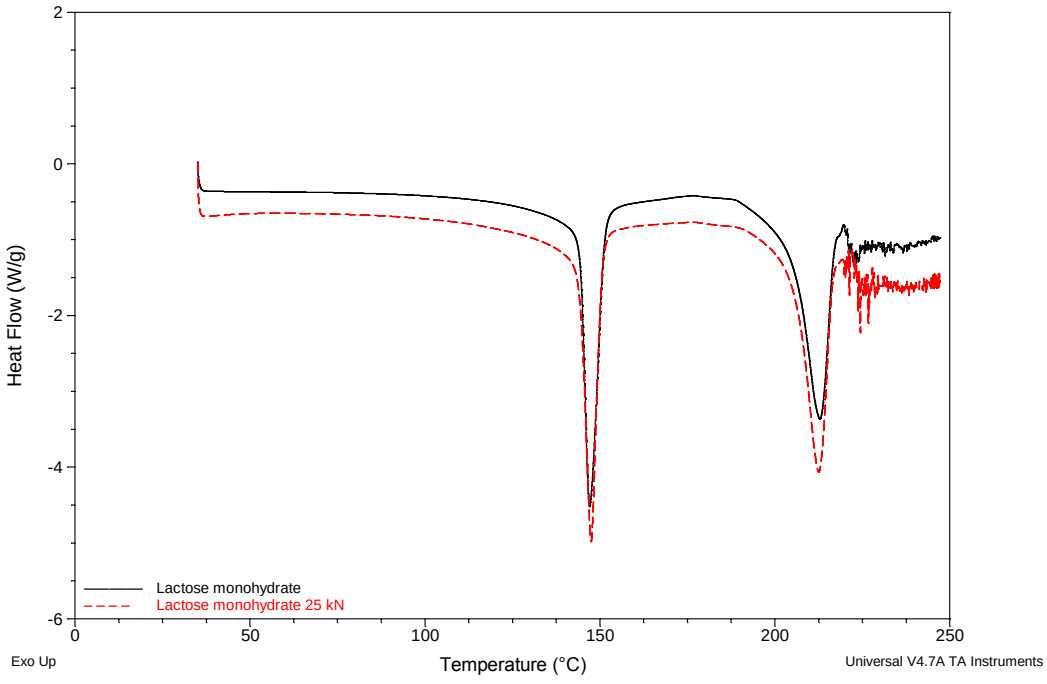

Figure 7.2.Representative DSC thermal profiles for lactose monohydrate powder and direct compression tablet at 25 kN.

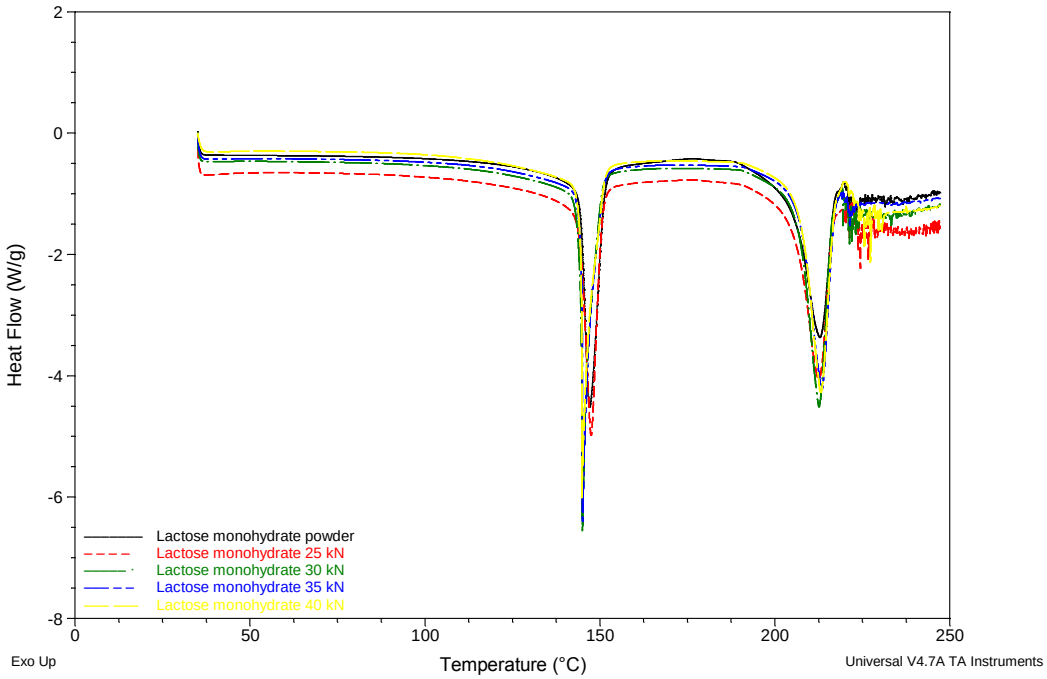

Figure 7.3. Representative DSC thermal profiles for lactose monohydrate powder and tablets under direct compression at 25, 30, 35 and 40 kN force.

Table 7.1. Summary of DSC results for lactose monohydrate powder and direct compression tablets at 25, 30, 35 and 40 kN.

	Dehydration endotherm (°C) Peak max	Dehydration enthalpy (J/g)	Melting endotherm (°C) Peak max	Melting enthalpy (J/g)
Powder	**147.07** (± 0.27)	**170.2** (± 2.9)	**212.58** (± 0.22)	**157.6** (± 0.8)
25 kN	**146.67** (± 0.74)	**181.5** (± 0.8)	**212.39** (± 0.20)	**157.7** (± 0.1)
30 kN	**145.16** (± 0.55)	**170.1** (± 1.2)	**212.69** (± 0.30)	**150.1** (± 3.3)
35 kN	**144.33** (± 0.69)	**162.6** (± 3.7)	**212.91** (± 0.29)	**154.1** (± 2.9)
40 kN	**145.07** (± 0.99)	**166.5** (± 2.1)	**212.64** (± 0.31)	**158.0** (± 6.5)

7.4.3 Powder x-ray diffraction results for lactose monohydrate compacts

PXRD patterns of lactose monohydrate powder and direct compression tablets were obtained (Figure 7.4). All PXRD patterns are consistent with literature patterns (Kirk et al., 2007, Lerk et al., 1984b). Figure 7.4 demonstrates that PXRD analysis of the ground compacted material shows very minimal decrease in the relative intensity of the diffraction maxima. However, no notable transformations of the lactose monohydrate are visible. This suggests any transition that may have occurred due to compaction could have only taken place on the tablet surface, and PXRD is infamous for its insensitivity towards detection of small amounts of disorder. Complementary DSC analysis was previously carried out (Figure 7.3 and Table 7.1) and showed a decrease in the dehydration onset, suggesting slight disruption of the crystalline water molecules with the crystalline lactose monohydrate.

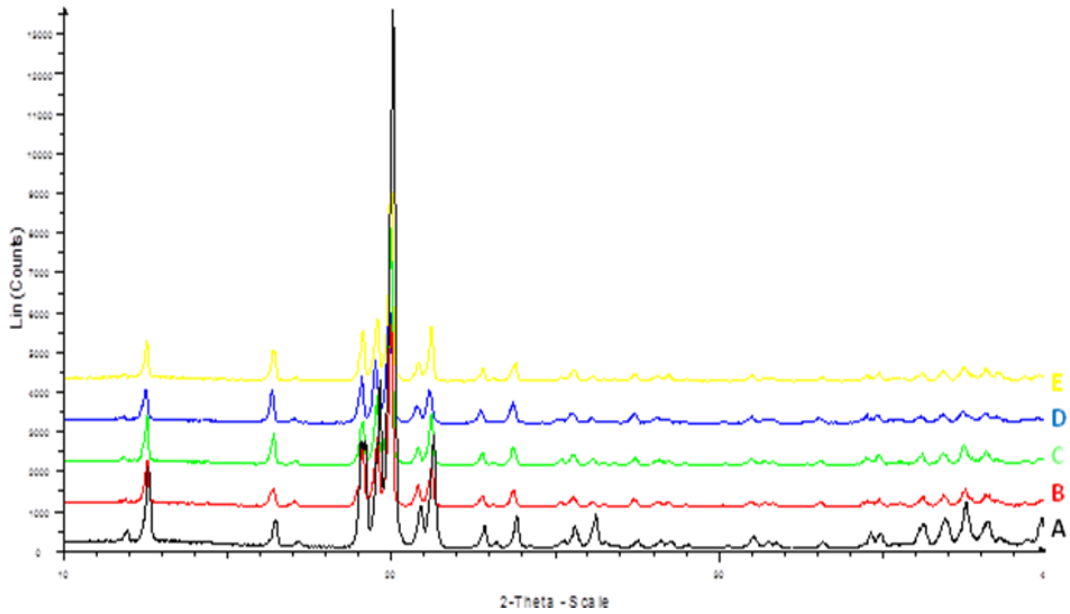

Figure 7.4. Powder x-ray diffraction patterns for lactose monohydrate powder and direct compression tablets at 25, 30, 35 and 40 kN.

A (black) = lactose monohydrate powder, B (red) = lactose monohydrate 25 kN, C (green) = lactose monohydrate tablet 30 kN, D (blue) = lactose monohydrate 35 kN, E (yellow) = lactose monohydrate 40 kN

7.4.4 Crushing strength results for lactose monohydrate compacts

Figure 7.5 summarises the compaction to force measurements graphically for lactose monohydrate direct compression tablets. Actual crushing strength data can be seen in Appendix 0.7. The data suggests that the general trend that is apparent is an increase in compaction force results in an increase in crushing strength.

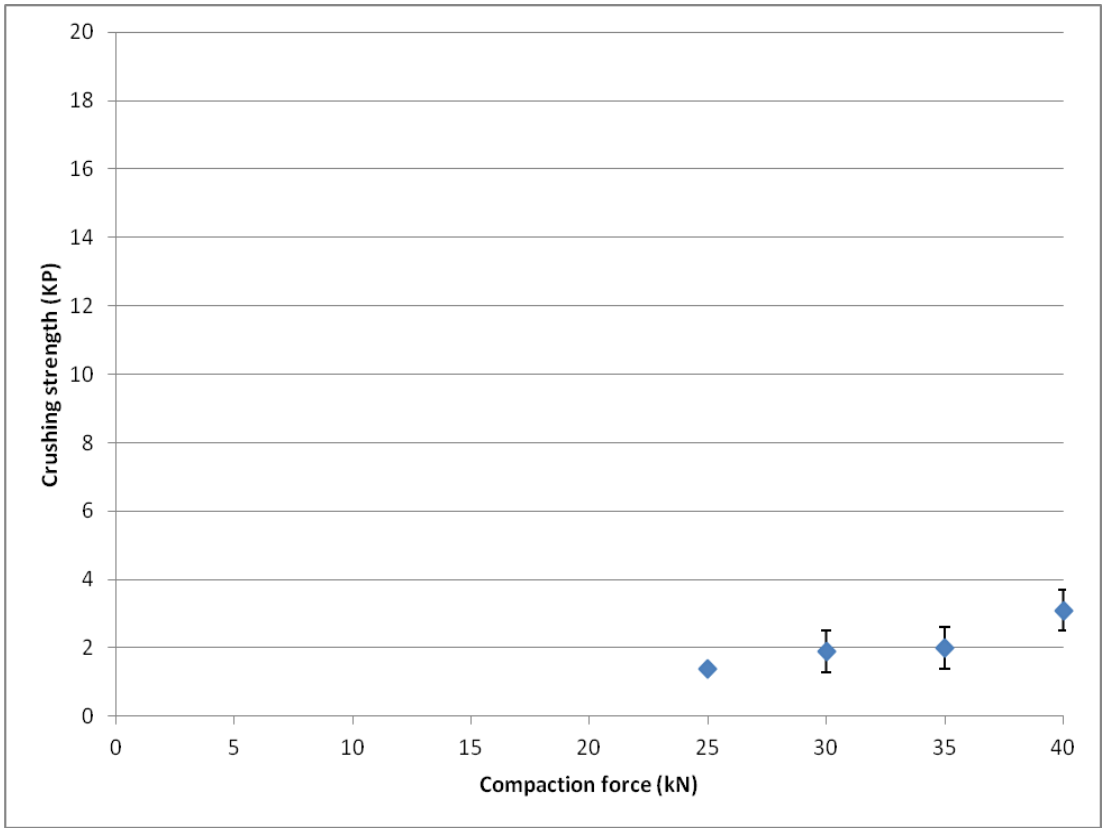

Figure 7.5. Compaction to force results for lactose monohydrate direct compression tablets at 25, 30, 35 and 40 kN

The tensile strength of the tablets was recorded to evaluate the effect of minor changes in compact weight and thickness upon the crushing strength, Figure 7.6 shows the resultant graph of the tensile strength measurements. The actual tensile strength data obtained can be seen in Appendix 0.8. The results of the tensile strength measurements did not indicate any changes in the data trends observed for the crushing strength results, suggesting that increased compaction force leads to the production of more rigid and robust tablets.

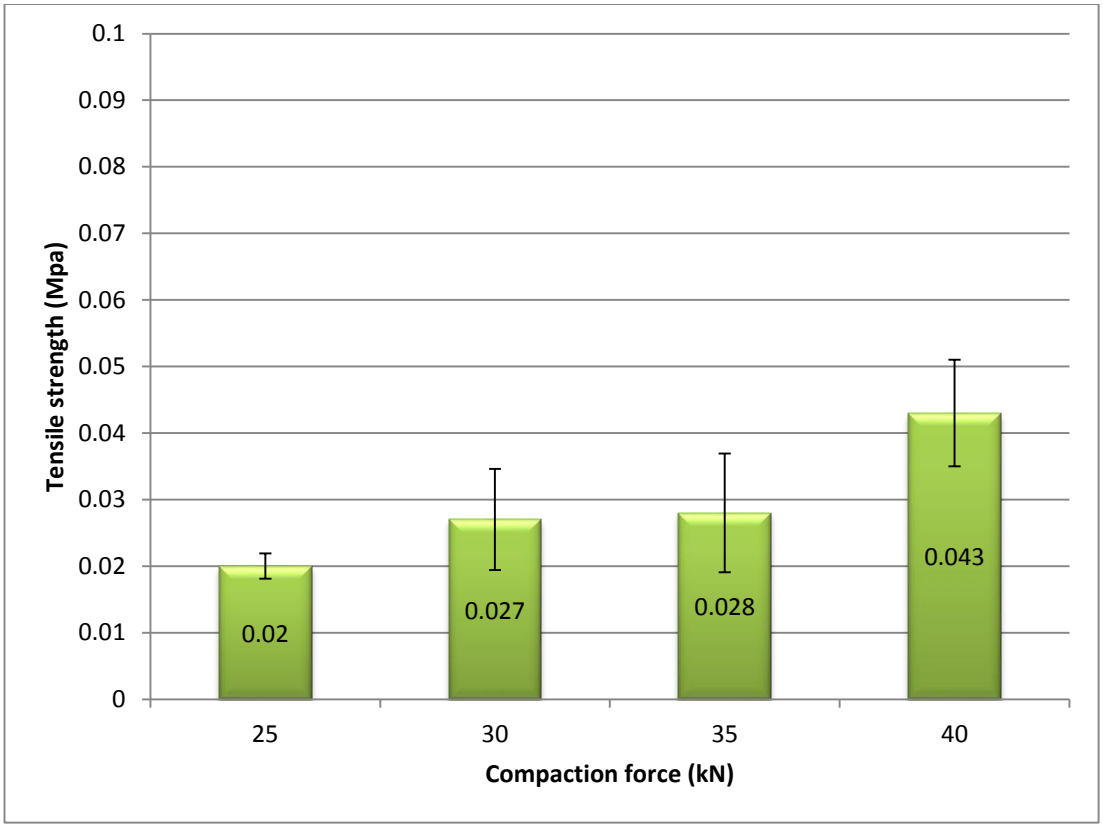

Figure 7.6. Tensile strength measurements for compacts of lactose monohydrate obtained after direct compression tablets at 25, 30, 35 and 40 kN

(Error bars denote SD, n=5)

7.4.5 Moisture profiles of compacts of lactose monohydrate

Moisture profiles for lactose monohydrate powder and resultant directly compressed tablets are shown in Figure 7.7 and final RH readings (the point taken to be the ERH value) are shown in Table 7.2.

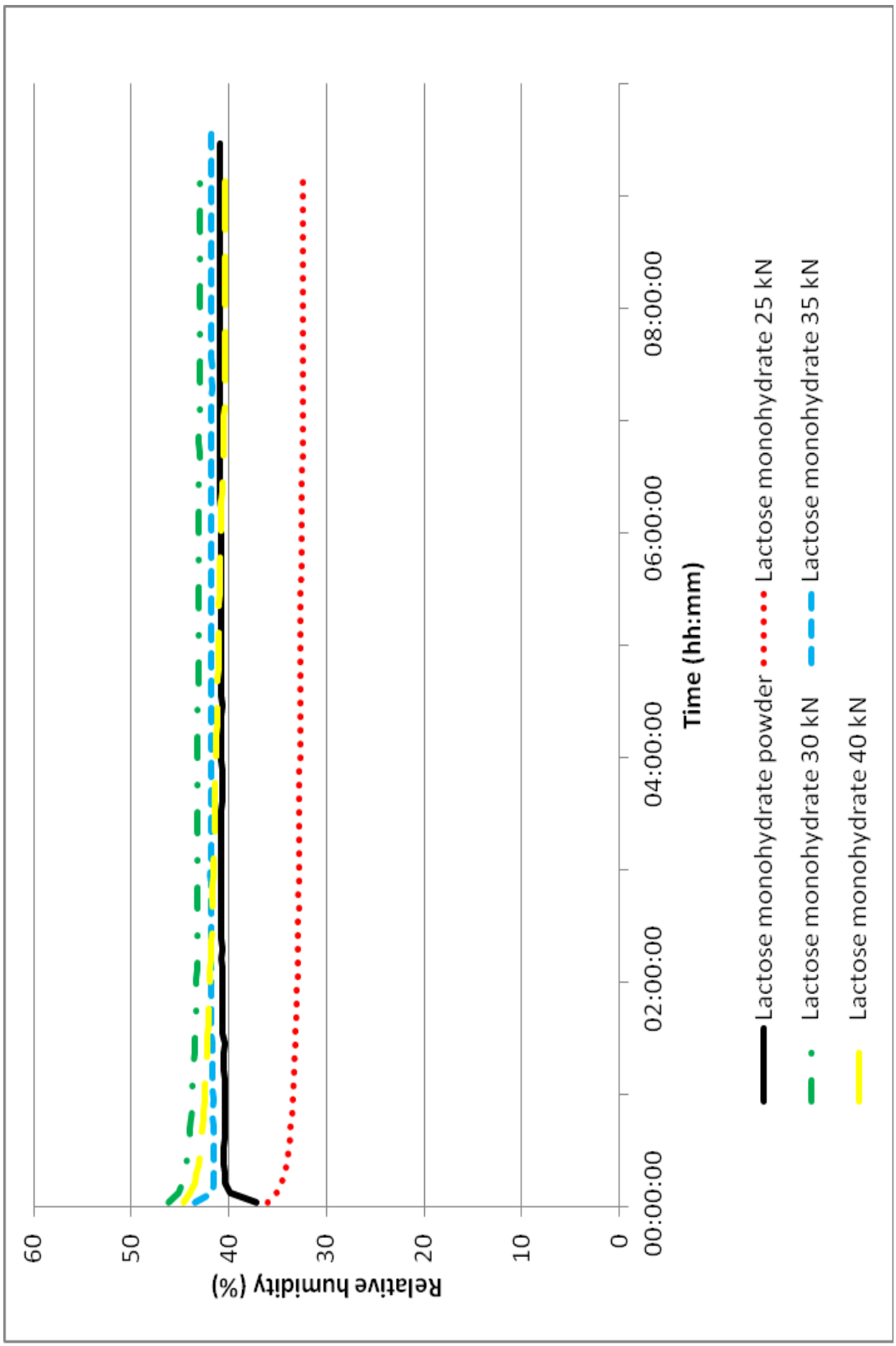

Figure 7.7. Representative moisture profiles for lactose monohydrate powder and its direct compression tablets obtained at 25, 30, 35 and 40 kN

From Figure 7.7 it is apparent that the moisture profile for lactose monohydrate tablets compacted at 25 kN has significantly different ERH values compared to the lactose monohydrate powder and tablets compressed at other compaction forces. Screening the solid-state data obtained, on examination of the DSC results obtained in Table 7.1, it is clear that the enthalpy associated with the dehydration endotherm for this sample is higher than that for the powder and other tablets at increased compaction forces. The implication is that the material has a stronger crystal lattice, and is therefore is harder to remove the water. Therefore the 25 kN compaction force appears to strengthen the crystal lattice (similar to a work hardening effect). Lower dehydration enthalpies are observed with increased compaction force, suggesting that forces above 25 kN cause the crystal lattice to be weakened. The stronger crystal lattice observed for the 25 kN compressed lactose monohydrate is responsible for the lower ERH value observed in the moisture profile, because the water is held more tightly, therefore there is less free water available. Therefore less moisture is available for exchange with the closed sample environment, so a lower RH is observed. Conversely, for the powder sample and the samples obtained at higher compaction forces, samples could possibly have a disrupted weaker lattice, so more water is accessible for exchange, thereby increasing the RH of the sample container, and the resultant ERH values.

Another possible explanation for the lower ERH of the 25 kN sample may lie in the porosity of the tablet being greater than the other tablets. Thus the higher porosity of the least compacted tablet may have allowed for an increased surface area. The

finding raised the interesting observation that would require more intensive investigation that ERH is not just weight dependent but is surface area dependent.

The behaviour exhibited by the material when within the sample environment is also useful in demonstrating how the material interacts with regard to moisture, regardless of the final ERH value attained. It is apparent that there is a difference between the behaviour of the lactose monohydrate powder and compacted material. Lactose monohydrate powder, exhibits a moisture profile that shows an initial increase in %RH before equilibrium is attained. This behaviour is indicative of the material exchanging moisture to the environment within the sample chamber. Conversely, all compacted material behaved in the opposite manner and all show an initial decrease in %RH before equilibrium is attained. This is indicative of the material taking in moisture from the sample chamber atmosphere. This therefore suggests that compaction of lactose monohydrate, causes the material to lose moisture and thus show an apparent increase in hygroscopicity by attempting to replenish the lost moisture when placed in the moisture profiler.

Table 7.2. Final RH readings for lactose monohydrate powder and direct compression tablets at 25, 30, 35 and 40 kN.

	Powder final RH reading (%)	25 kN final RH reading (%)	30 kN final RH reading (%)	35 kN final RH reading (%)	40 kN final RH reading (%)
Rep 1	40.9	32.5	42.9	41.7	40.4
Rep 2	40.8	31.4	43.5	41.7	40.5

Figure 7.8 demonstrates the effects of compaction on the ERH values of the lactose monohydrate powder and directly compressed tablets. Also demonstrating that the lactose monohydrate powder and tablets compacted at 30, 35 and 40 kN exhibit

similar ERH values. Whereas the tablets compacted at 25 kN have significantly lower ERH values.

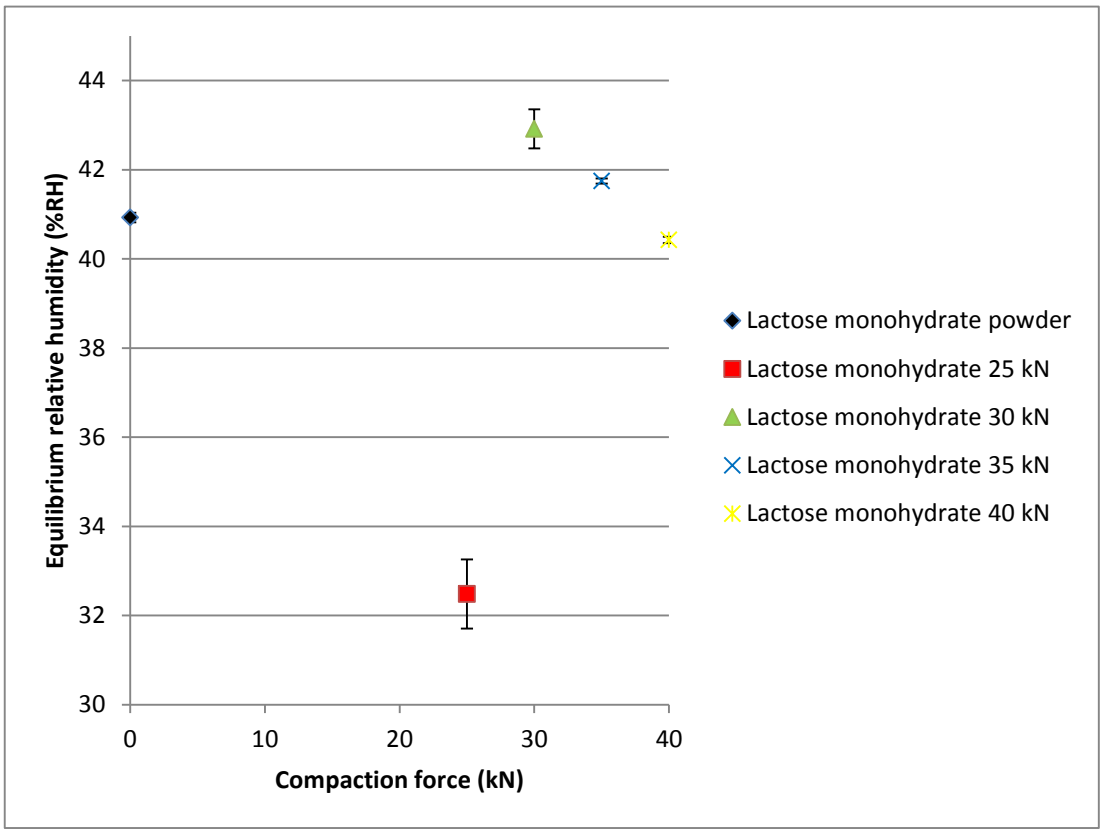

Figure 7.8. Effects of compaction on ERH for lactose monohydrate

7.5 Compacts of anhydrous lactose; Results and discussion

7.5.1 Thermogravimetric analysis results for compacts of anhydrous lactose.

TGA analysis of the initial powder with the various compaction forces used can be seen in Figure 7.9. These showed no notable difference and demonstrated characteristic behaviour of anhydrous lactose (Larhrib et al., 1999). No weight loss is apparent below 100°C, indicating that the anhydrous lactose did not contain a significant amount of free water. A very slight weight loss is observed after 100°C, confirming that the grade of lactose was present in predominately in the anhydrous form.

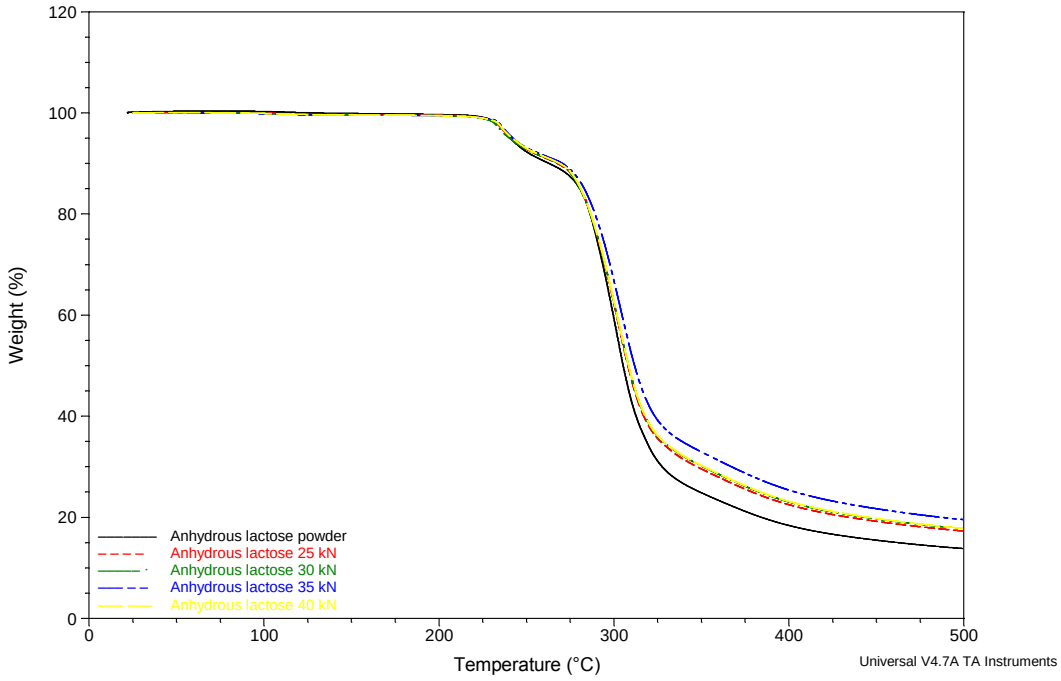

Figure 7.9. Representative TGA thermal profiles for anhydrous lactose powder and tablets under direct compression at 24, 30, 35 and 40 kN force

7.5.2 DSC results of compacts of anhydrous lactose

Representative DSC thermograms (Figure 7.10) exhibit an endothermic event at approximately 230°C which is characteristic of the crystalline melt associated with anhydrous β lactose (Listiohadi et al., 2008, Pitchayajittipong et al.). Absence of any peaks associated with anhydrous α-lactose, suggests that the sample was predominantly anhydrous β-lactose and levels of anhydrous α-lactose present were too low for its characteristic peaks to be detected. A slight dehydration endotherm is visible at approximately 120°C which is typical of anhydrous lactose (Lerk et al., 1984b) and supports the slight weight loss observed at 100°C in the TGA thermogram.

Table 7.3 shows a summary of the DSC results for anhydrous lactose powder and resultant compactions. The data shows the general trend that a decrease in the enthalpy associated with the melting endotherm is observed on compaction.

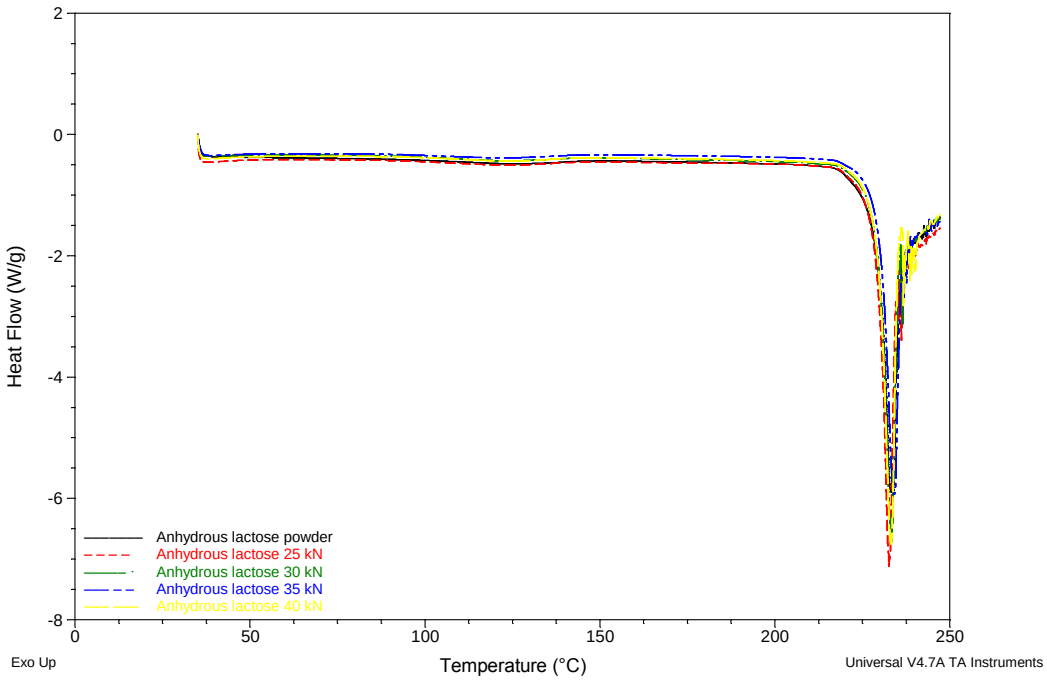

Figure 7.10. Representative DSC thermal profiles for anhydrous lactose tablets under direct compression at 25, 30, 35 and 40 kN force

Table 7.3. Summary of DSC results of anhydrous lactose powder and direct compression tablets at 25, 30, 35 and 40 kN tablets.

	Melting endotherm (°C) Peak max	Melting enthalpy (J/g)
Powder	**232.91** (± 0.31)	**152.8** (± 3.6)
25 kN	**232.99** (± 0.43)	**151.6** (± 4.5)
30 kN	**233.08** (± 0.22)	**142.4** (± 4.3)
35 kN	**233.13** (± 0.49)	**145.2** (± 5.5)
40 kN	**232.20** (± 1.58)	**145.6** (± 3.7)

7.5.3 Results of PXRD analysis of anhydrous lactose on compression

Powder diffractograms for anhydrous lactose and the corresponding directly compressed material are shown in Figure 7.11. The data demonstrates that no gross physical form change occurred when the anhydrous lactose powder was directly compressed. However, PXRD analysis was carried out on lightly ground compacted material; hence this indicates no visible transformations within the material as a whole. Transitions may have occurred due to compaction; they may have taken place upon the tablet surface and remained undetected by PXRD.

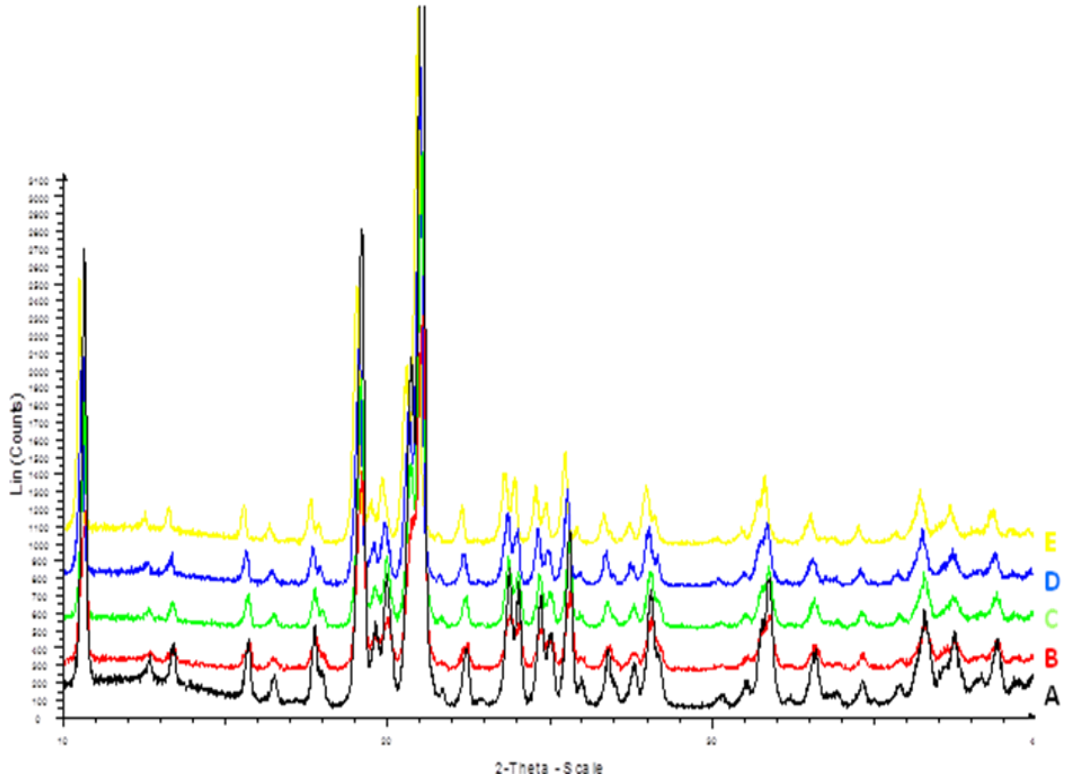

Figure 7.11. PXRD patterns for anhydrous lactose powder and direct compression tablets at 25, 30, 35 and 40 kN

A (black) = anhydrous lactose powder, B (red) = anhydrous lactose 25 kN, C (green) = anhydrous lactose 30 kN, D (blue) = anhydrous lactose 35 kN, E (yellow) = anhydrous lactose 40 kN

7.5.4 Crushing strength of anhydrous lactose compacts

Figure 7.12 summarises the compaction measurements graphically for anhydrous lactose direct compression tablets. Actual crushing data can be seen in Appendix 0.9. Evaluation of the data suggests that the general trend is an increase in crushing strength with increasing compaction force, which is expected. However, there is no significant difference in crushing strength of the tablets until a compaction force of 40 kN is applied.

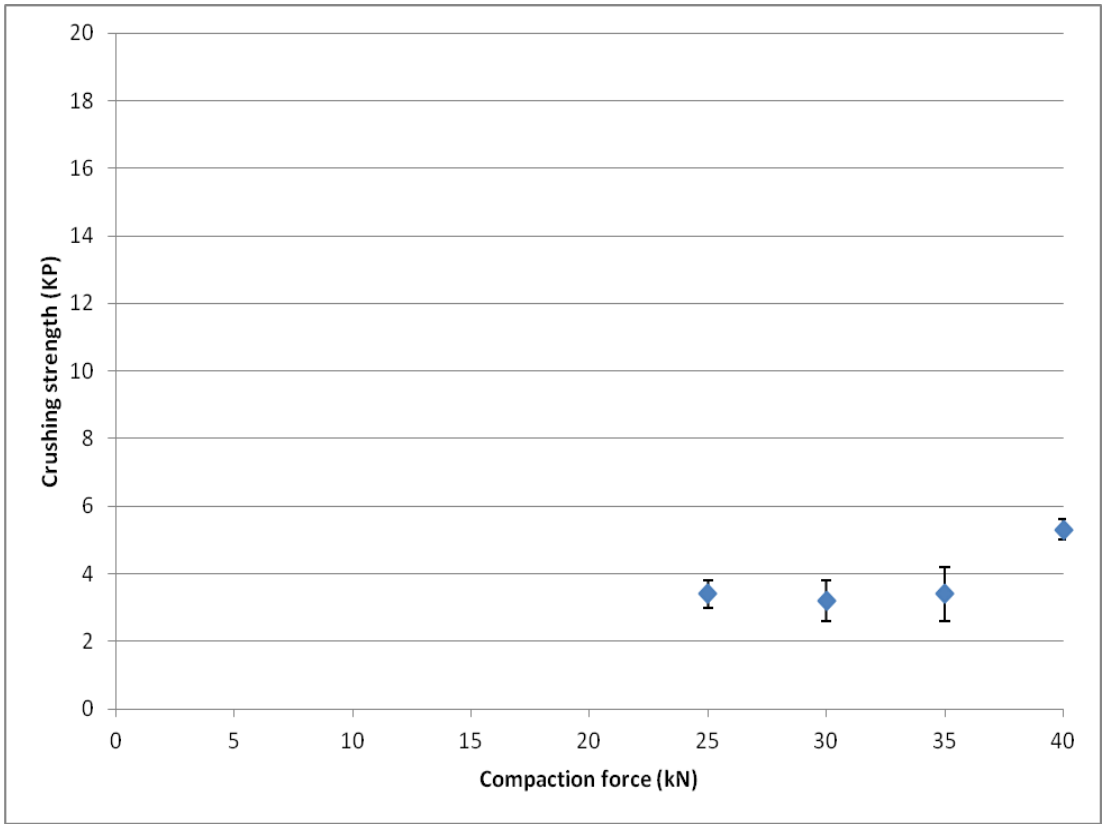

Figure 7.12. Compaction to force results for anhydrous lactose direct compression tablets at 25, 30, 35 and 40 kN

The tensile strength of the tablets was recorded to evaluate the effect of minor changes in compact weight and thickness upon the crushing strength. Figure 7.13 shows the resultant graph of the of the tensile strength measurements. The actual tensile strength data can be seen in Appendix 0.10. The results of the tensile strength measurements indicate that a relationship is apparent between the applied compaction force and the tensile strength, with higher compaction forces leading to tablets being produced with higher resultant tensile strengths.

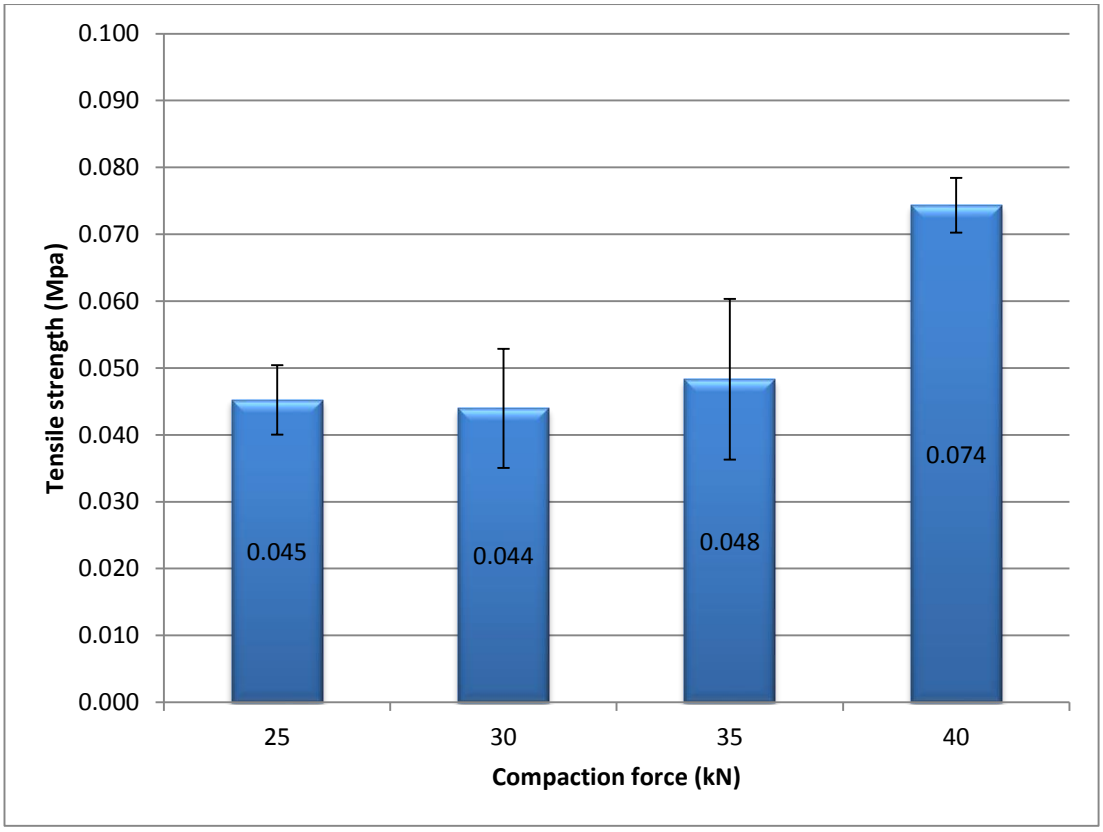

Figure 7.13. Tensile strength measurements for compacts of anhydrous lactose obtained after direct compression tablets at 25, 30, 35 and 40 kN

(Error bars denote SD, n=5)

7.5.5 Moisture profiles of compacts of anhydrous lactose

Moisture profiles for anhydrous lactose powder and resultant directly compressed tablets are shown in Figure 7.14 and final RH readings (consequently the ERH) are shown in Table 7.4.

Figure 7.14. Representative moisture profiles for anhydrous lactose powder and direct compression tablets at 25, 30, 35 and 40 kN

Table 7.4. Final ERH readings for anhydrous lactose powder and direct compression tablets at 25, 30, 35 and 40 kN

	Powder final RH reading (%)	25 kN final RH reading (%)	30 kN final RH reading (%)	35 kN final RH reading (%)	40 kN final RH reading (%)
Rep 1	35.2	37.9	41.4	38.3	42.0
Rep 2	34.4	38.2	41.9	38.0	41.1

From Figure 7.14, it is apparent that the ERH values displayed by the anhydrous lactose powder are lower than that for the compacted material. Figure 7.15 demonstrates that the powder exhibits significantly different lower ERH than the compacted material.

The lower ERH exhibited by the anhydrous lactose powder suggests that the moisture associated with the material is more firmly bound. It is difficult to associate any firm trends in the data. A possible explanation for the increase in ERH may be due to the formation of more hydrophobic surfaces during the compaction event. Further studies are required to investigate this.

The shape of the moisture profile produced by the material is also important and is able to give extra information about the behaviour of the material regardless of the final ERH value. From Figure 7.14, it is apparent that anhydrous lactose powder and compacts produced from it under the current experimental conditions does not readily reach equilibrium ERH. At risk of over interpreting the data beyond the above both the powder and the 25kN compact material display different behaviour to the remainder of the material compacted at higher forces. Anhydrous powder and the 25 kN direct compression tablet show an initial increase in RH, before attaining equilibrium. This is indicative of the material giving out moisture to the

surrounding sample environment. This therefore demonstrates the low hygroscopicity possessed by the anhydrous lactose powder, and in this case the 25kN direct compressed tablet. It is this characteristic that makes anhydrous lactose an ideal excipient choice as a filler/binder for moisture sensitive API's. So, although anhydrous lactose powder and 25 kN compacted tablets have the lowest ERH's.

However, the compacted anhydrous lactose at 30, 35 and 40 kN, display opposite behaviour, they show a sharp initial decrease in initial RH, before equilibrium is attained. This is indicative of the material taking in moisture from the surrounding sample chamber. This suggests that although a higher final ERH, compaction above pressures of 25 kN for anhydrous lactose, causes the behaviour to change, causing a slight increase in the initial hygroscopicity of the material.

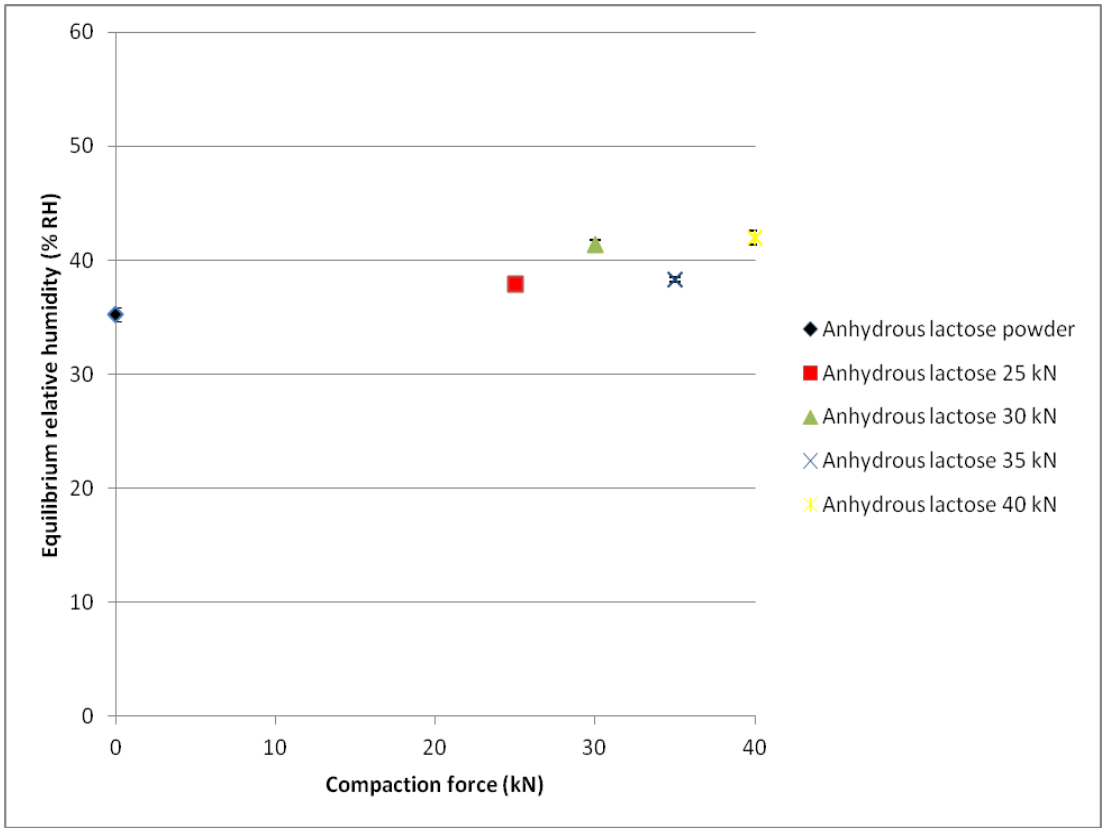

Figure 7.15. Effects of compaction on ERH on anhydrous lactose

7.6 Spray dried lactose; Results and discussion

7.6.1 Results of thermo gravimetric analysis of compacts of spray dried lactose

TGA analysis of the spray dried lactose powder and the resultant tablets produced with the various compaction forces can be seen in Figure 7.16. The data showed that the behaviour characteristic of spray dried lactose and the initial weight loss is due to loss of residual water from the spray drying process.

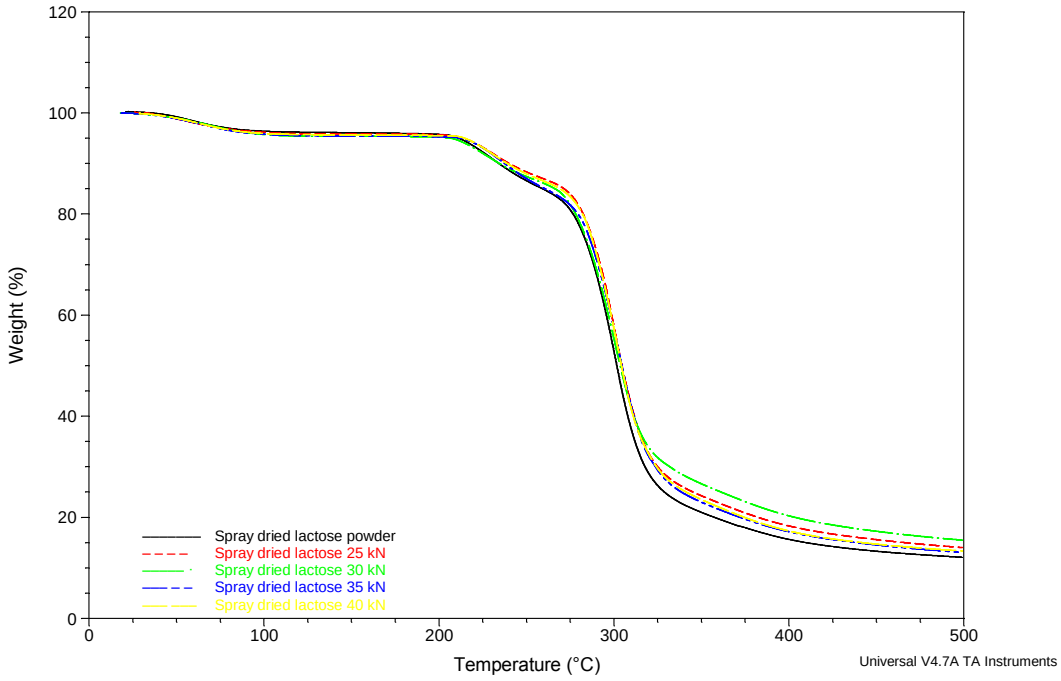

Figure 7.16. Representative TGA thermal profiles for spray dried lactose powder and direct compression tablets at 25, 30, 35 and 40 kN

7.6.2 Differential scanning calorimetry results of spray dried lactose compacts

Representative DSC thermal profiles can be seen in Figure 7.17. They display the characteristic behaviour of spray dried lactose and several thermal events are evident. The first endotherm is broad is at approximately 70°C is assigned to residual loss of water from the material as a result of the spray drying process. A disruption of the baseline is evident in the range 110-120°C, which given that the material is amorphous is attributed to the T_g. An exotherm is apparent at approximately 170°C which representative of crystallisation of the amorphous spray dried lactose (Sebhatu et al., 1994, Takeuchi et al., 1998). It is necessary to highlight that the material was initially amorphous prior to analysis, and that the DSC analysis facilitated the crystallisation. The final endotherms correspond to

melting of the crystalline spray dried lactose. There are two melting endotherms observed at approximately 216°C and 223°C in the thermal profiles for the compacted material, however the second endotherm is absent/unable to be distinguished from subsequent decomposition in the spray dried lactose powder thermal profile. This suggests that compaction may have facilitated the formation of both α and β lactose upon crystallisation within the DSC apparatus.

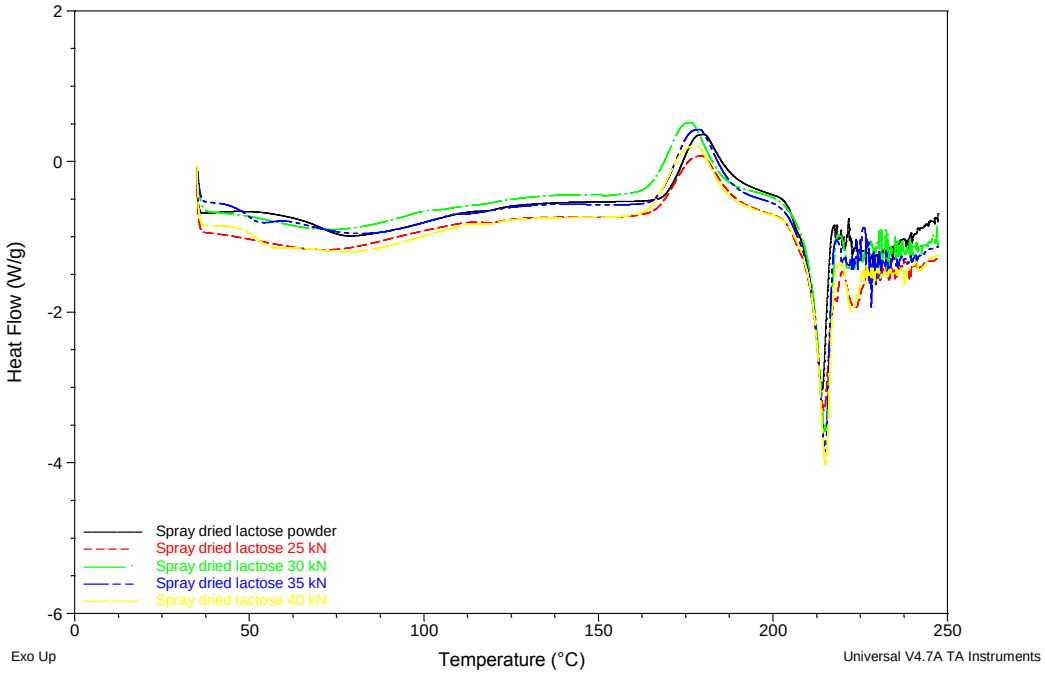

Figure 7.17. Representative DSC thermal profiles for spray dried lactose powder and direct compression tablets at 25, 30, 35 and 40 kN

Table 7.5.Summary of DSC results for spray dried lactose powder and direct compression tablet at 25, 30, 35 and 40 kN

	Crystallisation exotherm (°C) Peak max	Crystallis-ation enthalpy (J/g)	Melting endotherm (°C) Peak max	Melting enthalpy (J/g)	Melting endotherm (°C) Peak max	Melting enthalpy (J/g)
Powder	**180.12** (± 0.42)	**84.61** (± 4.92)	**214.04** (± 0.23)	**87.27** (± 11.38)	-	-
25 kN	**178.85** (± 0.58)	**89.19** (± 5.08)	**214.75** (± 0.35)	**67.93** (± 11.21)	**223.54** (± 0.33)	**15.25** (± 4.22)
30 kN	**174.30** (± 2.15)	**82.18** (± 4.97)	**215.41** (± 0.73)	**87.10** (± 2.69)	**222.75** (± 1.68)	**10.94** (± 2.45)
35 kN	**177.20** (± 2.04)	**86.12** (± 6.54)	**214.89** (± 0.25)	**86.76** (± 3.06)	**223.49** (± 0.69)	**10.79** (± 1.38)
40 kN	**176.79** (± 0.91)	**91.49** (± 7.29)	**214.77** (± 0.18)	**89.01** (± 3.96)	**222.28** (± 0.64)	**11.63** (± 0.84)

7.6.3 Powder x-ray diffraction analysis of compacts of spray dried lactose

Powder diffractograms for spray dried lactose and the corresponding directly compressed material are shown in Figure 7.18. The diffractograms suggest that the spray dried lactose has some crystalline material present and is not completely amorphous; however it also demonstrates that the sample remains in the same physical state throughout compaction.

PXRD analysis was carried out on lightly ground compacted material and no visible transformations are observed throughout the entire material. However transitions due to compaction may have occurred only on the tablet surface, which PXRD may

not have been able to detect the low level amount of disorder produced by compaction.

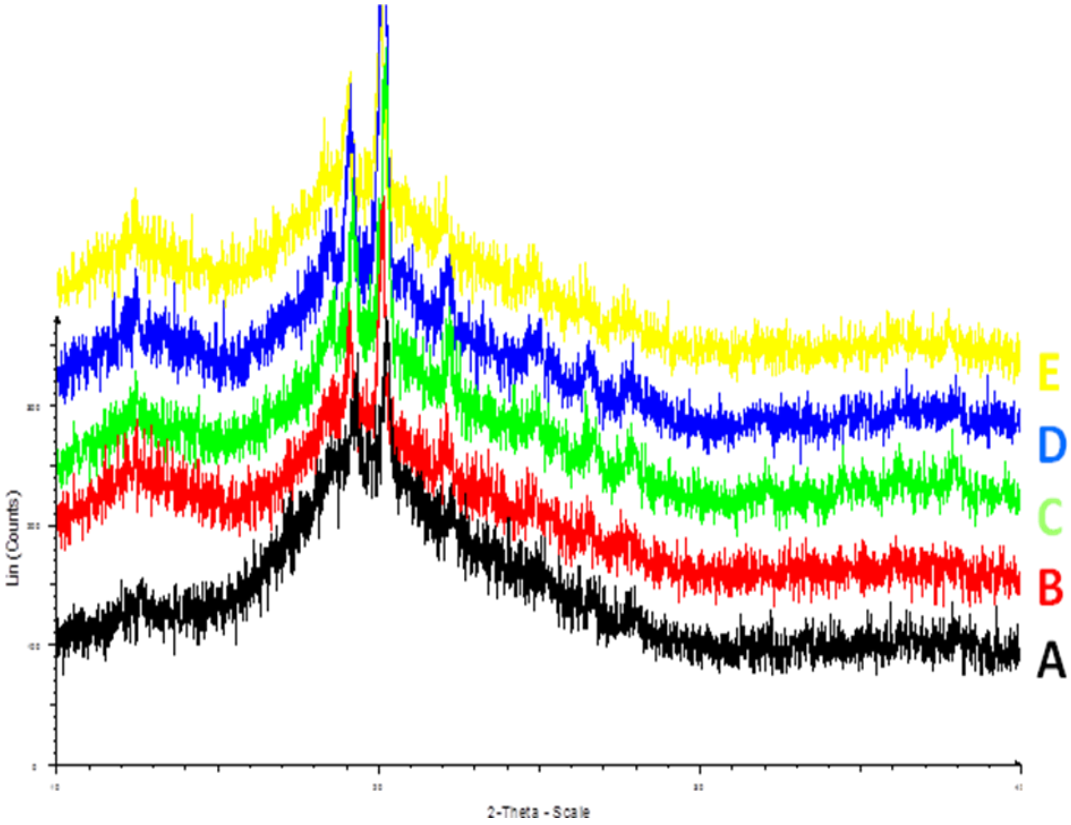

Figure 7.18. PXRD patterns for spray dried lactose powder and direct compression tablets at 25, 30, 35 and 40 kN

A (black) = spray dried lactose powder, B (red) = spray dried lactose 25 kN, C (green) = spray dried lactose 30 kN, D (blue) = spray dried lactose 35 kN, E (yellow) = anhydrous lactose 40 kN

7.6.4 Crushing strength of compacts of spray dried lactose

Figure 7.19 shows the crushing strength results for the spray dried lactose direct compression tablets, and the data is summarised in Appendix 0.11.

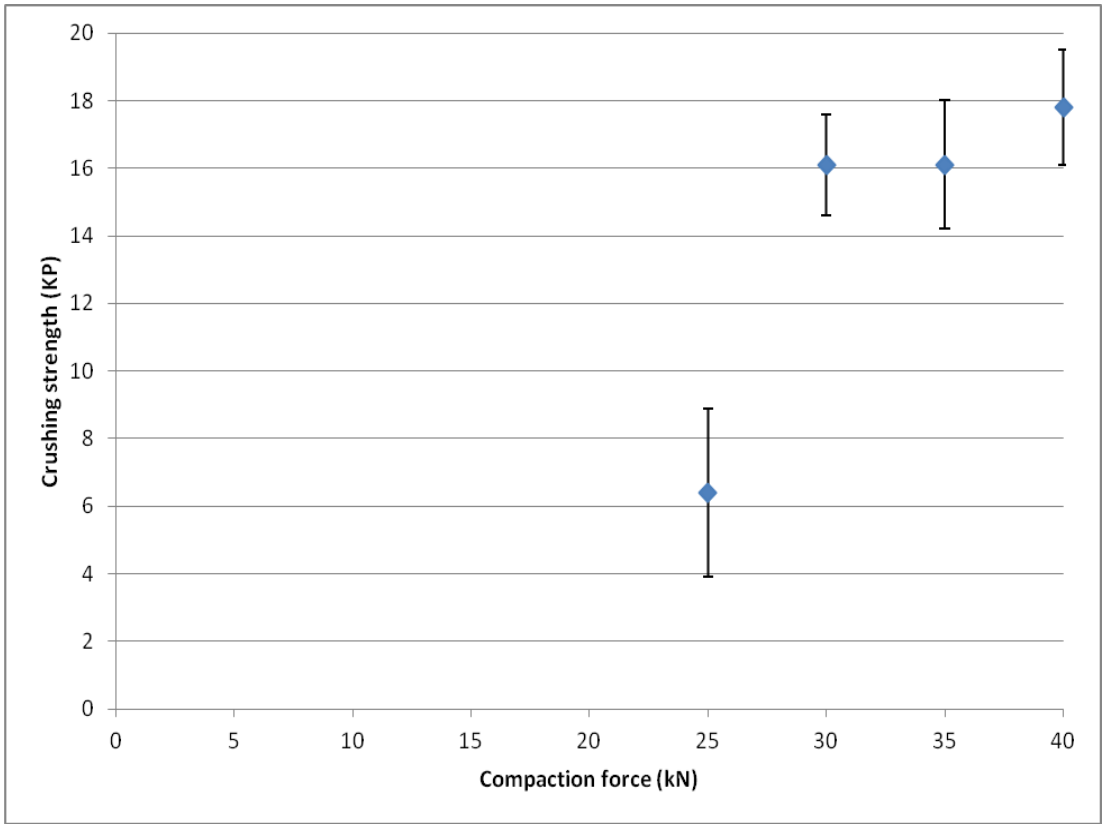

Figure 7.19. Compaction to force results for spray dried lactose direct compression tablets at 25, 30, 35 and 40 kN

The tensile strength of the tablets was calculated in order to evaluate the effect of minor changes in compact weight and thickness upon the crushing strength. Figure 7.20 shows the resultant tensile strength results. The tabulated tensile strength data is summarised in Appendix 0.12. The only notable difference being the material compacted at 25 kN, this does not seem to form as strong compacts as obtained with higher compaction forces.

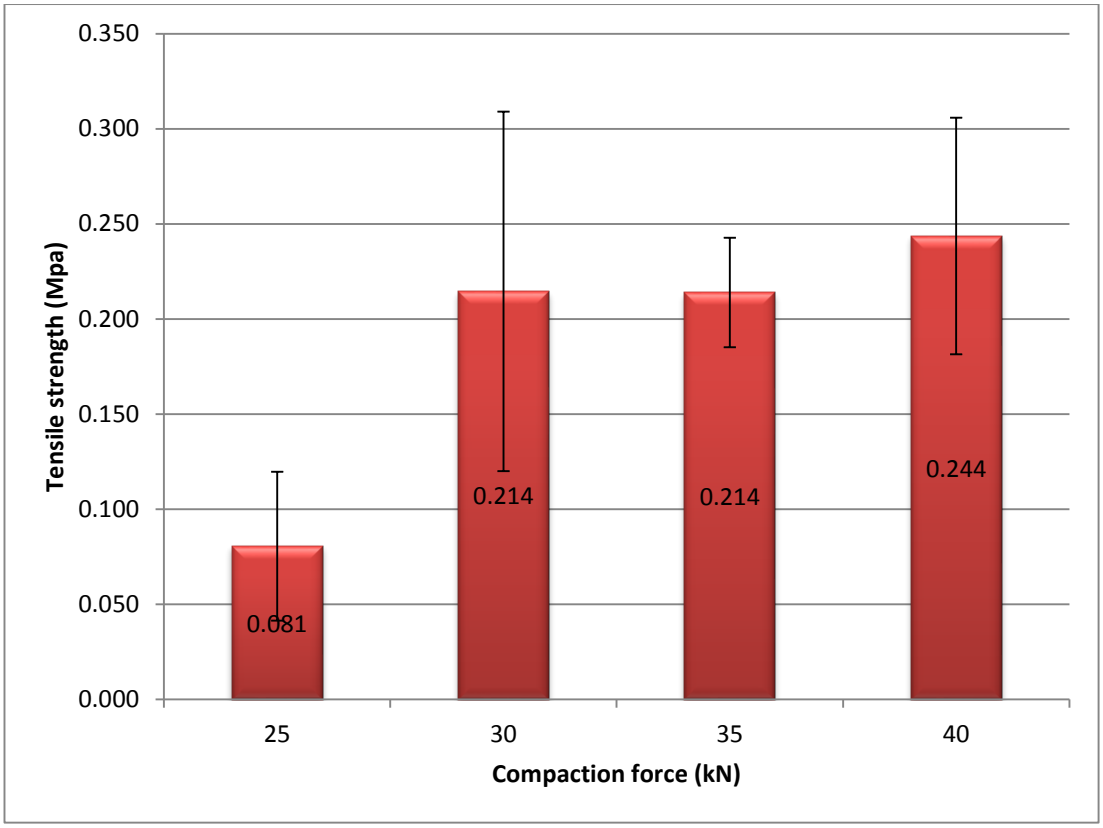

Figure 7.20. Tensile strength measurements for compacts of spray dried lactose obtained after direct compression tablets at 25, 30, 35 and 40 kN

(Error bars denote SD, n=5)

7.6.5 Moisture profiles of compacts of spray dried lactose

Moisture profiles for representative spray dried lactose powder and the resultant directly compressed tablets are shown in Figure 7.21 and the final RH readings, which is the point taken to be the ERH are shown in Table 7.6.

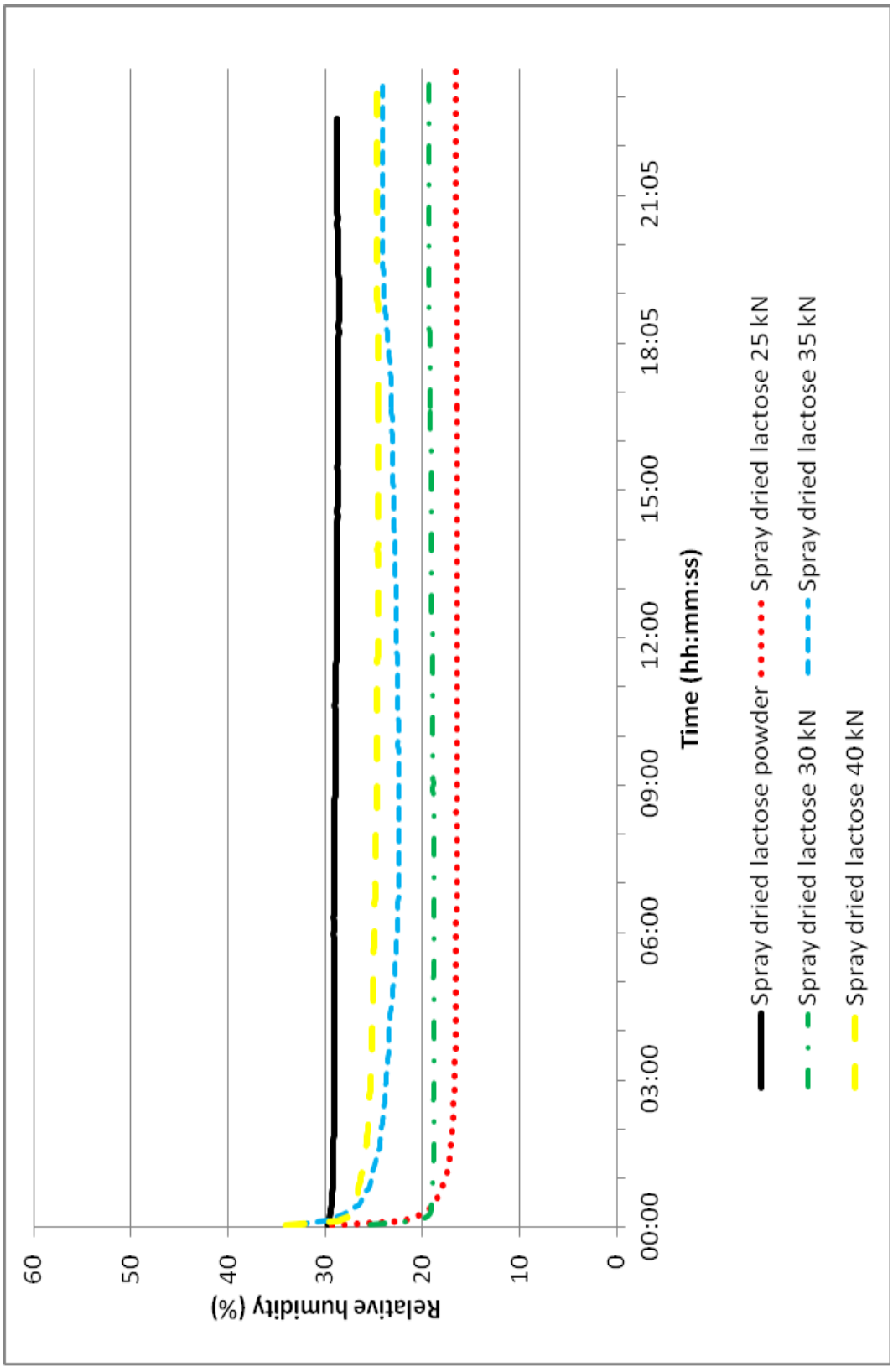

Figure 7.21. Representative moisture profiles for spray dried lactose powder and direct compression tablets at 25, 30, 35 and 40 kN

From Figure 7.21 it is apparent that the spray dried powder exhibits a higher ERH than any of the compacted material and that this increased ERH is different (Figure 7.22). This increased ERH is seen because the material is not compacted; therefore the free moisture is able to move out into the sample chamber more easily than the compacted material. Material compacted at 25 kN shows the lowest ERH, with ERH increasing with increasing compaction force, with 40 kN having the highest ERH of the compacts. In trying to conceptualise why increasing compaction pressures lead to higher ERH's it is useful to think about the compaction process. Spray dried lactose predominantly compacts by plastic deformation since no crystalline particles exist to fragment. Higher compaction pressures therefore give rise to lower porosities and increased bonding to yield higher crushing strengths. It is possible that during the compression event associated moisture is driven away from the spray dried lactose (friction causing higher temperatures). X-ray, DSC, and TGA analysis of the compacts show little difference in the solid state of lactose from any of the compacts. Thus as previously discussed, we have evidence that ERH not only reflects the physical state or weight of a material but also its porosity and surface area. The trend with lower ERH being observed for lower compaction force is consistent with higher compaction forces producing lower effective surface areas and therefore being less able to extract moisture from the sample chamber. This raised the interesting concept that apparent ERH may be reflective of the bonding that has taken place during a compaction event.

The shape of the moisture profile is also important and is able to give extra information about the behaviour of the material within the closed environment, regardless of the final ERH value. The spray dried powder appears to remain stable throughout analysis; however a slight initial decrease in RH is evident before equilibrium is reached. All compacted material show an obvious decrease in initial RH before equilibrium is attained. This initial decrease suggests the material takes in moisture from the sample chamber environment. This is indicative of a material being hygroscopic in nature and therefore suggests compaction causes apparent hygroscopicity to increase for spray dried lactose.

Table 7.6. Final ERH readings for spray dried lactose powder and direct compression tablets at 25, 30, 35 and 40 kN

	Powder final RH reading (%)	25 kN final RH reading (%)	30 kN final RH reading (%)	35 kN final RH reading (%)	40 kN final RH reading (%)
Rep 1	28.8	16.5	19.4	24.1	24.7
Rep 2	28.8	18.7	24.7	23.8	26.7

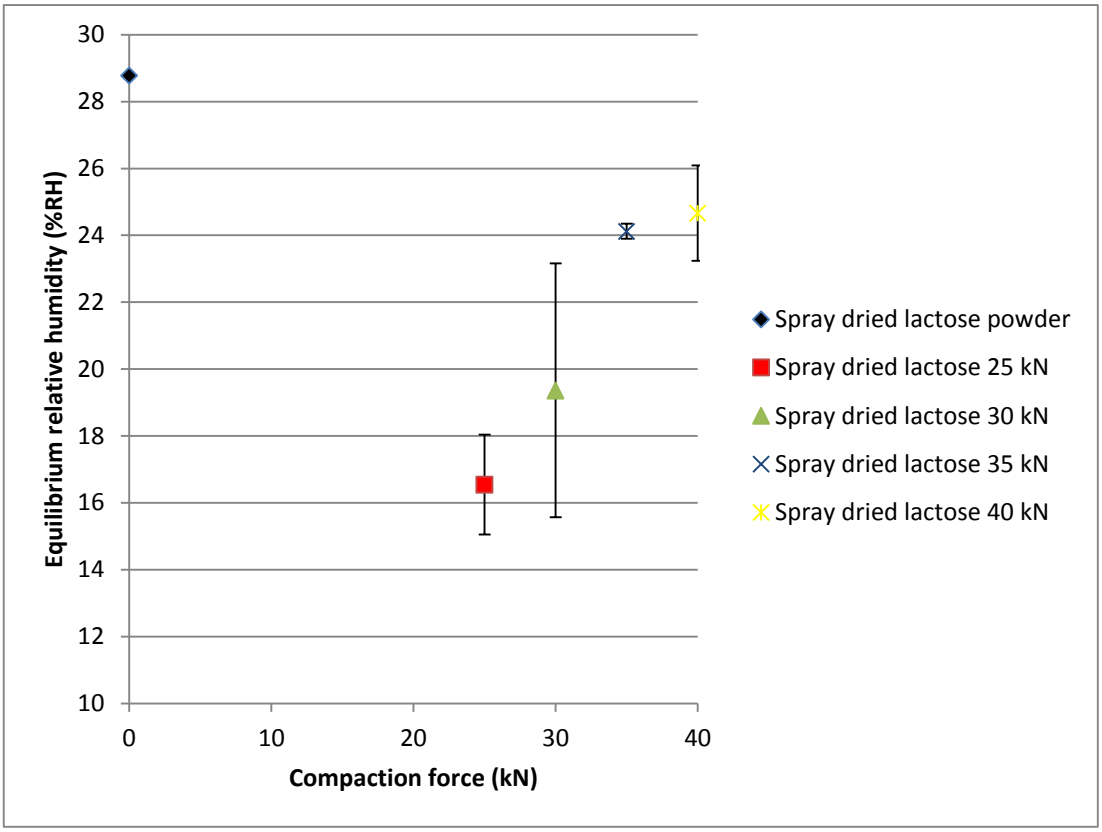

Figure 7.22. Effects of compaction force on ERH of spray dried lactose (n=5 for error bars)

7.7 Conclusion

From Figure 7.23 its is evident that compaction is able to effect the ERH of materials. In general lower ERH's were obtained at lower compaction pressure. For the materials studied compaction is able to alter how the material interacts with the surrounding atmospheric moisture. This is supported by the powdered form of the material exhibiting different ERH's than the compacted material. In this instance, anhydrous lactose is the most consistent with regards to ERH showing the least variation is observed between the ERH's for the anhydrous lactose powder and various direct compression tablets. This finding is attributed to its crystalline structure and reduced resistance to deformation. In the following chapter the effect of storing the compacts on physical and ERH behaviour will be examined.

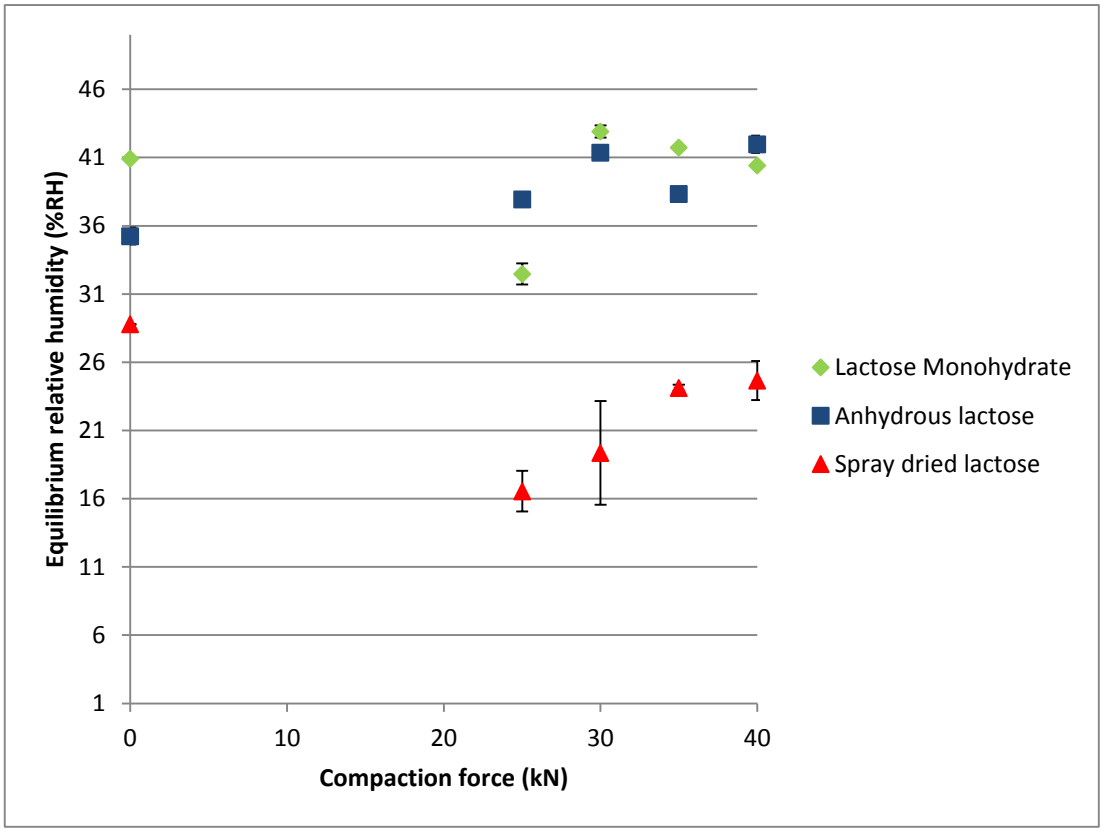

Figure 7.23. Summary of effect of compaction force on ERH for all lactose forms

8 INVESTIGATION INTO THE EFFECTS OF STORAGE RELATIVE HUMIDITY UPON COMPACT BEHAVIOUR AND THE RESULTANT MOISTURE PROFILE

8.1 Introduction

Water is able to interact with pharmaceutical solids at practically all stages of the manufacturing process; from synthesis of the raw material up to storage of the final prepared dosage form. Interaction of water with pharmaceutical solids is therefore an important factor that must be considered during formulation, processing and the product performance of solid pharmaceutical dosage forms.

It is known that RH during storage of solid dosages forms, such as a tablet, the relative humidity is able to influence their physical properties (Hendricks et al., 1996, Molokhia, 1984). The effects of storage conditions upon powders prior to tabletting has been previously studied; it was found that initial storage conditions had a notable effect on the final physical stability of the resultant tablet (York, 1976).

Therefore it is apparent that storage of the final solid dosage forms post-compaction can also be affected by storage conditions. Under extreme RH and temperatures the physical stability of even the most stable formulations can be dramatically altered; which can directly affect properties such as hardness and disintegration, hindering the desired effects.

Therefore in order to develop physically stable dosage forms many variables must be considered and consequently the role of water vapour must be considered. ERH moisture profiling can be used in order to monitor free moisture changes with regards to storage conditions in relation the raw materials and the final dosage form.

8.2 Objectives

Having obtained ERH profiles for well characterised compacts on their initial formation the overall aim of the chapter was to evaluate the effect of storage of the compacts at elevated RH upon the ERH that the compacts produced after storage. This was completed by:

- Examining the solid state properties and the resultant crushing and tensile strengths before and after storage.
- Examining the ERH value and the moisture profile to observe any effects due to storage and correlate these to the solid state analysis in order to explain any differences observed.

Lactose was again the selected material because as previously mentioned it is widely used within the industry and its physical behaviour is well documented within literature (Garnier et al., 2008, Listiohadi et al., 2009). Three different physical forms of lactose were selected; lactose monohydrate, anhydrous lactose and spray dried lactose. These were selected because they all exhibit different physical properties and therefore will behave differently under storage. Therefore, they may then behave differently within the moisture profiler, so the different forms were selected in order to give a better indication of how different materials behave within the profiler.

8.3 Methods

Samples of lactose monohydrate, anhydrous lactose and spray dried lactose were tabletted using direct compression. Direct compression of the material was performed using a single punch die. The material was weighed on an analytical

balance and then transferred manually into a 10 mm circular die. The weight of material was kept constant at 450 mg (± 1.99 mg) throughout, producing tablets of approximately 4.7 mm in thickness. Various compaction forces were employed during the compression; these were 25, 30, 35 and 40 kN. The compacted material was then placed into a desiccator, over saturated sodium chloride salt solution at ambient temperature (25-30°C) to give a resultant storage RH of 75%. They were stored for a period of 7 days.

In order to fully characterise any changes induced by storage of the direct compression tablets upon ERH, a variety of analytical techniques were employed.

8.4 Behaviour of lactose monohydrate on storage; results and discussion

8.4.1 TGA results of the effect of storage of lactose monohydrate compacts

Representative TGA analysis for direct compression lactose monohydrate tablets at 25 kN before and after storage can be seen in Figure 8.1. Representative thermal profiles for lactose monohydrate tablets at increased compaction forces (30, 35 and 40 kN) before and after storage can be seen in Appendix 0.1 - Appendix 0.3.

All (before and after storage) TGA profiles of lactose monohydrate show the behaviour characteristic of lactose monohydrate; water loss followed by melting and decomposition of the material. The theoretical expected water loss for lactose monohydrate is 5%, all show approximate 5% weight losses corresponding to water loss (Berlin et al., 1971, Otsuka et al., 1991).

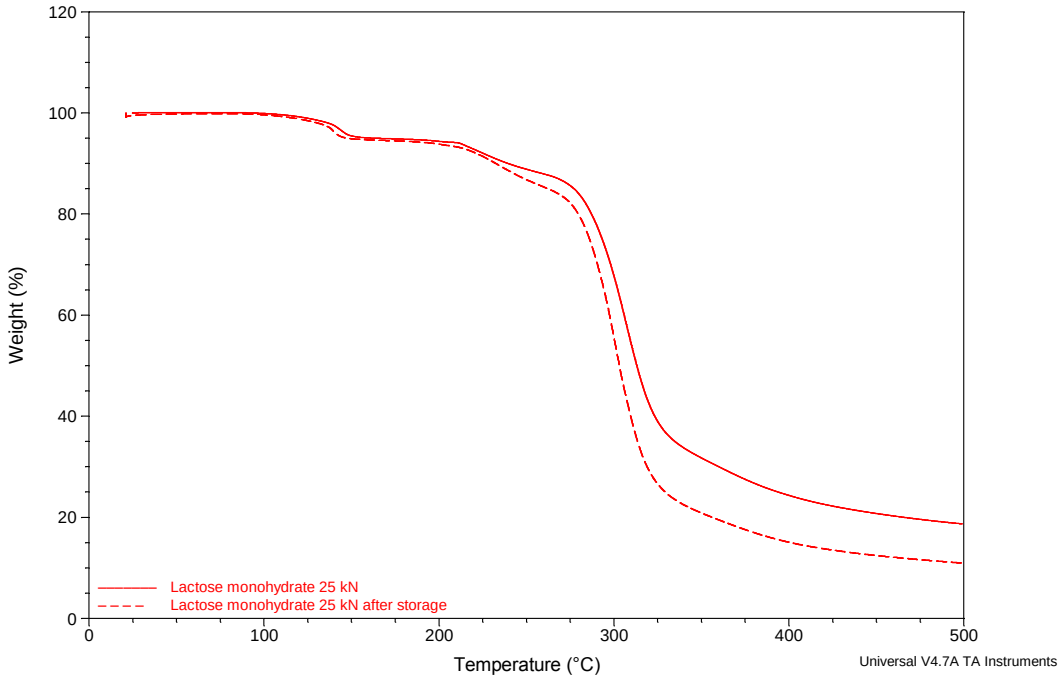

Figure 8.1. Representative TGA thermal profile for direct compression lactose monohydrate tablets at 25 kN, before and after storage

Results of the TGA analysis of all direct compression lactose monohydrate material with regards to water loss is shown in Table 8.2. At 25 kN, there is no evident difference in water loss, suggesting that the tablet has not taken up any moisture upon storage at elevated RH. Therefore indicates that compaction at 25 kN, does not cause any major structural disruption to the lactose monohydrate, which would then be able to facilitate moisture ingress. However, compaction may cause small changes which are undetectable, such as an increase in amorphous regions or tablet fracture, as in complementary thermal analysis (DSC) there is a decrease in the dehydration and melting enthalpies after storage, which is indicative that disruption of the crystal lattice has occurred.

From the data it is observed that at higher compaction forces there is an approximate 0.1-0.4% increase in water content after storage, which is attributed to amorphous material being created during the compaction process, which is able to take up moisture upon storage. It has been previously highlighted that processing is able to introduce considerable disorder upon crystalline solid surfaces, which is able to lead to a marked increase in the tendency to sorb water (Vippagunta et al., 2001).

Table 8.1. TGA data for lactose monohydrate direct compression tablets before and after storage (n=3)

	Water loss (%)	Standard deviation (%)
25 kN	5.130	± 0.004
25 kN after storage	5.130	± 0.231
30 kN	5.123	± 0.039
30 kN after storage	5.571	± 0.047
35 kN	5.182	± 0.003
35 kN after storage	5.595	± 0.091
40 kN	5.174	± 0.020
40 kN after storage	5.290	± 0.086

8.4.2 DSC results of the effect of storage of lactose monohydrate compacts

Representative DSC thermal profiles for lactose monohydrate before and after storage directly compressed at 25 kN is shown in Figure 8.2, thermal profiles for material compacted at 30, 35 and 40 kN can be seen in Appendix 0.4 - Appendix 0.6. All DSC profiles show characteristic behaviour of α lactose monohydrate, namely a dehydration endotherm at approximately 145°C , followed by a melting endotherm between 212-214°C. Above this temperature the material decomposed (Lerk et al., 1984a, Lerk et al., 1984b). Material before and after storage show these

characteristic peaks, therefore suggesting that storage of lactose monohydrate does not induce any change in the solid state.

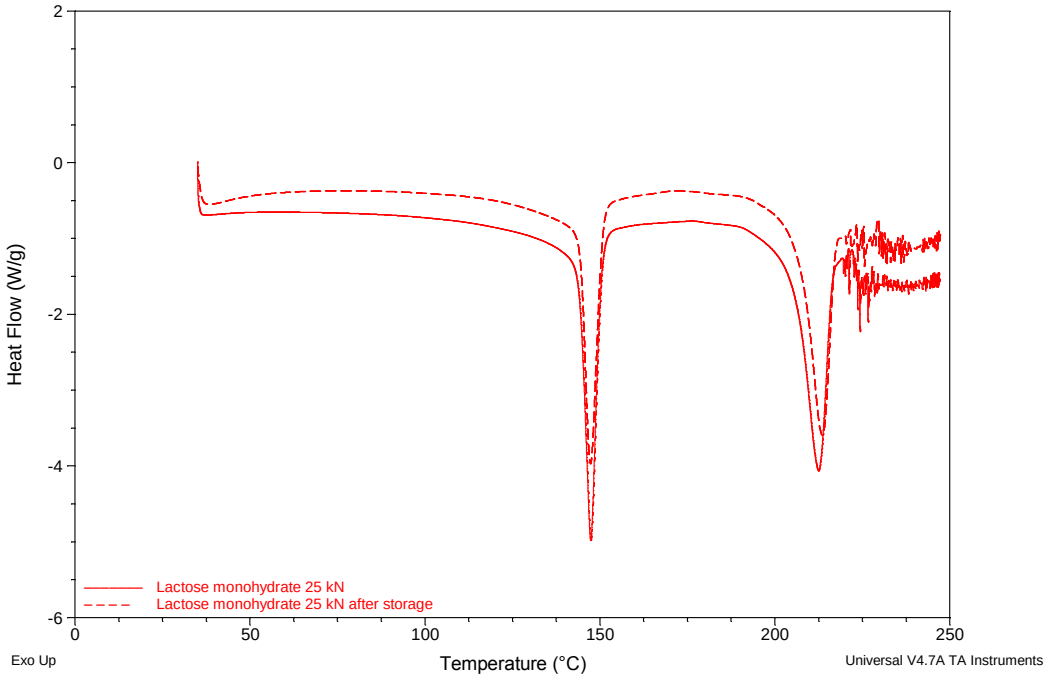

Figure 8.2. Representative DSC profiles for lactose monohydrate tablets produced under direct compression at 25 kN, before and after storage

Table 8.2. DSC dehydration and melting point values of lactose monohydrate before storage

n=3	Dehydration endotherm (°C) (Peak max)	Dehydration enthalpy (J/g) (Peak max)	Melting endotherm (°C) (Peak max)	Melting enthalpy (J/g) (Peak max)
25 kN	**146.67** (± 0.74)	**181.5** (± 0.8)	**212.39** (± 0.20)	**157.7** (± 0.1)
25 kN after storage	**146.27** (± 0.92)	**152.8** (± 1.5)	**214.20** (± 0.80)	**141.5** (± 1.0)
30 kN	**145.16** (± 0.55)	**170.1** (± 1.2)	**212.69** (± 0.30)	**150.1** (± 3.3)
30 kN after storage	**146.65** (± 0.71)	**168.1** (± 12.0)	**213.23** (± 0.33)	**151.2** (± 6.7)
35 kN	**144.33** (± 0.69)	**162.6** (± 3.7)	**212.91** (± 0.29)	**154.1** (± 6.5)
35 kN after storage	**145.3** (± 0.53)	**161.5** (± 8.2)	**213.80** (± 0.72)	**150.7** (± 9.7)
40 kN	**145.07** (± 0.99)	**166.50** (± 2.1)	**212.64** (± 0.31)	**158.0** (± 6.5)
40 kN after storage	**147.39** (± 0.49)	**172.8** (± 9.6)	**212.74** (± 0.4)	**151.0** (± 2.7)

DSC dehydration and melting data is also presented graphically**.** The data in Figure 8.3 shows that there is notable change upon storage in the peak max temperature/position associated with the dehydration and melting endotherms. Therefore, indicating that storage does not cause a complete change in physical form, because if this had occurred it would have resulted in a temperature change of the peak max of the endotherms.

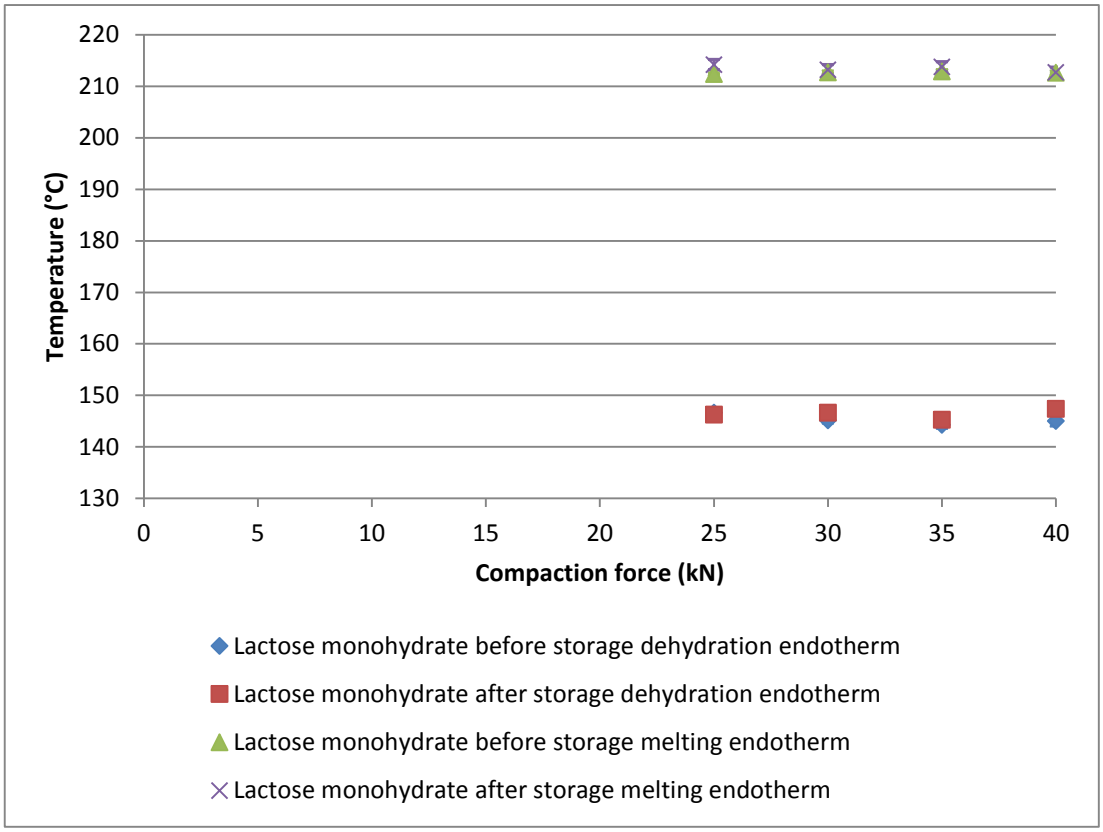

Figure 8.3. Summary of DSC peak max dehydration and melting endotherms for lactose monohydrate before and after storage

From Figure 8.4 it is evident that there is a notable decrease in both the dehydration and melting enthalpies associated with the lactose monohydrate compacted at 25 kN after storage (dehydration enthalpy decreases by 30 J/g and the melting enthalpy decreases by 16 J/g). The finding is consistent with the idea that there is some physical change to the physical state of the material that has been induced during the compaction process. Thereby reinforcing the conclusion formed during the previous TGA analysis (section 8.4.1), that the physical changes that were induced were small enough so that no notable moisture ingress was possible. This therefore may imply that the crystals were fractured upon

compaction rather than amorphous regions being formed, as amorphous regions would readily absorb the moisture available upon storage.

At increased compaction pressures above 25 kN the difference in the dehydration and melting enthalpies are not as obviously decreased. This is attributed to amorphous regions that may have been generated at the higher compaction forces employed, thereby allowing moisture ingress. The amorphous material is more susceptible to moisture and is able to take up moisture present due to the elevated storage RH. When the moisture is absorbed into the amorphous regions, it is able to act as a plasticiser, which is the cause of the decrease in enthalpies, but is able to make the tablets more robust, which is substantiated by an increase in both crushing and tensile strength.

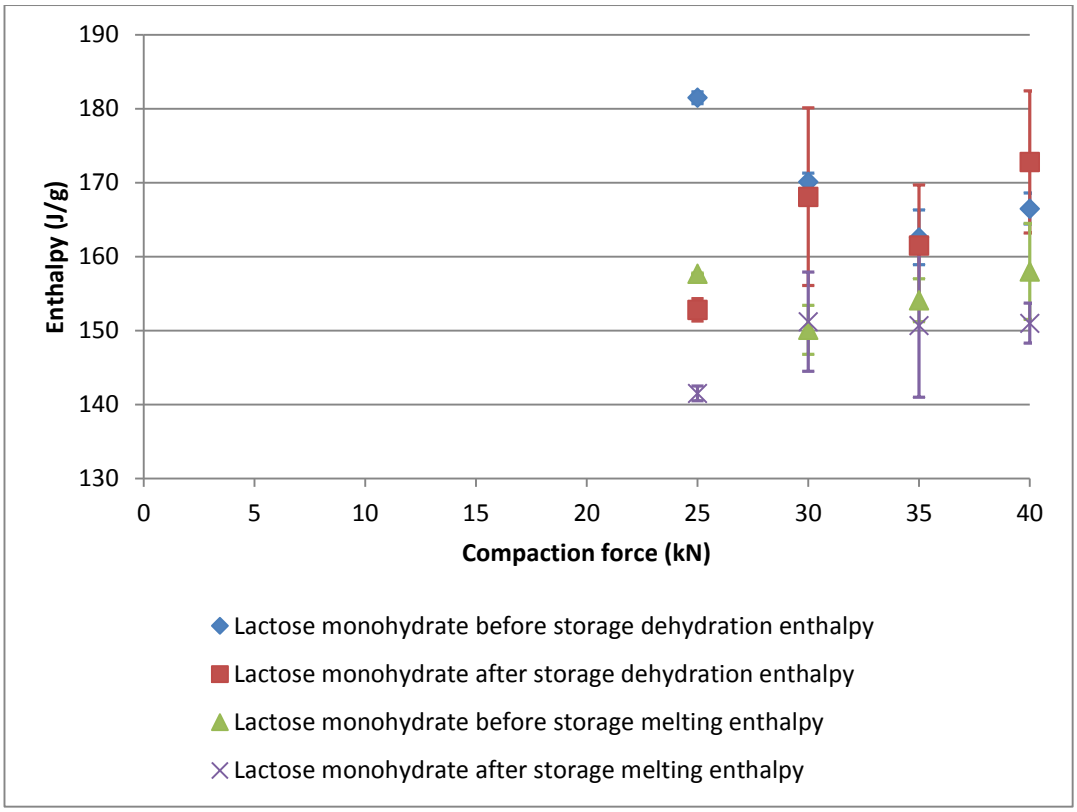

Figure 8.4. Summary of DSC results for dehydration and melting enthalpies for lactose monohydrate before and after storage

8.4.3 Compact crushing strength

Figure 8.6 shows the crushing strength results for lactose monohydrate before and after storage; data is shown in Appendix 0.7.

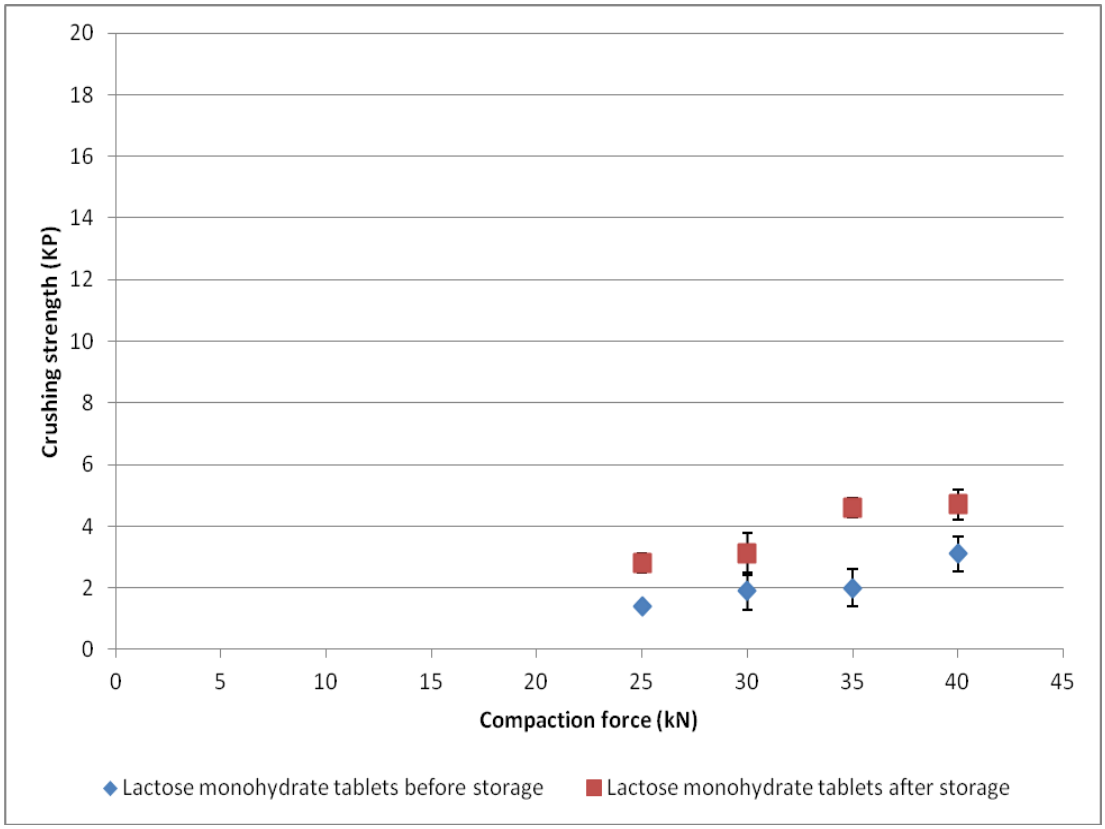

Figure 8.5. Compaction to force results for lactose monohydrate direct compression tablets before and after storage

The data presented shows the general trend of higher compaction forces producing higher compact crushing strengths. Increased crushing strength after storage indicates and reiterates the previous conclusions drawn from prior analysis that storage at RH above lactose monohydrates critical relative humidity, allows moisture to enable bonds to form between the components of the compact.

8.4.4 Tensile strength results on storage of lactose monohydrate compacts

The tensile strength of the tablets was calculated in order to eliminate the effect that minor changes in the compact weight and consequently tablet thickness may

have upon the crushing strength. Figure 8.6 shows the resultant tensile strength results. Tabulated data can be seen in Appendix 0.8. The results of the tensile strength measurements are consistent with reinforcing the conclusions drawn from the crushing strength measurements; that after storage there is a notable difference.

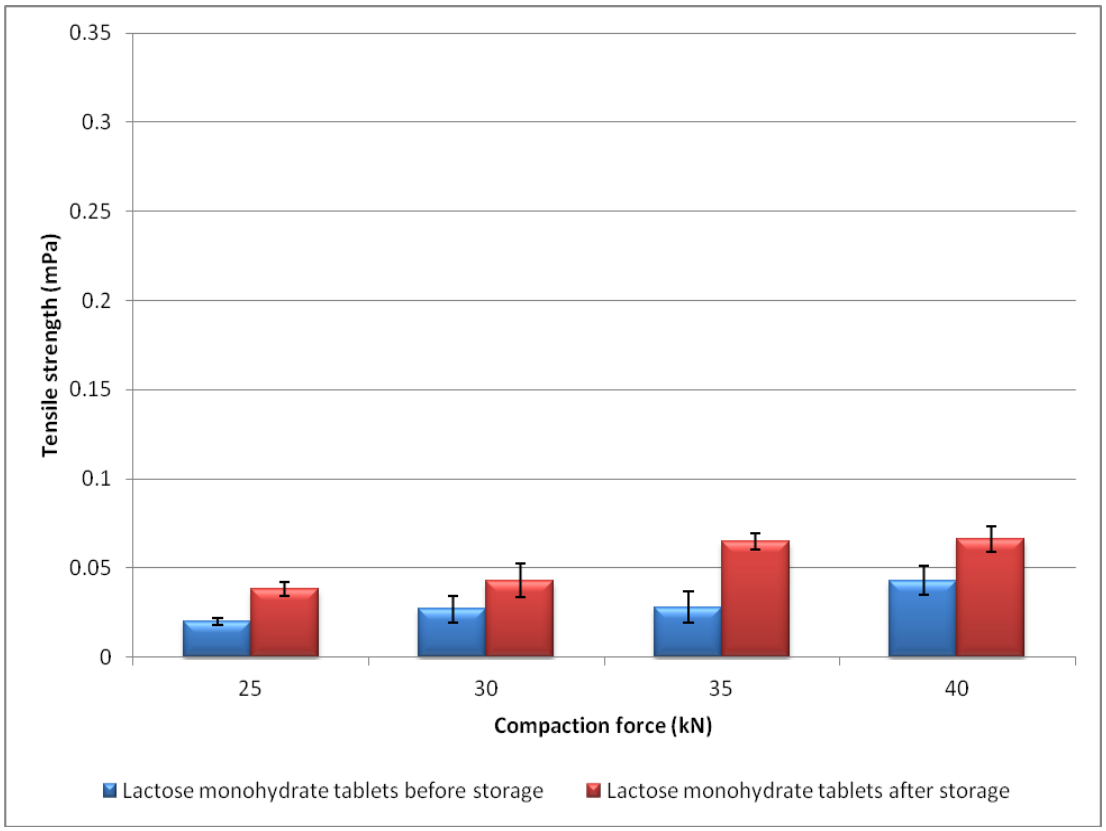

Figure 8.6. Summary of tensile strength measurements for lactose monohydrate direct compression tablets at 25, 30, 35 and 40 kN, before and after storage

8.4.5 Tablet thickness on storage of lactose monohydrate compacts

Tablet thickness was recorded both before and after storage to enable the tensile strength to be calculated but also to give an indication of the effects of storage at the increased RH with regards to moisture. Table 8.3 shows a summary of the tablet thickness of the tablets before and after storage. The data shows no significant

change in thickness of the tablets before and after storage. Previously, a decrease in tablet thickness that was observed was attributed to the plasticising effect of the moisture available upon storage (Dawoodbhai and Rhodes, 1989).

Table 8.3. Summary of tablet thickness measurements for lactose monohydrate tablets before and after storage

(n=5)	Initial tablet thickness (mm)	After storage tablet thickness (mm)	Change in thickness (mm)
25 kN	**4.701** (± 0.029)	**4.692** (± 0.039)	**-0.009**
30 kN	**4.601** (± 0.027)	**4.600** (± 0.028)	**-0.001**
35 kN	**4.515** (± 0.018)	**4.518** (± 0.028)	**+0.003**
40 kN	**4.525** (± 0.025)	**4.524** (± 0.028)	**-0.001**

8.4.6 Weight measurements on storage of lactose monohydrate compacts

Weight measurements were recorded of the initial tablets and after storage, in order to observe any changes that may have occurred due to storage at an elevated RH. Table 8.4 shows that there was no notable difference in weight change for lactose monohydrate tablets upon storage.

Table 8.4. Summary of weight measurements before and after storage for lactose monohydrate tablets before and after storage

n=5	Initial weight (mg)	After storage weight (mg)	Weight change (mg)
25 kN	**452.5** (± 2.0)	**452.3** (± 2.0)	**-0.2**
30 kN	**454.5** (± 1.3)	**454.5** (± 0.8)	**0.0**
35 kN	**451.6** (± 1.7)	**452.6** (± 1.9)	**+1.0**
40 kN	**455.1** (± 3.0)	**454.8** (± 3.1)	**-0.3**

8.4.7 PXRD results of the effect of storage of lactose monohydrate compacts

Powder diffractograms for lactose monohydrate material compacted at 25 kN before and after storage are shown in Figure 8.7. Powder diffractograms for material compacted at higher compaction forces both before and after storage can be seen in Appendix 0.9- Appendix 0.11.

The similarity of the diffractograms before and after storage show that no physical change occurred on storage and are consistent with a crystalline material. The powder diffractograms obtained correspond well with those reported in the literature (Kirk et al., 2007) .

Minor fluctuations in relative intensity were observed. However, PXRD analysis was performed on slightly ground material; hence the analysis only demonstrates that no visible transformations occurred within the material as whole. This does not definitively show that transitions may not have occurred upon the tablet surface, as

small amounts of disorder may not have been detected by the PXRD, as the limit of detection for PXRD is 5%.

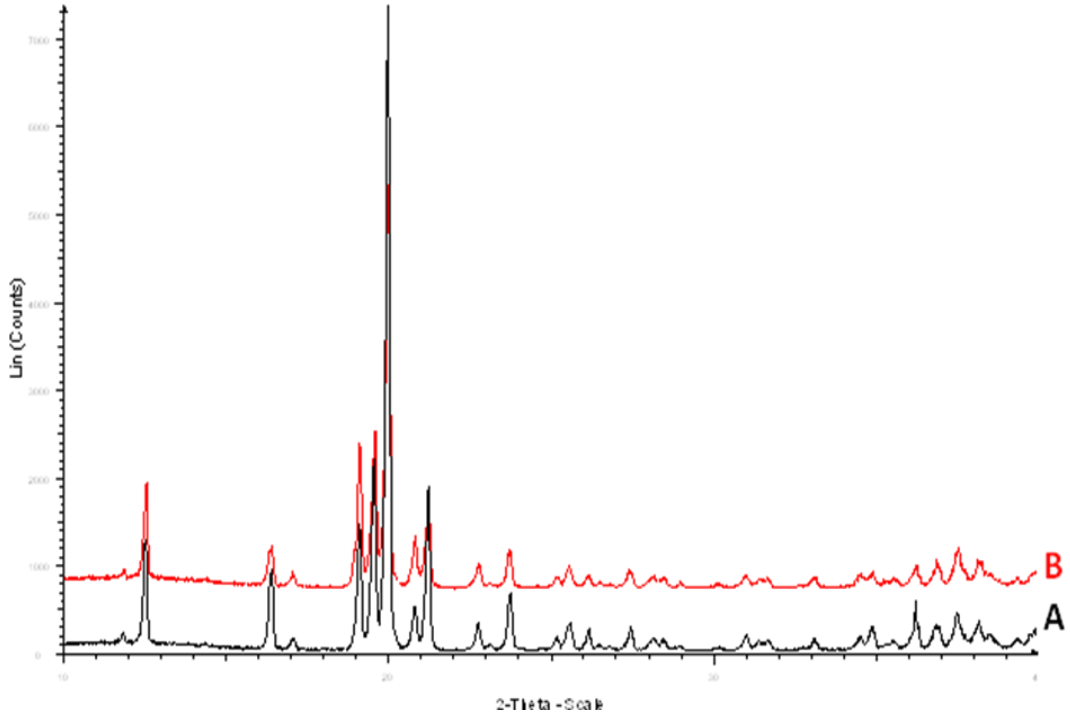

Figure 8.7. Powder x-ray diffraction patterns for lactose monohydrate direct compression tablets at 25 kN, before and after storage.

A (Black) = after storage (1 week at 75 % RH), B (Red) = before storage

8.4.8 Moisture profiling results of the effect of storage of lactose monohydrate compacts

Moisture profiles for lactose monohydrate direct compression tablets before and after storage are shown in Figure 8.8 and Figure 8.9, respectively, the final RH readings, which is the point taken to be the ERH value are shown in

Table 8.5.

It is apparent that before storage material compacted at 25 kN has notably different ERH values in comparison to material compacted at 30, 35 and 40 kN. It is

evident that after storage there is an increase in ERH value for compacted material at 25 kN. Material compacted at 30, 35 and 40 kN shows a slight variation in ERH after storage, however no notable changes are observed. Interestingly the general moisture profile behaviour for the compacts before and after compaction is similar; the lower ERH values obtained for the compact at 25 kN could be consistent with the compact's likely increase in porosity. The increase in ERH for this compact after storage at elevated RH is consistent with an increase in bonding (to give the observed increase in tensile strength) on storage and a reduction in porosity.

Behaviour within the moisture profile is also important in demonstrating how the material interacts with the surrounding environment with regards to moisture. In this instance material before storage and after storage behaved differently, immediately suggesting that although storage had little effect on actual ERH values, the way the compacted material behaved within the closed environment was altered. Before storage all material showed an initial decrease in %RH before equilibrium was attained, which is indicative of the material taking in moisture from the surrounding closed environment. Therefore, suggesting that when lactose monohydrate was compacted it exhibits some hygroscopic behaviour. After storage, the material compacted at 40 kN displayed different behaviour; initially there was a sharp increase of % RH within the first hour, then material exhibited a decrease in %RH whilst attaining equilibrium. The material initially displayed behaviour characteristic of the material actively wanting to give moisture out to the sample environment, hence the increase in the RH observed. The instability of the profile

could be due to changes occurring in the compact on exposure to the moisture profiler environment.

Table 8.5. Final RH readings for lactose monohydrate direct compression tablets, before and after storage

	25 kN final RH readings (%)		30 kN final RH readings (%)		35 kN final RH readings (%)		40 kN final RH readings (%)	
Before storage	32.5	31.4	43.0	43.6	41.7	41.7	40.4	40.5
After storage	37.0	34.3	41.0	41.1	42.6	42.6	41.6	42.8

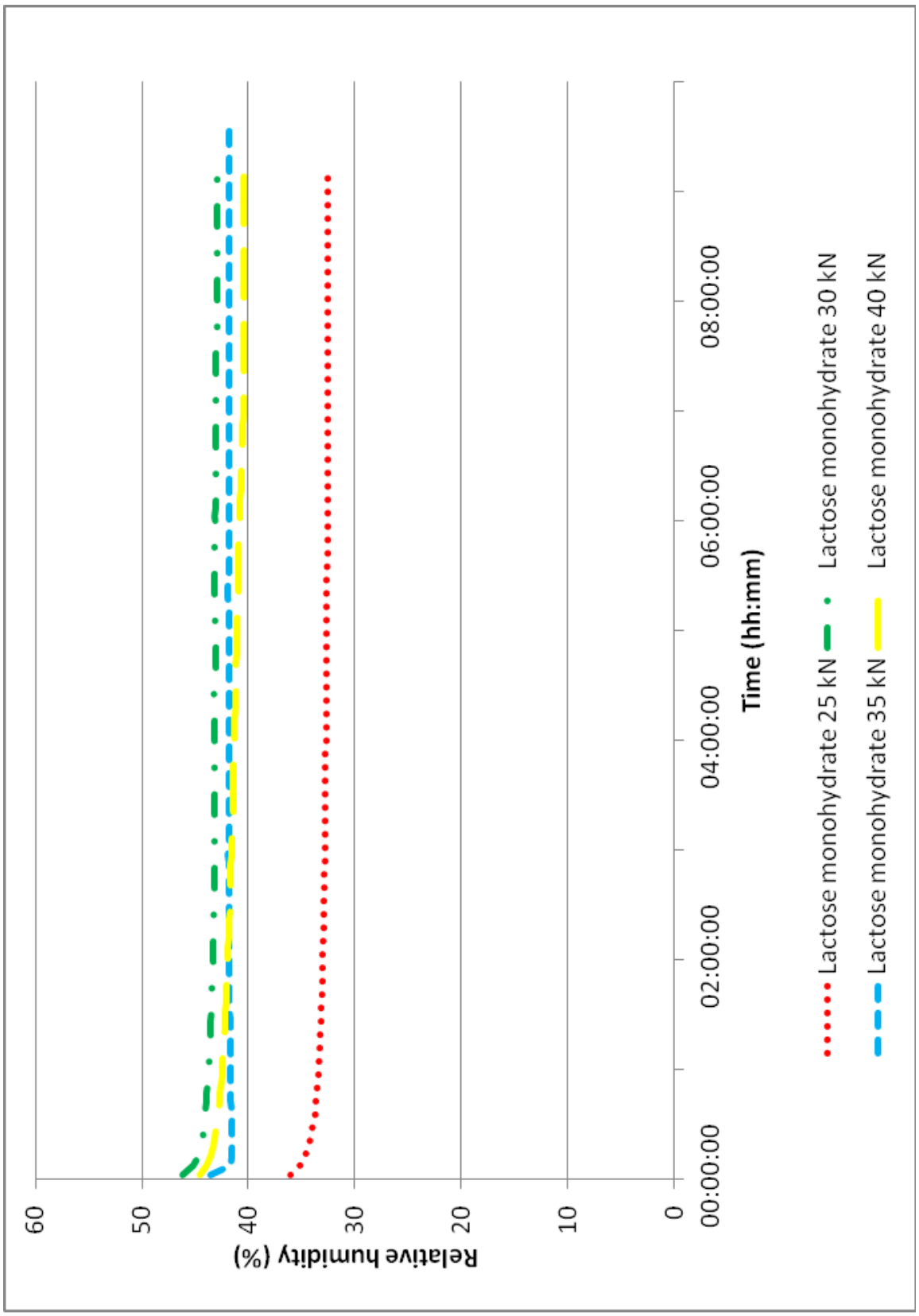

Figure 8.8. Moisture profiles of lactose monohydrate tablets before storage

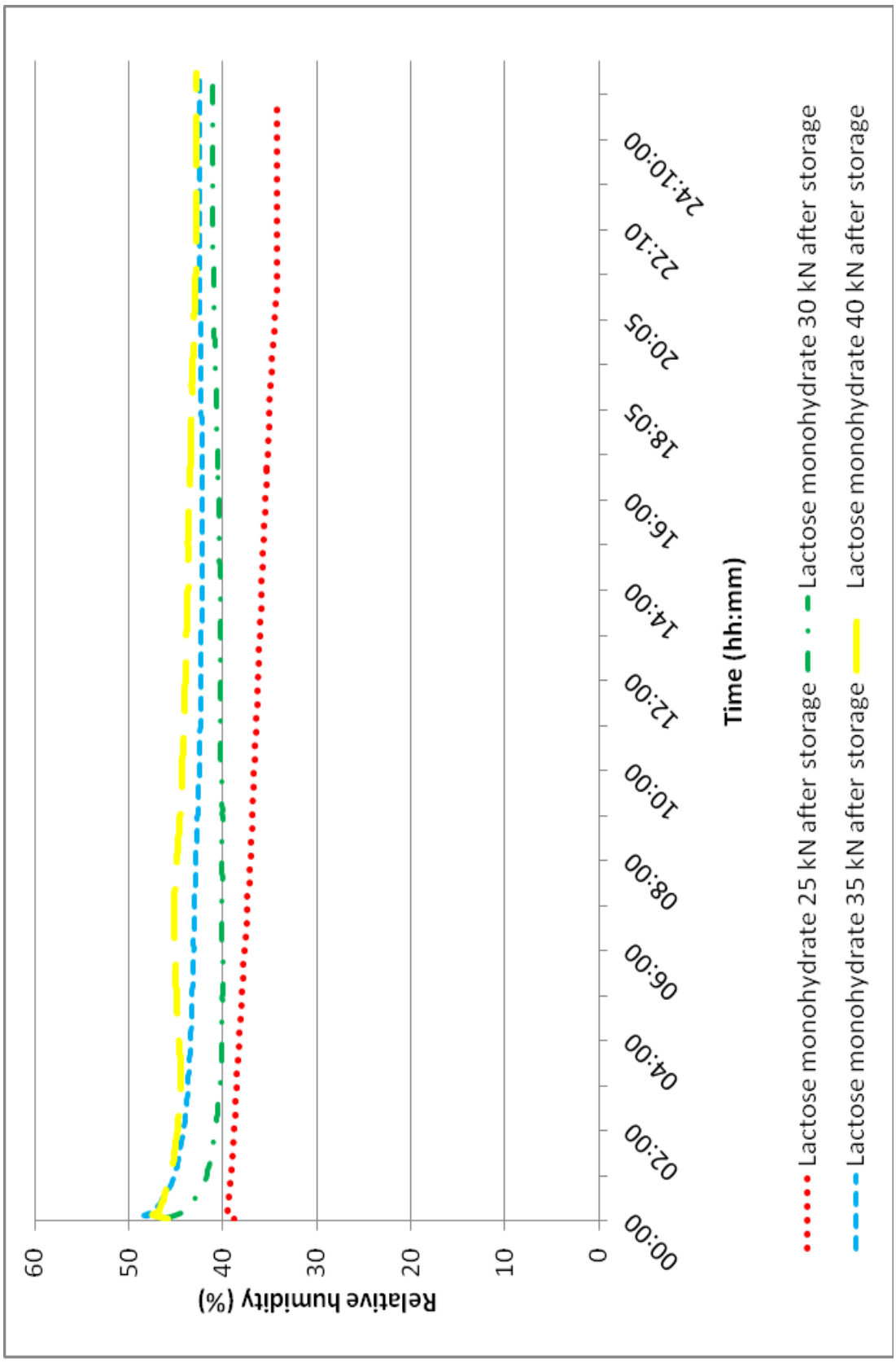

Figure 8.9. Moisture profiles of lactose monohydrate tablets after storage

8.5 Behaviour of anhydrous lactose compacts on storage; results and discussion

8.5.1 DSC results of the effect of storage of anhydrous lactose compacts

Representative DSC thermal profiles for directly compressed anhydrous lactose at 25 kN before and after storage can be seen in Figure 8.10. Representative DSC thermal profiles for anhydrous lactose tablets at increased compaction forces (30, 35 and 40 kN) can be seen in Appendix 0.15 - Appendix 0.17. All DSC profiles exhibit similar characteristic endotherms, which are distinctive to anhydrous lactose. A small dehydration endotherm is visible; this is attributed to it being a commercial sample which has small amounts of monohydrate present. Melting endotherm visible at approximately 230°C, which is indicative of β polymorph (Listiohadi et al., 2009). A summary of the thermal events within the DSC thermal profiles before and after storage are shown in Table 8.6.

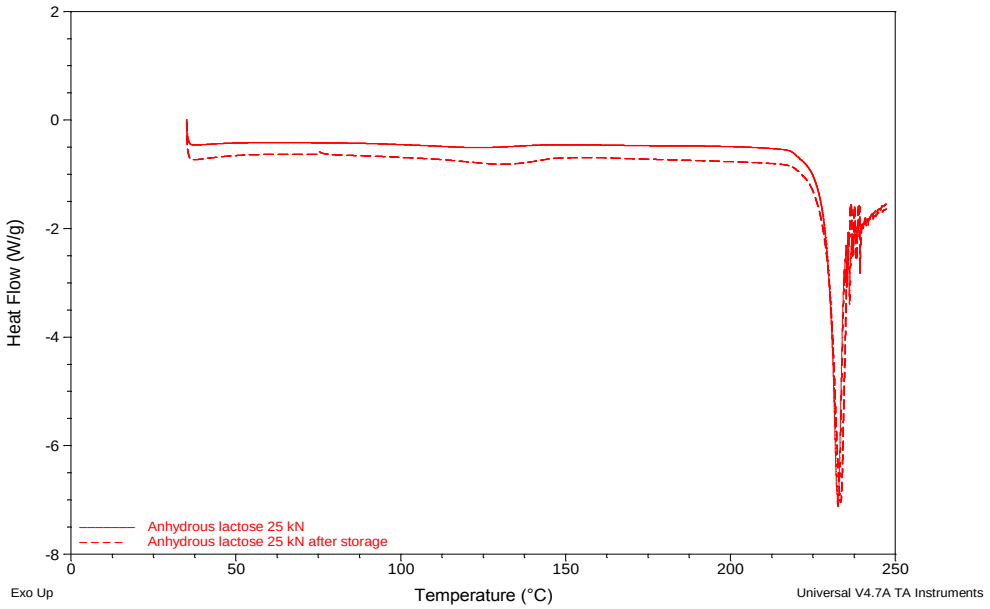

Figure 8.10. Representative DSC profile for anhydrous lactose tablets compacted at 25 kN, before and after storage

Table 8.6. Summary of anhydrous lactose direct compression tablets DSC results before and after storage

	Dehydration endotherm (°C) (Peak max)	Dehydration enthalpy (J/g) (Peak max)	Melting endotherm (°C) (Peak max)	Melting enthalpy (J/g) (Peak max)
25 kN	**117.39** (± 4.63)	**12.55** (± 0.90)	**232.99** (± 0.43)	**151.6** (± 4.5)
25 kN after storage	**128.79** (± 0.28)	**27.24** (± 1.53)	**232.37** (± 1.77)	**187.43** (± 7.49)
30 kN	**121.93** (± 1.18)	**13.50** (± 0.28)	**233.08** (± 0.22)	**142.4** (± 4.3)
30 kN after storage	**128.32** (± 0.87)	**28.53** (± 0.47)	**231.46** (± 0.84)	**171.73** (± 5.86)
35 kN	**122.77** (± 2.07)	**13.12** (± 1.32)	**233.13** (± 0.49)	**145.2** (± 5.5)
35 kN after storage	**128.59** (± 1.19)	**26.7** (± 2.45)	**233.19** (± 0.67)	**182.8** (± 7.7)
40 kN	**121.93** (± 1.29)	**12.96** (± 0.84)	**232.20** (± 1.58)	**145.6** (± 3.7)
40 kN after storage	**128.47** (± 0.71)	**26.50** (± 3.41)	**233.45** (± 0.59)	**174.2** (± 8.5)

From the data in Table 8.6, Figure 8.11 and Figure 8.12 it is evident that storage has a notable effect upon the thermal events with respect to DSC. It is apparent that upon storage of anhydrous lactose the peak max associated with the minor dehydration endotherm is increased, hence found at a higher temperature. It is expected that continued storage at the increased RH would eventually lead to the position of the dehydration endotherm to be approximately 145°C, which corresponds to dehydration of the crystal lattice (Lerk et al., 1984b), suggesting prolonged storage would facilitate conversion of an anhydrous lactose to the

monohydrate, as anhydrous lactose is able to convert to the monohydrate form at 70% RH at room temperature (Academy of Pharmaceutical and Pharmaceutical Society of Great, 1986).

Figure 8.11 shows that there is no variation in the peak max associated with the melting endotherm. No notable changes in the peak max indicate that no transition between α and β has occurred. Over time at increased storage RH it is expected that more moisture would be picked up, which would subsequently cause the endotherm associated with the β melt to gradually diminish and an endotherm associated with the α melt would become prominent, as the anhydrous from is converted into the hydrate.

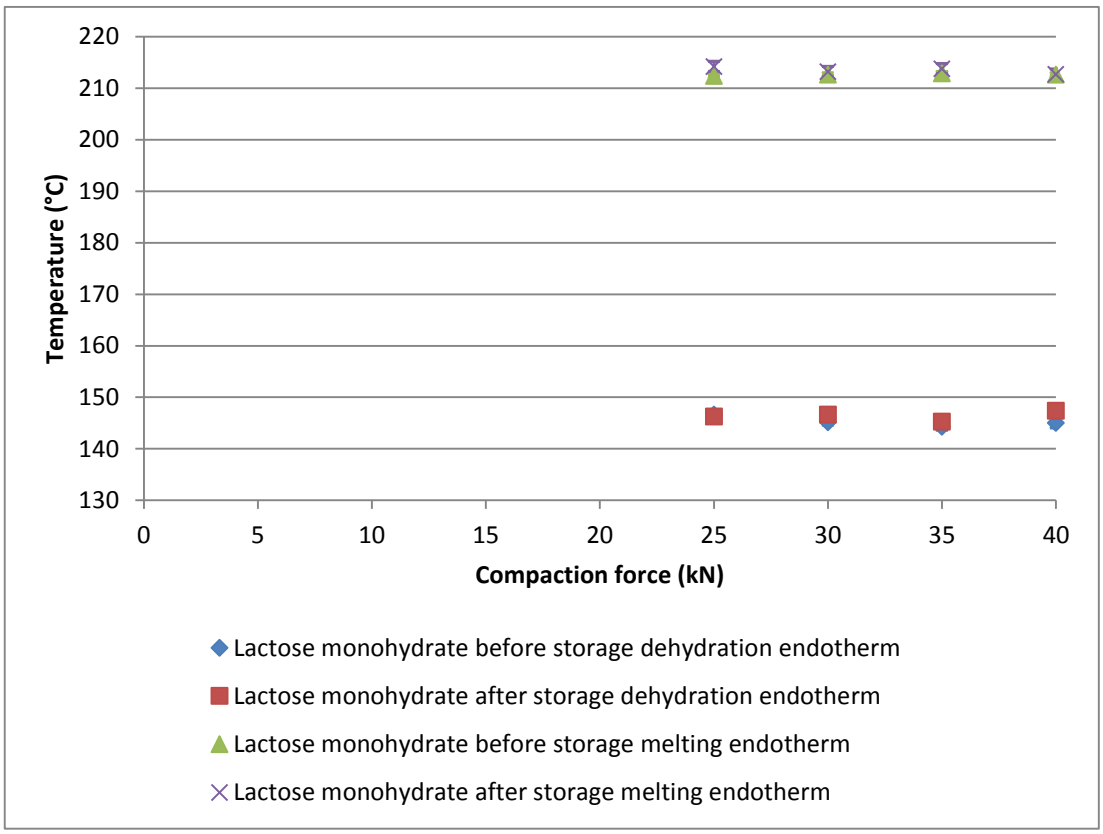

Figure 8.11. Summary of anhydrous lactose tablets before and after storage dehydration and melting endotherms

Figure 8.12 shows the summary of the enthalpies associated with the endothermic events from the DSC thermal profiles. This demonstrates that after storage there is a notable increase in the enthalpies associated with both the dehydration and the melting endotherms. It is expected that an increase in enthalpy coupled to the dehydration endotherm would be observed, because of the previous increase in peak max due to moisture ingress from the storage RH. A notable increase in the enthalpies associated with the melting endotherms is also evident. This therefore reiterates the conclusions drawn from the previous results; storage at the elevated RH cause's moisture to promote crystallisation of any disordered system. However the moisture does not facilitate conversion of the anhydrous form to the hydrate, within the storage time period of this study.

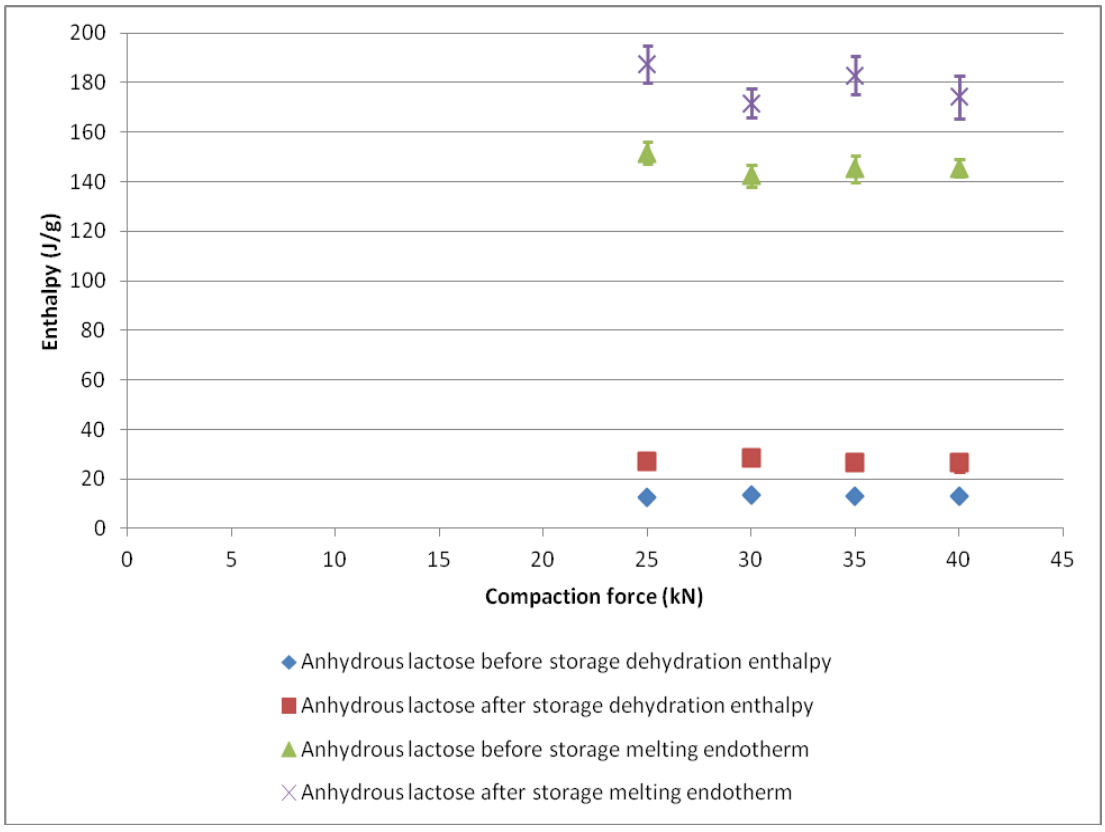

Figure 8.12. Summary of anhydrous lactose tablets before and after storage dehydration and melting enthalpies

8.5.2 Compact crushing strength on storage of anhydrous lactose

Figure 8.13 shows the crushing strength results for anhydrous lactose tablets before and after storage, data is shown in Appendix 0.18. From this it is evident that there is a notable difference of crushing strength upon storage of the anhydrous lactose tablets. As an increase in crushing strength is observed, this suggests that the high storage RH allows moisture ingress, in which the water is able to promote bonding, which leads to stronger more robust tablets.

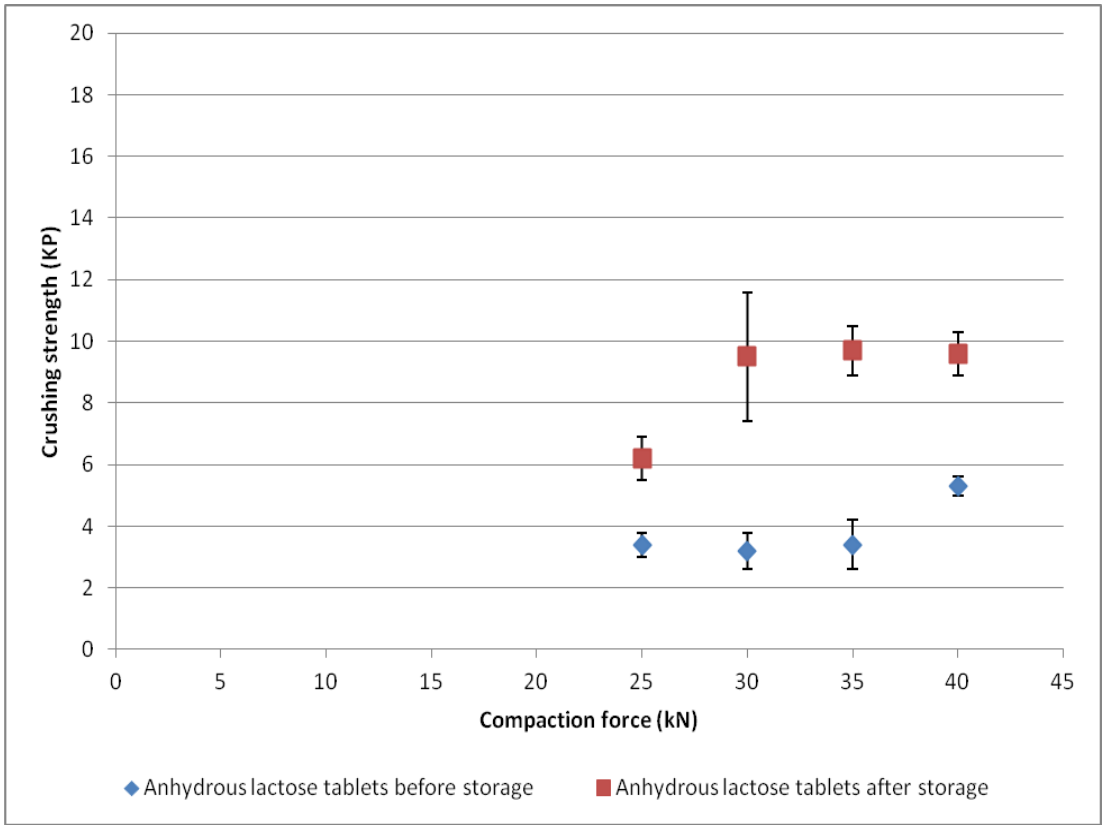

Figure 8.13. Compaction to force results for anhydrous lactose direct compression tablets before and after storage

8.5.3 Tensile strength results on storage of anhydrous lactose compacts

The tensile strength of the tablets was calculated in order to eliminate the effect that minor fluctuations in initial compact weight and corresponding tablet thickness may have upon crushing strength. Figure 8.14 shows the summary of tensile strength results, data can be seen in Appendix 0.19. The results of the tensile strength measurements indicate and reinforce the conclusions drawn from the crushing strength data, that storage at elevated RH causes moisture to act to produce stronger more robust tablets.

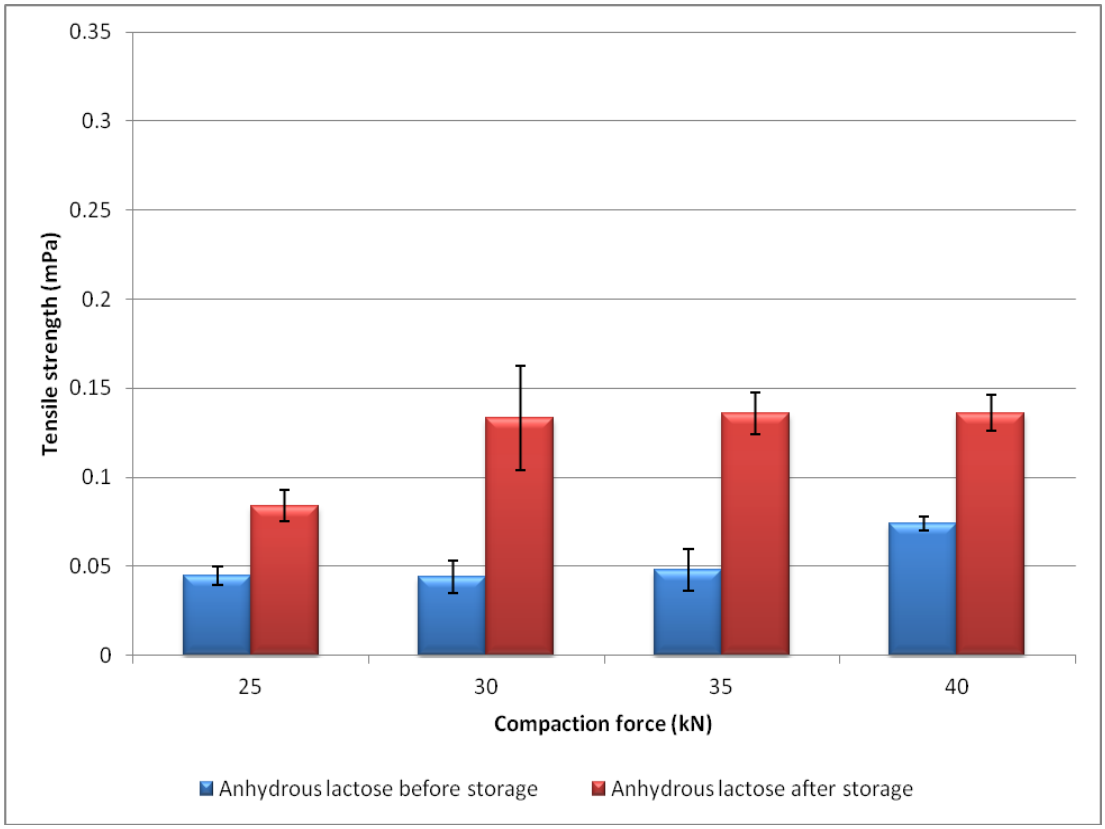

Figure 8.14. Summary of tensile strength measurements for anhydrous lactose tablets before and after storage

8.5.4 Tablet thickness on storage of anhydrous lactose compacts

Tablet thickness was recorded both before and after storage to enable the tensile strength to be calculated. Compact thickness can also be used to give an indication of the effects of moisture with storage, for example if the high storage RH has caused the tablet to swell. Table 8.7 shows a summary data of the tablet thickness, demonstrating that no significant change was observed.

Table 8.7. Summary of tablet thickness measurements before and after storage for anhydrous lactose

(n=5)	Initial tablet thickness (mm)	After storage tablet thickness (mm)	Change in thickness (mm)
25 kN	**4.728** (± 0.030)	**4.715** (± 0.027)	**-0.013**
30 kN	**4.574** (± 0.032)	**4.573** (± 0.028)	**-0.001**
35 kN	**4.535** (± 0.029)	**4.536** (± 0.026)	**+0.001**
40 kN	**4.523** (± 0.030)	**4.512** (± 0.027)	**-0.011**

8.5.5 Compact weight measurements on storage of anhydrous lactose compacts

Weight measurements were recorded of the tablets initially after compaction and then again after storage. Table 8.8 shows that after storage the tablet thickness increased upon storage. However, the weight increase in terms of percentage weight loss ranges from 0.40-0.78%, which is not a very notable increase.

Table 8.8. Summary of tablet weight before and after storage for anhydrous lactose

(n=5)	Initial tablet weight (mg)	After storage tablet weight (mg)	Change in weight after storage (mg)
25 Kn	**454.18** (± 1.31)	**456.00** (± 1.34)	**+1.82**
30 Kn	**453.16** (± 1.47)	**455.18** (± 1.75)	**+2.02**
35 Kn	**455.08** (± 2.41)	**457.22** (± 2.64)	**+2.14**
40 kN	**455.36** (± 2.97)	**458.94** (± 1.43)	**+3.58**

8.5.6 PXRD results of the effect of storage of anhydrous lactose compacts

Powder diffractograms for anhydrous lactose compacted at 25 kN before and after storage are shown in Figure 8.15, powder diffractograms for material compacted at increased compaction forces (30, 35 and 40 kN) before and after storage are shown in Appendix 0.20 - Appendix 0.22. These show that no physical change occurred before and after storage. There is a strong characteristic peak at approximately 10.5° 2θ, which is present both before and after storage.

PXRD analysis was performed on slightly ground material; the PXRD analysis shows that no visible transformations occurred within the material as a whole. This is not to say that transitions may not have occurred upon the tablet surface, as PXRD is insensitive to small amounts of disorder.

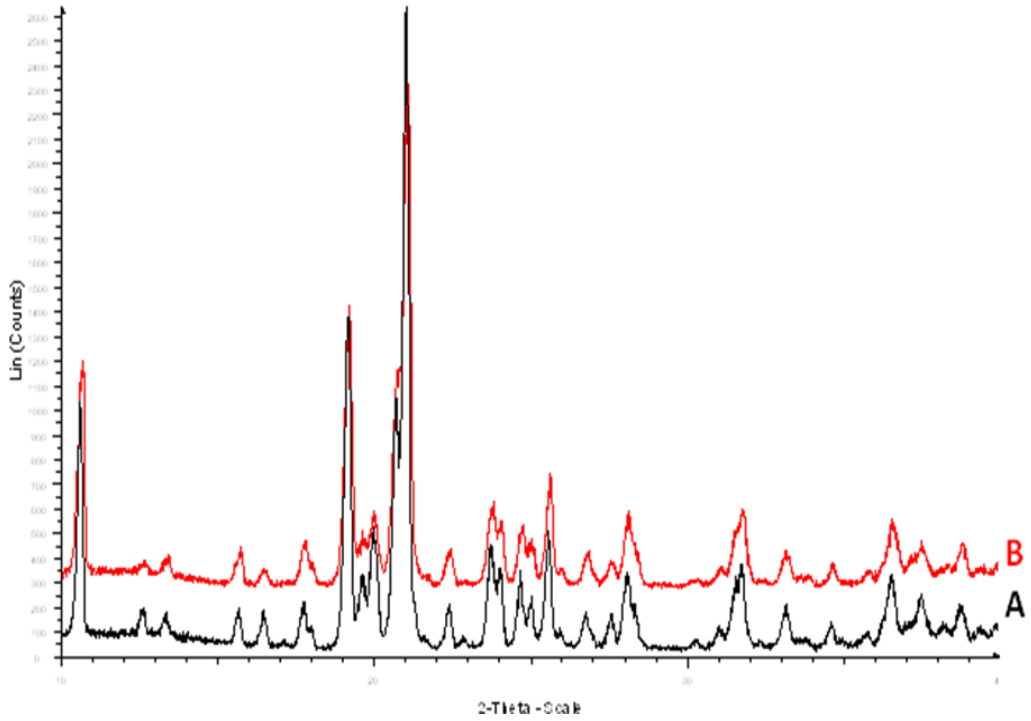

Figure 8.15. Powder x-ray diffraction patterns for anhydrous lactose direct compression tablets at 25 kN before and after storage

A (Black) = after storage, B (Red) = before storage

8.5.7 Moisture profiling results of the effect of storage of anhydrous lactose compacts

Moisture profiles for anhydrous lactose before and after storage are shown in Figure 8.16 and Figure 8.17 respectively. Final ERH readings, which is the point taken to be the ERH are shown in Table 8.9.

After initial compaction of the material before storage, all material displayed similar ERH values, suggesting that compaction force had no notable effect in this instance upon ERH value. After storage there was no notable change in ERH values.

The shape of the moisture profile produced by the material is important in indicating the behaviour of the material. Before storage, the majority of the compacted material displayed an initial decrease before ERH was attained; which is indicative of the material taking in moisture from the surrounding sample environment. The 25 kN compacted material behaves differently; displaying an initial increase in RH before equilibrium is reached, representing the material giving out moisture to the sample chamber environment.

After storage, moisture profiles for the compacted material all show a slight increase in RH, before gradually decreasing and reaching equilibrium. This is different behaviour to the majority of the moisture profiles before storage. This increase in RH is indicative of the material initially giving out moisture which is attributed to an initial rapid equilibrium after storage at elevated RH. Material then demonstrates a gradual decrease in RH, which is indicative of the material taking in moisture from the sample chamber atmosphere, almost reverting back to the behaviour observed prior to storage. The trend in the final ERH values after storage (Table 8.9) is that increased compaction pressure is once again associated with an increase in ERH. It is postulated that the decreased porosity of the more highly compressed material offers less surface area to interact with the moisture in the environment and thus produce the higher ERH. In summary the results of the moisture profiles for anhydrous lactose in this instance indicate that storage at 75 % RH does not affect the amount of free water available, to a large extent.

Table 8.9. Final RH readings for anhydrous lactose direct compression tablets before and after storage

	25 kN final RH readings (%)		30 kN final RH readings (%)		35 kN final RH readings (%)		40 kN final RH readings (%)	
Before storage	37.9	38.2	41.3	41.9	38.3	38.0	42.0	41.1
After storage	36.8	35.3	37.9	39.0	38.7	39.1	41.6	40.8

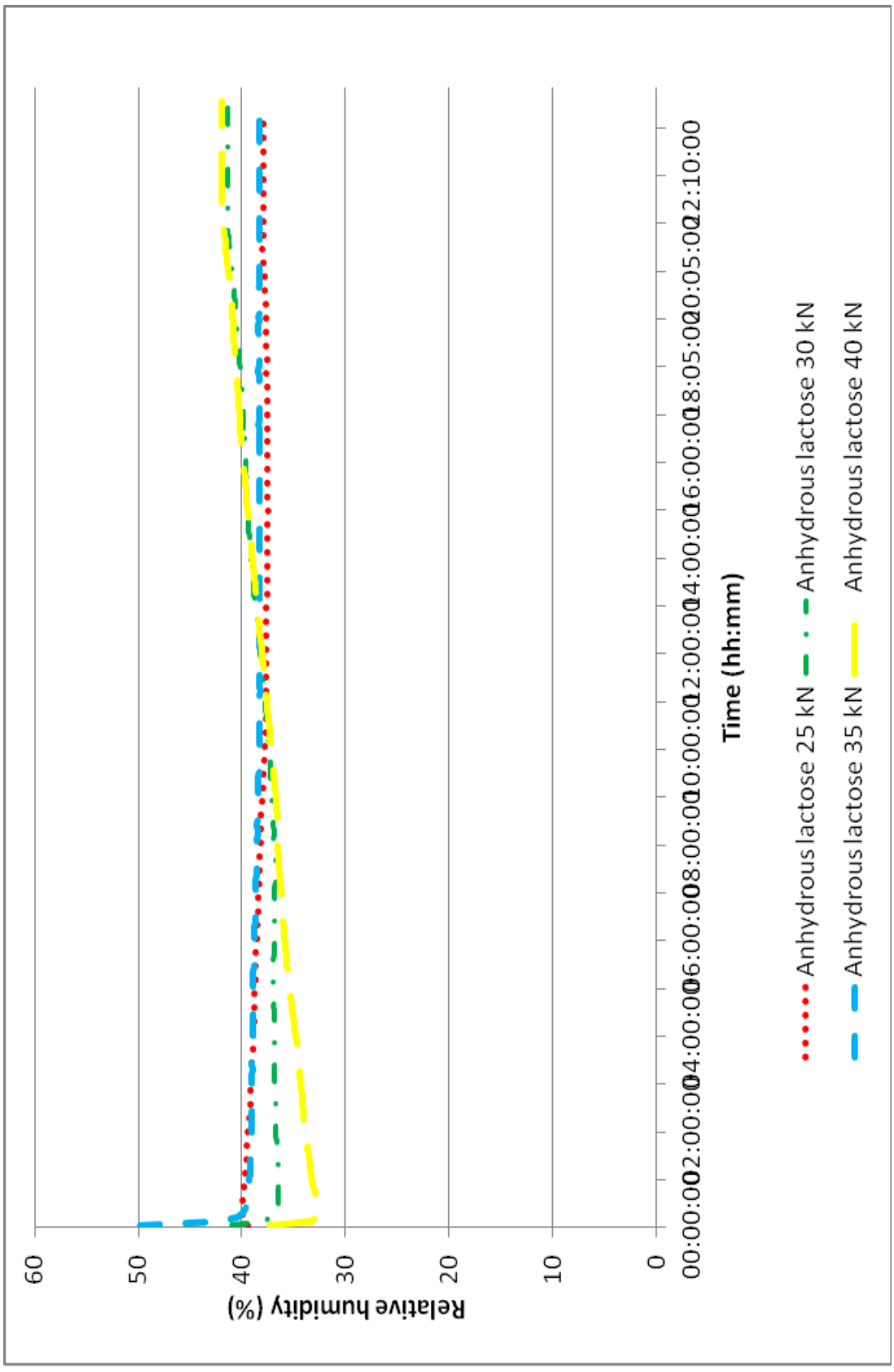

Figure 8.16. Moisture profiles of anhydrous lactose tablets before storage

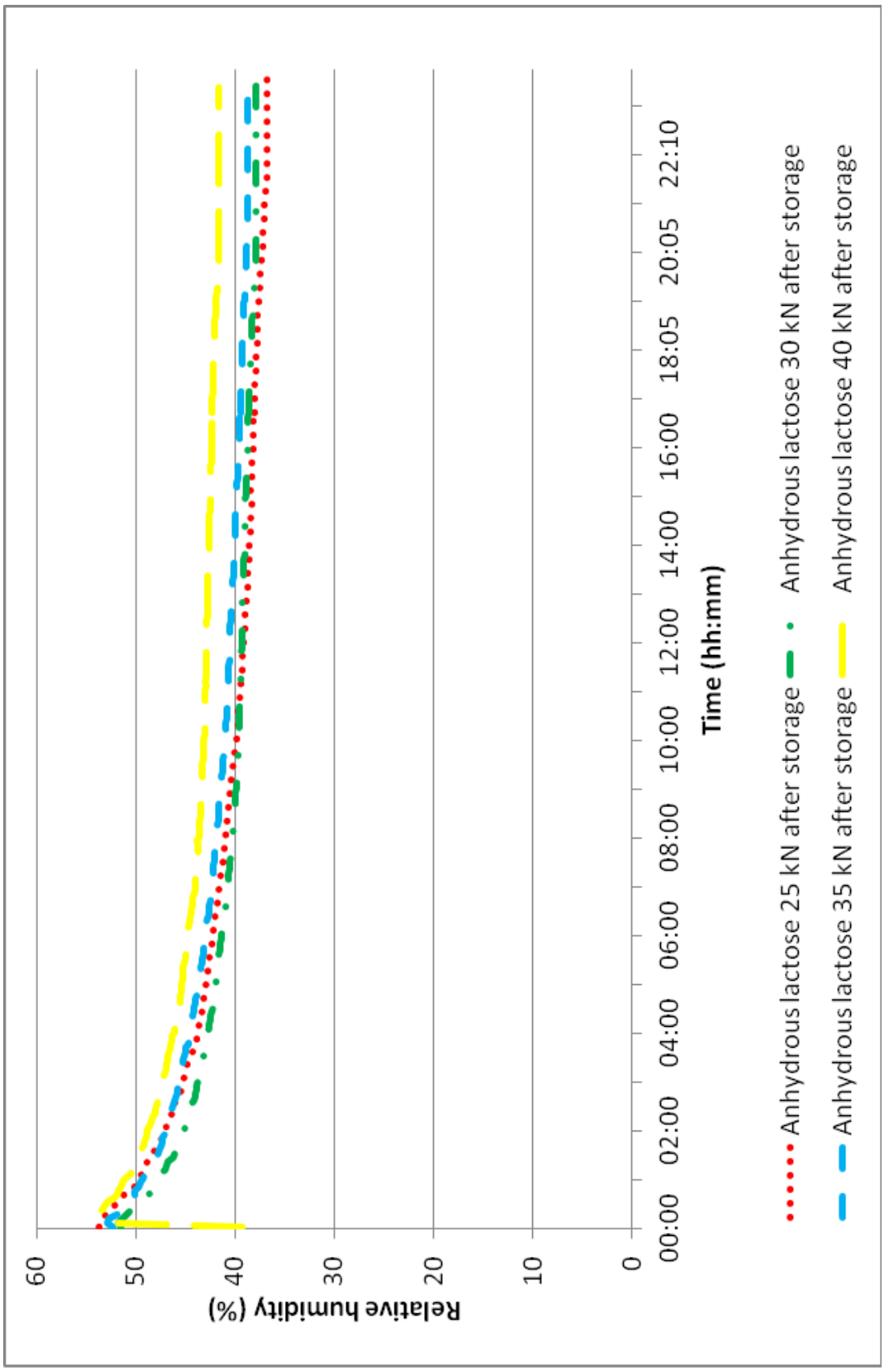

Figure 8.17. Moisture profiles for anhydrous lactose tablets after storage

8.6 Behaviour of spray dried lactose compacts; results and discussion

8.6.1 TGA results of the effect of storage of spray dried lactose compacts

Representative TGA thermal profiles for spray dried lactose tablets at 25 kN before and after storage can be seen in Figure 8.18. Representative thermal profiles for spray dried tablets at increased compaction forces (30, 35 and 40 kN) before and after storage can be seen in Appendix 0.23 - Appendix 0.25. All thermal profiles before storage demonstrate the characteristic behaviour of spray dried lactose. The first initial weight loss is due to residual water present from the spray drying process and hence is present at a lower temperature than if it was crystalline lattice water.

All thermal profiles before storage demonstrate the characteristic behaviour of spray dried lactose. The first initial weight loss is due to residual water present from the spray drying process and hence is present at a lower temperature than if it was crystalline lattice water.

The representative thermal profile for material after storage is notably different to material before storage. After storage the thermal profile is more characteristic of that of lactose monohydrate in that a water loss is followed by melting and decomposition. However, spray dried lactose samples before storage contain a higher weight loss percentage that is attributed water; this is attributed to the residual water that remains after the spray drying process. Spray dried lactose samples after storage have a lower percentage weight loss than material before storage, therefore below the 5% that is expected for lactose monohydrate. This

would suggest that total conversion of amorphous to monohydrate form did not occur upon storage.

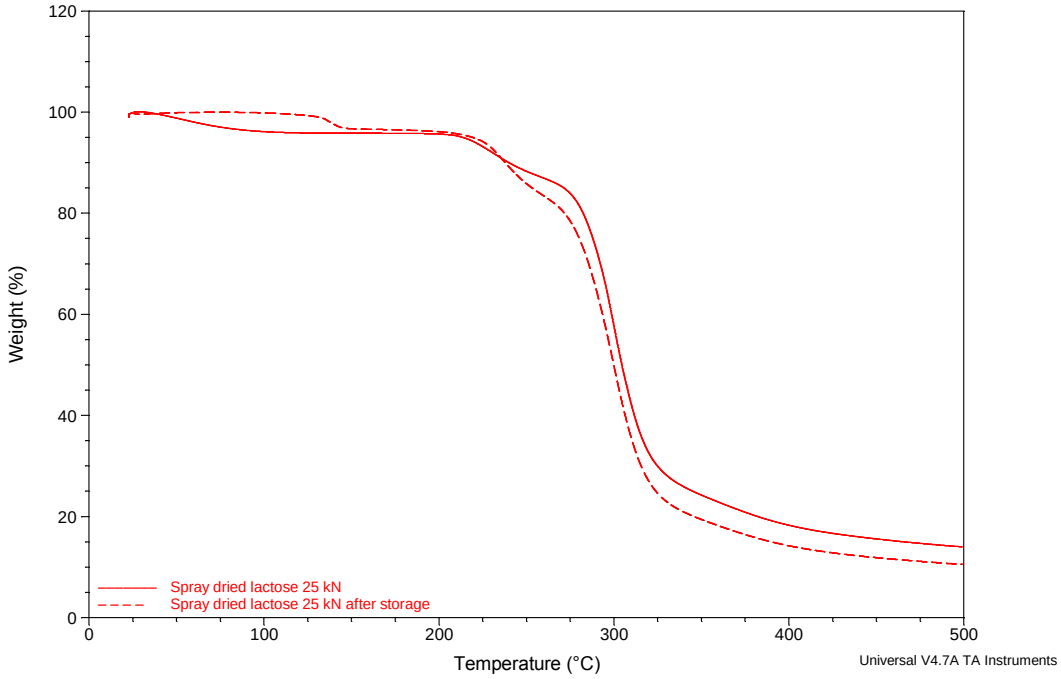

Figure 8.18. Representative TGA thermal profiles for spray dried lactose tablets at 25 kN, before and after storage

Table 8.10. Summary of TGA data for spray dried lactose direct compression tablets before and after storage

(n=3)	Water loss (%)	Standard deviation (%)
25 kN	4.214	± 0.338
25 kN after storage	2.625	± 0.244
30 kN	4.118	± 0.230
30 kN after storage	2.860	± 0.171
35 kN	4.257	± 0.183
35 kN after storage	2.863	± 0.256
40 kN	4.283	± 0.229
40 kN after storage	2.617	± 0.574

8.6.2 DSC results of the effect of storage of spray dried lactose compacts

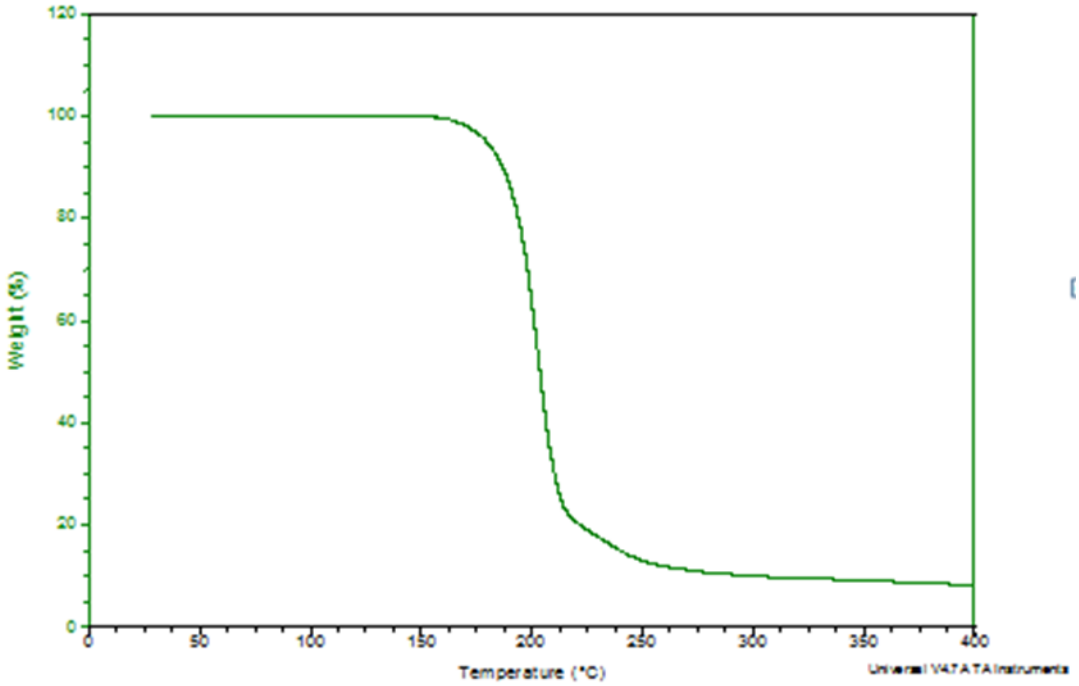

Representative DSC thermal profiles for spray dried lactose compacts produced with a compaction pressure of 25 kN before and after storage can be seen in Figure 8.19. Representative DSC thermal profiles for spray dried lactose compacts produced at increased compaction forces (30, 35 and 40 kN) can be seen in

Appendix 0.26 - Appendix 0.28.

Before storage it is evident that all thermal profiles display the behaviour that is characteristic of spray dried lactose. The first endotherm visible is a broad endotherm with a peak max at approximately 75°C is assigned to the loss of residual water as a direct result of the spray drying process and corresponds to the

initial weight loss observed within the TGA thermal profile. Disruption of the baseline is evident in the region 115-125°C, which given that the material is amorphous in nature; this is attributed to the T_g. The exotherm visible at approximately 170°C is indicative of crystallisation of the amorphous material; the crystallisation was facilitated by the DSC analysis and was amorphous prior to analysis (Sebhatu et al., 1994). Two melting endotherms are observed at approximately 216°C and 223°C which is attributed to the melting of α and β forms respectively (Islam and Langrish, 2010) . The endotherm corresponding to the α melt is more sharper than the β melting endotherm, suggesting that upon recrystallisation within the DSC, α is the prominent form.

After storage it is evident from the thermal profiles that the material has physically changed. After storage there was no residual moisture, instead this was replaced with a dehydration endotherm at approximately 145°C, which is indicative of the dehydration of the monohydrate (Ticehurst et al., 1996) . Two melting endotherms are visible within the thermal profile at approximately 214°C and 230°C, which is attributed to the melting of α and β forms respectively. The second endotherm which is due to the β melt is notably sharper and has a higher enthalpy than the α melt, suggesting that storage at the elevated RH facilitates crystallisation to predominantly β form.

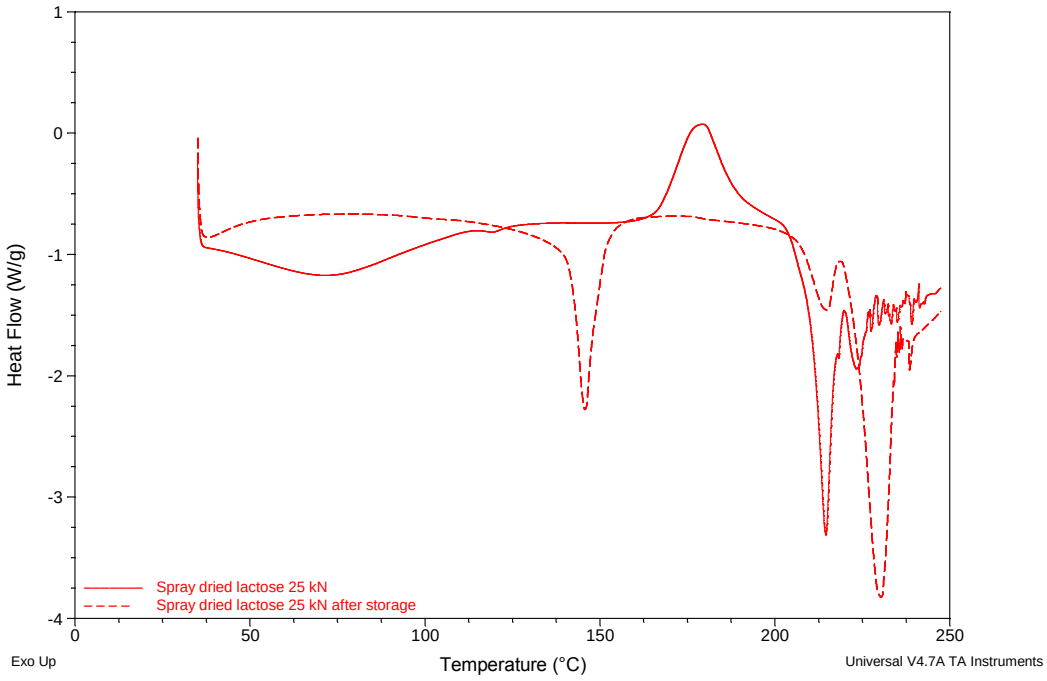

Figure 8.19. Representative DSC thermal profiles for spray dried lactose at 25 kN, before and after storage

8.6.3 Compact crushing strength results on storage of spray dried lactose

Figure 8.20 shows the crushing strength for spray dried lactose tablets before and after storage, data is shown in Appendix 0.29. From this it is evident that there is no notable difference before and after storage with regards to the 25 kN compacted material. However, with regards to the 30, 35 and 40 kN compacted material, there is a notable decrease in crushing strength after storage. The decrease reinforces earlier discussion which suggested that amorphous spray dried lactose is converted at least in part to the crystalline lactose monohydrate. The evidence for this includes that lactose monohydrate previously displayed crushing strengths below 6 KP.

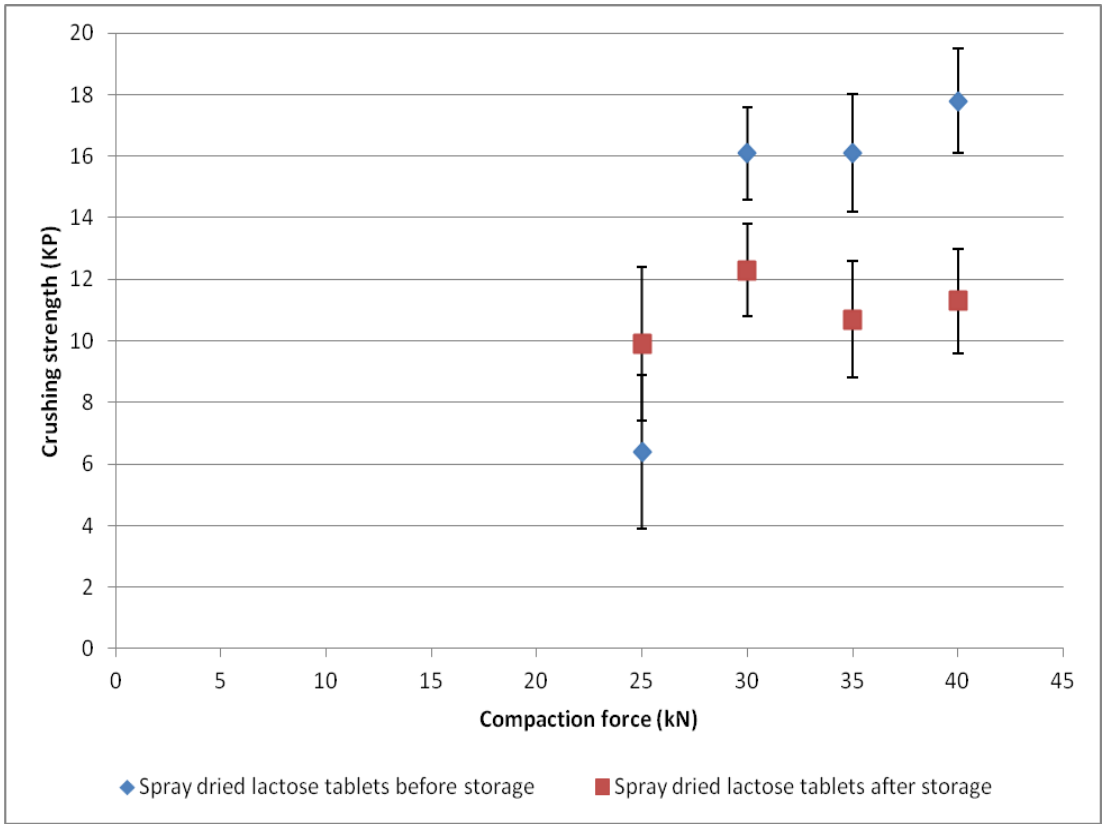

Figure 8.20. Compaction to force results for spray dried lactose direct compression tablets before and after storage

8.6.4 Tensile strength results on storage of spray dried compacts

Tensile strength of the compacts were calculated in order to eliminate minor fluctuations in initial compact weight and the corresponding tablet thickness may have upon crushing strength. Figure 8.21 shows the summary of tensile strength results, data can be seen in Appendix 0.30. The results reinforce the conclusions drawn from crushing strength analysis in that apart from the 25 kN compacted material there is a decrease in tensile strength after storage. However it is only a significant decrease with respect to material compacted at 35 and 40 kN. It is expected that prolonged exposure to the elevated storage RH would cause further decrease until a range similar to that previously seen for lactose monohydrate is reached.

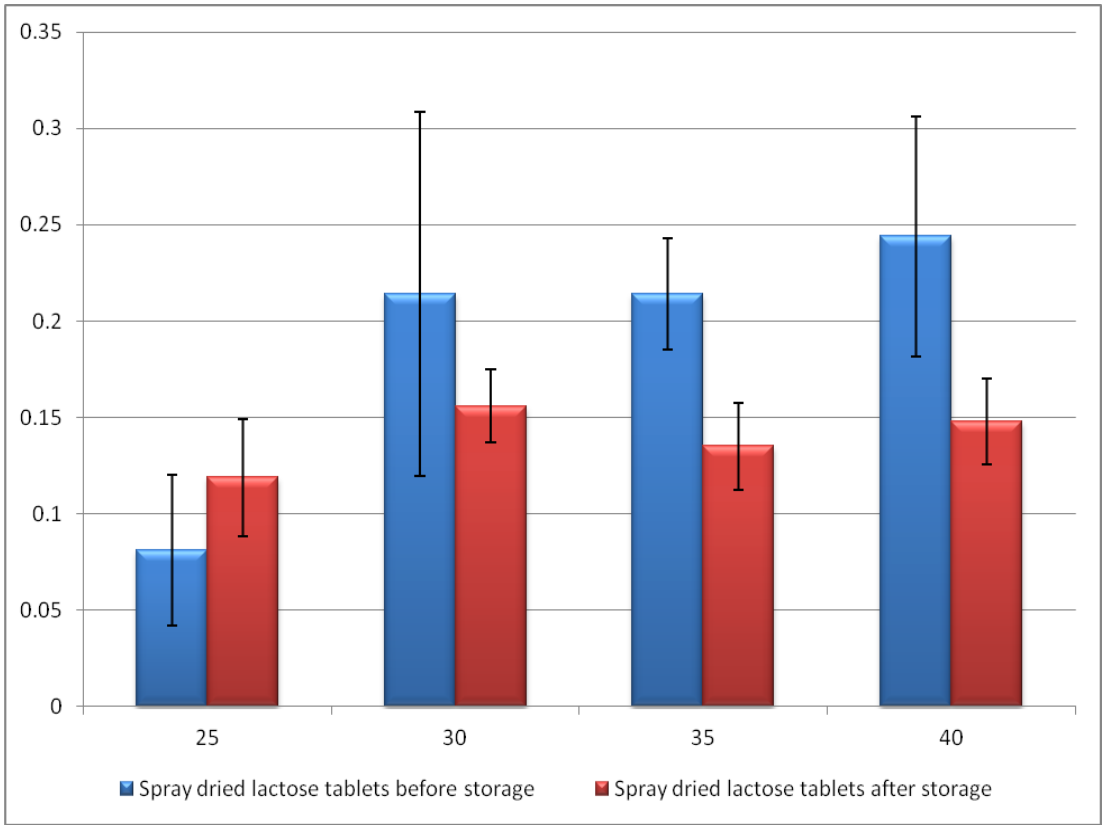

Figure 8.21. Summary of tensile strength measurements for spray dried lactose tablets before and after storage

8.6.5 Tablet thickness results on storage of spray dried lactose compacts

Tablet thickness was recorded both before and after storage to enable tensile strength to be calculated, but it can also be used to give an indication of the effects of storage with regards to moisture. The results show that there are no notable differences in the thickness of the tablets before and after storage indicating that no gross physical changes have occurred within the tablets upon storage at elevated RH.

Table 8.11. Summary of tablet thickness measurements before and after storage for spray dried lactose

(n=5)	Initial tablet thickness (mm)	After storage tablet thickness (mm)	Change in thickness (mm)
25 kN	**4.728** (± 0.030)	**4.715** (± 0.027)	**-0.013**
30 kN	**4.574** (± 0.032)	**4.573** (± 0.028)	**-0.001**
35 kN	**4.535** (± 0.029)	**4.536** (± 0.026)	**+0.001**
40 kN	**4.523** (± 0.030)	**4.512** (± 0.027)	**-0.011**

8.6.6 PXRD results of the effect of storage of spray dried lactose compacts

Powder diffractograms for spray dried lactose compacted at 25 kN before and after storage are shown in Figure 8.22. Powder diffractograms for material compacted at higher compaction forces (30, 35 and 40 kN) before and after storage can be seen in Appendix 0.31 - Appendix 0.33. All powder diffractograms show the same trend, initially mainly amorphous material which upon storage converts to a somewhat crystalline.

Before storage the material is mainly amorphous, however evidence of some low level crystallinity is observed, which may be a direct result of the time PXRD analysis takes as the material is hygroscopic and is able to pick up atmospheric moisture easily. After storage the diffractogram evidently demonstrates a high degree of crystallinity; suggesting that the storage RH caused conversion to a crystalline form

of lactose. The diffractogram exhibits peaks that are characteristic to both α and β lactose, suggesting that upon recrystallisation both α and β polymorphs are present. Both α and β forms are found because prior to dehydration (either by spray drying or freeze drying processes), muto-rotation may occur, which is dependent upon temperature, concentration and time, hence the degree of muto-rotation and therefore the anomeric content will vary depending upon the individual parameters employed (Haque and Roos, 2005).

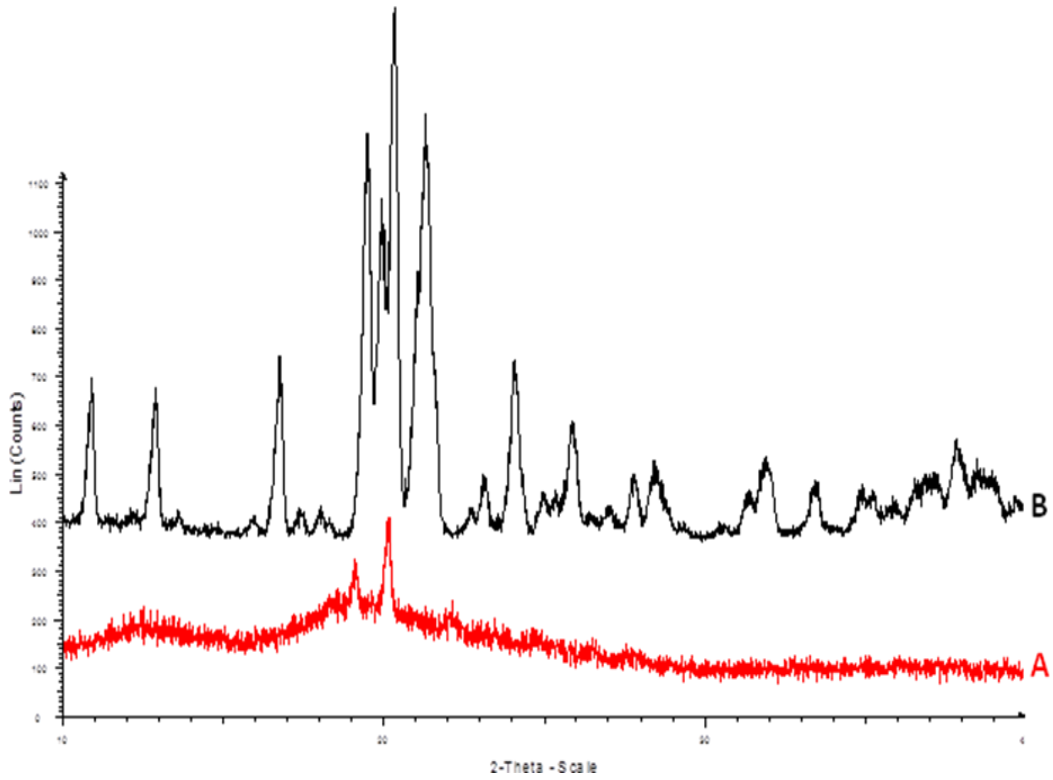

Figure 8.22. Powder x-ray diffraction patterns for spray dried lactose direct compression tablets at 25 kN before and after storage

A (Red) = before storage, B (Black) = after storage

8.6.7 Moisture profiling results of the effect of storage of spray dried lactose compacts

Moisture profiles for spray dried lactose tablets before and after storage are shown in Figure 8.23 and Figure 8.24 respectively. The final RH readings, which is the point taken to be the ERH are shown in Table 8.13.

From Figure 8.23 it is apparent that tablets compacted at 25 kN exhibits the lowest ERH values, with the general trend for this material being that increasing compaction forces results in an increase in ERH value. This is directly attributed to compaction; lower force results in less disruption to the material, so the material is able to retain more of its amorphous character.

After storage Figure 8.24, it is evident that that the same trend is apparent as before storage; 25 kN has the lowest ERH ascending to 40 kN which displays the highest ERH value. However, it is obvious that after storage the tablets show an increase in ERH values when compared to before storage. The increase in ERH is obviously a direct result of the elevated storage RH. From the final ERH values in Table 8.13 it is obvious that there is a dramatic increase in ERH values upon storage. The ERH exhibited by the tablets after storage are within the same range of those obtained for lactose monohydrate tablets previously (section **Error! Reference source not found.**), reiterating conclusions drawn from the previous analysis (section 8.6.1 - 8.6.6), that the amorphous material was converted to the crystalline monohydrate form.

The trend with lower ERH being observed for lower compaction force is consistent with higher compaction forces producing lower effective surface areas and

therefore being less able to extract moisture from the sample chamber. This raises the interesting concept that apparent ERH may be reflective of the bonding that has taken place during a compaction event. The higher ERH values obtained on storage are consistent with the loss of effective surface area that is known to occur when amorphous lactose crystallises. The conversion to crystalline forms of lactose is accompanied by a loss of compact strength, reflecting the different compaction and bonding mechanisms of the two different solid state forms.

The shape of the moisture profile is important as it is able to give extra information about the behaviour of the material within a closed environment. Before storage all spray dried material demonstrated the same behaviour; an initial decrease in RH before equilibrium is reached. The decrease in RH is indicative of the material being hygroscopic in nature. After storage the same behaviour is displayed by all of the compacted material, an initial decrease before equilibrium is then reached, this behaviour is indicative of hygroscopicity. However, the initial decrease in material after storage is much less pronounced than before storage material, suggesting that although the material retains some hygroscopic nature it is altered upon storage. This again reinforces the results observed in previous solid state analysis that transformation occurred from the amorphous to the crystalline state. Lactose in its amorphous form is highly hygroscopic but it is the form that determines how much water is actually absorbed. The amorphous form is far more hygroscopic than the crystalline lactose monohydrate (Tamime, 2009). Therefore, in this instance the moisture profile displayed the decrease in hygroscopicity, which is another indication of form conversion.

Table 8.13. Final RH values for spray dried lactose tablets before and after storage

	25 kN final RH readings (%)		30 kN final RH readings (%)		35 kN final RH readings (%)		40 kN final RH readings (%)	
Before storage	16.5	18.662	19.4	24.7	24.1	23.8	24.7	26.7
After storage	30.7	30.9	33.2	33.9	38.9	37.4	39.8	40.1

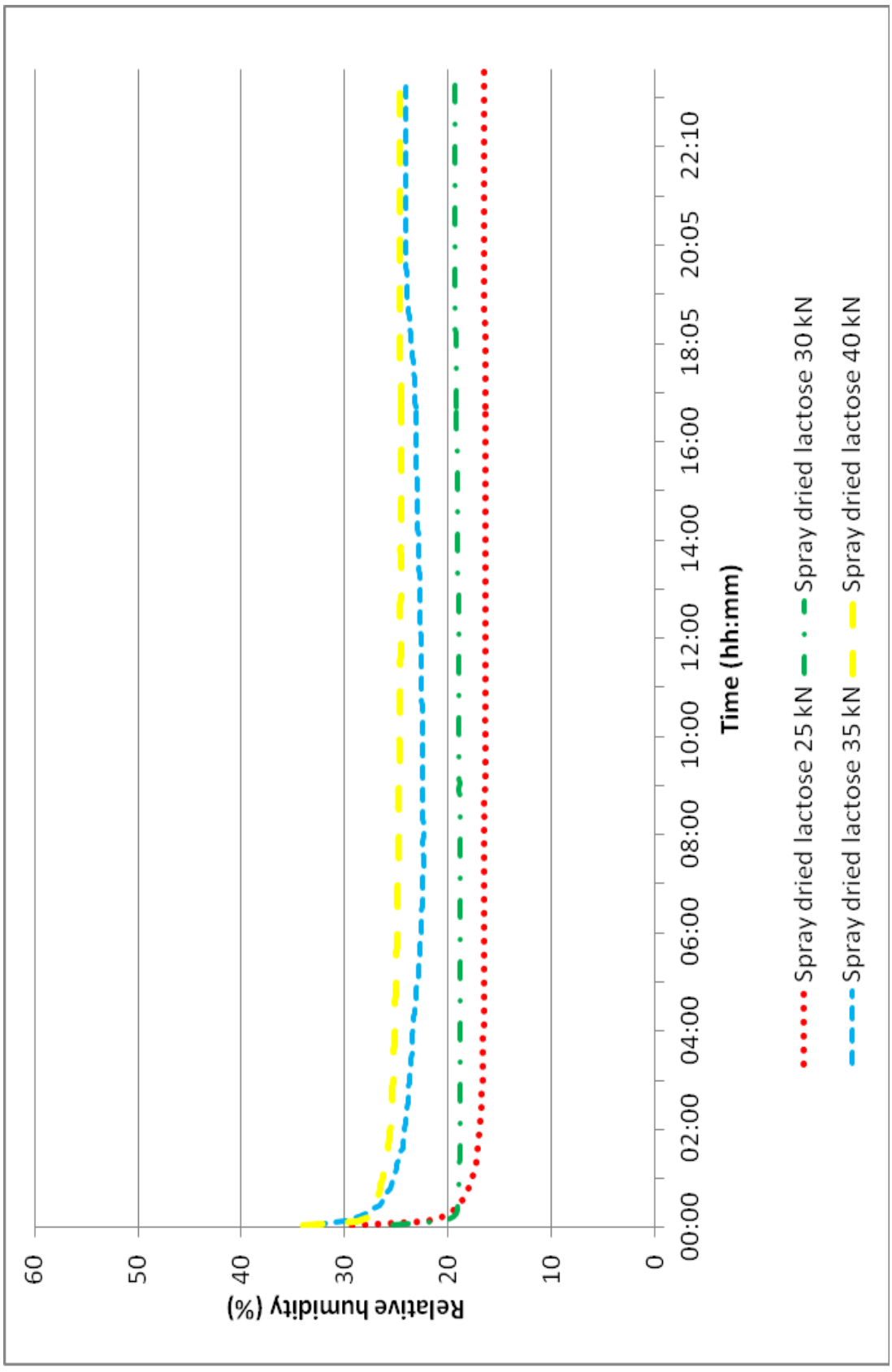

Figure 8.23. Representative moisture profiles for spray dried lactose tablets before storage

Figure 8.24. Representative moisture profiles for spray dried lactose tablets after storage

8.7 Discussion

Storage of lactose monohydrate compacts and subsequent solid state analysis showed that no physical form change was induced during the storage period. However after storage a notable increase in both crushing strength and tensile strength was observed due to elevated storage RH allowing moisture to act to promote bonding. Moisture profiles showed that storage RH in general had no notable effect upon the final ERH values. However, there was a difference in the behaviour of the 25 kN compacted material. The lower ERH values obtained for the compact at 25 kN could be consistent with the compact's likely increased porosity. The increase in ERH for this compact after storage at elevated RH is consistent with an increase in bonding (to give the observed increased tensile strength) on storage and a reduction in porosity.

Storage of anhydrous lactose tablets and subsequent solid state analysis showed that no physical change was induced during the storage period, although minor changes within the DSC profiles were observed. Crushing strength and tensile strength results demonstrated an increase after storage; this is attributed to the storage RH acting as a source of moisture, which is then able to act to promote inter-particular bonding producing stronger tablets. Moisture profiles showed that storage had no impact upon ERH values. The trend in the final ERH values after storage (Table 8.9) is that increased compaction pressure is once again associated with an increase in ERH. It is postulated that the decreased porosity of the more highly compressed material offers less surface area to interact with the moisture in the environment and thus produce the higher ERH. Storage of spray dried lactose

tablets and subsequent solid state analysis showed that during the storage period, the conditions caused conversion of the amorphous material to a part crystalline material. Crystallisation was facilitated by the elevated RH, forming both α and β polymorphs. Crushing strength and tensile strength generally decreased, suggesting that spray dried lactose produces more robust tablets initially, but these are susceptible to form conversion, which will consequently alter physical properties. The results of moisture profiling showed that storage affected the final ERH value, before storage ERH values were a direct result of the influence of the compaction force employed. After storage, all samples exhibited higher ERH values in a similar range, which were more uniform and correlated well with those observed initially for crystalline lactose monohydrate. The higher ERH values obtained on storage are consistent with the loss of effective surface area that is known to occur when amorphous lactose crystallises. The conversion to crystalline forms of lactose is accompanied by a loss of compact strength, reflecting the different compaction and bonding mechanisms of the two different solid state forms.

From the work in this chapter we have evidence of a positive correlation of moisture profile determined ERH and compact force. We have tentative evidence of ERH providing insight into compact bonding processes. As such moisture profiling shows promise as a valuable analytical tool and to be complementary to other conventional analytical methods that are currently employed, such as TGA, DSC and XRPD, due to its higher sensitivity. Also beneficial was that material did not have to be physically ground prior to analysis, which therefore allowed for samples to be

analysed as a whole, therefore eliminating the possibility of physically altering and inducing changes within the samples by grinding.

9 CONCLUSION AND FURTHER WORK

9.1 Conclusion

At the outset the question the thesis attempted to address is whether it is possible to obtain information on the physical form of a material and consequently its behaviour or performance by assessing equilibrium relative humidity with time. To date single point ERH values are routinely determined and used to indicate the likelihood of microbial growth. To the best of the author's knowledge, in this thesis profiles have been obtained and for the first time the potential of moisture profiling to demonstrate micrometric sample differences and process/environment induced changes documented. The results in the thesis highlight the promise of moisture profiling as a tool towards predicating a process endpoint or process performance. The sub-aims of this thesis were explored in several of the chapters.

In chapter 3 the establishment and assessment of the validity of a novel instrument that monitors equilibrium relative humidity with time (moisture profiler) was demonstrated. This was performed using several different methods using standards. The moisture profiler showed linearity within the range 0-100% RH. The moisture profiler provided reliable reproducibility in both inter and intra-day measurements, suggesting the technique is sensitive and repeatable. Robustness of the technique was assessed and demonstrated that the effect of sample size on the ERH and profile is material dependent. In order to achieve optimal ERH measurements and performance, we recommend the use of the same weight within the sample holder regardless of the material. It was also shown that the starting RH within the sample chamber can affect the resultant ERH for some materials. The thesis has evidenced

that for best results the starting RH within the sample chamber should be higher than the samples eventual ERH. The thesis has also shown that control of temperature and sample weight is important. It is clear that for ERH measurements to be useful the most appropriate method of their measurement is required.

In Chapter 6 we exposed samples of different solid state forms to elevated humidity. After placing the stored samples into the moisture profiler, the moisture profiles were indicative of the solid state changes induced by storage at elevated storage RH. X-ray, DSC and TGA measurements provided data which supported the changes in solid-state properties indicated by the moisture profiler.

In later chapters we investigated the effects of compaction to different compaction forces and characterised the solid-state consequence of that process by a range of solid-state techniques. We were able to infer changes in solid-state properties with reference to the moisture profiles. We demonstrated the sensitivity of ERH to compaction forces for some materials. In general lower ERH's were obtained at lower compaction pressure. For the materials studied we suggested that compaction is able to alter how the material interacts with the surrounding atmospheric moisture to reach its ERH. The clearest evidence to support this came from the powdered form of the lactose materials exhibiting different ERH's than the compacted material. Anhydrous lactose was found to be the most consistent with regards to ERH showing the least variation is observed between the ERH's for the anhydrous lactose powder and various direct compression tablets obtained at different compaction force. We suggested that its crystalline structure and resistance to deformation contributed to this result.

In the final results chapter the effect of storing compacts at elevated humidity on solid-state properties and compact properties was evaluated by a range of techniques. Relative to anhydrous lactose and lactose monohydrate compacts, storage of spray dried lactose tablets and their subsequent solid state analysis showed the most change. The conditions caused conversion of the amorphous material to a part crystalline material. The results of moisture profiling showed that storage affected the final ERH value, before storage ERH values were a direct result of the influence of the compaction force employed. After storage, all samples exhibited higher ERH values in a similar range, which were more uniform and correlated well with those observed initially for crystalline lactose monohydrate. The higher ERH values obtained on storage are consistent with the loss of effective surface area that is known to occur when amorphous lactose crystallises. The conversion to crystalline forms of lactose is accompanied by a loss of compact strength, reflecting the different compaction and bonding mechanisms of the two different solid state forms.

Whilst preliminary in nature the evidence of a positive correlation of moisture profile determined ERH and compact force for materials is significant since it can potentially give an insight into the micrometric properties of a material. The tentative evidence of ERH providing insight into compact bonding processes needs to be complemented with a wider study. The simplicity of the technique once orthogonally validated demands further evaluation so that it can form part of the toolkit complementing existing techniques such as TGA, DSC and XRPD.

9.2 Proposals for further work

Throughout the experimental works carried out to produce this thesis the possibilities and ideas for further work arose.

With respect to the design of the moisture profiler itself, incorporating a temperature control within the actual instrument would be beneficial to minimise temperature dependent ERH values. The design of software to enable an automated endpoint recognition would be hugely beneficial, because presently this is user defined.

With respect to research application, a number of areas for further work evolved. Firstly, only lactose and its different forms were studied in depth, therefore it would be useful to study a wider range of excipients. In this thesis storage at elevated RH was studied. It would be interesting to examine ERH of materials after desiccation for example.

Solid state analysis revealed that storage of amorphous lactose at the elevated humidity facilitated conversion to the crystalline form in both powder and tablets. It is of interest to carry out thermal activity monitoring (TAM) analysis alongside moisture profiling to try to relate low levels of amorphicity to the ERH values obtained. The fact that TAM is more sensitive than PXRD for determining amorphous content makes this a viable option.

A more in-depth study of the relationship between ERH and surface area or porosity would be welcome using well characterised defined starting materials.

10 REFERENCES

ABDELWAHED, W., DEGOBERT, G., STAINMESSE, S. & FESSI, H. (2006) Freeze-drying of nanoparticles: Formulation, process and storage considerations. *Advanced Drug Delivery Reviews,* 58**,** 1688-1713.

ACADEMY OF PHARMACEUTICAL, S. & PHARMACEUTICAL SOCIETY OF GREAT, B. (1986) *Handbook of pharmaceutical excipients*, American Pharmaceutical Association.

AHLNECK, C. & ZOGRAFI, G. (1990) THE MOLECULAR-BASIS OF MOISTURE EFFECTS ON THE PHYSICAL AND CHEMICAL-STABILITY OF DRUGS IN THE SOLID-STATE. *International Journal of Pharmaceutics,* 62**,** 87-95.

AHUJA, S. & DONG, M. W. (2005) *Handbook of pharmaceutical analysis by HPLC*, Elsevier Academic Press.

AMERICAN CHEMICAL, S. & AMERICAN CHEMICAL SOCIETY. COMMITTEE ON ANALYTICAL, R. (2006) *Reagent chemicals: specifications and procedures : American Chemical Society specifications, official from January 1, 2006*, American Chemical Society.

AMIDON, G. E. & MIDDLETON, K. R. (1988) Accelerated physical stability testing and long-term predictions of changes in the crushing strength of tablets stored in blister packages. *International Journal of Pharmaceutics,* 45**,** 79-89.

ANDERSON, N. G. (2000) *Practical process research & development*, Academic Press.

ANGBERG, M. (1995) Lactose and thermal analysis with special emphasis on microcalorimetry. *Thermochimica Acta,* 248**,** 161-176.

ARAUJO, P. (2009) Key aspects of analytical method validation and linearity evaluation. *Journal of Chromatography B,* 877**,** 2224-2234.

AULTON, M. E. (2002) *Pharmaceutics: the science of dosage form design*, Churchill Livingstone.

AULTON, M. E. (2009) *Aulton's pharmaceutics : the design and manufacture of medicines,* Edinburgh, Churchill Livingstone Elsevier.

BANKER, G. S. & RHODES, C. T. (2002) *Modern pharmaceutics*, Marcel Dekker.

BARBOSA-CÃ¡NOVAS, G. V. (2007) *Water activity in foods: fundamentals and applications*, Blackwell Pub.

BELL L & LABUZA, T. P. (2000) *Moisture sorption: practical aspects of isotherm measurement and use*, American Association of Cereal Chemists.

BERGREN, M. S. (1994) AN AUTOMATED CONTROLLED-ATMOSPHERE MICROBALANCE FOR THE MEASUREMENT OF MOISTURE SORPTION. *International Journal of Pharmaceutics,* 103**,** 103-114.

BERLIN, E., KLIMAN, P. G., ANDERSON, B. A. & PALLANSCH, M. J. (1971) Calorimetric measurement of the heat of desorption of water vapor from amorphous and crystalline lactose. *Thermochimica Acta,* 2**,** 143-152.

BHUGRA, C. & PIKAL, M. J. (2008) Role of thermodynamic, molecular, and kinetic factors in crystallization from the amorphous state. *Journal of Pharmaceutical Sciences,* 97**,** 1329-1349.

BLANCO, M., CUEVA-MESTANZA, R. & PEGUERO, A. Controlling individual steps in the production process of paracetamol tablets by use of NIR spectroscopy. *Journal of Pharmaceutical and Biomedical Analysis,* 51**,** 797-804.

BOND, L., ALLEN, S., DAVIES, M. C., ROBERTS, C. J., SHIVJI, A. P., TENDLER, S. J. B., WILLIAMS, P. M. & ZHANG, J. X. (2002) Differential scanning calorimetry and

scanning thermal microscopy analysis of pharmaceutical materials. *International Journal of Pharmaceutics,* 243**,** 71-82.

BRACKEL, U. (2007) *Product design and engineering: best practices*, Wiley-VCH.

BRITTAIN, H. G. (1995) *Physical characterization of pharmaceutical solids,* New York, Dekker.

BROADHEAD, J., ROUAN, S. K. E. & RHODES, C. T. (1992) THE SPRAY DRYING OF PHARMACEUTICALS. *Drug Development and Industrial Pharmacy,* 18**,** 1169-1206.

BROOK, D. B. & MARSHALL, K. (1968) "Crushing-strength" of compressed tablets I. Comparison of testers. *Journal of Pharmaceutical Sciences,* 57**,** 481-484.

BUCKTON, G., YONEMOCHI, E., HAMMOND, J. & MOFFAT, A. (1998) The use of near infra-red spectroscopy to detect changes in the form of amorphous and crystalline lactose. *International Journal of Pharmaceutics,* 168**,** 231-241.

BUGAY, D. E. (2001) Characterization of the solid-state: spectroscopic techniques. *Advanced Drug Delivery Reviews,* 48**,** 43-65.

BUMA, T. J. & WIEGERS, G. A. (1967) *X-ray Powder Patterns of Lactose and Unit Cell Dimensions of B. Lactose*.

BUSIGNIES, V., TCHORELOFF, P., LECLERC, B., BESNARD, M. & COUARRAZE, G. (2004) Compaction of crystallographic forms of pharmaceutical granular lactoses. I. Compressibility. *European Journal of Pharmaceutics and Biopharmaceutics,* 58**,** 569-576.

BYRN, S. R., PFEIFFER, R. R., STEPHENSON, G., GRANT, D. J. W. & GLEASON, W. B. (1994) SOLID-STATE PHARMACEUTICAL CHEMISTRY. *Chemistry of Materials,* 6**,** 1148-1158.

BYRN, S. R., PFEIFFER, R. R. & STOWELL, J. G. (1999) *Solid-state chemistry of drugs*, SSCI, Inc.

CAL, S., RODRIGUEZPUENTE, B., SOUTO, C., CONCHEIRO, A., GOMEZAMOZA, J. L. & MARTINEZPACHECO, R. (1996) Comparison of a spray-dried alpha-lactose monohydrate with a fully hydrated roller-dried beta-lactose. *International Journal of Pharmaceutics,* 136**,** 13-21.

CHIDAVAENZI, O. C., BUCKTON, G., KOOSHA, F. & PATHAK, R. (1997) The use of thermal techniques to assess the impact of feed concentration on the amorphous content and polymorphic forms present in spray dried lactose. *International Journal of Pharmaceutics,* 159**,** 67-74.

CLARKE, B. L. (1947) Introductory Remarks. *Analytical Chemistry,* 19**,** 943-943.

COLUMBANO, A., BUCKTON, G. & WIKELEY, P. (2002) A study of the crystallisation of amorphous salbutamol sulphate using water vapour sorption and near infrared spectroscopy. *International Journal of Pharmaceutics,* 237**,** 171-178.

CORRIGAN, O. I. (1995) Thermal analysis of spray dried products. *Thermochimica Acta,* 248**,** 245-258.

CRAIG, D. Q. M., ROYALL, P. G., KETT, V. L. & HOPTON, M. L. (1999) The relevance of the amorphous state to pharmaceutical dosage forms: glassy drugs and freeze dried systems. *International Journal of Pharmaceutics,* 179**,** 179-207.

CUI, Y. (2007) A material science perspective of pharmaceutical solids. *International Journal of Pharmaceutics,* 339**,** 3-18.

DALTON, C. R. & HANCOCK, B. C. (1997) Processing and storage effects on water vapor sorption by some model pharmaceutical solid dosage formulations. *International Journal of Pharmaceutics,* 156**,** 143-151.

DARCY, P. & BUCKTON, G. (1997) The influence of heating/drying on the crystallisation of amorphous lactose after structural collapse. *International Journal of Pharmaceutics,* 158**,** 157-164.

DAWOODBHAI, S. & RHODES, C. T. (1989) THE EFFECT OF MOISTURE ON POWDER FLOW AND ON COMPACTION AND PHYSICAL STABILITY OF TABLETS. *Drug Development and Industrial Pharmacy,* 15**,** 1577-1600.

EBBING, D. D. & GAMMON, S. D. (2009) *General Chemistry*, Brooks/Cole.

ELMONSEF OMAR, A. M. & ROOS, Y. H. (2007) Glass transition and crystallization behaviour of freeze-dried lactoseâ€"salt mixtures. *LWT - Food Science and Technology,* 40**,** 536-543.

F. DOHERTY, M., VALENTIN, P. & PAUL SERBAN, A. (2007) Crystal engineering for product and process design. *Computer Aided Chemical Engineering.* Elsevier.

FLORENCE, A. T. & ATTWOOD, D. (2006) *Physicochemical principles of pharmacy,* London, Pharmaceutical Press.

FORD, J. L. & TIMMINS, P. (1989) *Pharmaceutical thermal analysis: techniques and applications*, E. Horwood.

FRANKS, F. (1998) Freeze-drying of bioproducts: putting principles into practice. *European Journal of Pharmaceutics and Biopharmaceutics,* 45**,** 221-229.

GABBOTT, P. (2008) *Principles and applications of thermal analysis*, Blackwell Pub.

GAD, S. C. (2007) *Handbook of pharmaceutical biotechnology*, Wiley-Interscience.

GARNIER, S., PETIT, S., MALLET, F., PETIT, M. N., LEMARCHAND, D., COSTE, S., LEFEBVRE, J. & COQUEREL, G. (2008) Influence of ageing, grinding and preheating on the thermal behaviour of Î±-lactose monohydrate. *International Journal of Pharmaceutics,* 361**,** 131-140.

GIRON, D. (1995) Thermal analysis and calorimetric methods in the characterisation of polymorphs and solvates. *Thermochimica Acta,* 248**,** 1-59.

GOMBÃS, Ã., SZABÃ³-RÃ©VÃ©SZ, P., KATA, M., REGDON, G. & ERÅ‘S, I. (2002) Quantitative Determination of Crystallinity of Î±-Lactose Monohydrate by DSC. *Journal of Thermal Analysis and Calorimetry,* 68**,** 503-510.

GOULA, A. M. & ADAMOPOULOS, K. G. (2005) Spray drying of tomato pulp in dehumidified air: II. The effect on powder properties. *Journal of Food Engineering,* 66**,** 35-42.

GUSTAVO GONZÁLEZ, A. & ÁNGELES HERRADOR, M. (2007) A practical guide to analytical method validation, including measurement uncertainty and accuracy profiles. *TrAC Trends in Analytical Chemistry,* 26**,** 227-238.

HALEBLIAN, J. & MCCRONE, W. (1969) Pharmaceutical applications of polymorphism. *J Pharm Sci,* 58**,** 911-29.

HAMMOND, C. (2009) *The basics of crystallography and diffraction*, Oxford University Press.

HANCOCK, B. C. & ZOGRAF, G. (1997) Characteristics and significance of the amorphous state in pharmaceutical systems. *Journal of Pharmaceutical Sciences,* 86**,** 1-12.

HAQUE, M. K. & ROOS, Y. H. (2005) Crystallization and X-ray diffraction of spray-dried and freeze-dried amorphous lactose. *Carbohydrate Research,* 340**,** 293-301.

HEIDEMANN, D. R. & JAROSZ, P. J. (1991) PREFORMULATION STUDIES INVOLVING MOISTURE UPTAKE IN SOLID DOSAGE FORMS. *Pharmaceutical Research,* 8**,** 292-297.

HENDRICKS, M. M. W. B., DE BOER, J. H. & SMILDE, A. K. (1996) *Robustness of Analytical Chemical Methods and Pharmaceutical Technological Products*, Elsevier.

HOGAN, S. E. & BUCKTON, G. (2001) The application of near infrared spectroscopy and dynamic vapor sorption to quantify low amorphous contents of crystalline lactose. *Pharmaceutical Research,* 18**,** 112-116.

HUYNH-BA, K. (2008) *Handbook of Stability Testing in Pharmaceutical Development: Regulations, Methodologies, and Best Practices*, Springer.

IBACH, A. & KIND, M. (2007) Crystallization kinetics of amorphous lactose, whey-permeate and whey powders. *Carbohydrate Research,* 342**,** 1357-1365.

ISLAM, M. I. U. & LANGRISH, T. A. G. (2010) An investigation into lactose crystallization under high temperature conditions during spray drying. *Food Research International,* 43**,** 46-56.

JIVRAJ, M., MARTINI, L. G. & THOMSON, C. M. (2000) An overview of the different excipients useful for the direct compression of tablets. *Pharmaceutical Science & Technology Today,* 3**,** 58-63.

JONES, M. D., HOOTON, J. C., DAWSON, M. L., FERRIE, A. R. & PRICE, R. (2006) Dehydration of trehalose dihydrate at low relative humidity and ambient temperature. *International Journal of Pharmaceutics,* 313**,** 87-98.

KENNON, N. F. (1978) *Patterns in crystals,* Chichester (etc.)), Wiley.

KHANKARI, R. K. & GRANT, D. J. W. (1995) PHARMACEUTICAL HYDRATES. *Thermochimica Acta,* 248**,** 61-79.

KHANKARI, R. K., LAW, D. & GRANT, D. J. W. (1992) Determination of water content in pharmaceutical hydrates by differential scanning calorimetry. *International Journal of Pharmaceutics,* 82**,** 117-127.

KIRK, J. H., DANN, S. E. & BLATCHFORD, C. G. (2007) Lactose: A definitive guide to polymorph determination. *International Journal of Pharmaceutics,* 334**,** 103-114.

L.O, F. (1993) The physical modification of lactose and its thermoanalytical identification. *Thermochimica Acta,* 222**,** 187-194.

LARHRIB, H., ZENG, X. M., MARTIN, G. P., MARRIOTT, C. & PRITCHARD, J. (1999) The use of different grades of lactose as a carrier for aerosolised salbutamol sulphate. *International Journal of Pharmaceutics,* 191**,** 1-14.

LERK, C. F., ANDREAE, A. C., DE BOER, A. H., DE HOOG, P., KUSSENDRAGER, K. & VAN LEVERINK, J. (1984a) Alterations of α-lactose during differential scanning calorimetry. *Journal of Pharmaceutical Sciences,* 73**,** 856-857.

LERK, C. F., ANDREAE, A. C., DE BOER, A. H., DE HOOG, P., KUSSENDRAGER, K. & VAN LEVERINK, J. (1984b) Transitions of lactoses by mechanical and thermal treatment. *Journal of Pharmaceutical Sciences,* 73**,** 857-859.

LEVINSON, R. (2001) *More Modern Chemical Techniques*, Royal Society Of Chemistry.

LEWIS, I. R. & EDWARDS, H. G. M. (2001) *Handbook of Raman spectroscopy : from the research laboratory to the process line,* New York, Marcel Dekker.

LIEBERMAN, H. A., LACHMAN, L. & SCHWARTZ, J. B. (1989) *Pharmaceutical dosage forms : tablets. Vol. 1,* New York, Dekker.

LISTIOHADI, Y., HOURIGAN, J. A., SLEIGH, R. W. & STEELE, R. J. (2008) Moisture sorption, compressibility and caking of lactose polymorphs. *International Journal of Pharmaceutics,* 359**,** 123-134.

LISTIOHADI, Y., HOURIGAN, J. A., SLEIGH, R. W. & STEELE, R. J. (2009) Thermal analysis of amorphous lactose and α-lactose monohydrate. *Dairy Sci. Technol.,* 89**,** 43-67.

LLINÀS, A. & GOODMAN, J. M. (2008) Polymorph control: past, present and future. *Drug Discovery Today,* 13**,** 198-210.

LLOYD, R. J., DONG CHEN, X. & HARGREAVES, J. B. (1996) Glass transition and caking of spray-dried lactose. *International Journal of Food Science & Technology,* 31**,** 305-311.

MACKIN, L., ZANON, R., PARK, J. M., FOSTER, K., OPALENIK, H. & DEMONTE, M. (2002) Quantification of low levels (< 10%) of amorphous content in micronised active batches using dynamic vapour sorption and isothermal microcalorimetry. *International Journal of Pharmaceutics,* 231**,** 227-236.

MOIR, P. (2007) A new approach to equilibrium relative humidity testing for moisture sorption studies in pharmaceutical stability. *Tablets and capsules,* 5**,** 18-25.

MOLOKHIA, A. M. (1984) Effect of storage on crushing strength, disintegration and drug release from mixed tablet bases. *International Journal of Pharmaceutics,* 22**,** 127-130.

MORISSETTE, S. L., ALMARSSON, Ö., PETERSON, M. L., REMENAR, J. F., READ, M. J., LEMMO, A. V., ELLIS, S., CIMA, M. J. & GARDNER, C. R. (2004) High-throughput crystallization: polymorphs, salts, co-crystals and solvates of pharmaceutical solids. *Advanced Drug Delivery Reviews,* 56**,** 275-300.

NEWMAN, A. W. & BRITTAIN, H. G. (1995) *Physical characterisation of pharmaceutical solids*, New York: Marcel Dekker.

NICKERSON, T. A. (1962) Lactose Crystallization in Ice Cream. IV. Factors Responsible for Reduced Incidence of Sandiness. *Journal of Dairy Science,* 45**,** 354-359.

OTSUKA, M., OHTANI, H., KANENIWA, N. & HIGUCHI, S. (1991) Isomerization of Lactose in Solid-state by Mechanical Stress During Grinding. *Journal of Pharmacy and Pharmacology,* 43**,** 148-153.

PIKAL, M. J., LUKES, A. L., LANG, J. E. & GAINES, K. (1978) Quantitative crystallinity determinations for β-lactam antibiotics by solution calorimetry: Correlations with stability. *Journal of Pharmaceutical Sciences,* 67**,** 767-773.

PITCHAYAJITTIPONG, C., PRICE, R., SHUR, J., KAERGER, J. S. & EDGE, S. Characterisation and functionality of inhalation anhydrous lactose. *International Journal of Pharmaceutics,* 390**,** 134-141.

QIU, Y. (2009) *Developing solid oral dosage forms : pharmaceutical theory & practice,* Amsterdam ; Oxford, Academic.

RODRÍGUEZ-SPONG, B., PRICE, C. P., JAYASANKAR, A., MATZGER, A. J. & RODRÍGUEZ-HORNEDO, N. (2004) General principles of pharmaceutical solid polymorphism: A supramolecular perspective. *Advanced Drug Delivery Reviews,* 56**,** 241-274.

ROOS, Y. (1995) *Phase transitions in foods*, Academic Press, San Diego, USA.

ROOS, Y. & KAREL, M. (1990) Differential scanning calorimetry study of phase transitions affecting the quality of dehydrated materials. *Biotechnology Progress,* 6**,** 159-163.

ROUQUEROL, F., ROUQUEROL, J. & SING, K. S. W. (1999) *Adsorption by powders and porous solids : principles, methodology and applications,* San Diego, Calif., Academic Press.

ROZET, E., CECCATO, A., HUBERT, C., ZIEMONS, E., OPREAN, R., RUDAZ, S., BOULANGER, B. & HUBERT, P. (2007) Analysis of recent pharmaceutical regulatory documents on analytical method validation. *Journal of Chromatography A,* 1158**,** 111-125.

SANDERS, G. H. W., ROBERTS, C. J., DANESH, A., MURRAY, A. J., PRICE, D. M., DAVIES, M. C., TENDLER, S. J. B. & WILKINS, M. J. (2000) Discrimination of polymorphic forms of a drug product by localized thermal analysis. *Journal of Microscopy-Oxford,* 198**,** 77-81.

SEBHATU, T., AHLNECK, C. & ALDERBORN, G. (1997) The effect of moisture content on the compression and bond-formation properties of amorphous lactose particles. *International Journal of Pharmaceutics,* 146**,** 101-114.

SEBHATU, T., ANGBERG, M. & AHLNECK, C. (1994) Assessment of the degree of disorder in crystalline solids by isothermal microcalorimetry. *International Journal of Pharmaceutics,* 104**,** 135-144.

SHAH, B., KAKUMANU, V. K. & BANSAL, A. K. (2006) Analytical techniques for quantification of amorphous/crystalline phases in pharmaceutical solids. *Journal of Pharmaceutical Sciences,* 95**,** 1641-1665.

SHAH, K. R., HUSSAIN, M. A., HUBERT, M. & FARAG BADAWY, S. I. (2008) Form conversion of anhydrous lactose during wet granulation and its effect on compactibility. *International Journal of Pharmaceutics,* 357**,** 228-234.

SHAM, J. O. H., ZHANG, Y., FINLAY, W. H., ROA, W. H. & LÖBENBERG, R. (2004) Formulation and characterization of spray-dried powders containing nanoparticles for aerosol delivery to the lung. *International Journal of Pharmaceutics,* 269**,** 457-467.

SHARIARE, M. H., DE MATAS, M., YORK, P. & SHAO, Q. The impact of material attributes and process parameters on the micronisation of lactose monohydrate. *International Journal of Pharmaceutics,* 408**,** 58-66.

SHUKLA, A. J. & PRICE, J. C. (1991) Effect of Moisture Content on Compression Properties of Directly Compressible High Beta-Content Anhydrous Lactose. *Drug Development and Industrial Pharmacy,* 17**,** 2067-2081.

SING, K. S. W., EVERETT, D. H., HAUL, R. A. W., MOSCOU, L., PIEROTTI, R. A., ROUQUEROL, J. & SIEMIENIEWSKA, T. (1985) REPORTING PHYSISORPTION DATA FOR GAS SOLID SYSTEMS WITH SPECIAL REFERENCE TO THE

DETERMINATION OF SURFACE-AREA AND POROSITY (RECOMMENDATIONS 1984). *Pure and Applied Chemistry,* 57**,** 603-619.

SINGHAL, D. & CURATOLO, W. (2004) Drug polymorphism and dosage form design: a practical perspective. *Advanced Drug Delivery Reviews,* 56**,** 335-347.

SLADE, L., LEVINE, H. & REID, D. S. (1991) Beyond water activity: Recent advances based on an alternative approach to the assessment of food quality and safety. *Critical Reviews in Food Science and Nutrition,* 30**,** 115-360.

STOLOFF, L. (1978) CALIBRATION OF WATER ACTIVITY MEASURING-INSTRUMENTS AND DEVICES - COLLABORATIVE STUDY. *Journal of the Association of Official Analytical Chemists,* 61**,** 1166-1178.

STRICKLEY, R. G. & ANDERSON, B. D. (1997) Solid-state stability of human insulin II. Effect of water on reactive intermediate partitioning in lyophiles from pH 2–5 solutions: Stabilization against covalent dimer formation. *Journal of Pharmaceutical Sciences,* 86**,** 645-653.

STRYDOM, S., LIEBENBERG, W., YU, L. & DE VILLIERS, M. (2009) The effect of temperature and moisture on the amorphous-to-crystalline transformation of stavudine. *International Journal of Pharmaceutics,* 379**,** 72-81.

SUGIMOTO, K., DINNEBIER, R. E. & ZAKRZEWSKI, M. (2007) Structural characterization of anhydrous naloxone- and naltrexone hydrochloride by high resolution laboratory X-ray powder diffraction and thermal analysis. *Journal of Pharmaceutical Sciences,* 96**,** 3316-3323.

TAJBER, L., CORRIGAN, D. O., CORRIGAN, O. I. & HEALY, A. M. (2009) Spray drying of budesonide, formoterol fumarate and their composites--I. Physicochemical characterisation. *International Journal of Pharmaceutics,* 367**,** 79-85.

TAKEUCHI, H., YASUJI, T., HINO, T., YAMAMOTO, H. & KAWASHIMA, Y. (1998) Spray-dried composite particles of lactose and sodium alginate for direct tabletting and controlled releasing. *International Journal of Pharmaceutics,* 174**,** 91-100.

TAMIME, A. (2009) *Dairy Powders and Concentrated Products*, John Wiley & Sons.

TEUNOU, E. & FITZPATRICK, J. J. (1999) Effect of relative humidity and temperature on food powder flowability. *Journal of Food Engineering,* 42**,** 109-116.

TICEHURST, M. D., YORK, P., ROWE, R. C. & DWIVEDI, S. K. (1996) Characterisation of the surface properties of Î±-lactose monohydrate with inverse gas chromatography, used to detect batch variation. *International Journal of Pharmaceutics,* 141**,** 93-99.

TROY, H. C. & SHARP, P. F. (1930) Î± and Î² Lactose in Some Milk Products. *Journal of Dairy Science,* 13**,** 140-157.

TSINONTIDES, S. C., RAJNIAK, P., PHAM, D., HUNKE, W. A., PLACEK, J. & REYNOLDS, S. D. (2004) Freeze drying--principles and practice for successful scale-up to manufacturing. *International Journal of Pharmaceutics,* 280**,** 1-16.

UNITED STATES PHARMACOPEIAL CONVENTION. (1995) *The United States pharmacopeia,* Rockville, United States Pharmacopeial Convention.

VACLAVIK, V. A. (2007) *Essentials of Food Science*, SPRINGER VERLAG NY.

VAN CAMPEN, L., AMIDON, G. L. & ZOGRAFI, G. (1983) Moisture sorption kinetics for water-soluble substances I: Theoretical considerations of heat transport control. *Journal of Pharmaceutical Sciences,* 72**,** 1381-1388.

VELARDI, S. A. & BARRESI, A. A. (2008) Development of simplified models for the freeze-drying process and investigation of the optimal operating conditions. *Chemical Engineering Research and Design,* 86**,** 9-22.

VIPPAGUNTA, S. R., BRITTAIN, H. G. & GRANT, D. J. W. (2001) Crystalline solids. *Advanced Drug Delivery Reviews,* 48**,** 3-26.

VISHWESHWAR, P., MCMAHON, J. A., BIS, J. A. & ZAWOROTKO, M. J. (2006) Pharmaceutical co-crystal. *Journal of Pharmaceutical Sciences,* 95**,** 499-516.

WHITEMAN, M. & YARWOOD, R. J. (1988) The Evaluation of Six Lactose-Based Materials as Direct Compression Tablet Excipients. *Drug Development and Industrial Pharmacy,* 14**,** 1023-1040.

WILLSON, R. J. & BEEZER, A. E. (2003) The determination of equilibrium constants, Delta G, Delta H and Delta S for vapour interaction with a pharmaceutical drug, using gravimetric vapour sorption. *International Journal of Pharmaceutics,* 258**,** 77-83.

WINSTON, P. W. & BATES, D. H. (1960) Saturated Solutions For the Control of Humidity in Biological Research. *Ecology,* 41**,** 232-237.

YORK, P. (1976) A preliminary study of the physical stability of tablets prepared from powders stored under tropical conditions. *Pharmazie. 1976 Jun;31(6):383-6.*

YORK, P. (1981) Analysis of moisture sorption hysteresis in hard gelatin capsules, maize starch, and maize starch: drug powder mixtures. *Journal of Pharmacy and Pharmacology,* 33**,** 269-273.

YORK, P. (1983) Solid-state properties of powders in the formulation and processing of solid dosage forms. *International Journal of Pharmaceutics,* 14**,** 1-28.

YU, L. (2001) Amorphous pharmaceutical solids: preparation, characterization and stabilization. *Advanced Drug Delivery Reviews,* 48**,** 27-42.

ZIFFELS, S. & STECKEL, H. Influence of amorphous content on compaction behaviour of anhydrous Î±-lactose. *International Journal of Pharmaceutics,* 387**,** 71-78.

ZOGRAFI, G. (1988) States of Water Associated with Solids. *Drug Development and Industrial Pharmacy,* 14**,** 1905-1926.

ZOGRAFI, G., GRANDOLFI, G. P., KONTNY, M. J. & MENDENHALL, D. W. (1988) PREDICTION OF MOISTURE TRANSFER IN MIXTURES OF SOLIDS - TRANSFER VIA THE VAPOR-PHASE. *International Journal of Pharmaceutics,* 42**,** 77-88.

ZOGRAFI, G. & HANCOCK, B. (1994) *WATER-SOLID STATE INTERACTIONS IN PHARMACEUTICAL SYSTEMS,* Stuttgart, Medpharm Gmbh Scientific Publ.

11. APPENDIX

Appendix 0.1.Representative TGA thermal profile acesulfame potassium

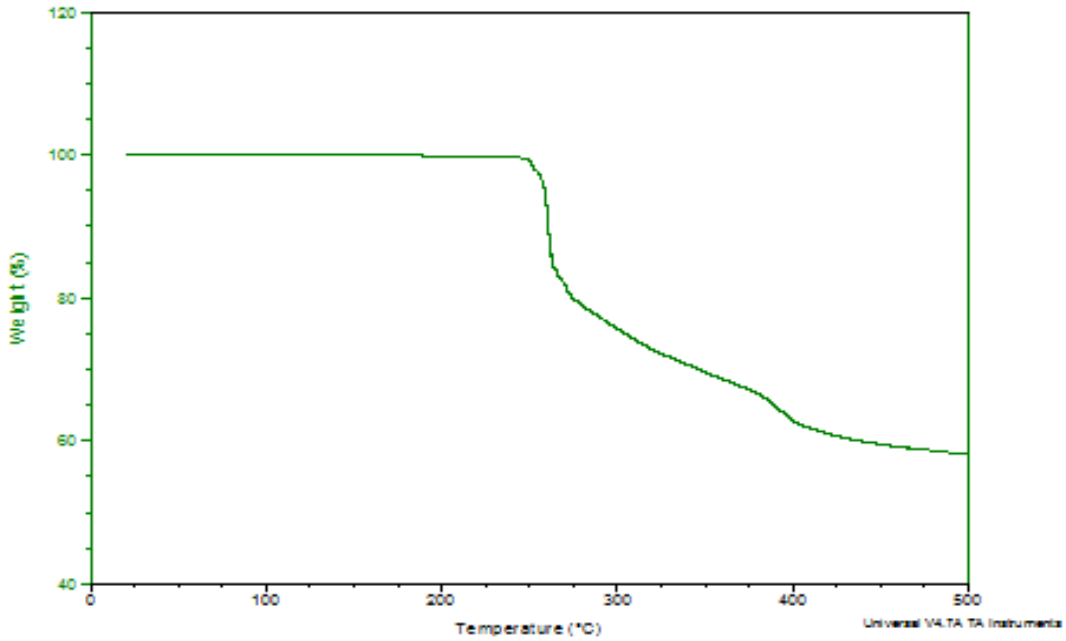

Appendix 0.2. Representative DSC thermal profile for acesulfame potassium

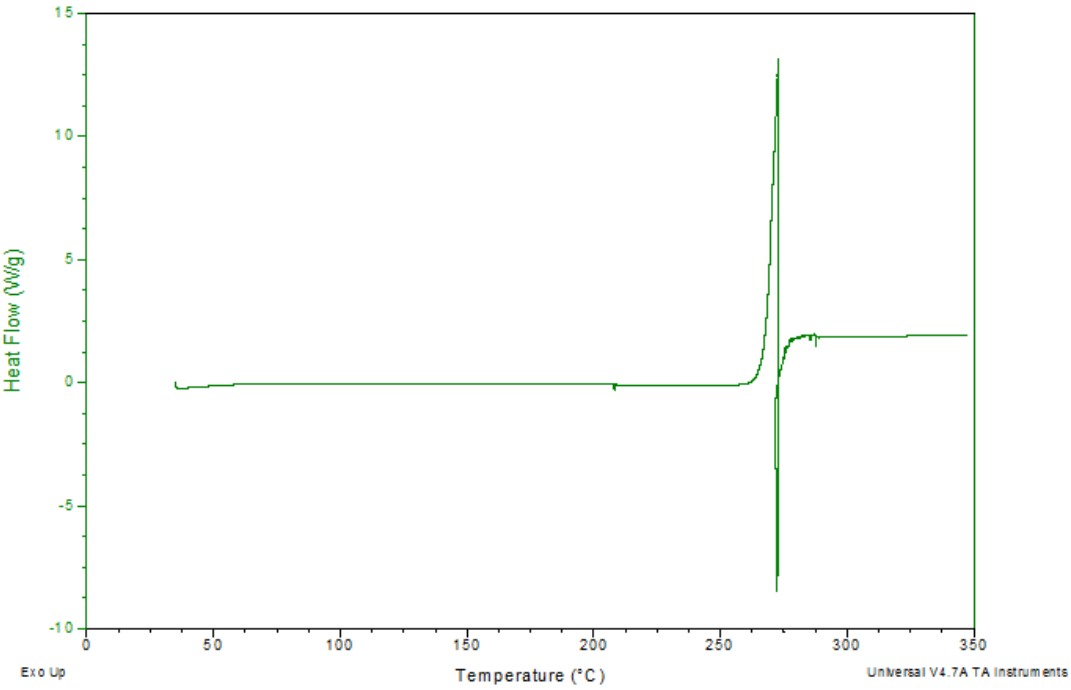

Appendix 0.3. Representative PXRD pattern for acesulfame potassium

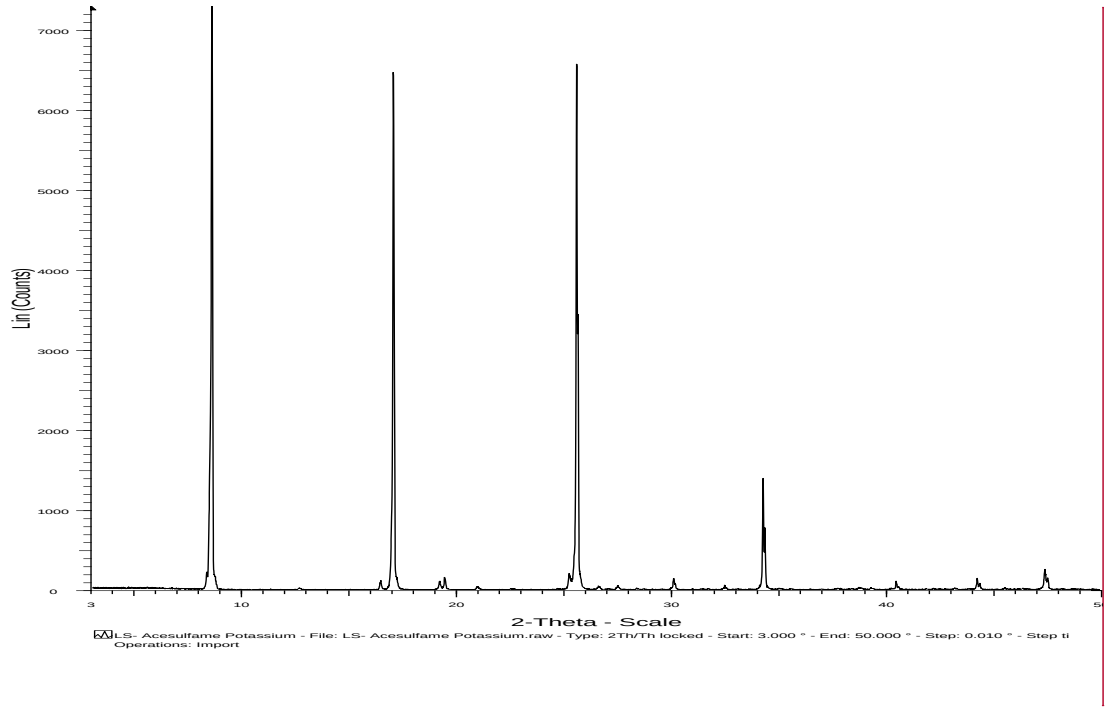

Appendix 0.4. Representative TGA thermal profile for citric acid

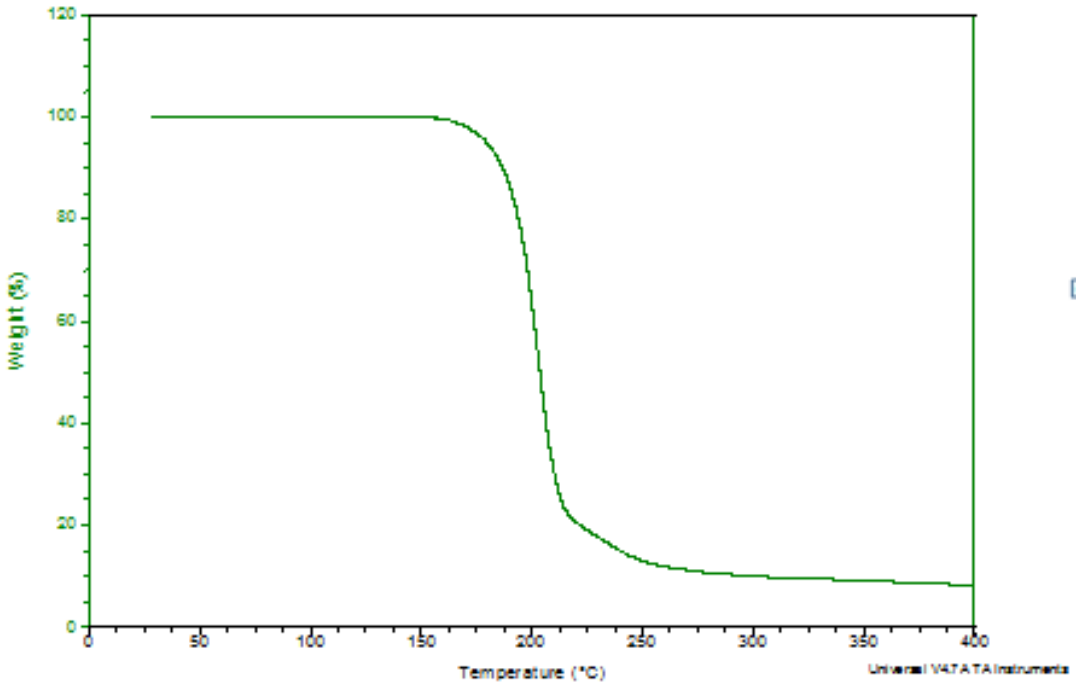

Appendix 0.5. Representative DSC thermal profile for citric acid

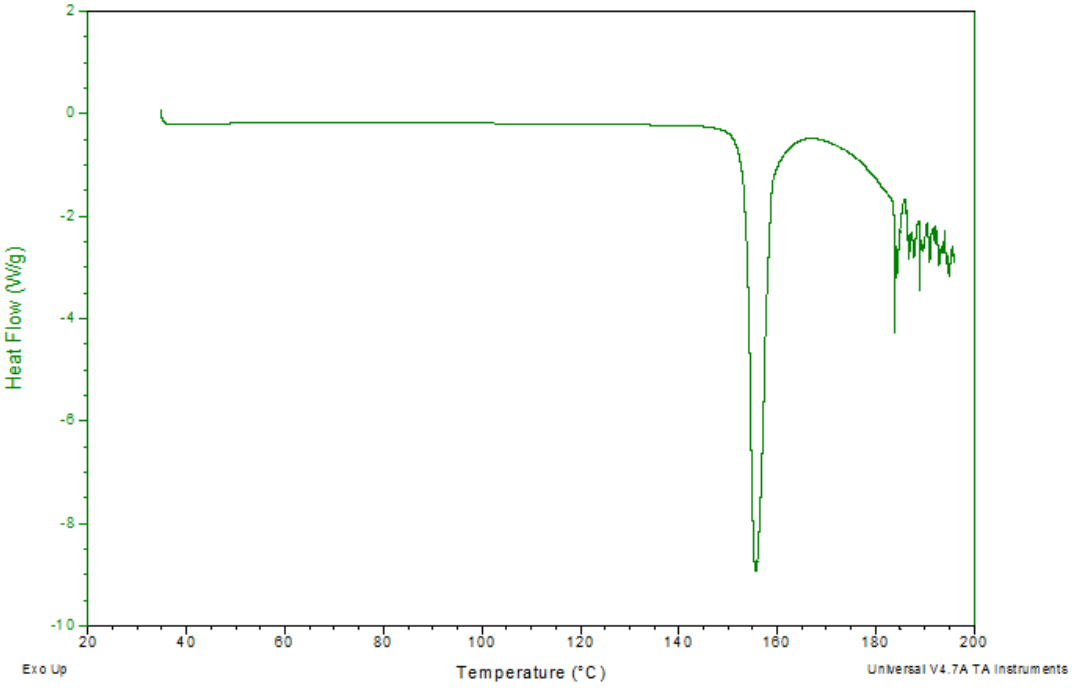

Appendix 0.6. Representative PXRD pattern for citric acid

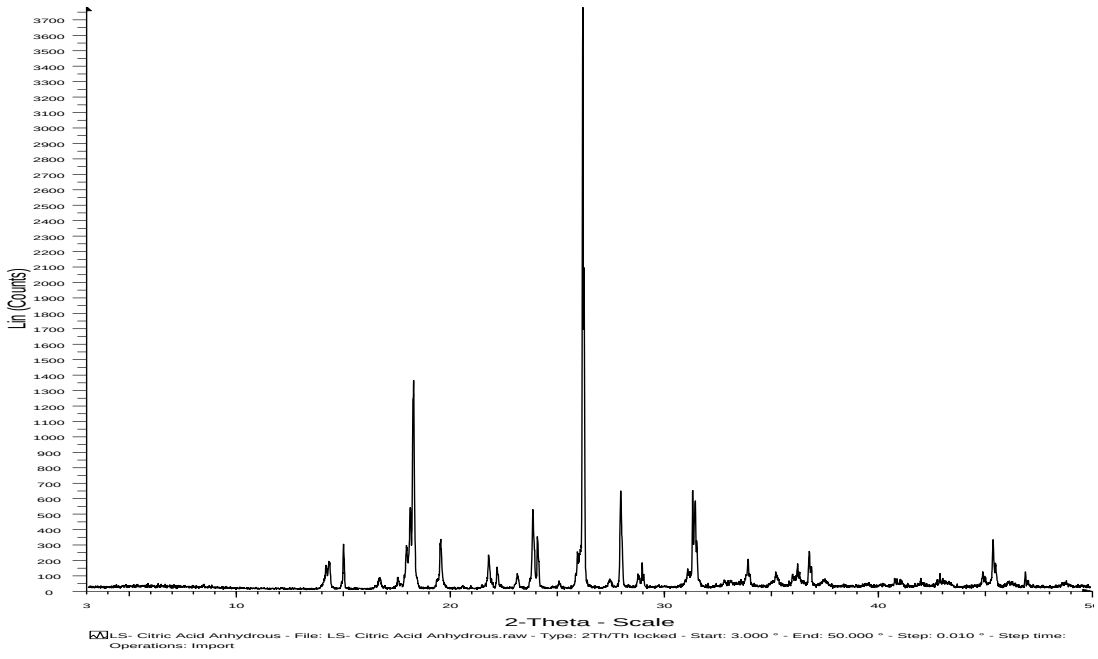

Appendix 0.7. Representative DSC thermal profile for maize/starch

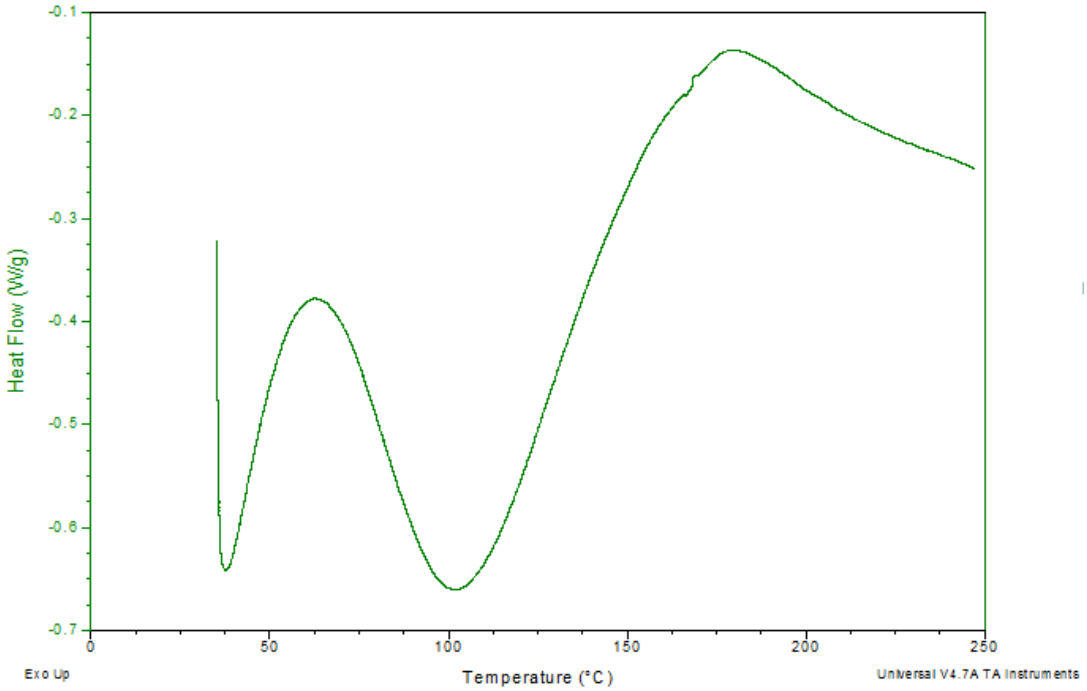

Appendix 0.8. Representative PXRD pattern for maize/starch

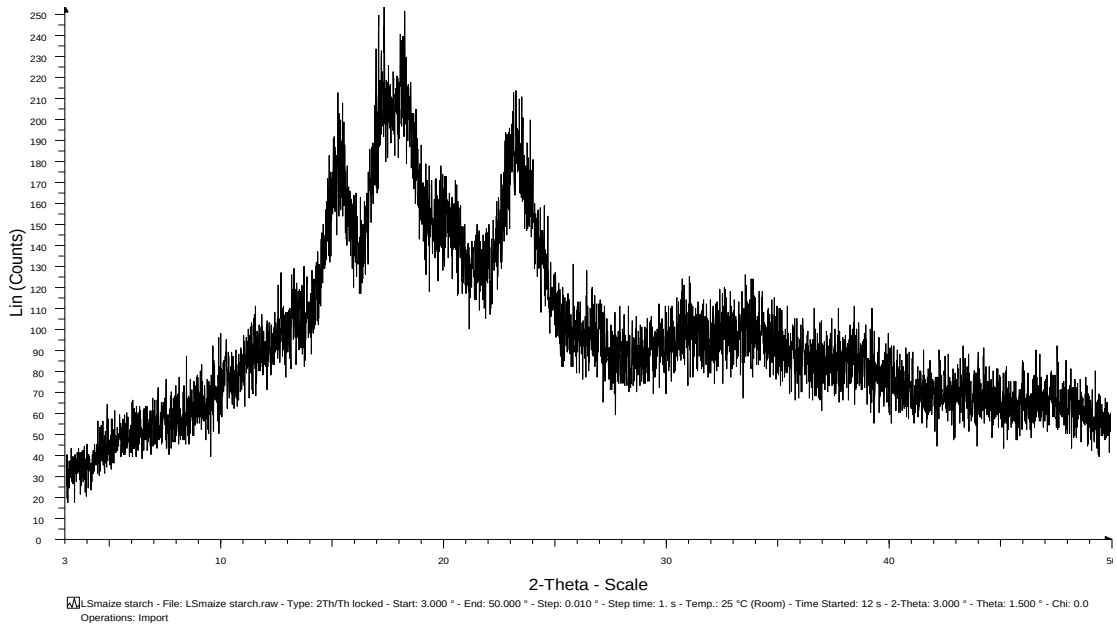

Appendix 0.9. Representative TGA thermal profile for magnesium stearate

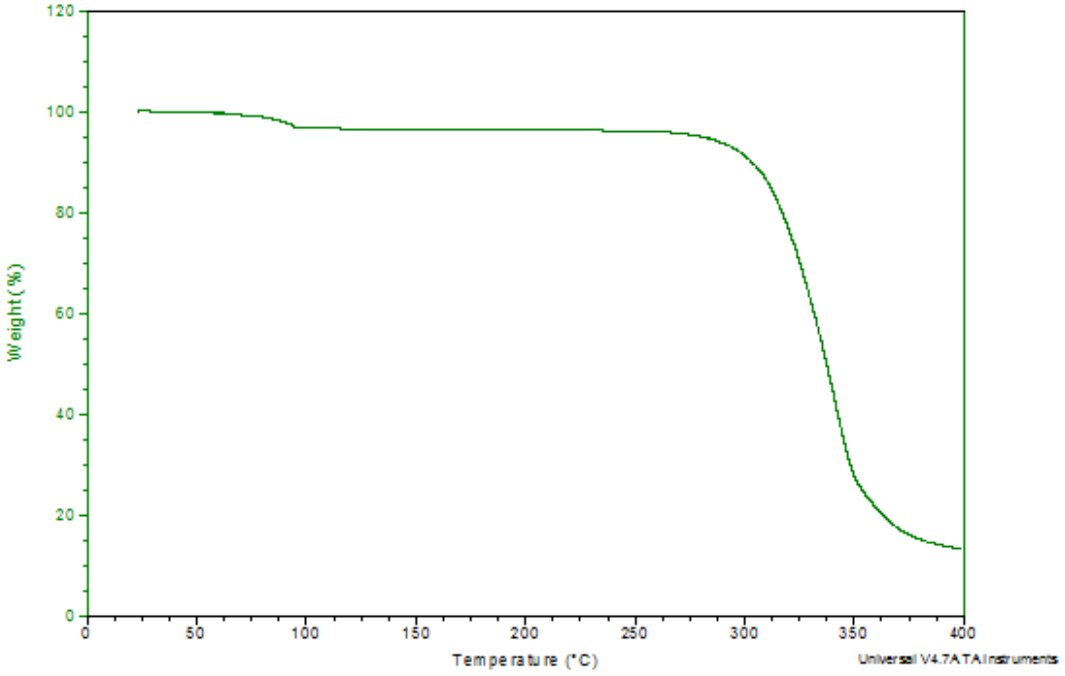

Appendix 0.40. Representative DSC thermal profile for magnesium stearate

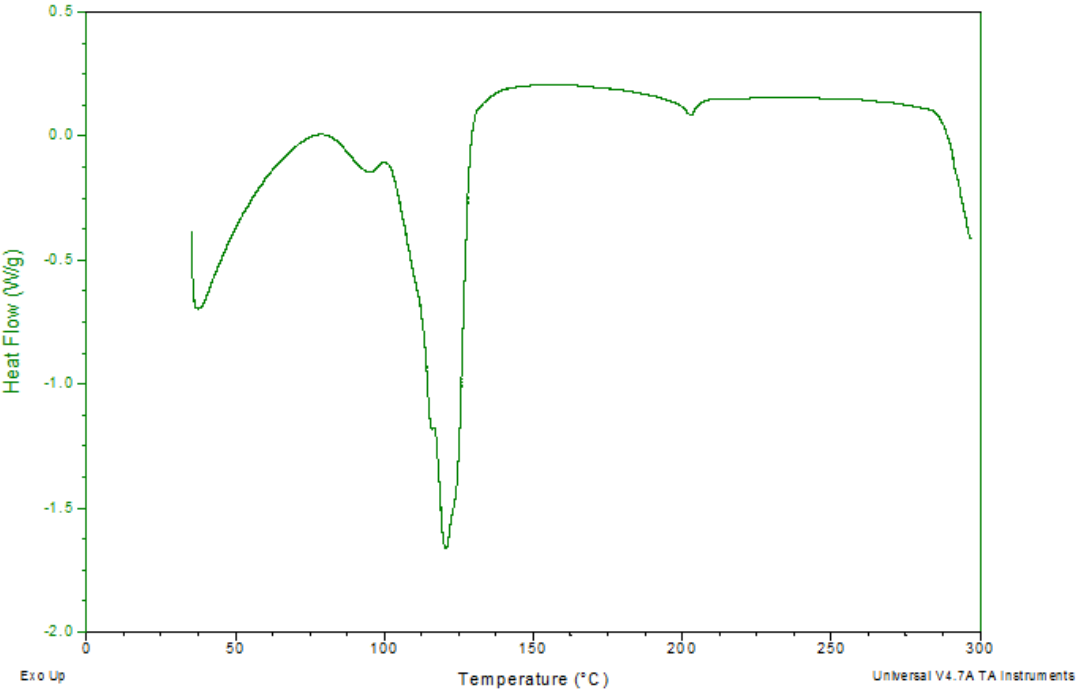

Appendix 0.11. Representative PXRD pattern for magnesium stearate

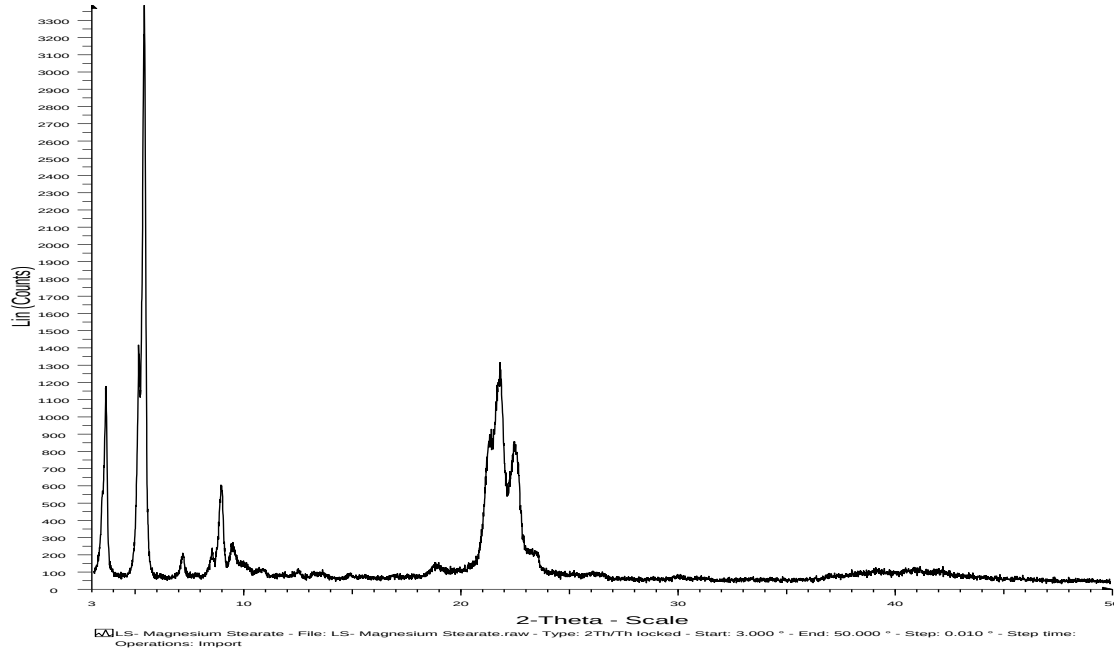

Appendix 0.11. Representative TGA thermal profile for povidone

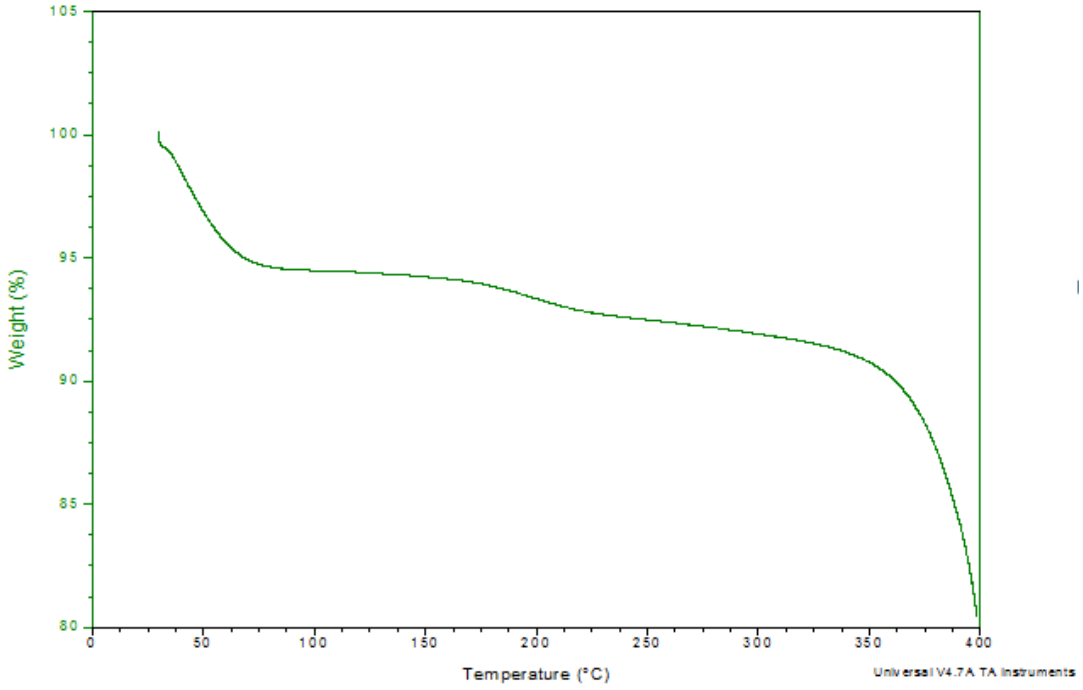

Appendix 0.5. Representative DSC thermal profile for povidone

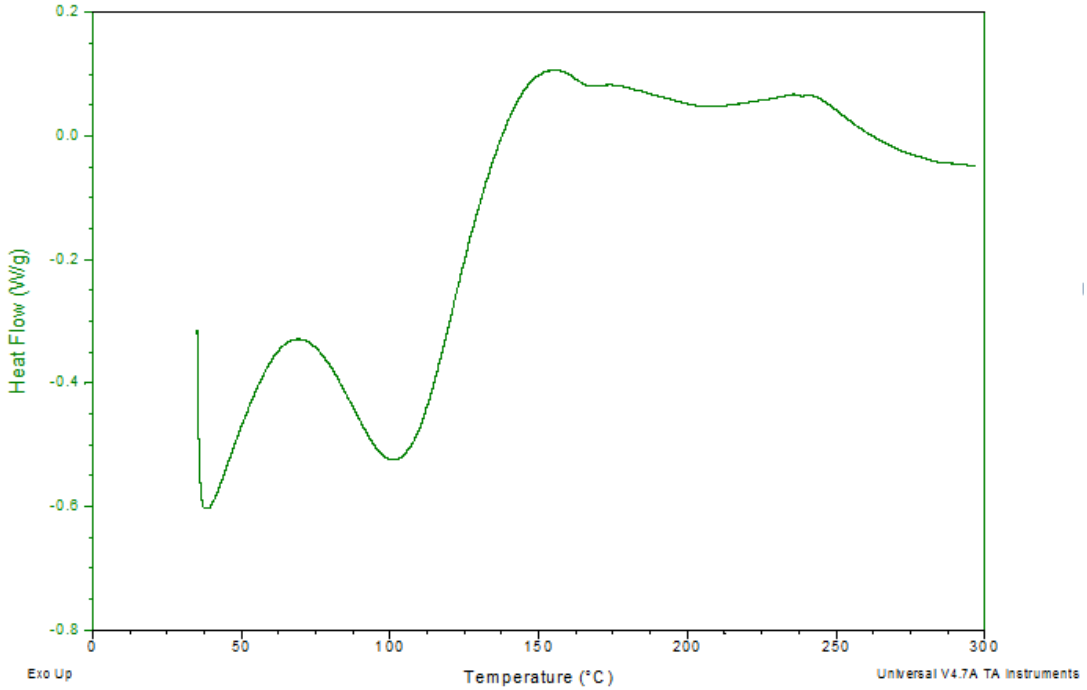

Appendix 0.13. Representative PXRD pattern for povidone

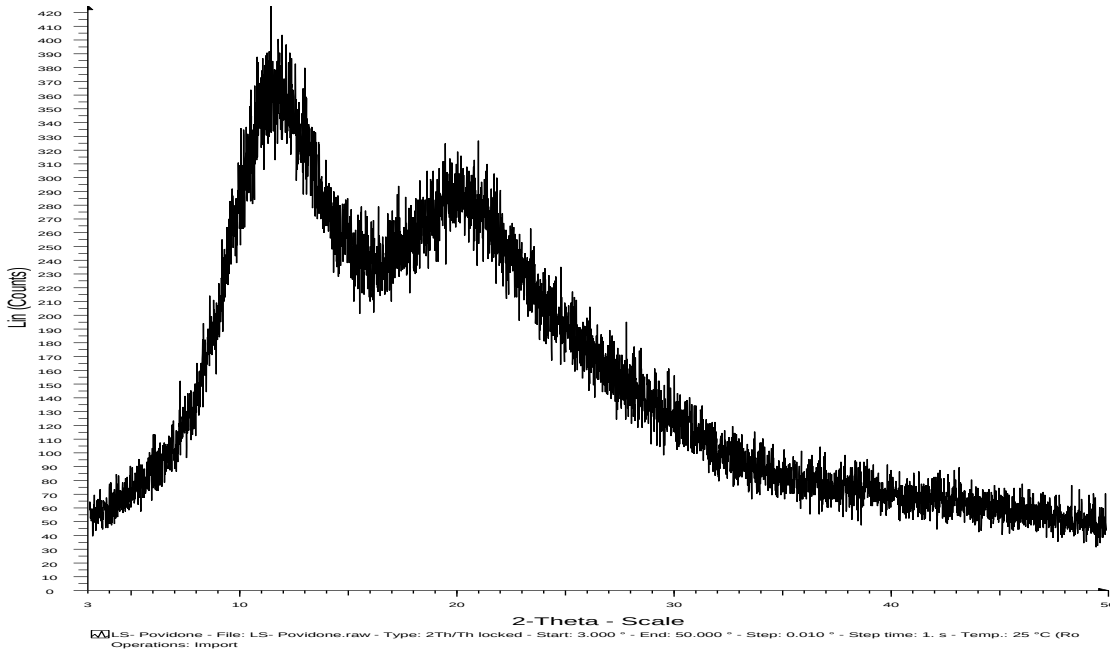

Appendix 0.64. Representative TGA thermal profile for sodium citrate

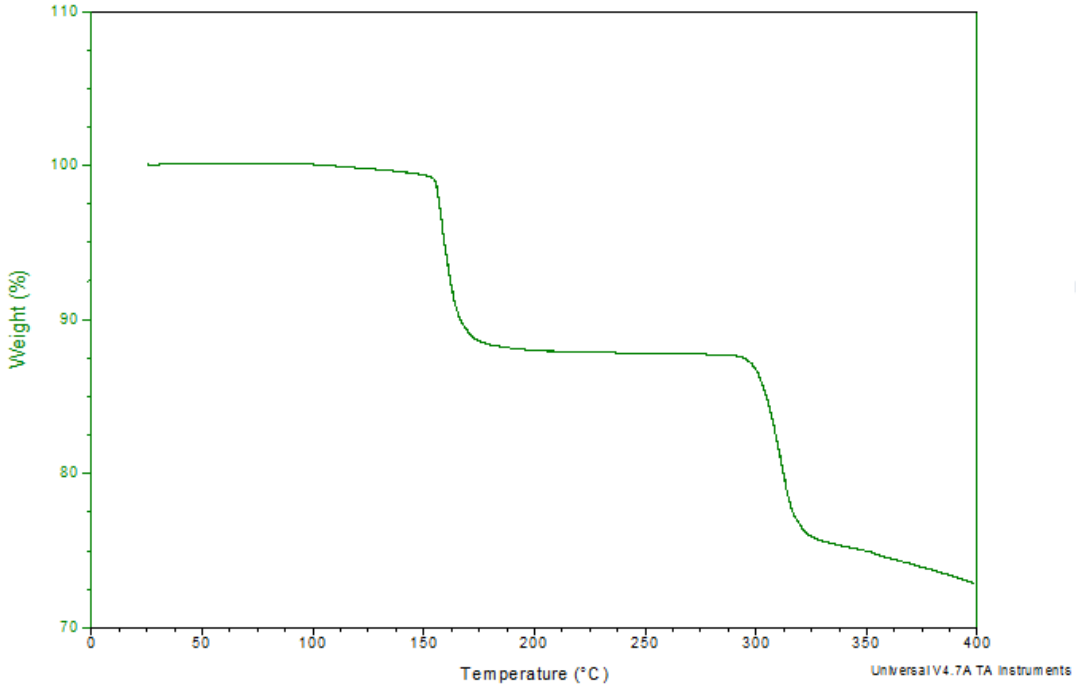

Appendix 0.15. Representative DSC thermal profile for sodium citrate

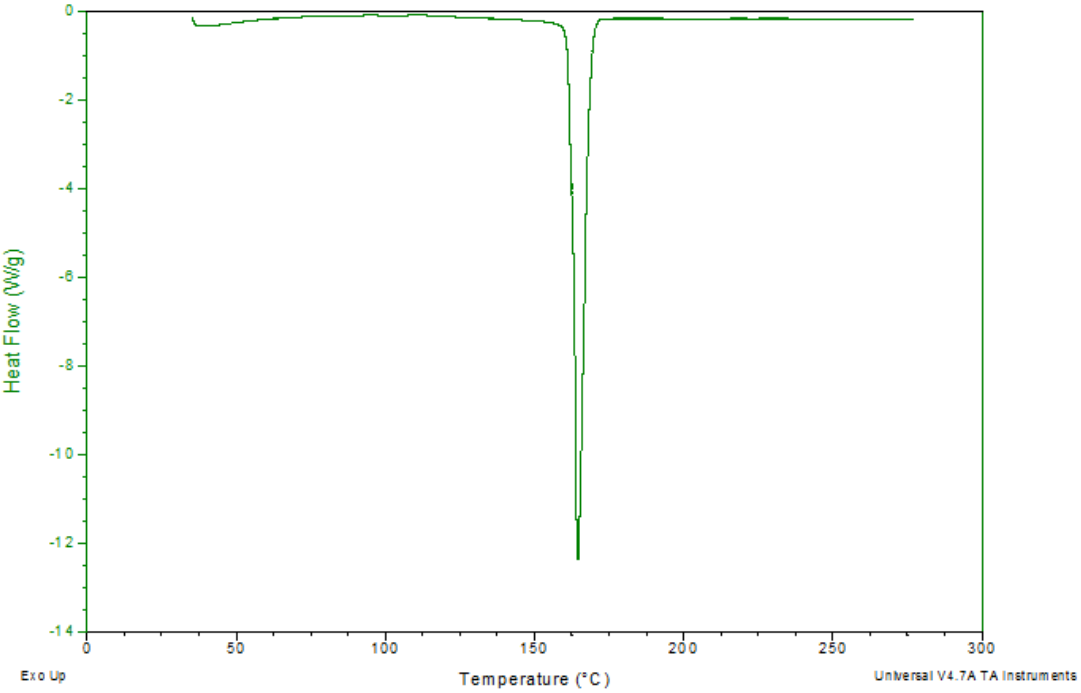

Appendix 0.16. Representative PXRD pattern for sodium citrate

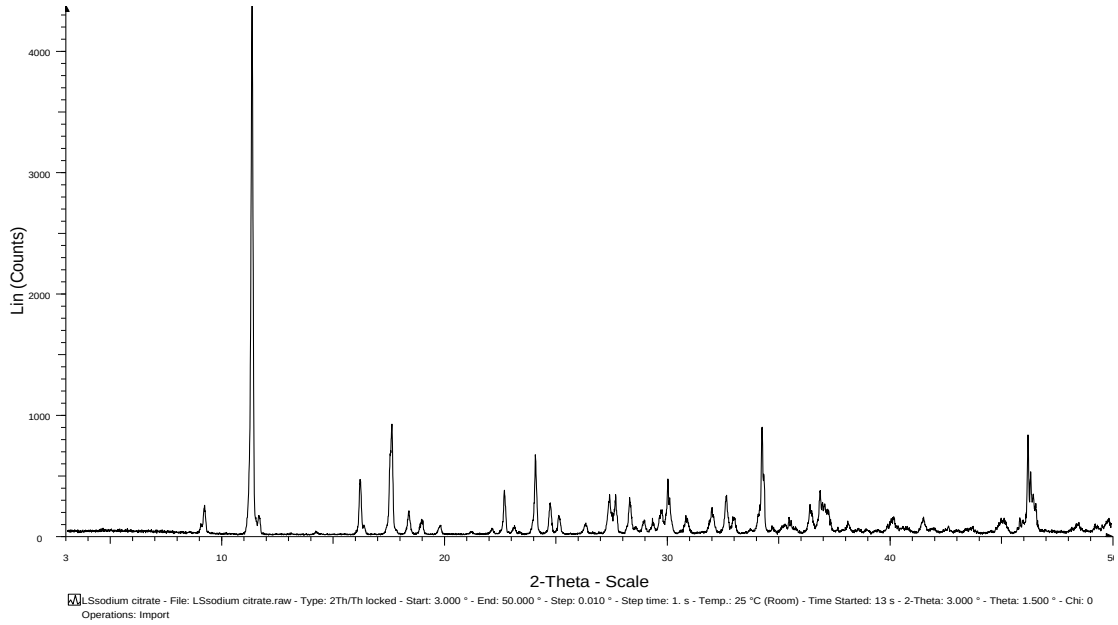

Appendix 0.7. Crushing strength data for lactose monohydrate tablets produced by direct compression

	Crushing (KP)					Average (n = 5)	Standard deviation (KP)
25 kN	1.6	1.5	1.5	1.3	1.3	**1.4**	± 0.1
30 kN	2.9	1.6	1.7	2.0	1.6	**1.9**	± 0.6
35 kN	2.5	1.4	1.9	2.8	1.4	**2.0**	± 0.6
40 kN	3.6	2.1	3.4	3.1	3.1	**3.1**	± 0.6

Appendix 0.8. Tensile strength data for lactose monohydrate tablets produced by direct compression

	Tensile strength (mPa)					Average (n=5)	Standard deviation (mPa)
25 kN	0.022	0.020	0.020	0.017	0.018	**0.020**	± 0.002
30 kN	0.040	0.022	0.024	0.028	0.022	**0.027**	± 0.008
35 kN	0.035	0.020	0.027	0.039	0.022	**0.028**	± 0.009
40 kN	0.051	0.030	0.048	0.044	0.043	**0.043**	± 0.008

Appendix 0.9. Crushing strength data for anhydrous lactose tablets produced by direct compression

	Crushing (KP)					Average (n=5)	Standard deviation (KP)
25 kN	3.6	3.5	3.4	3.6	2.7	**3.4**	± 0.4
30 kN	2.4	2.6	3.6	3.9	3.3	**3.2**	± 0.6
35 kN	2.8	2.9	3.0	4.8	3.7	**3.4**	± 0.8
40 kN	5.3	5.4	4.8	5.5	5.4	**5.3**	± 0.3

Appendix 0.10. Tensile strength data for anhydrous lactose tablets produced by direct compression

	Tensile strength (mPa)					Average (n=5)	Standard deviation (mPa)
25 kN	0.049	0.047	0.046	0.048	0.036	**0.045**	± 0.005
30 kN	0.033	0.036	0.050	0.054	0.045	**0.044**	± 0.009
35 kN	0.039	0.041	0.042	0.068	0.052	**0.048**	± 0.012
40 kN	0.075	0.077	0.067	0.077	0.076	**0.074**	± 0.004

Appendix 0.11. Crushing strength data for spray dried lactose tablets produced by direct compression

	Crushing (KP)					Average (n=5)	Standard deviation (KP)
25 kN	5.1	2.5	9.8	9.5	4.9	**6.4**	± 3.8
30 kN	8.4	25.1	9.4	16.3	21.1	**16.1**	± 7.2
35 kN	14.3	16.7	14.9	19.5	15.0	**16.1**	± 2.1
40 kN	21.5	22.3	17.9	11.4	15.9	**17.8**	± 4.4

Appendix 0.12. Tensile strength data for spray dried lactose tablets produced by direct compression

	Tensile strength (mPa)					Average (n=5)	Standard deviation (mPa)
25 kN	0.066	0.031	0.124	0.117	0.065	**0.081**	± 0.039
30 kN	0.115	0.334	0.127	0.219	0.278	**0.214**	± 0.095
35 kN	0.191	0.222	0.197	0.261	0.198	**0.214**	± 0.029
40 kN	0.299	0.306	0.243	0.156	0.215	**0.244**	± 0.062

Appendix 0.1. Representative TGA thermal profiles for lactose monohydrate tablets produced by direct compression at 30 kN, before and after storage

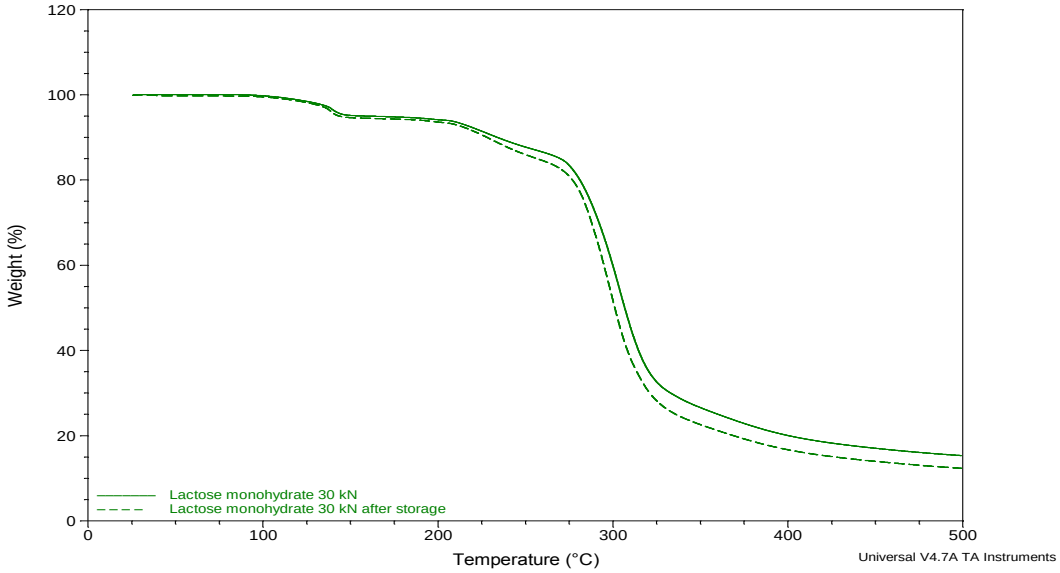

Appendix 0.2. Representative TGA thermal profiles for lactose monohydrate tablets produced by direct compression at 35 kN, before and after storage

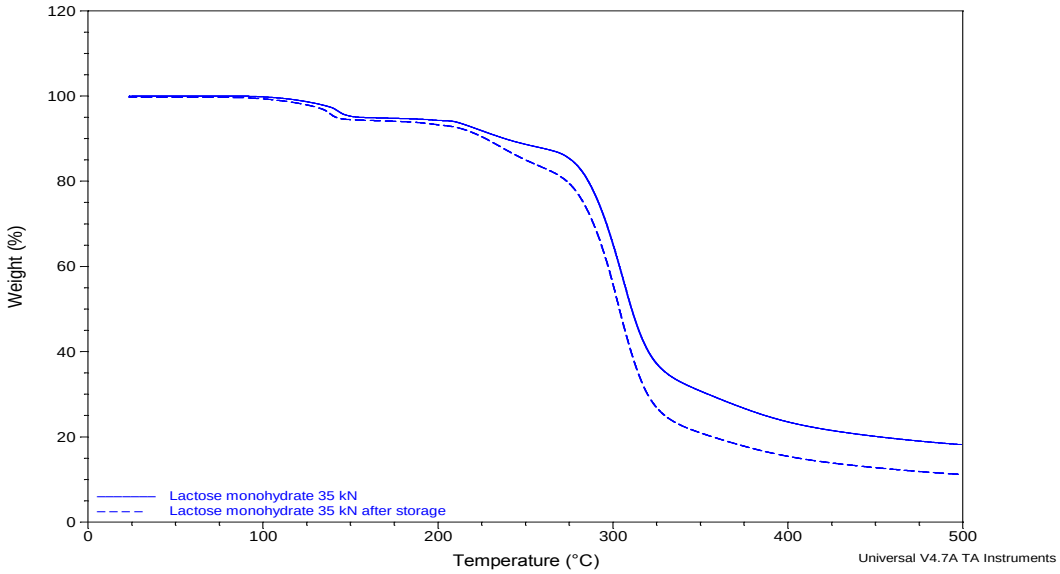

Appendix 0.3. Representative TGA thermal profiles for lactose monohydrate tablets produced by direct compression at 40 kN, before and after storage

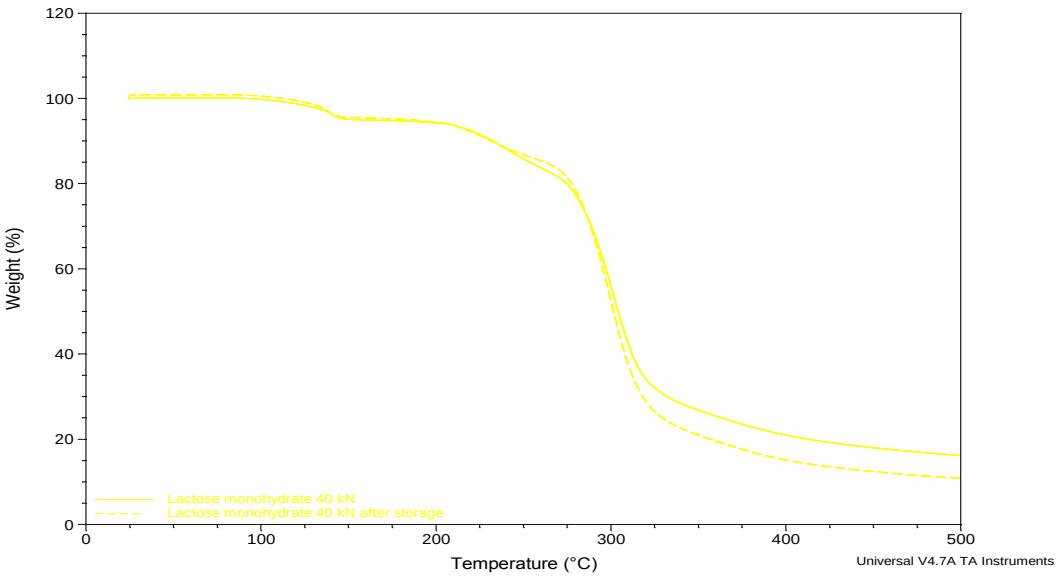

Appendix 0.4. Representative DSC thermal profiles for lactose monohydrate tablets produced by direct compression at 30 kN, before and after storage

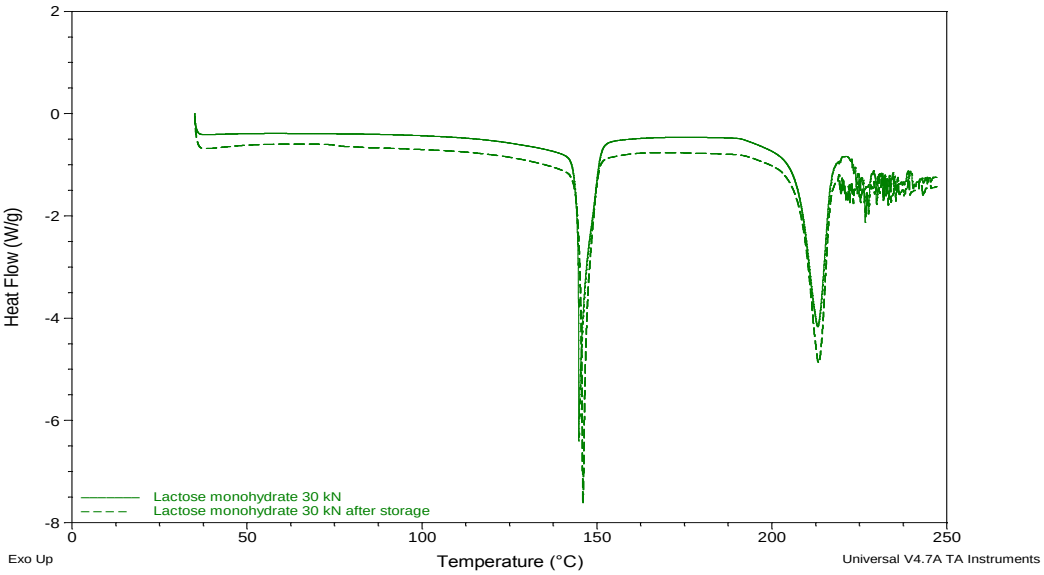

Appendix 0.5. Representative DSC thermal profiles for lactose monohydrate tablets produced by direct compression at 35 kN, before and after storage

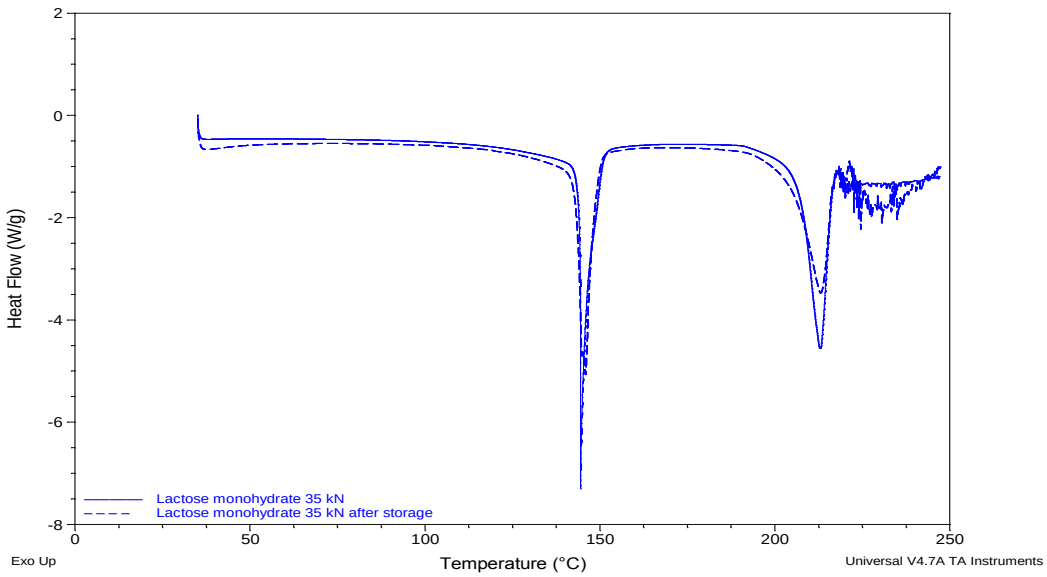

Appendix 0.6. Representative DSC thermal profiles for lactose monohydrate tablets produced by direct compression at 40 kN, before and after storage

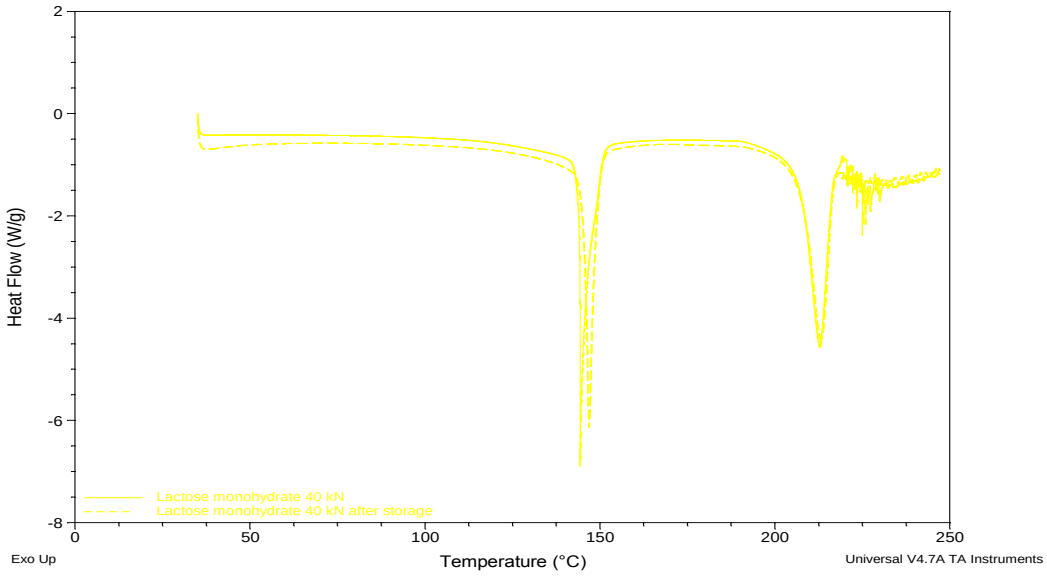

Appendix 0.7. Crushing strength data for lactose monohydrate tablets produced by direct compression, before and after storage at various compaction forces

	Crushing (kP)					Average (n = 5)	Standard deviation (kP)
25 kN	1.6	1.5	1.5	1.3	1.3	**1.4**	± 0.1
25 kN after storage	2.8	2.5	3.2	2.6	2.8	**2.8**	± 0.27
30 kN	2.9	1.6	1.7	2.0	1.6	**1.9**	± 0.6
30 kN after storage	2.4	3.9	3.7	2.5	3.2	**3.1**	± 0.68
35 kN	2.5	1.4	1.9	2.8	1.4	**2.0**	± 0.6
35 kN after storage	4.5	4.8	5.0	4.2	4.5	**4.6**	± 0.31
40 kN	3.6	2.1	3.4	3.1	3.1	**3.1**	± 0.6
40 kN after storage	5.1	5.0	4.7	3.8	4.9	**4.7**	± 0.52

Appendix 0.8. Tensile strength data for lactose monohydrate tablets produced by direct compression, before and after storage at various compaction forces

	Tensile strength (mPa)					Average (n=5)	Standard deviation (mPa)
25 kN	0.022	0.020	0.020	0.017	0.018	**0.020**	± 0.002
25 kN after storage	0.038	0.034	0.044	0.035	0.038	**0.038**	± 0.004
30 kN	0.040	0.022	0.024	0.028	0.022	**0.027**	± 0.008
30 kN after storage	0.033	0.054	0.052	0.035	0.044	**0.043**	± 0.010
35 kN	0.035	0.020	0.027	0.039	0.022	**0.028**	± 0.009
35 kN after storage	0.063	0.068	0.071	0.059	0.063	**0.065**	± 0.005
40 kN	0.051	0.030	0.048	0.044	0.043	**0.043**	± 0.008
40 kN after storage	0.072	0.071	0.066	0.054	0.068	**0.066**	± 0.007

Appendix 0.9. PXRD patterns for lactose monohydrate tablets produced by direct compression at 30 kN

A (Black) = after storage, B (Green) = before storage

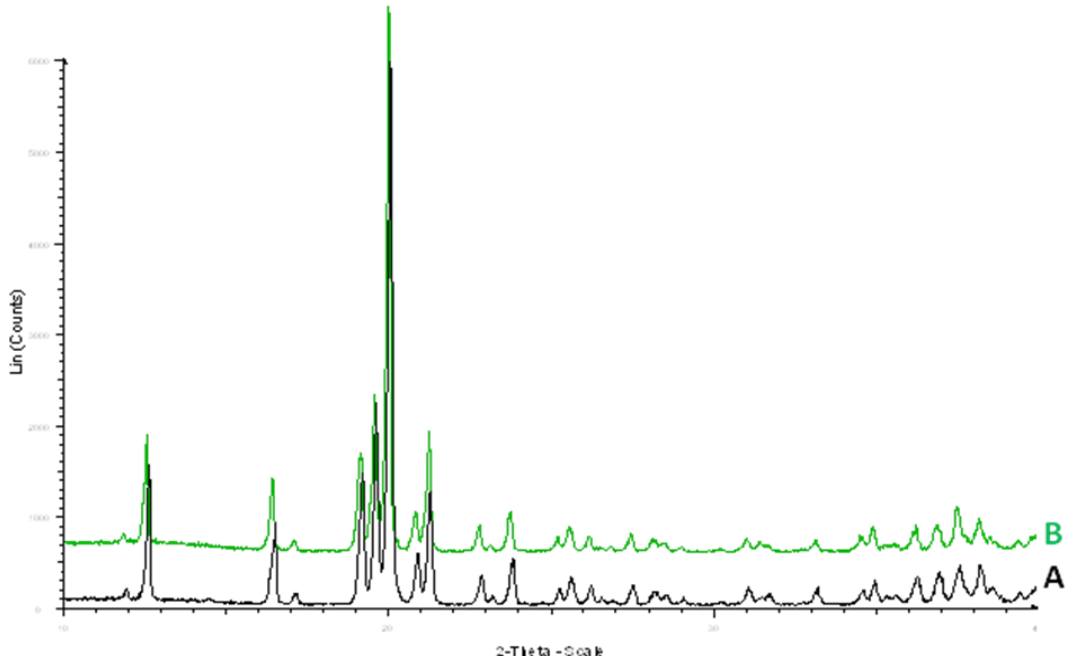

Appendix 0.10. PXRD patterns for lactose monohydrate tablets produced by direct compression at 35 kN.

A (Black) = after storage, B (Blue) = before storage

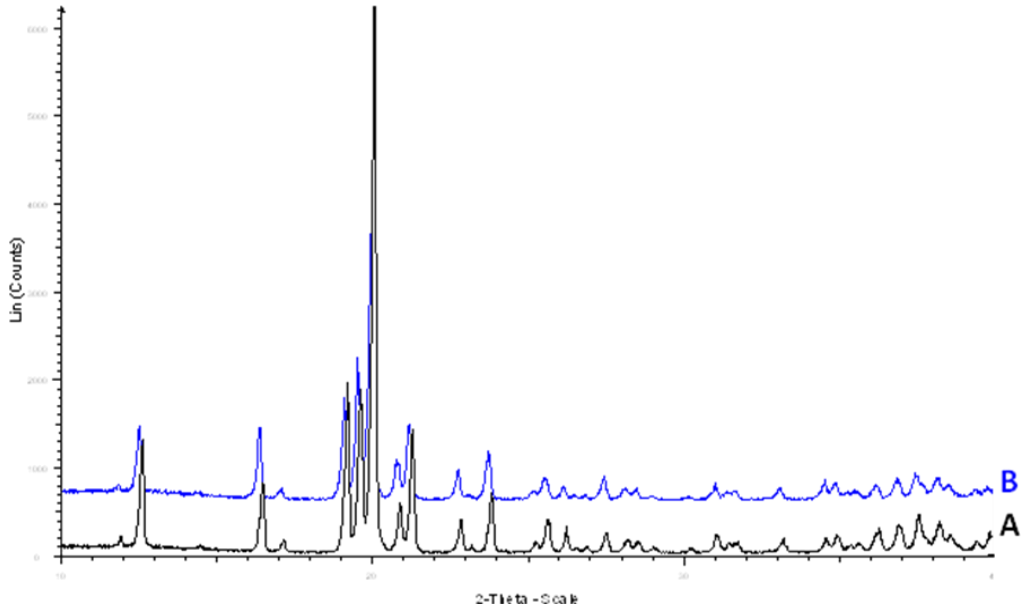

Appendix 0.11. PXRD patterns for lactose monohydrate tablets produced by direct compression at 40 kN

A (Black) = after storage, B (Yellow) = before storage

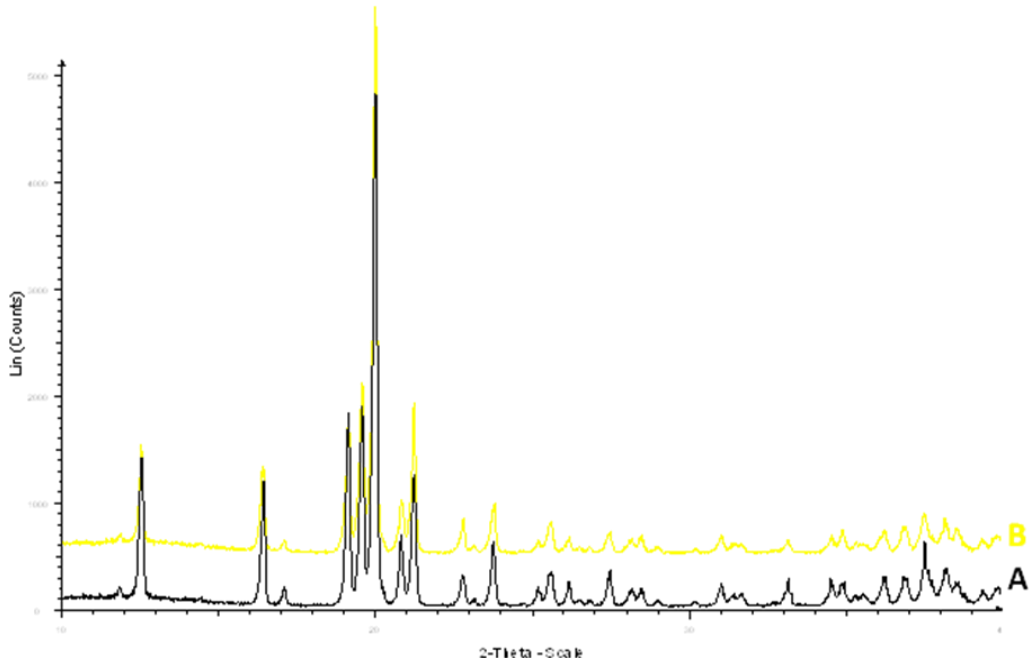

Appendix 0.12. Representative TGA thermal profiles for anhydrous lactose tablets produced by direct compression at 30 kN, before and after storage

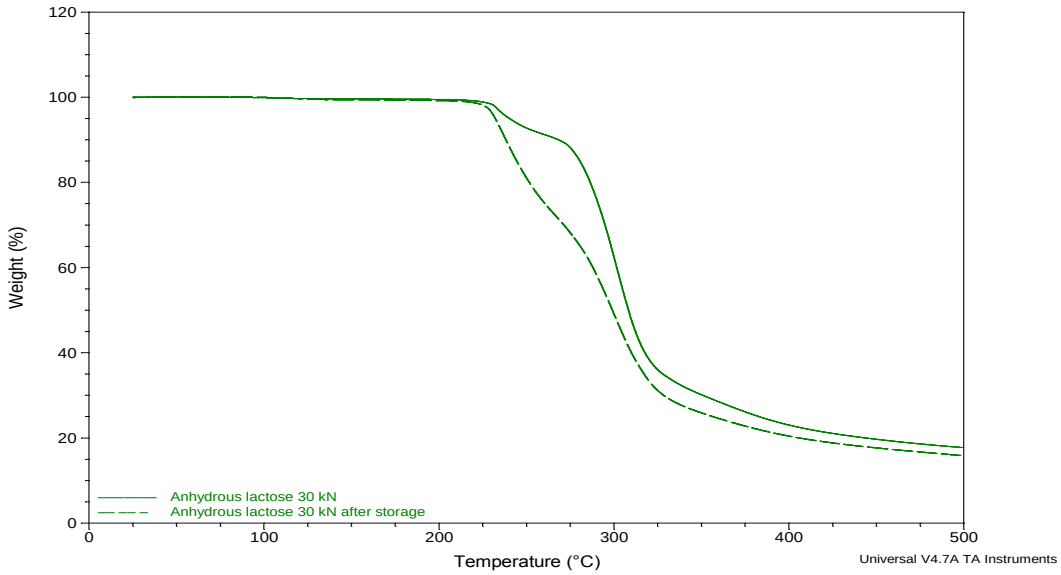

Appendix 0.13. Representative TGA thermal profile for anhydrous lactose tablets produced by direct compression at 35 kN, before and after storage

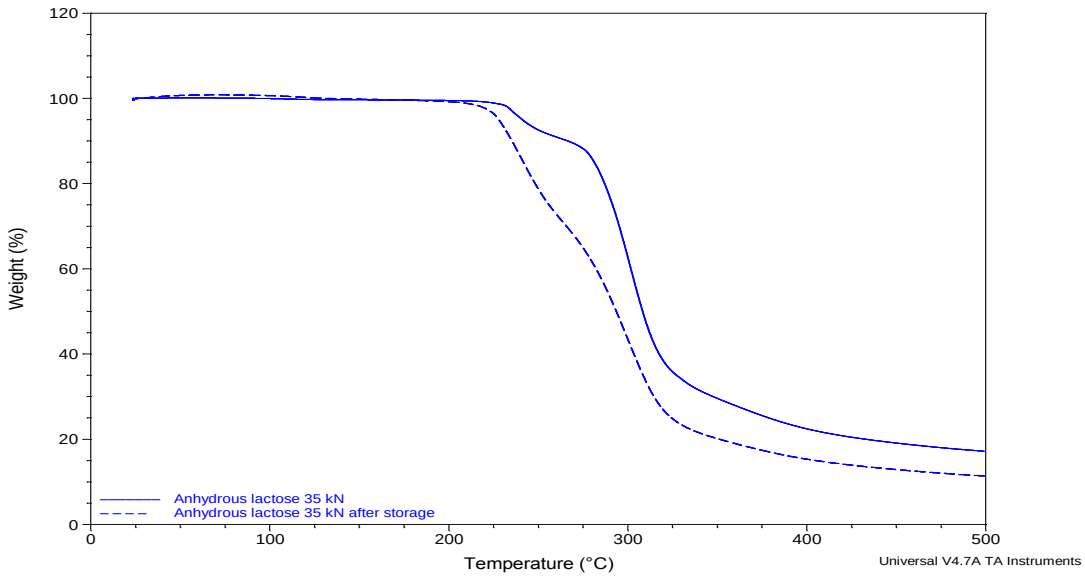

Appendix 0.14. Representative TGA thermal profile for anhydrous lactose tablets produced by direct compression at 40 kN, before and after storage

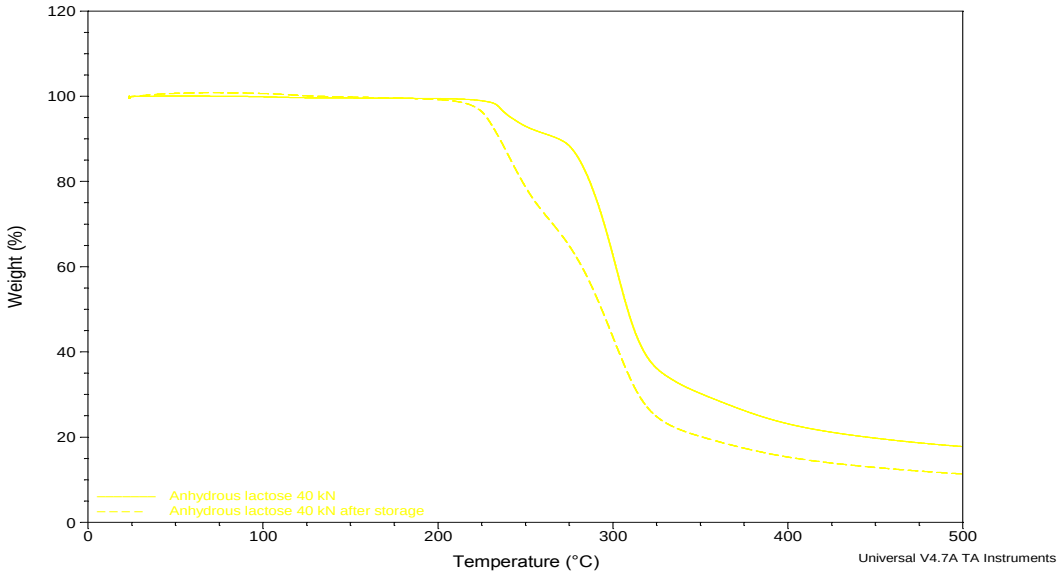

Appendix 0.15. Representative DSC thermal profile for anhydrous lactose tablets produced by direct compression at 30 kN, before and storage

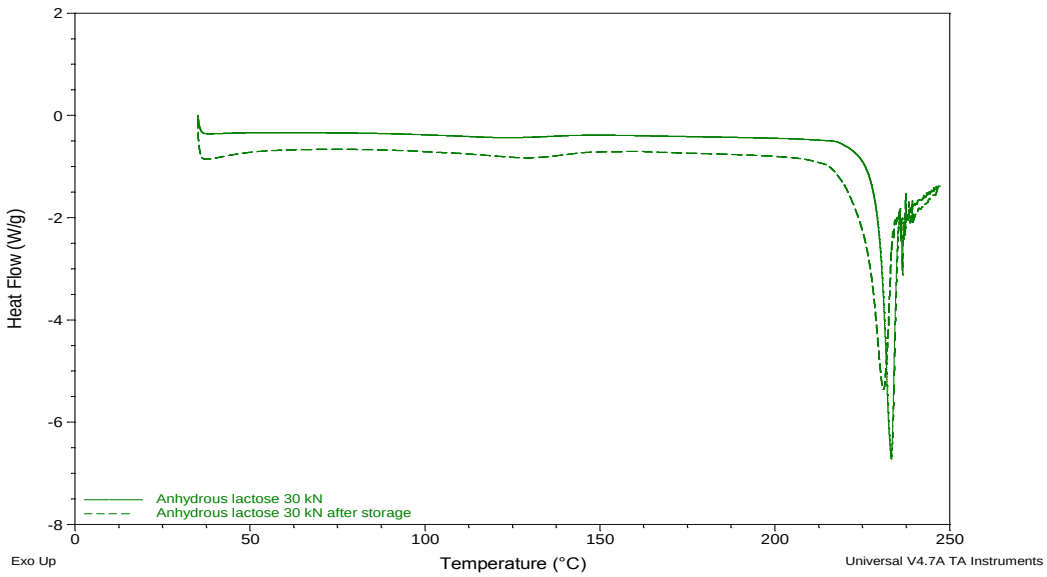

Appendix 0.16. Representative DSC thermal profiles for anhydrous lactose produced by direct compression at 35 kN, before and after storage

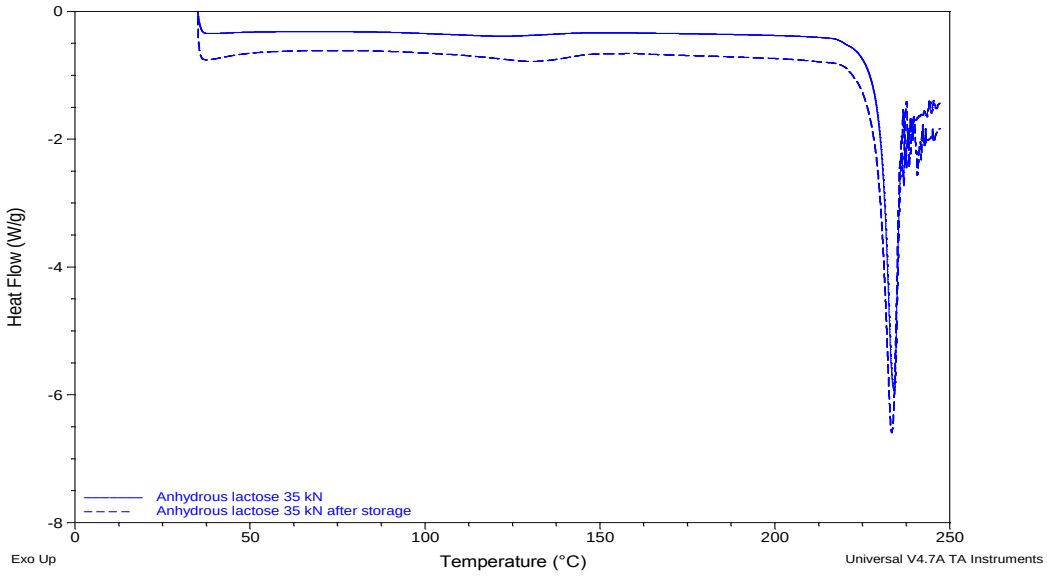

Appendix 0.17. Representative DSC thermal profiles for anhydrous lactose produced by direct compression at 40 kN, before and after storage

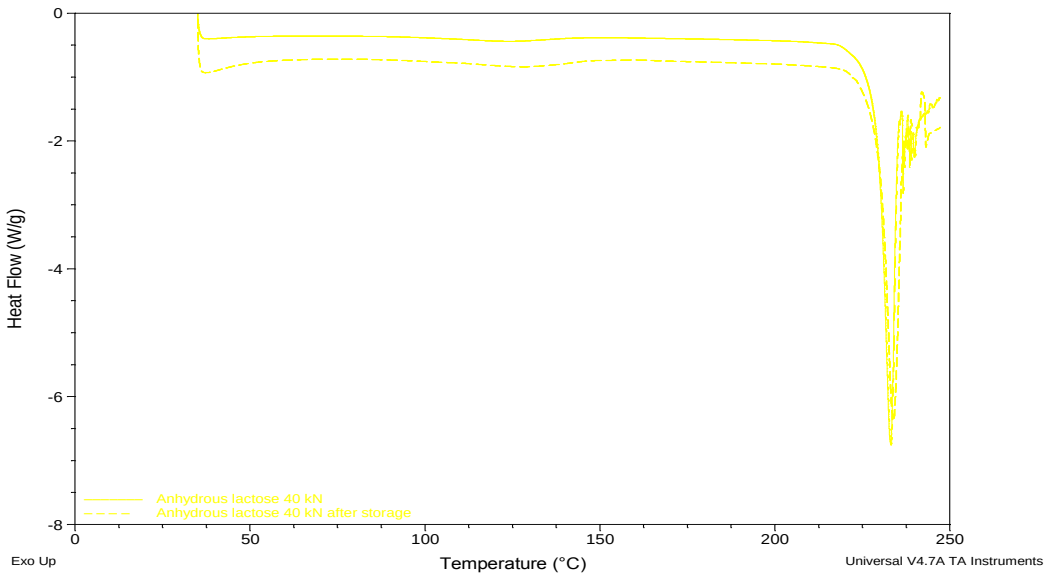

Appendix 0.18. Crushing strength data for anhydrous lactose tablets produced by direct compression, before and after storage at various compaction forces

	Crushing (KP)					Average (n=5)	Standard deviation (KP)
25 kN	3.6	3.5	3.4	3.6	2.7	**3.4**	± 0.4
25 kN after storage	5.3	6.5	5.9	7.1	6.3	**6.2**	± 0.7
30 kN	2.4	2.6	3.6	3.9	3.3	**3.2**	± 0.6
30 kN after storage	12.3	7.8	11.0	7.4	9.2	**9.5**	± 2.1
35 kN	2.8	2.9	3.0	4.8	3.7	**3.4**	± 0.8
35 kN after storage	10.0	8.7	9.0	10.2	10.7	**9.7**	± 0.8
40 kN	5.3	5.4	4.8	5.5	5.4	**5.3**	± 0.3
40 kN after storage	9.4	9.3	9.1	10.9	9.4	**9.6**	± 0.7

Appendix 0.19. Tensile strength data for anhydrous lactose tablets produced by direct compression, before and after storage at various compaction forces

	Tensile strength (mPa)					Average (n=5)	Standard deviation (mPa)
25 kN	0.049	0.047	0.046	0.048	0.036	**0.045**	± 0.005
25 kN after storage	0.072	0.088	0.079	0.095	0.085	**0.084**	± 0.008
30 kN	0.033	0.036	0.050	0.054	0.045	**0.044**	± 0.009
30 kN after storage	0.172	0.109	0.154	0.103	0.127	**0.133**	± 0.029
35 kN	0.039	0.041	0.042	0.068	0.052	**0.048**	± 0.012
35 kN after storage	0.139	0.122	0.127	0.143	0.150	**0.136**	± 0.012
40 kN	0.075	0.077	0.067	0.077	0.076	**0.074**	± 0.074
40 kN after storage	0.133	0.132	0.128	0.154	0.132	**0.136**	± 0.010

Appendix 0.20. PXRD patterns for anhydrous lactose tablets produced by direct compression at 30 kN, before and after storage

A (Black) = after storage, B (Green) = before storage

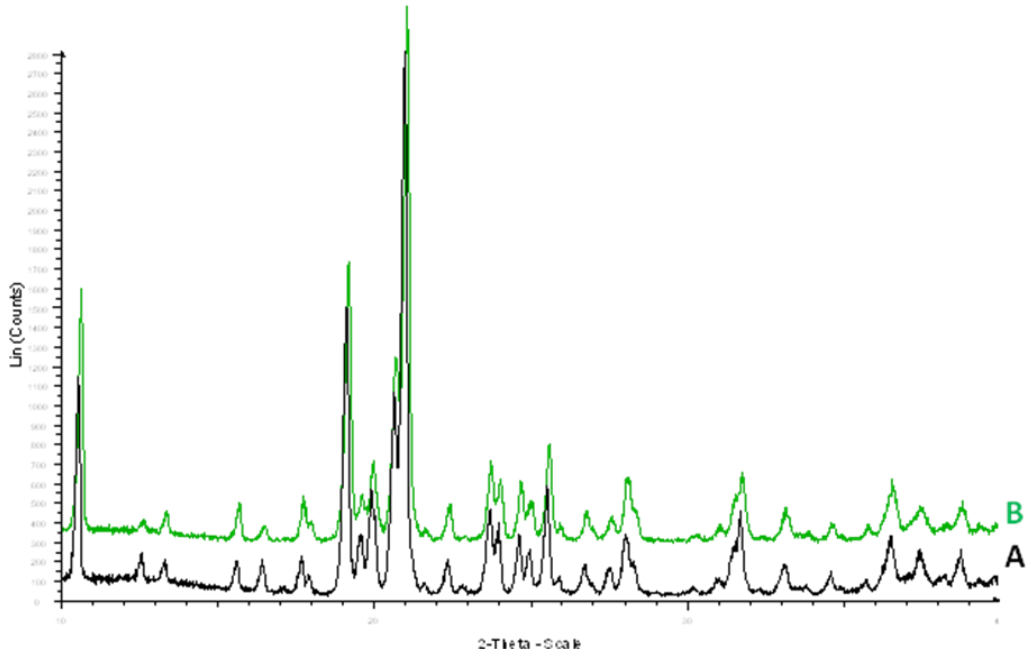

Appendix 0.21. PXRD patterns for anhydrous lactose tablets produced by direct compression at 35 kN

A (Black) = after storage, B (Blue) = before storage

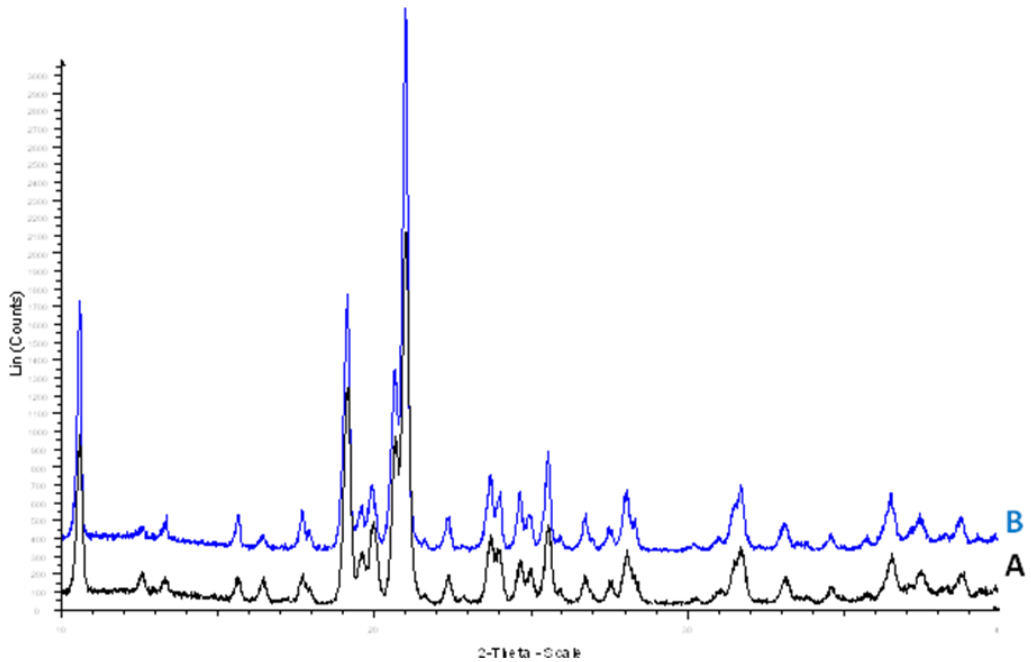

Appendix 0.22. PXRD patterns for anhydrous lactose tablets produced by direct compression at 40 kN

A (Black) = after storage, B (Yellow) = before storage

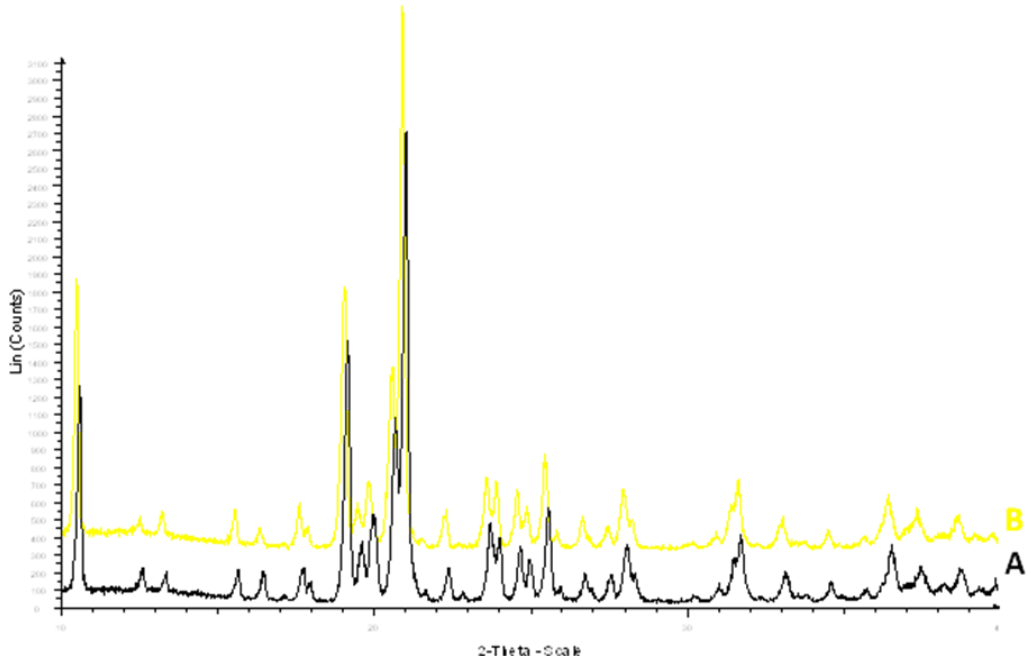

Appendix 0.23. Representative TGA thermal profile for spray dried lactose tablets produced by direct compression at 30 kN, before and after storage

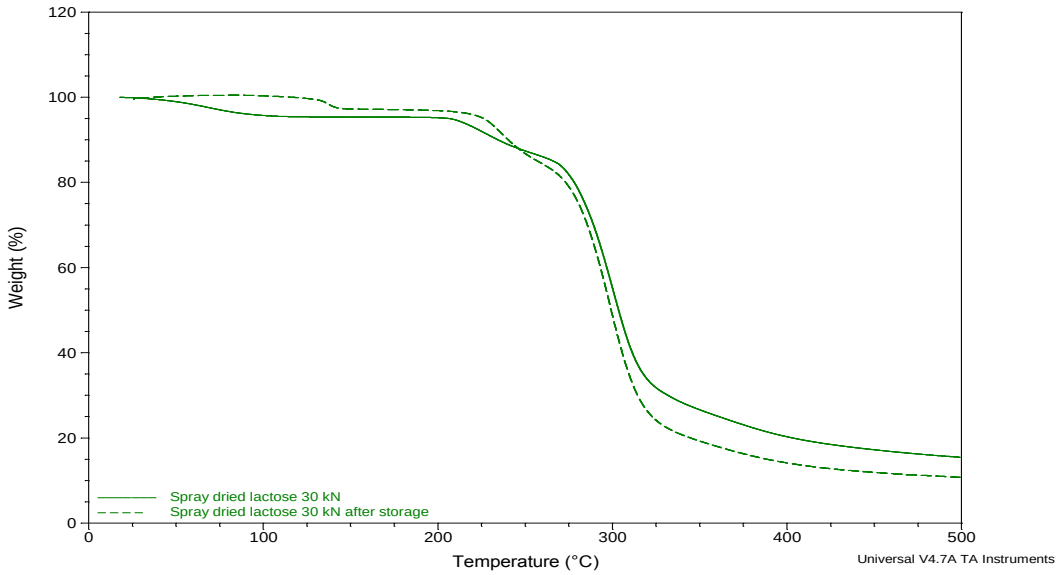

Appendix 0.24. Representative TGA thermal profile for spray dried lactose tablets produced by direct compression at 35 kN, before and after storage

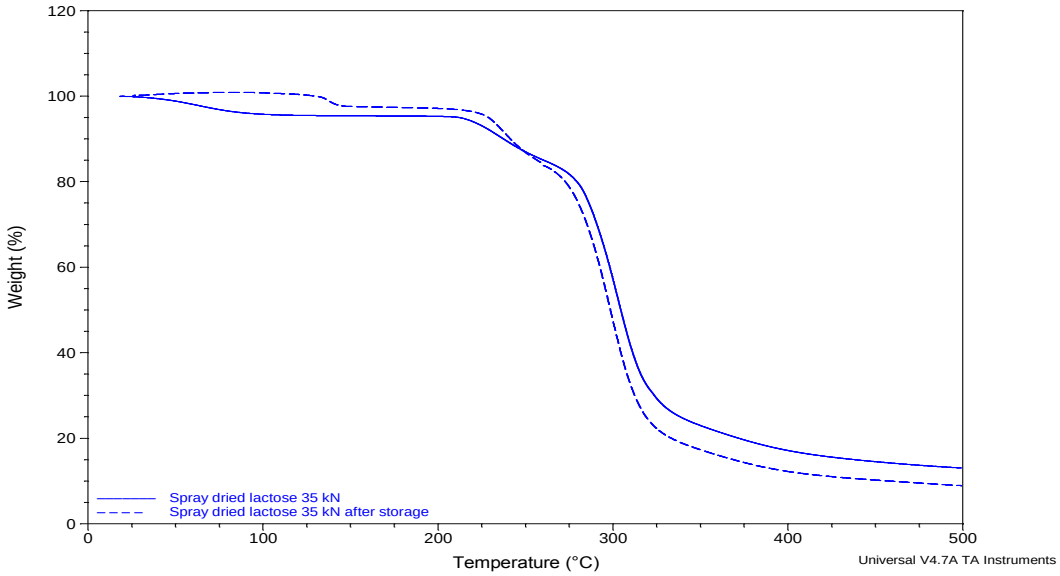

Appendix 0.25. Representative TGA thermal profile for spray dried lactose tablets produced by direct compression at 40 kN, before and after storage

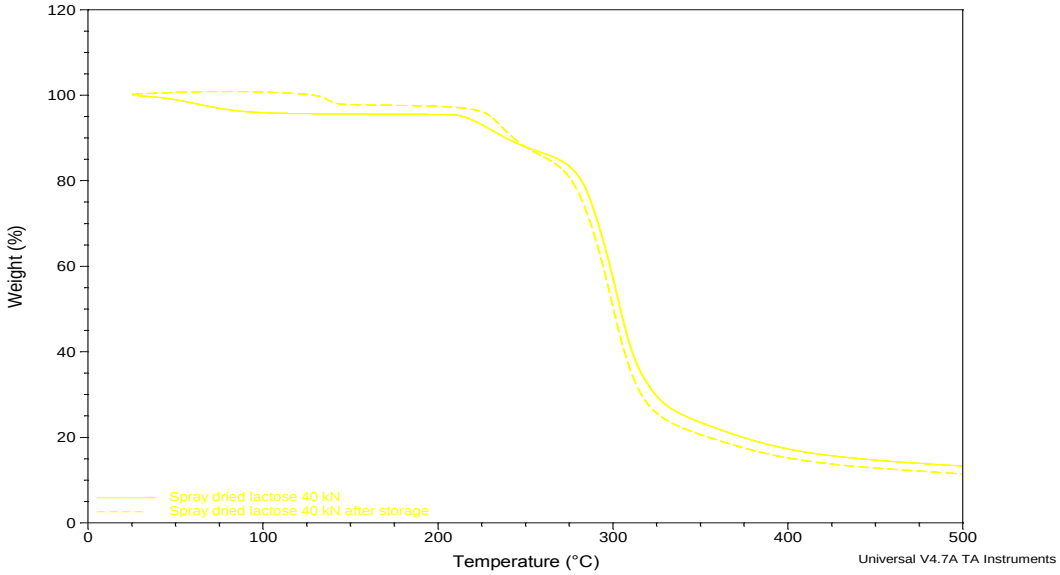

Appendix 0.26. Representative DSC thermal profile for spray dried lactose tablets produced by direct compression at 30 kN, before and after storage

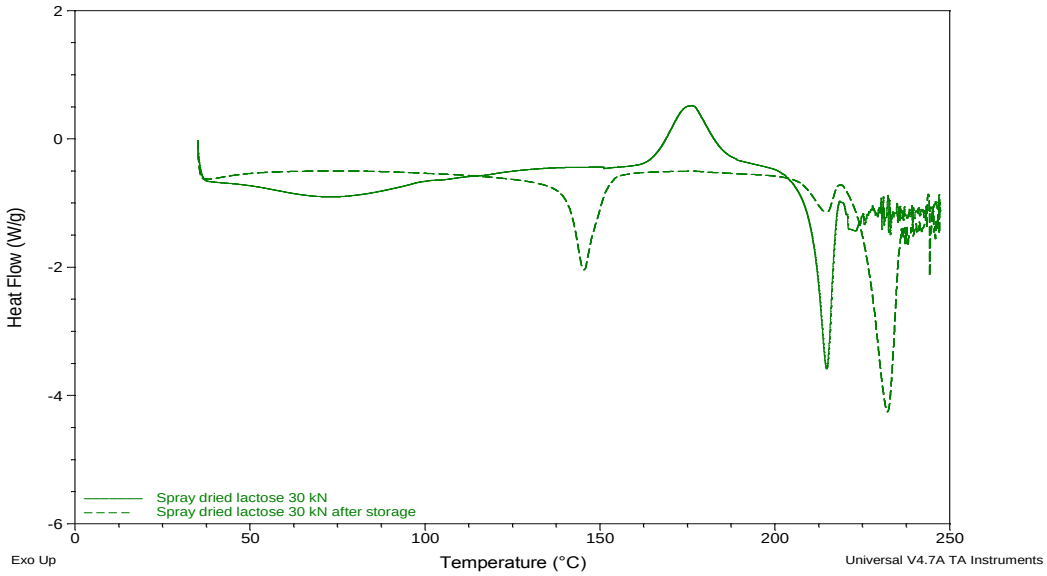

Appendix 0.27. Representative DSC thermal profile for spray dried lactose tablets produced by direct compression at 35 kN, before and after storage

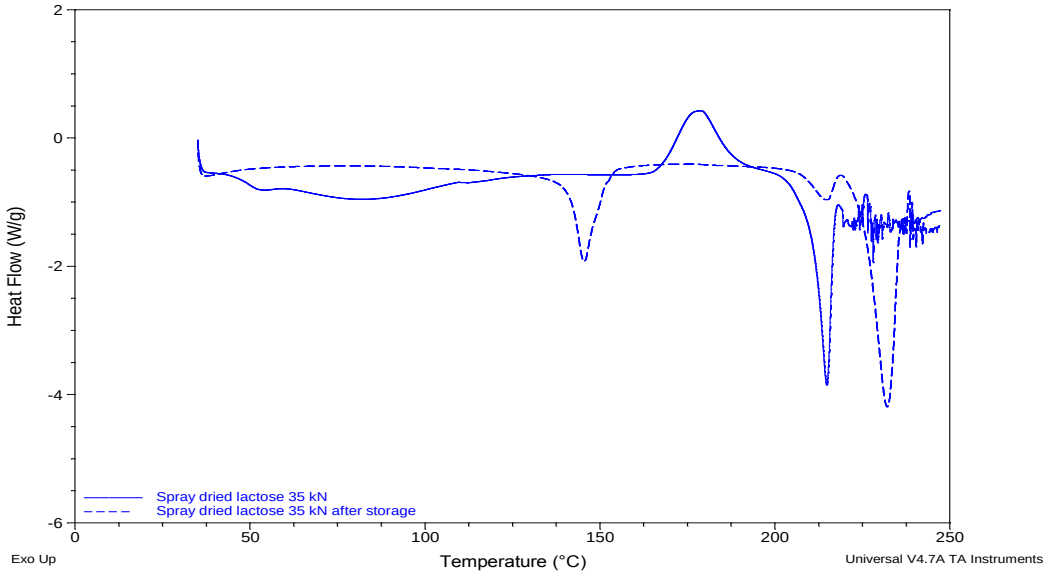

Appendix 0.28. Representative DSC thermal profiles for spray dried lactose tablets produced by direct compression at 40 kN, before and after storage

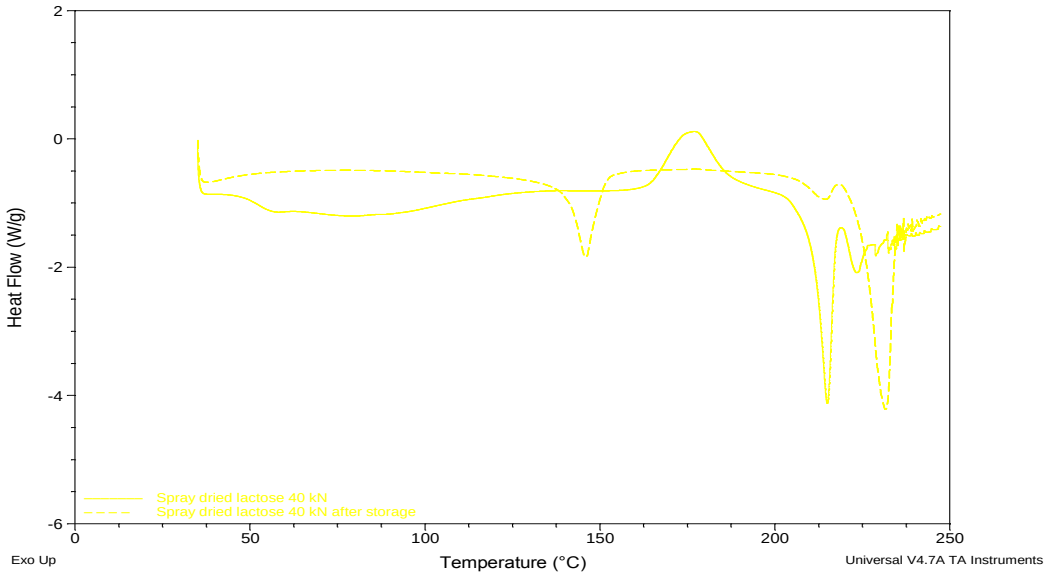

Appendix 0.29. Crushing strength data for spray dried lactose tablets produced by direct compression, before and after storage at various compaction forces

	Crushing (KP)					Average (n =5)	Standard deviation (KP)
25 kN	5.1	2.5	9.8	9.5	4.9	**6.4**	± 3.8
25 kN after storage	12.1	11.5	11.0	6.0	8.9	**9.9**	± 2.5
30 kN	8.4	25.1	9.4	16.3	21.1	**16.1**	± 7.2
30 kN after storage	12.5	13.4	13.9	10.8	10.7	**12.3**	± 1.5
35 kN	14.3	16.7	14.9	19.5	15.0	**16.1**	± 2.1
35 kN after storage	10.8	9.8	14.0	9.0	10.0	**10.7**	± 1.9
40 kN	21.5	22.3	17.9	11.4	15.9	**17.8**	± 4.4
40 kN after storage	13.5	10.0	9.3	11.7	12.2	**11.3**	± 1.7

Appendix 0.30. Tensile strength data for spray dried lactose tablets produced by direct compression, before and after storage at various compaction forces

	Tensile strength (mPa)					Average (n=5)	Standard deviation (mPa)
25 kN	0.066	0.031	0.124	0.117	0.065	**0.081**	± 0.039
25 kN after storage	0.148	0.135	0.130	0.070	0.112	**0.119**	± 0.030
30 kN	0.115	0.334	0.127	0.219	0.278	**0.214**	± 0.095
30 kN after storage	0.162	0.168	0.176	0.139	0.133	**0.156**	± 0.019
35 kN	0.191	0.222	0.197	0.261	0.198	**0.214**	± 0.029
35 kN after storage	0.136	0.125	0.173	0.115	0.126	**0.135**	± 0.023
40 kN	0.299	0.306	0.243	0.156	0.215	**0.244**	± 0.062
40 kN after storage	0.175	0.131	0.120	0.153	0.161	**0.148**	± 0.022

Appendix 0.31. PXRD pattern for spray dried lactose tablets produced by direct compression at 30 kN

A (Green) = before storage, B (Black) = after storage

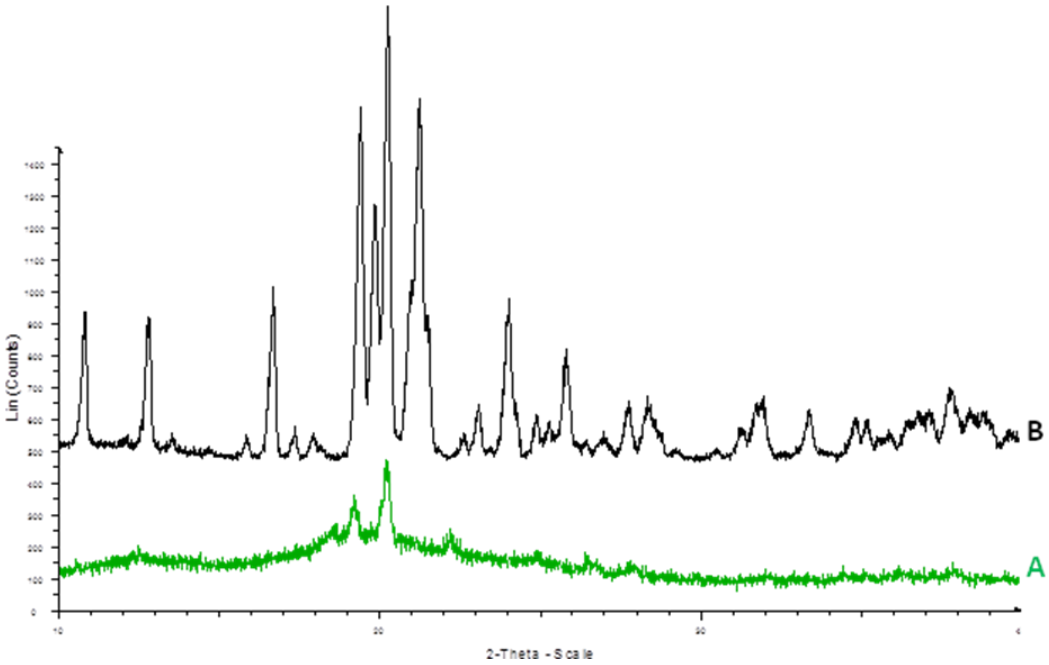

Appendix 0.32. PXRD patterns for spray dried lactose tablets produced by direct compression at 35 kN

A (Blue) = before storage, B (Black) = after storage

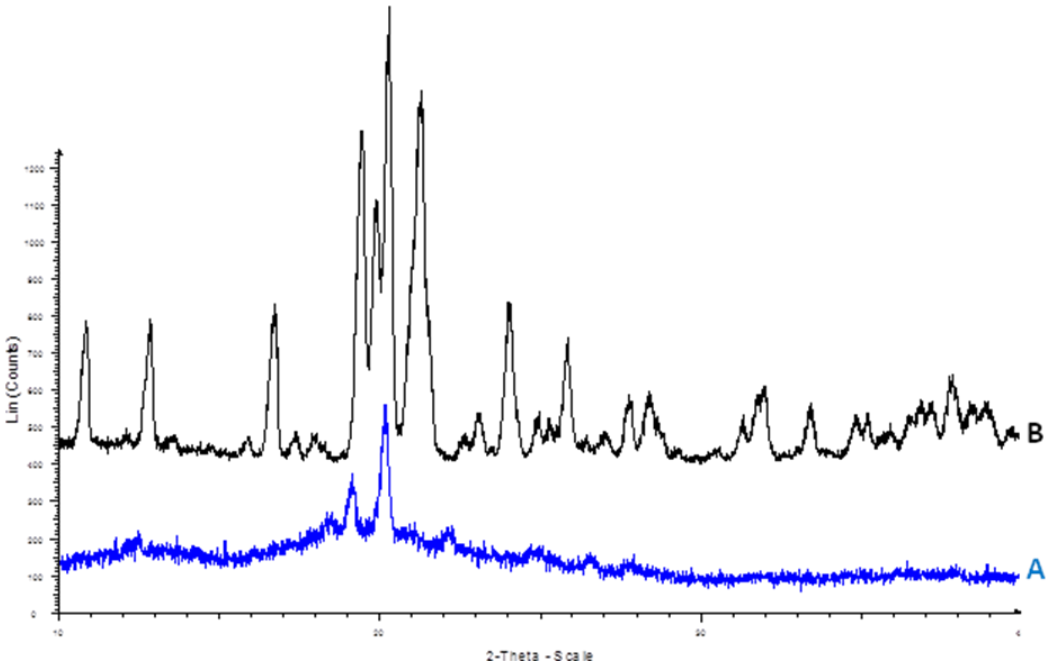

Appendix 0.33. PXRD patterns for spray dried lactose tablets produced by direct compression at 40 kN

A (Yellow) = before storage, B (Black) = after storage

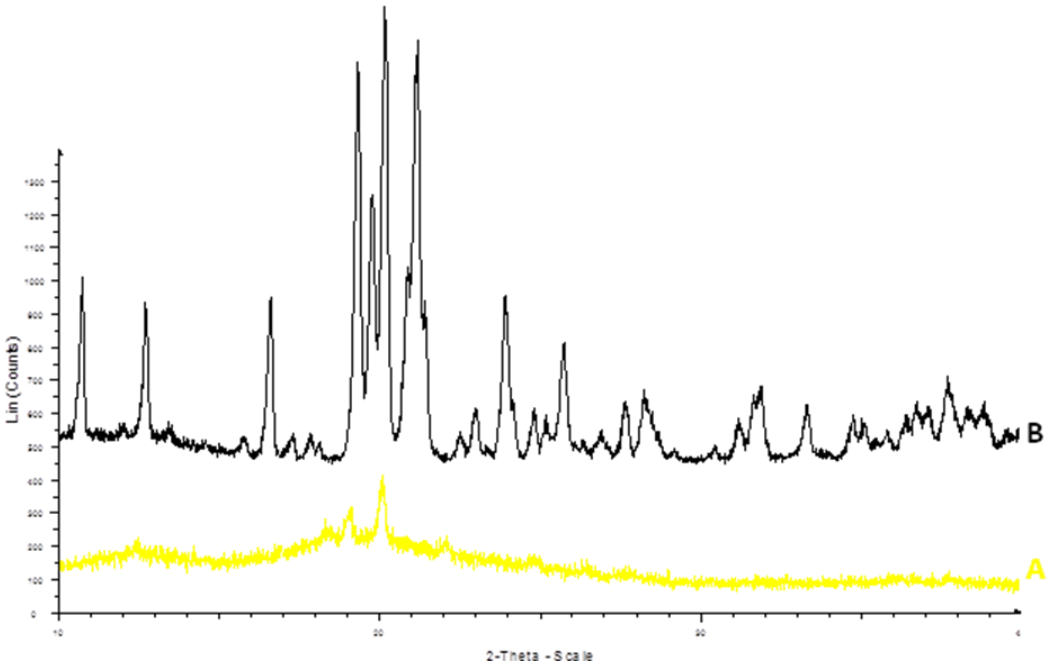

Sections of this work have previously been presented or published in the following forms:

The use of material generated moisture profiling to probe physical form change.
Seymour, L., Forbes, R. T., Hulse, W. L.
Poster presentation, at the American Association of Pharmaceutical Scientists Annual Meeting.
New Orleans, United States of America, 14th-18th November 2010.